Characterisation of novel TLR-dependent immunomodulators from tropical plant extracts

Khalil Thirlaway, BSc

Thesis submitted to the University of Nottingham for the degree of Doctor of Philosophy

School of Veterinary Medicine and Science

September 2016

“Just keep swimming”

Dory, *Finding Nemo*

Abstract

Toll-like receptors (TLRs) recognise a wide range of molecular patterns, and are key in activation and coordination of the innate and adaptive immune responses. TLR ligands include pathogen-associated and damage-associated molecular patterns (PAMPs and DAMPs, respectively), as well as an increasing number of plant-derived ligands. Novel TLR ligands represent promising potential therapeutics, for example as vaccine adjuvants or selectively immunosuppressive drugs.

Exploiting Malaysia's diverse and largely unexplored repertoire of endemic plant species, lyophilised extracts of leaf and bark tissue from various species were screened for stimulatory or inhibitory activity in four stably transfected HEK cell lines expressing TLR 2/1, 2/6, 4 and 5. Extracts showing significant changes in CXCL8 production relative to controls were fractionated to identify active components, and chemically modified to identify functional molecular groups. To better assess biological relevance of any effects, active extracts were tested for modulation of class-switching and proliferation in primary murine splenic B-lymphocytes.

Of the 21 extracts screened, three showing interactions with TLR2/6 were chosen for further analysis: 1402EtL and 1412EtB showed stimulatory activity and 1404EtL showed inhibitory activity. 1402EtL was insoluble in aqueous solution, which prevented further characterisation, but a >100kDa active fraction of 1412EtB and a 10-30kDa active fraction of 1404EtL were identified. Neither boiling nor acid-treatment affected the stimulatory activity of 1412EtB, but oxidation with metaperiodate eliminated activity. None of the three treatments affected the inhibitory activity of 1404EtL. In primary murine B-cells 1402EtL was found to induce IgG1 isotype switching and crude 1412EtB induced proliferation and upregulation of IgM expression. The acid-treated, boiled and >100kDa forms of 1412EtB produced a stronger proliferative and IgM response, as well as inducing IgG1 class switching.

These data suggest that these plants represent promising candidates for development of novel TLR-mediated immunomodulatory pharmaceuticals.

Acknowledgements

This work was carried out at the University of Nottingham's School of Veterinary Medicine and Science as part of the BBSRC-funded Doctoral Training Partnership.

There are many without whom this thesis would not have been possible, and to mention them all individually would take more space than can be spared here. If you're one of those people, you will already know. That said, there are some who certainly must be mentioned.

My supervisors Dr. Robin Flynn and Prof. David Haig have steered me through the past four years and without their support I wouldn't have got very far at all. The support of the rest of the Flynn group was also invaluable, and for that I'd like to thank Tan, Azad, Kate, Cat, Parul, Mayowa and Divya.

My collaborators Dr. Kang Nee Ting (Crops for the Future research centre, University of Nottingham Malaysia Campus) and Dr. Andy Bottley (Plant Sciences, University of Nottingham) kindly supplied the plant extracts tested herein, along with as much information as they were able to provide. The assistance of Dr. David Onion (Life Sciences, University of Nottingham) and the use of the Flow Cytometry Facility were also much appreciated.

There are several of the research staff and postgraduates of the SVMS who helped me to retain some shreds of sanity during the difficult patches. Their advice, consolation, inspiration, motivation and catharsis will not be forgotten. Similarly, the members of the University of Nottingham Wing Chun Kung Fu Club are the greatest mental health asset I could ask for. Kapow.

Finally, I'd like to thank Hans Zimmer and Tangerine Dream for providing the soundtrack to the writing of this thesis.

Contents

Abstract i

Acknowledgements ii

Contents iii

List of Figures vii

List of Tables ix

List of Abbreviations x

Chapter 1. Introduction 1

1.1 Overview of mammalian immunity 1

1.1.1 Innate immunity 1

1.1.2 Adaptive immunity 3

1.1.2.1 T lymphocytes 3

1.1.2.2 B lymphocytes 4

1.1.2.3 Ig classes 4

1.1.2.4 Importance of innate immunity to adaptive immunity 6

1.2 Pattern Recognition Receptors 6

1.2.1 TLRs 7

1.2.1.1 TLR signalling 11

1.2.1.2 TLR dysfunction and pathology 14

1.3 Clinical TLR modulation 16

1.3.1 TLR stimulation 16

1.3.2 TLR inhibition 18

1.4 Plant-derived medicine 19

1.4.1 Plant-derived immunomodulators 20

1.4.1.1 Plant-derived TLR agonists 21

1.4.1.2 Plant-derived TLR antagonists 22

1.5 Rationale and aims/objectives 25

1.5.1 Rationale 25

1.5.2 Aims/objectives 25
Chapter 2. Materials and Methods 26
2.1 Plant extracts 26
2.1.1 Extracts from Crops for the Future research centre (CftF) 26
2.1.2 Extracts from Plant Sciences, University of Nottingham 27
2.1.3 Plant-based controls 27
2.1.4 Dialysis 27
2.1.5 Fluorescent Lectin Stain 28
2.1.6 Extract modification 29
2.1.6.1 Acid treatment 29
2.1.6.2 Heat inactivation 30
2.1.6.3 Metaperiodate carbohydrate oxidation 30
2.1.7 Sodium dodecyl sulphate polyacrylamide gel electrophoresis (SDS-PAGE) 30
2.1.8 Size fractionation 31
2.2 Cells and culture techniques 33
2.2.1 Human embryonic kidney (HEK) cell lines 33
2.2.1.1 Growth media and conditions 33
2.2.1.2 Cytotoxicity assay 34
2.2.1.3 Stimulation experiments 35
2.2.1.4 Inhibition experiments 35
2.2.2 Murine B lymphocytes 35
2.2.2.1 Isolation and culture conditions 35
2.2.2.2 Stimulation 36
2.2.2.3 Flow cytometry 37
2.3 Supernatant assays 38
2.3.1 LDH assay 38
2.3.2 CXCL8 ELISA 38
2.4 Statistical analysis 41

Chapter 3. Screening for modulation of extracellular TLRs by plant extracts 42
3.1 Introduction 42
3.2 Results 47
3.2.1 Cytotoxicity of plant extracts 47
3.2.2 Stimulation of transfected HEK293 TLR cell lines. 49
3.2.3 Inhibition of HEK293 TLR cells with plant extracts 64
3.2.4 Summary 71
3.3 Discussion 72
3.3.1 Cytotoxicity of plant extracts 72
3.3.2 TLR5 data 73
3.3.3 Extracts from CftF 74
3.3.4 Extracts from Plant Sciences Dept., Nottingham 77
3.3.5 Conclusions 77
Chapter 4. Chemical and size characterisation of putative TLR ligands in three plant extracts 79
4.1 Introduction 79
4.2 Results 84
4.2.1 Solubility of plant extracts in PBS 84
4.2.2 Fluorescent Lectin Stain 88
4.2.3 Chemical modification of plant extracts 90
4.2.4 Fractionation of plant extracts 94
4.2.4.1 SDS-PAGE 94
4.2.4.2 Sequential filtration 96
4.2.5 Summary 100
4.3 Discussion 101
Chapter 5. Effects of plant extracts on proliferation and immunoglobulin class-switching in primary B cells 106
5.1 Introduction 106
5.2 Results 110

5.2.1 Cell proliferation (Ki-67 expression) 110
5.2.2 IgM expression 112
5.2.3 Antibody class switching - IgG1 expression 114
5.3 Discussion 116
Chapter 6. General Discussion 121
6.1 TLR-modulatory properties of plant extracts tested 121
6.2 Characterisation of selected extracts 122
6.3 B-cell *in vitro* modulation by selected extracts 123
6.4 Evaluation of 1412EtB, ethanolic extract of bark of *F. ribes* 124
6.5 Contextual considerations 125
6.6 Study limitations and further work 127
6.7 Concluding remarks 129
Bibilography 130
Appendix A Flow cytometry data 160
A.1 Proliferation - Ki-67 160
A.2 IgM 167
A.3 IgG1 174
A.4 Proliferation and antibody expression analysis 181
Appendix B PIPS Placement with The Naked Scientists 191
Appendix C Conferences and meetings attended 193

List of Figures

Figure 1.1 Generic TLR tertiary structure 9

Figure 1.2. Mammalian TLR signalling pathways..... 12

Figure 2.1. Membrane layout for fluorescent lectin stain optimisation 29

Figure 2.2 10-200kDa ladder used in SDS-PAGE..... 31

Figure 2.3. Method for sequential filtration through progressively-smaller molecular weight cut-off (MWCO) membranes..... 32

Figure 2.4. Layout of CXCL8 ELISA plates..... 40

Figure 3.1. Lactate dehydrogenase (LDH) cytotoxicity assay 48

Figure 3.2. TLR2/1 screening results 50

Figure 3.3. TLR2/1 screening results 54

Figure 3.4. TLR4 screening results 58

Figure 3.5. TLR5 screening results 62

Figure 3.6. TLR2/1 inhibition screening results 65

Figure 3.7. TLR2/6 inhibition screening results 67

Figure 3.8. TLR4 inhibition screening results..... 69

Figure 4.1. Stimulation of CXCL8 production by HEK293-TLR2/6 cells in response to 1402EtL in aqueous or DMSO solution..... 85

Figure 4.2. Inhibition of CXCL8 production by HEK293-TLR2/6 cells in response to 1404EtL in aqueous or DMSO solution..... 86

Figure 4.3. Stimulation of CXCL8 production by HEK293-TLR2/6 cells in response to 1412EtB in aqueous or DMSO solution..... 87

Figure 4.4. Fluorescent lectin stain optimisation 89

Figure 4.5. Inhibition of TLR2/6-mediated CXCL8 production by 1404EtL and its chemically modified variants..... 91

Figure 4.6. Stimulation of TLR2/6-mediated CXCL8 production by 1412EtB and its chemically modified variants..... 93

Figure 4.7 Polyacrylamide gel electrophoresis (PAGE) of crude extracts 95

Figure 4.8. Inhibition of TLR2/6-mediated CXCL8 production by 1404EtL and fractions..... 97

Figure 4.9. Stimulation of TLR2/6-mediated CXCL8 production by 1412EtB and fractions 99

Figure 5.1. Summary of the effects of crude, modified and fractionated extracts on Ki-67 expression..... 111

Figure 5.2. Summary of the effects of crude, modified and fractionated extracts on IgM expression..... 113

Figure 5.3. Summary of the effects of crude, modified and fractionated extracts on IgG1 expression..... 115

Figure 0.1. FACS readouts for Ki-67 in murine splenic B-cells..... 160

Figure 0.2. FACS readouts for IgM in murine splenic B-cells..... 167

Figure 0.3. FACS readouts for IgG1 in murine splenic B-cells..... 174

Figure 0.4. Summary FACS scatter plots for Ki67, IgM and IgG1 in murine splenic B-cells.... 181

List of Tables

Table 1.1. Main classes of pattern recognition receptors 7

Table 1.2. TLRs, their locations and ligands 10

Table 1.3. Overview of known plant-derived TLR modulators. 24

Table 2.1. Plant extracts provided by Dr. Ting 26

Table 2.2. HEK cell lines used in this study. 34

Table 2.3. Treatments used in B cell stimulation experiments 37

Table 3.1. Summary heat map of screening results. 71

Table 4.1. Summary heat map of characterisation results 100

List of Abbreviations

ANOVA	Analysis of variance
AP-1	Activator protein 1
APC	Antigen-presenting cell
APC	Allophycocyanin
AS01	Adjuvant system 1
AS02	Adjuvant system 2
AS03	Adjuvant system 3
AS04	Adjuvant system 4
BCG	Bacillus Calmette-Guérin
BCR	B cell receptor
BSA	Bovine serum albumin
CD14	Cluster of differentiation 14
CD19	Cluster of differentiation 19
CD4	Cluster of differentiation 4
CD40	Cluster of differentiation 40
CD8	Cluster of differentiation 8
CF	Cystic fibrosis
CFSE	Carboxyfluorescein succinimidyl ester
CftF	Crops for the Futre research centre
CLR	C-type lectin receptor
ConA	Concanavalin A
COX	Cyclooxygenase
CpG ODN	Cytosine-guanine-rich oligodeoxynucleotide
CSR	Class switch recombination
CXCL	C-X-C motif ligand
CXCR	C-X-C chemokine receptor
DAMP	Damage-associated molecular pattern
DC	Dendritic cell
DDA	Dioctadecyl ammonium bromide
DMEM	Dulbecco's modified Eagle's medium
DMSO	Dimethyl sulphoxide
DNA	Deoxyribonucleic acid
ds	Double-stranded

EDTA	Ethylenediaminetetraacetic acid
EEM	Ethanolic extract of *Eupatorium makinoi*
EGCG	(–)-epigallocatechin-3-gallate
ELISA	Enzyme-linked immunosorbent assay
ELR	Glutamic acid-leucine-arginine motif
ERK	Extracellular-signal-related kinase
FACS	Fluorescence-activated cell sorting
FCS	Foetal calf serum
FDA	U.S. Food and Drug Administration
FITC	Fluorescein isothiocyanate
Fla-ST	*Salmonella typhimurium* flagellin
FSC	Forward-scattered light
GPI	Glycosylphosphatidylinositol
GSK	GlaxoSmithKline
HCl	Hydrochloric acid
HRP	Horse radish peroxidase
IFN-γ	Interferon-gamma
Ig	Immunoglobulin
IκB	Inhibitor κB
IKK	IκB kinase
IL	Interleukin
iNOS	Inducible nitric oxide synthase
IRAK	IL-1 receptor-associated kinase
IRF	Interferon regulatory factor
ISCOM	Immunostimulatory complex
JAK	Janus kinase
JNK	c-Jun N-terminal kinase
kDa	Kilodalton
LC-MS	Liquid chromatography mass spectrometry
LDH	Lactate dehydrogenase
LM	Lipomannan
LRR	Leucine-rich repeat
LPS	Lipopolysaccharide
LSD	Lysergic acid diethylamine
LTA	Lipoteichoic acid

M2	Alternatively-activated macrophage
MACS	Magnetic-activated cell sorting
MALP-2	Macrophage-activating lipopeptide 2
MAPK	Mitogen-activated protein kinase
MHC	Major histocompatability complex
miRNA	Micro RNA
Mϕ	Macrophage
MPL	Monophosphoryl lipid A
MRSA	Methicillin-resistant *Staphylococcus aureus*
MTT	3-(4,5-dimethylthiazol-2-yl)-2,5-diphenyltetrazolium bromide
MWCO	Molecular weight cut-off
MyD88	Myeloid differentiation factor 88
NF-κB	Nuclear factor kappa B
NK	Natural killer cell
NLR	NOD-like receptor
NO	Nitric oxide
NOD	Nucleotide oligomerisation domain
ODN	Oligodeoxynucleotide
OMP	Outer membrane protein
PAGE	Polyacrylamide gel electrophoresis
Pam2CSK4	S-[2,3-bis(palmitoyloxy)-(2RS)-propyl]-cysteinyl-seryl-lysyl-lysyl-lysyl-lysine
Pam2Cys	S-[2,3-bis(palmitoyloxy)propyl]cysteine
PAMP	Pathogen-associated molecular pattern
PBS	Phosphate-buffered saline
PE	R-phycoerythrin
PEG	Polyethylene glycol
PG	Platycodon grandiflorum polysaccharide
PGG	β-1,2,3,4,6-penta-O-galloyl-D-glucopyranose
PGN	Peptidoglycan
PLM	Phospholipomannan
PRR	Pattern recognition receptor
PSM	PAMP-sensitising molecule
RIG1	Retinoic-acid-inducible gene 1
RLR	RIG1-like receptor
RNA	Ribonucleic acid

RPMI	Roswell Park Memorial Institude medium
RT	Room temperature
SDS-PAGE	Sodium dodecyl sulphate polyacrylamide gel electrophoresis
SEAP	Secreted embryonic alkaline phosphatase
ss	Single-stranded
SSC	Side-scattered light
STAT	Signal transducer and activator of transcription
TBK	Tank-binding kinase
TBS	Tris-buffered saline
Tc	Cytotoxic T cell
Th	Helper T cell
THF	2',5,6',7-tetrahydroxyflavanonol
TIR	Toll/IL-1 receptor
TIRAP	TIR-domain-containing adaptor protein
TLR	Toll-like receptor
TMB	Tetramethylbenzidine
TNF-α	Tumour necrosis factor alpha
TRAF	TNF-receptor-associated factor
Treg	Regulatory T cell
TRIF	TIR-domain-containing adapter-inducing interferon-beta
WT	Wild type

Chapter 1. Introduction

1.1 Overview of mammalian immunity

The mammalian immune system is a complex and highly-evolved network of pattern detectors, signalling pathways and effector mechanisms which protects us from both exogenous insults such as infection and endogenous threats such as cancer. It is often broadly divided into innate and adaptive systems, with the innate arm providing more immediate detection and protection, and the adaptive arm providing protection which is slower to activate but highly specific. There is abundant cross-talk both within and between these systems to maintain a dynamic equilibrium between protective activity and immunopathogenesis. The discovery of new pathways (such as TLR10 signalling; Jiang et al. 2016), receptors (such as HHLA2; Janakiram et al. 2015) and cell phenotypes (such as $CD8^+$ Treg cells; Suzuki et al. 2012) is an ongoing process and our understanding of immunity is constantly improving.

1.1.1 Innate immunity

Innate immunity is important in many aspects of health. As well as forming the first line of defence against pathogens, its functions include pathogen recognition, activation of adaptive immunity and anti-tumour activity. Dysregulation of these functions can lead to pathologies ranging from allergy to lethal sepsis. This array of functions is mediated by a combination of phagocytic antigen-presenting cells (APCs, principally dendritic cells (DC) and macrophages (Mϕ)) and granulocytes (neutrophils, mast cells, basophils and eosinophils) (Murphy 2012).

Upon infection a pathogen will encounter APCs, either in the form of patrolling Mϕ or DC both patrolling and embedded within the epithelial barrier. APCs are equipped with an array of receptors which bind pathogen molecules and cause the pathogen to be phagocytosed by the cell (Mogensen 2009). The pathogen is digested and peptides from it are presented as

antigens on major histocompatibility complex (MHC) class II molecules on the surface of the APC (Springer 1990). Secretion of proinflammatory cytokines is followed by rapid cytokine-mediated chemotaxis of granulocytes to the site of infection. Different pathogens bind and activate distinct sets of immune receptors, eliciting a pathogen-specific cytokine profile which summons appropriate immune effector cells (Huang 2001; Mrabet-Dahbi et al. 2009; Mogensen 2009).

As well as providing host protection against pathogens, the innate immune system also plays an important role in recognition and control of developing tumours (Barth et al., 1991; Zitvogel et al., 2008). As a result of oncomutation the incipient tumour cell's gene expression profile will alter, changing the protein profile of the interior of the cell, in some cases resulting in a mutated protein or abnormal expression of a protein normally expressed at very low levels or only at certain developmental stages (Neville et al., 1975). These changes in protein composition will be exhibited on the tumour cell surface in the form of peptides bound to MHC class I molecules. This abnormal antigenic profile is recognised by APCs which activate both innate and adaptive immune effector cells such as natural killer (NK) and T cytotoxic (Tc) cells. These bring about the destruction of the cancerous cells by several means, including tumour necrosis alpha (TNF-α) secretion, perforin-mediated cell lysis and the Fas apoptotic pathway (Grivennikov et al. 2010). IFN-γ produced by NK cells summons additional Mϕ and upregulates MHC class I expression on tumour cells, further increasing their antigenicity. This system of antigen monitoring and cytotoxic enforcement is known as immunosurveillance. However, it only targets tumour cells with antigenic mutations, leading to a process termed immunoediting whereby non-antigenic cancers can continue to develop, a state known as immunotolerance (Murphy 2012). Conversely, the subset of alternatively activated Mϕ known as M2 have been found to have a pathological effect, actually contributing to tumour growth and spread. M2 secrete growth factors that stimulate both

tumour cell proliferation and angiogenesis (Biswas et al. 2006). They also degrade the extracellular matrix, facilitating tumour dissemination (Quail & Joyce 2013).

1.1.2 Adaptive immunity

1.1.2.1 T lymphocytes

Once antigens from an internalised or degraded pathogen are presented on the APC's MHC class II molecules the APC matures and migrates to the lymph nodes where activation of adaptive immunity begins. The MHC-antigen complex (along with co-stimulatory DC surface molecules such as CD80, CD86 and CD40 (Yoshimura et al. 2001)) is detected by and activates naïve CD4+ T helper lymphocytes (Th0). These then proceed to proliferate and differentiate, depending on the cytokine environment, into effector T helper cells of the Th1, Th2 or Th17 phenotypes, which set in motion the appropriate immune response via further cytokine secretion. A Th1-type response protects the host from intracellular pathogens and is mediated mainly by Mϕ, $CD8^+$ cytotoxic Tc and IgG^+ B cells. Interferon gamma (IFN-γ) secreted by Th1 cells stimulates phagocytosis by Mϕ and induces production of nitric oxide free radicals to kill intracellular pathogens, while Tc cells detect and destroy infected host cells by lysis using either perforins or the Fas apoptotic pathway. Activation of the Fas receptor (also known as Apo-1 or CD95) leads to the activation of a series of caspases which mediate cell death (Waring & Müllbacher 1999). A Th2-type response is raised against infection by multicellular parasites such as helminths. IL-5 causes eosinophils to degranulate and attack the parasite with an array of toxic compounds, and IL-4 and immunoglobulins (Ig) of the IgE class stimulate the release of chemicals such as histamine and serotonin to aid expulsion of the parasite. The Th17-type response primarily combats extracellular bacterial and fungal infections. Tumour necrosis factor alpha (TNF-α) recruits and activates neutrophils, and IL-6 activates components of the complement system to directly attack the

pathogens. In addition to these three distinct helper subsets, some activated T lymphocytes differentiate into memory cells which persist following clearance of infection. These are quickly reactivated upon re-exposure to the original antigen and allow the adaptive immune system to provide lasting protection against reinfection. T lymphocytes also function to activate B lymphocytes, the major cell type involved in antibody-mediated immunity.

1.1.2.2 B lymphocytes

The primary role of B lymphocytes is the production and secretion of antibodies, also known as immunoglobulins. Upon activation by a combination of antigen and Th cells, or by a T-independent antigen alone, immature B cells proliferate and mature into antibody-producing plasma cells and long-lasting memory cells. During the maturation process the cells undergo somatic hypermutation of the variable regions of antibody genes to increase the variety of Ig produced and thus the probability of an Ig clone with improved antigen-specific affinity being found. B cell clones are selected for antigen affinity through competition for resources in the germinal centres, mediated by antigen-presenting follicular DC. In addition to this selection process for antigen affinity, B cells are capable of producing different classes of Ig by varying the non-mutating portion of the molecule. This process, known as class switch recombination (CSR), allows differentiation of antibody functions and localisations appropriate to the type of antigen detected.

1.1.2.3 Ig classes

IgM is produced early during the course of infection; its pentameric structure prevents it from diffusing from the blood into extravascular sites but increases the pentamer's avidity and thus its complement activation efficacy. IgG antibodies (divided into subclasses IgG1, IgG2, IgG3 and IgG4 in humans) are monomers found both in the blood and extracellular fluid. They fulfil a variety of roles including neutralisation of pathogens and toxins, opsonisation of pathogens for phagocytosis and activation of the complement system. IgG is

the dominant isotype in most mammalian vaccine responses (Siegrist 2008). IgA is produced in both monomeric and dimeric forms. The monomeric form is found in the blood and extracellular spaces, fulfilling opsonisation and complement activation functions. The dimeric form is secreted into the lumen of the gut where it neutralises toxins and pathogens before they can cross the epithelial layer. IgE is predominantly bound to the surface of mast cells, activated in response to parasite infection. In addition to Ig production, B lymphocytes are also capable of acting as APCs and either inducing tolerance or activating immune responses (Rodríguez-Pinto 2005). By endocytosing antigens bound to the B cell receptor (BCR) and presenting them on MHC class II molecules, B lymphocytes can play an important role in the generation of immunity in response to vaccines (Hon et al. 2005).

Their antibody production and secondary antigen presentation functions make B cells the principal effectors of the response to vaccination. However, the highly purified antigens in modern vaccines are often insufficiently immunogenic to generate a strong enough immune response. Adjuvants are added to enhance the immunogenicity of vaccines by targeting the innate immune system via a variety of mechanisms. Aluminium salt-based adjuvants (alum) activate innate immune receptors in the inflammasome (Li et al. 2008); emulsion-based adjuvants such as Freund's adjuvant slow down the release of antigen at the delivery site, prolonging the activation of APCs (known as a *depot effect*) (Awate et al. 2013); liposomal adjuvants provide both depot effect and, depending on the composition of the liposome, targeted immunogenicity (Henriksen-Lacey et al. 2010). For example, the surfactant dimethyl dioctadecyl ammonium bromide (DDA) stimulates a Th1-type response (Holten-Andersen et al. 2004). Vaccination has yielded some immensely important successes such as the eradication of smallpox and the near-eradication of polio, and is almost certain to be crucial to solving some of the medical problems of the present and future, such as novel influenza strains, HIV and many others.

1.1.2.4 Importance of innate immunity to adaptive immunity

Complex and effective as adaptive immunity may be, to function properly it requires direction from the innate immune system. This is illustrated in a study by Pannicke et al. (2013) which found that patients with a homozygous mutation in the gene encoding IKK2, a key part of the NF-κB pathway in innate immune signalling, had strongly impaired immunity in both innate and adaptive arms. The specificity and efficacy of innate immunity are key to the activation and direction of both innate and adaptive effector mechanisms in response to both infectious and endogenous threats. Conversely, the innate immune system can exhibit aberrant behaviour which leads to pathological conditions. The activation and regulation of innate immune activation is governed by cellular receptors detailed in the following sections.

1.2 Pattern Recognition Receptors

Pattern recognition receptors (PRRs) are highly conserved transmembrane proteins which play a crucial role in pathogen detection and categorisation. PRRs are expressed constitutively on certain cell types, mainly but not exclusively immune cells (especially APCs), for example toll-like receptor (TLR) 2, 3 and 4 are also expressed in intestinal epithelial cells (Cario et al., 2000) and TLR3 is expressed on human neurons (Lafon et al. 2006). They are germline-encoded and non-clonal, so their ligand specificity is fixed. PRRs bind a variety of self and non-self ligands, termed pathogen-associated molecular patterns (PAMPs) and damage-associated molecular patterns (DAMPs). PAMPs are molecular patterns conserved within a group of pathogens, often crucial to their survival and/or pathogenesis. PRR-binding PAMPs are a diverse group including proteins, carbohydrates, nucleic acids, lipoproteins, glycolipids and many more. DAMPs are endogenous molecular motifs such as heat-shock proteins or degraded components of the extracellular matrix, which tend to be only present in large amounts in damaged tissue (Okamura et al. 2001; Wallin et al. 2002).

There are four main groups of PRRs (Table 1.1): Toll-like receptors (TLR), NOD-like receptors (NLR), C-type lectin receptors (CLR) and RIG-1-like receptors (RLR). This study focuses on the TLRs.

Table 1.1. Main classes of pattern recognition receptors

PRR	Cell types and localisation	Known ligands
TLR	Plasma membrane and endosome of various cell types (distributions vary) inc. DC, Mϕ, B & T lymphocytes, mast cells and epithelial cells. See Table 1.2	Wide range of PAMP and DAMP ligands inc. cell wall components, nucleic acids and heat shock proteins. See Table 1.2
NLR	Cytosol of most cell types, primarily DC and Mϕ	Bacterial cell wall components, toxins and DAMPs
CLR	Plasma membrane of most cell types (many CLRs also have an adhesion function), primarily DC and Mϕ	Carbohydrates and carbohydrate-containing molecules
RLR	Cytosol, primarily DC, Mϕ and fibroblasts	Viral double-stranded RNA (dsRNA)

1.2.1 TLRs

TLRs are so called because of their similarity to the Toll gene first discovered in *Drosophila melanogaster*. Initially identified as critical in the development of embryonic dorsoventral polarity (Anderson et al., 1985), it was later found to play a crucial role in the fly's antifungal immune response (Lemaitre et al., 1996). A Toll-like protein in humans (now designated TLR4) was also found to activate the innate immune response to bacterial lipopolysaccharide (LPS; Medzhitov et al., 1997), and since then ten human TLRs have so far been characterised (Table 1.2), along with others present in other mammals. Humans do possess a TLR11 gene, however nonsense mutations have introduced stop codons and no functional protein has been detected (Lauw et al., 2005). TLRs are type 1 transmembrane proteins with an intracellular Toll-interleukin-1-receptor homology (TIR) domain and an extracellular domain containing between 19 and 25 leucine-rich repeats (LRR), connected by a single transmembrane helix (Botos et al. 2011). It is these LRR which give the extracellular domain

its characteristic solenoid structure due to the formation of hydrogen-bonded β-sheets on the concave side and less compact α-helices on the convex side (Figure 1.1.A).

TLRs exist mostly as homodimers, with the exception of TLR1, 6 and 10 which instead heterodimerise with TLR2 (Hasan et al. 2005). The TLR2/1 and 2/6 heterodimers enhance the ligand specificity of TLR2, whereas TLR10 appears to act as an anti-inflammatory inhibitor of other TLR signalling, primarily in B cells (Hornung et al. 2002; Oosting et al. 2014; Jiang et al. 2016). When TLRs dimerise, the C-terminal regions of their extracellular domains converge, while the N-terminal regions diverge (Gao & Li 2017), resulting in a shape which somewhat resembles the letter "M" (Figure 1.1.B).

PAMP binding sites are formed by insertions in the extracellular LRR domain (Bell et al. 2003). The location and mechanism of ligand binding vary with receptor and ligand structure (Jin & Lee 2008). For example, TLR2/1 recognises triacylated lipopeptides by binding the ligand's lipid chains in hydrophobic channels at the central/c-terminal domains of the convex face of its extracellular regions. Two lipid chains are bound to TLR2, and the other to TLR1 (Jin et al. 2007). TLR2/6 binds diacylated lipopeptides because in TLR6 the hydrophobic channel is truncated, preventing binding of a third lipid chain (Kang et al. 2009). On TLR3, the hydrophilic residues required to bind dsRNA are found at both the N-terminal and C-terminal domains of the lateral face of the extracellular region, meaning that a ligand of sufficient length (40-50 base pairs) can bind up to four times on a TLR3 dimer (Liu et al. 2008). TLR4 enlists co-receptors such as CD14 and MD2 to assist in binding ligands such as LPS. CD14 helps transfer LPS to the TLR4-MD2 complex, and MD2 forms a β-cup with a hydrophobic interior and a positively-charged exterior, well-suited for binding negatively charged amphipathic molecules such as LPS to the receptor (Kim et al. 2007). These examples serve to highlight the diversity of TLR ligand binding mechanisms.

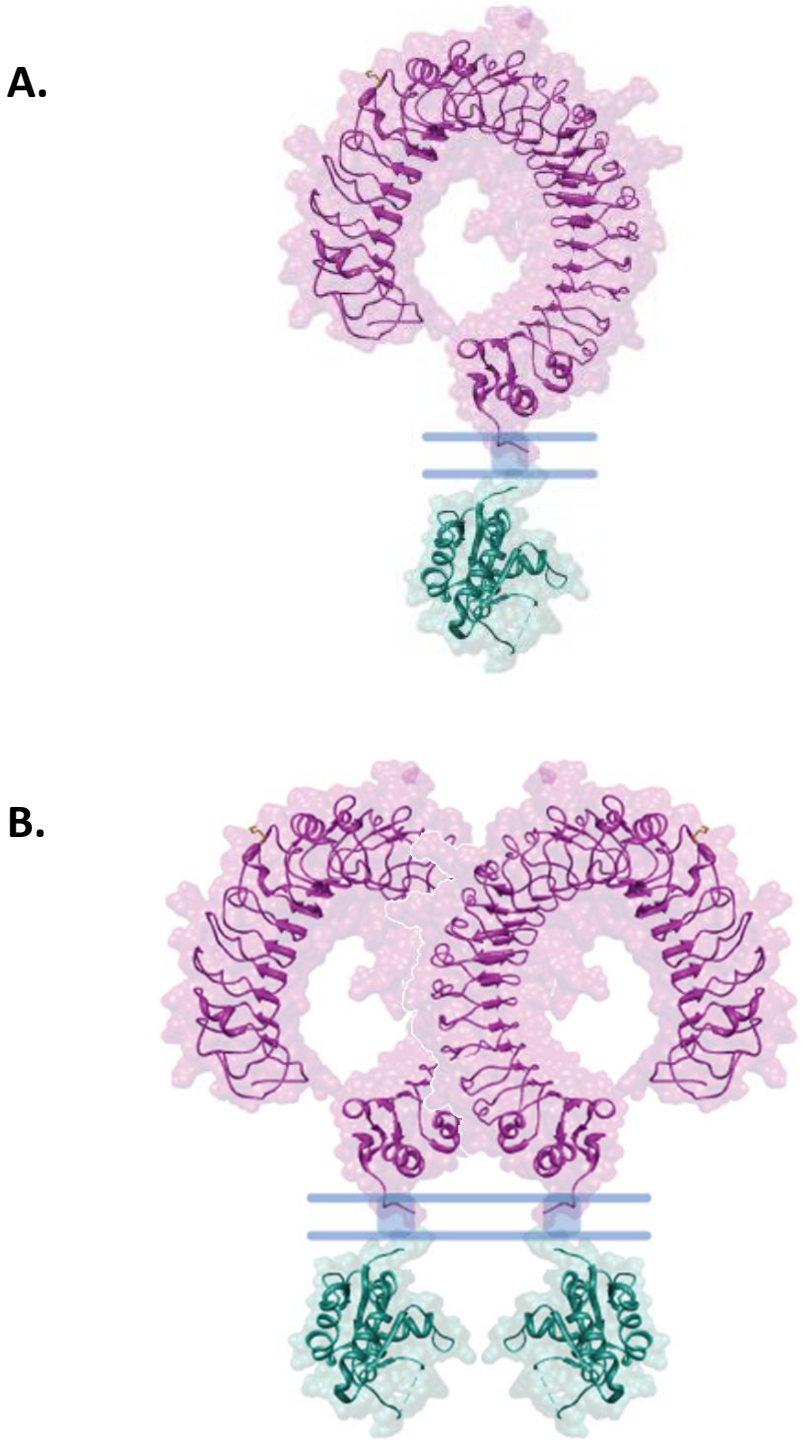


Figure 1.1 Generic TLR tertiary structure. A: generic TLR monomer; B: generic TLR dimer. The turquoise region is the intracellular C-terminal TIR domain, the blue region shows the location of the transmembrane helix and the purple region is the extracellular N-terminal LRR-containing domain. Adapted from Berger et al. (2015).

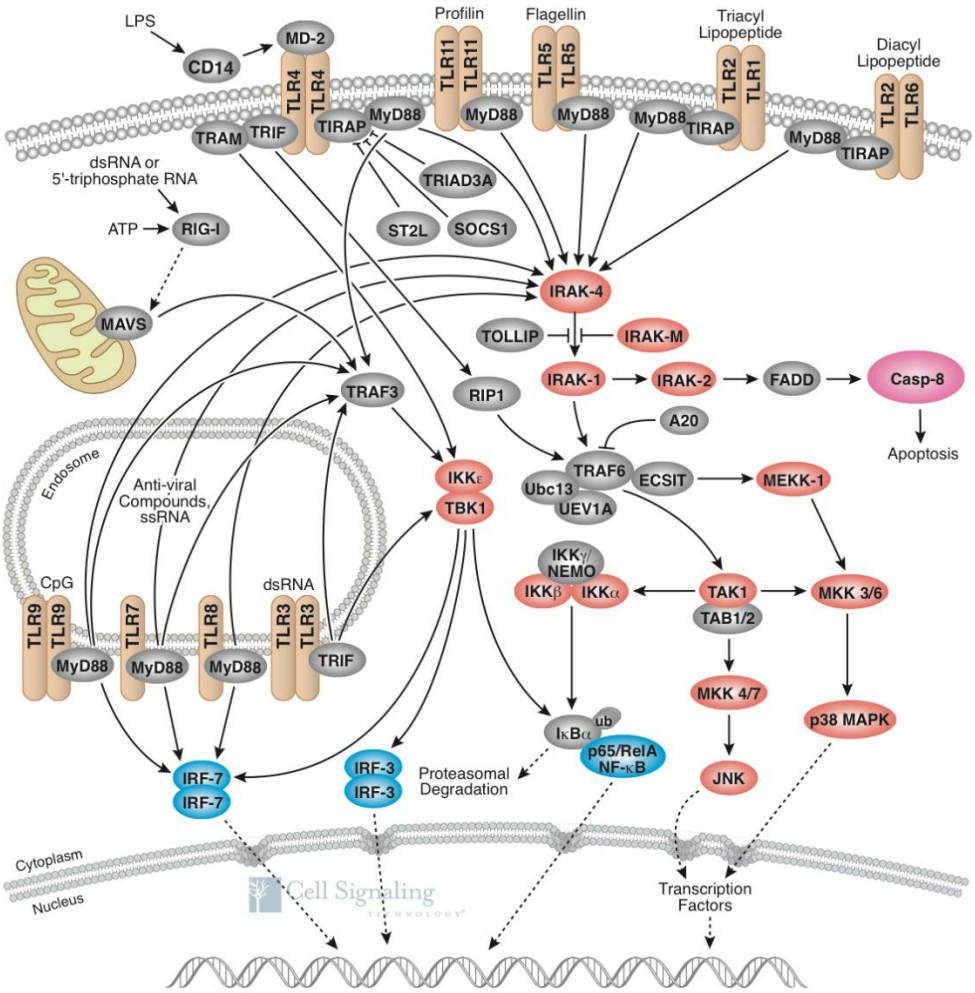
Table 1.2. TLRs, their locations and ligands.

TLR	Localisation	Cell types	Known ligands (non-synthetic)	Ligand origins	Response
TLR2	Plasma membrane	DC, Mϕ, Mo, MC	Glycolipids	Bacteria	Inflammatory and Th2-inducing cytokines
			Lipoproteins	Bacteria	
			Lipoteichoic acid	Gram-positive bacteria	
			Peptidoglycan	Gram-positive bacteria	
			Zymosan	Fungi	
			Heat shock proteins	Host cells	
			High mobility group proteins	Host cells	
			Proteoglycans	Host cells	
TLR2+1	Plasma membrane	DC, Mϕ, Mo, B	Triacyl lipopeptides	Gram-negative bacteria	Inflammatory cytokines
TLR2+6	Plasma membrane	Mϕ, Mo, MC, B	Diacyl lipopeptides	Gram-positive bacteria	Inflammatory cytokines
TLR2+10	Plasma membrane	DC, B	Unknown	Unknown	Inhibition of TLR signalling
TLR3	Endosome	DC, B, T, NK, neuron	dsRNA	Viruses	Type 1 IFN and inflammatory cytokines
TLR4	Plasma membrane and endosome	DC, Mϕ, Mo, MC, IE	LPS	Gram-negative bacteria	Type 1 IFN and inflammatory cytokines
			Heat shock proteins	Host cells	
			High mobility group proteins	Host cells	
			Proteoglycans	Host cells	
			Fibronectin	Host cells	
			Tenascin-C	Host cells	
TLR5	Plasma membrane	DC, Mϕ, Mo, IE	Flagellin	Bacteria	Inflammatory cytokines
TLR7	Endosome	DC, Mϕ, Mo, B	ssRNA	Viruses	Type 1 IFN and inflammatory cytokines
TLR8	Endosome	DC, Mϕ, Mo, MC	ssRNA	Viruses	Type 1 IFN and inflammatory cytokines
TLR9	Endosome	DC, Mϕ, Mo, B	Unmethylated CpG DNA	Bacteria and viruses	Type 1 IFN and inflammatory cytokines
			Chromatin-IgG complex	Host cells	

Summary of human TLR localisation, ligands and resulting immune responses. DC: dendritic cell, Mϕ: macrophage, Mo: monocyte, MC: mast cell, B: B lymphocyte, T: T lymphocyte, NK: natural killer cell, IE: intestinal epithelium. Adapted from Waltenbaugh et al. (2008).

1.2.1.1 TLR signalling

Upon binding of a ligand to its respective TLR, intracellular signalling pathways are set in motion resulting in activation of various transcription factors and release of a range of cytokines and costimulatory molecules (Kawai & Akira 2010). The signalling pathways and effector molecules vary between TLRs and cell types (with TLR4 signalling also varying with intracellular localisation), but a common feature to all is activation of the transcription factor NF-κB (Figure 1.2). With the exception of TLR3 and intracellular TLR4, all human TLR signal pathways are dependent upon the adaptor molecule myeloid differentiation factor 88 (MyD88), which interacts with TLRs via its own C-terminal TIR domain and recruits IL-1 receptor associated kinases (IRAK-4 and IRAK-1) via the N-terminal death domain common to all three molecules. The complex is completed by the recruitment of TNF receptor-associated factor 6 (TRAF6). IRAK-1 is phosphorylated by IRAK-4 and, together with TRAF6, dissociates from the TLR. TRAF6 then forms a new complex with TAK1, TAB1, TAB2, Ubc13 and Uev1A, resulting in the activation of TAK1, which phosphorylates the IκB kinase (IKK) complex and mitogen-activated protein kinases (MAPK). The activated IKK complex degrades the NF-κB inhibitor IκB, while MAP kinases such as c-Jun N-terminal kinase (JNK) activate transcription factors such as AP-1 and interferon regulatory factor (IRF) 5. Thereafter the transcription of pro-inflammatory cytokine genes occurs, resulting in an inflammatory immune response.



Key:

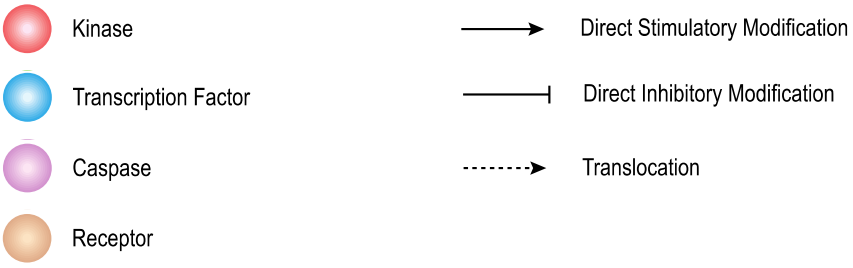


Figure 1.2. Mammalian TLR signalling pathways. Binding of ligand to TLRs leads both directly and indirectly to the activation of various transcription and regulatory factors. The TLR11 pathway included is found in mice but not humans. Adapted from (Mandrekar 2012)

A variation on the MyD88 pathway is found at the endosomes on which the intracellular TLRs reside. An additional signalling protein, TRAF3, is localised exclusively to this organelle and is not found on the plasma membrane (Barton & Kagan 2009). It interacts with MyD88 at activated TLR7, 8 or 9 to trigger an alternative pathway whereby IκB is degraded not by the

IKK complex but by a complex of IKKε and TANK-binding kinase 1 (TBK1). This does not result in the same activation profile of transcription factors, activating IRF3 and IRF7 and resulting in production of type 1 interferon (IFN-α or -β). The confinement of immobile TRAF3 to the endosome allows MyD88 to activate two signalling pathways, distinct in both outcome and cellular localisation. This compartmentalisation of MyD88-dependent TLR signalling is due to the TLRs found at each location and their respective ligands. Plasma membrane TLR2/1, 2/6, 4 and 5 detect extracellular PAMPs such as LPS and flagellin which are indicative of bacterial infection and necessitate an inflammatory response. The nucleic acid ligands for TLR3 (double-stranded RNA (dsRNA)), 7 and 8 (single-stranded RNA (ssRNA)) and 9 (unmethylated cytosine-guanine (CpG) DNA) are found within the host cell and result in a more IFN-biased response as these receptors are associated with detection of viral infection.

One peculiar characteristic of TLR4 is that following ligand binding and MyD88-dependent signalling, it translocates from the plasma membrane to the endosome and triggers an entirely separate signalling pathway, known as the MyD88-independent, or TRIF-dependent, pathway (Barton & Kagan 2009). TIR-domain-containing adapter-inducing interferon-β (TRIF) is the adaptor molecule recruited to the cytoplasmic portion of the TLR in this case. TRIF activates TRAF3 (a component common to both endosomal TLR signal transduction pathways), and from this point onwards the signal progresses similarly to the endosomal version of the MyD88-dependent pathway, resulting in a mixed inflammatory and IFN response. This pathway is activated by both TLR3 and intracellular TLR4.

TLR signalling is regulated mainly by ubiquitination and deubiquitination of signalling components such as TRAF6 and the IKK complex (Boone et al., 2004; Lowe et al., 2006). Splice variation also contributes to TLR signal regulation. A splice variant of MyD88 known as MyD88s prevents recruitment of IRAK-4 to the TLR, thus inhibiting NF-κB activation (Janssens et al., 2003). Interestingly, the inhibitory effect is limited to NF-κB, with AP-1 activity

remaining unaffected. This indicates that the pathways to NF-κB and AP-1 activation are distinct post-MyD88, and that splice variation plays a role in the tuning of TLR responses.

The immobilisation and segregation of TRAF3 is key to retaining the distinction between the inflammatory and IFN responses, transferring a moving receptor to an immobile adaptor (instead of vice versa). If, like TLR4, a receptor is to activate both, it must translocate between the two separate sites.

1.2.1.2 TLR dysfunction and pathology

Dynamic homeostatic regulation of the immune system is crucial for mounting appropriate defences while avoiding damage to the host. Dysregulation of innate immunity can lead to a wide range of pathologies, including immunodeficiency (Pannicke et al. 2013), allergy (Dekruyff et al. 2014), neurodegeneration (Heneka et al. 2014) and autoimmune conditions such as Crohn's (Muzes et al. 2013).

Deficiency in TLRs or their adapters and downstream signalling molecules has been shown to result in ineffective or uncoordinated activation of immunity. For example, Zhang et al. (2007) found that children carrying a dominant-negative TLR3 allele are more prone to develop herpes simplex encephalitis from infection by herpes simplex virus 1. The fact that it is expressed in epithelial cells and neurons of the central nervous system lends weight to the idea that the evolution and maintenance of TLR3 is linked to such neurotropic viruses. When infected experimentally with intracellular protozoan parasite *Toxoplasma gondii*, TLR9-deficient ($TLR9^{-/-}$) mice did not mount the Th1 response required to clear the parasite (Minns et al., 2006). As a consequence, they exhibited significantly elevated parasite burdens compared to wild type (WT) mice, but did not suffer the acute ileitis and subsequent mortality of the WT individuals either. Deficiencies in signalling molecules can leave the host vulnerable to infection too, as evidenced by the susceptibility of IRAK-4 and MyD88 deficient patients to recurrent invasive bacterial infection (Picard et al., 2011). However, immunity is

rarely that simple. Mice homozygous for null TLR4 were shown to be highly susceptible to infection by Gram-negative bacteria but resistant to LPS-induced sepsis (Poltorak, 1998). The absence of TLR4 activity hindered mobilisation of an effective immune response to the bacterial infection but also prevented the over-stimulation of inflammatory pathways and subsequent septic shock. This is a demonstration of the principle that the outcome of infection is often the product of a trade-off between resistance and tolerance, balancing pathogen clearance against the risk of immunopathology (Medzhitov et al. 2012; Muzes et al. 2013; Chua et al. 2013).

Interplay between the effects of different PRRs can complicate matters further. When challenged by *Borrelia hermsii* infection, $TLR2^{-/-}$ mice suffered both impaired antibody response and septic shock. Mϕ lacking both TLR2 and NOD2 (an intracellular NLR) exhibited further impairment, with significantly reduced cytokine output. However, $TLR2^{-/-}$ $NOD2^{-/-}$ mice had lower mortality than $TLR2^{-/-}$ individuals (Dickinson et al., 2010). This indicates that TLR2 is important in defence against *B. hermsii*, but in its absence other stimulated PRRs can cause fatally dysregulated inflammation, possibly due to the absence of a TLR2-mediated Th2 response allowing the Th1 response to exaggerate into lethal sepsis.

Excessive, repeated or persistent TLR stimulation can result in pathological responses which have been linked to asthma, atherosclerosis, autoimmunity and sepsis. In autopsied human atherosclerotic lesions and murine models elevated TLR4 expression was detected relative to non-atherosclerotic lesions and normal aortic tissue, with TLR4 co-localised with Mϕ. *In vitro* expression of TLR4 by human Mϕ was upregulated by oxidised low-density lipoprotein (oxLDL) (Xu et al., 2001). Another study observed TLR4-mediated differentiation of Mϕ into foam cells (the cells responsible for atherosclerotic lesions) which has inhibited by pre-treatment with TLR4 blocking antibody and exacerbated by co-stimulation with a TLR4 agonist (LPS) (Howell et al., 2011). Necrotic synovial fluid cells have been shown to induce TLR3-mediated activation of synovial fibroblasts, the major cell type associated with

rheumatoid arthritis (Brentano et al., 2005; Huber et al., 2006). Lupus-prone mice, when given TLR9-inhibitory oligodeoxynucleotides (ODNs), displayed both reduced both morbidity and mortality (Lenert, 2006).

TLR activation can be pathological even in an infectious situation. $TLR9^{-/-}$ mice experimentally given polymicrobial peritonitis by caecal ligation and puncture showed drastically reduced mortality compared with WT individuals. DCs transferred from $TLR9^{-/-}$ mice conferred protection upon WT recipients, as did treatment with TLR9-inhibitory ODN (Plitas et al., 2008). These findings suggest that, although beneficial in less heterogeneous infections, TLR9 signalling is pathological in polymicrobial infection. This may be because the widespread and wholesale TLR stimulation likely to occur from a diverse range of pathogens pushes the inflammatory response past the point of protection and into exaggerated pathological territory.

1.3 Clinical TLR modulation

Given their crucial role in coordinating immunity, TLRs are a promising target for therapeutic immune modulation.

1.3.1 TLR stimulation

TLR agonists are under investigation for a range of applications, and some are already in clinical use, particularly as vaccine adjuvants (Toussi & Massari 2014; Dowling & Mansell 2016). The TLR4 ligand monophosphoryl lipid A (MPL) is a derivative of the active lipid A fraction of LPS, which retains TLR4-stimulatory activity but is 0.1% as toxic (Qureshi et al. 1982). It is used in a range of adjuvant formulations, including GlaxoSmithKline (GSK)'s adjuvant system 1 (AS01) in conjunction with saponins and liposomes, adjuvant system 2 (AS02) in an oil-water emulsion and with alum in adjuvant system 4 (AS04; (Garçon et al.

2007). Gram-negative bacterial outer membrane proteins (OMP) stimulate TLR2 (Latz et al. 2004) and are used as a component of immunostimulatory complexes (ISCOM; Kersten et al. 1988) and conjugate vaccines (Latz et al. 2004; Holst et al. 2009).

Vaccine adjuvancy is not the only application of TLR agonists under investigation. For example, TLR stimulation by DAMPs released by dying cells activates anti-tumour immunity (Kroemer et al. 2013), making TLRs a potential target for anti-cancer therapeutics. SMP105 (Dainippon Sumitomo Pharma) is an emulsion-based preparation of *Mycobacterium bovis* BCG which activates TLR2 and has been shown in pre-clinical trials to stimulate anti-cancer $CD8^+$ T cells and IFN production, reducing tumour growth in mice (Murata 2008; Miyauchi et al. 2012). The active component was identified as arabino-mycolate glycolipids (Miyauchi 2011). Participants are currently being recruited for phase II clinical trials into the use of flagellin-derived TLR5 ligand CBLB502 (also known as Entolimod) in immunotherapy for colorectal cancer (Dowling & Mansell 2016). The TLR7 ligand Imiquimod is licensed for treatment of superficial non-melanoma skin cancers (Scheel et al. 2006; Iribarren et al. 2015), although there is ongoing uncertainty regarding the degree to which the therapeutic response is TLR7-dependent (Walter et al. 2013). Due to the complex role of immunity in tumour progression, DAMPs can sometimes elicit a response which promotes tumour growth and metastasis (Krysko et al. 2013), substantially complicating the development of cancer immunotherapies. Another clinical use of Entolimod under investigation is its ability to mitigate kidney damage caused by ischemia. Fukuzawa et al. (2011) found that treatment of an ischemic kidney within 30 minutes of blood supply restriction protected the organ from damage by reducing the production of neutrophil-attracting chemokines CXCL1 and CXCL2.

There are a wide variety of potential clinical applications of TLR agonists in use and under investigation, and more are likely to be found as our understanding of the multi-faceted roles of TLRs deepens.

1.3.2 TLR inhibition

A range of TLR antagonists are also being investigated for therapeutic use such as VIPER, a peptide-based TLR4 inhibitor derived from vaccinia virus protein A46. VIPER inhibits TLR4 signalling by blocking interactions between the TIR domains of the TLR and signalling molecules MyD88/TRIF (Lysakova-Devine et al. 2010). It ameliorated hypertension and inflammatory symptoms in rats predisposed to hypertension (Dange et al. 2015). AV411 (known as Ibudilast), another TLR4 inhibitor, is in phase II clinical trials for the treatment of progressive multiple sclerosis (MS; Fox et al. 2016) and has completed a phase I trial for reducing glial-cell-mediated methamphetamine-related neuroinflammation and neurodegradation (Worley et al. 2016). Ibudilast is a phosphodiesterase inhibitor as well as a TLR4 antagonist, and it is not yet entirely clear how these two functions are related (Kay et al. 2014). Like the TLR4 agonist MPL, E5564 (known as Eritoran) is a derivative of the lipid A component of LPS. The functional difference is that Eritoran binds but does not activate the TLR4-MD2 complex (Kim et al. 2007). It was found to inhibit production of LPS-induced TNFα in human monocytes (Czeslick et al. 2006), and reached phase III trials for treatment of sepsis but failed to meet the desired clinical endpoint targets and was abandoned.

A monoclonal anti-TLR2 antibody known as OPN-305 is under investigation by Opsona Therapeutics for the prevention of TLR2-mediated damage to kidney tissue following ischemia or transplantation (Leemans et al. 2005). Phase I clinical trials have been completed and OPN-305 is currently undergoing phase II trials (Reilly et al. 2013; Dowling & Mansell 2016). This is a similar clinical application to one proposed for the TLR5 agonist Entolimod (mentioned in the previous section), highlighting the multifactorial balancing act which is a product of the complex signalling and cross-talk of the innate immune system. Whether stimulatory or inhibitory, research into clinical applications of TLR modulators brings the challenge of implementation as well as the prospect of powerful therapeutic benefits.

1.4 Plant-derived medicine

Before the advent of scientific advances such as synthetic chemistry, humans derived medicines from natural sources such as plant, mineral and animal products (De Pasquale 1984). Even with the modern synthetic capabilities we have today, more than 60% of the 1,562 new drugs approved by the FDA between 1981 and 2014 were naturally-derived or synthetic mimics thereof (Newman & Cragg 2016). Many plant-derived compounds, including globally important drugs such as morphine (from *Papaver somniferum*) and Artemisinin (from *Artemisia annua*, and for which Tu YouYou was awarded half of the 2015 Nobel Prize for Physiology or Medicine; Tu 2011; Van Voorhis et al. 2015) were derived from plants and others are undergoing clinical trials (Saklani & Kutty 2008). There is still a large pool of plant species yet to be investigated, with a 2005 review by Soejarto et al. finding that only 15-20% of terrestrial plants had been evaluated for pharmaceutical potential. There are even companies such as Phytotitre (Caithness Biotechnologies) which specialise in providing libraries of plant extracts for pharmacological screening, facilitating the process of plant-derived drug discovery.

The role of traditional medicine in providing candidates for pharmacological investigation is a subject of some controversy, as these remedies inherently lack rigorous scientific data to support their claims. On the other hand, however flawed the theoretical basis behind many traditional remedies might be, they are the product of hundreds, sometimes thousands, of years of trial and observation. This does not mean that they are necessarily effective, but that the lack of scientific data should act as an incentive for further investigation, rather than an obstacle. Saslis-Lagoudakis et al. (2012) analysed the phylogenies of traditional medicinal plants and found that related plants in different regions were often used in similar enthomedicinal context, and also clustered with species from which modern pharmaceutical

drugs had been derived. This demonstrates the utility of traditional medicine in bioprospecting for novel pharmaceutical compounds.

1.4.1 Plant-derived immunomodulators

Of the numerous applications of plant-derived medicines, immunomodulators and anti-inflammatories are well represented. Immunostimulatory complex (ISCOM) vaccine adjuvants are primarily based upon saponins such as QS21 derived from *Quillaja saponaria*, a tree native to central Chile (Morein et al. 1995). ISCOMs generate a range of stimulatory responses, including activating and upregulating MHC class II expression on APCs (Behboudi et al. 1996; Bergstrom-Mollaoglu et al. 1992) and activation of $CD4^+$ and $CD8^+$ T cell responses (Maloy et al. 1995; Takahashi et al. 1990). In addition, colchicine, derived from *Colchicum autumnale*, remains the gold standard drug for treatment of the inherited systemic autoimmune condition known as familial Mediterranean fever (Zadeh et al. 2011).

A number of plant-derived immunomodulators are currently undergoing clinical trials (reviewed in Jantan et al. 2015). For example, an extract of the herb *Andrographis paniculata* is currently undergoing phase II clinical trials for the treatment of ulcerative colitis (Balzola et al. 2013) and has completed a clinical pilot study for the treatment of fatigue symptoms caused by multiple sclerosis (Bertoglio et al. 2016).

Pre-clinical *in vitro* studies continue in the search for plant-based potential pharmaceuticals. Arabinogalactan fractions from *Juniperus scopolourm* were shown to induce Mϕ proliferation and activity in vitro (Schepetkin et al., 2005) and arabinogalactan-heavy glycoproteins from *Baptista tinctorum* and *Echinacea pallida* stimulated cytokine production by LPS-insensitive mouse splenocytes and Mϕ as well as splenocyte proliferation (Classen et al., 2006). Interestingly, *Echinacea purpurea* extract showed little to no effect in this study, despite being the most commercially utilised species of *Echinacea*.

1.4.1.1 Plant-derived TLR agonists

Due to their crucial role in activation and regulation of immunity, as well as our increasing understanding of TLR signalling, there is substantial interest in plant-derived TLR modulators (Chahal et al. 2013). Many candidates under investigation are TLR agonists, for example a polysaccharide derived from *Dendrobium huoshanense* was found to activate TLR4 in RAW264.7 and primary peritoneal murine Mϕ, upregulating transcription factors such as ERK, JNK Akt and p38 (Xie et al. 2016). In some cases, TLR stimulation can result in suppression of immunopathology due to signalling interactions between different immune pathways. For example, levan is a fructan product of the fermentation of the soya bean *Glycine max* which, via TLR4-dependent IL-12-mediated Th1 activation, suppresses Th2 activity and reduces serum IgE in ovalbumin-immunised mice (Xu et al. 2006). This approach, if successfully developed, could lead to a novel drug for treatment of Th2-mediated immunopathologies such as allergic conditions.

Recent debate over the absorption (or not) of dietary-derived microRNAs (miRNA) from the mammalian digestive system (Zhang et al. 2012; Zhou et al. 2014; Witwer & Hirschi 2014; Yang et al. 2015; Yarmarkovich & Hirschi 2015) has ignited interest into plant miRNAs as potential immunomodulators, particularly targeting the RNA-sensing TLRs 3, 7 and 8. Evidence from *in vitro* studies by Cavalieri et al. (2016) suggests that plant miRNAs inhibit DC-mediated T cell proliferation via TLR3 in a manner independent of miRNA sequence or species of origin, but dependent upon plant-characteristic 3' -OH-methylation. *In vivo*, plant miRNAs were able to reduce spinal cord immune cell infiltration and demyelination associated with experimental autoimmune encephalomyelitis. These results are promising and could form the basis of a novel branch of research into therapeutic TLR modulation.

1.4.1.2 Plant-derived TLR antagonists

TLR antagonists typically function at three stages of TLR activity: degradation or inactivation of ligands, inhibition of receptor binding or dimerisation and disruption of downstream signalling. With regard to ligand neutralisation, polyphenols 2',5,6',7-tetrahydroxyflavanonol (THF) from *Scutellaria baicalensis* and β-1,2,3,4,6-penta-O-galloyl-D-glucopyranose (PGG) from *Radix paeoniae rubra* have both been shown to neutralise LPS both in vitro and in vivo, protecting mice against LPS-induced sepsis (Fu et al. 2008; Genfa et al. 2005).

At a receptor level, 6-shogaol, a phenol component of ginger *Zingiberis rhizoma*, was found to inhibit TLR4 dimerisation in murine Mϕ culture (Ahn et al. 2009). Similar results have been reported with isoliquiritigenin from liquorice *Glycyrrhiza uralensis* (Park & Youn 2010) and curcumin from turmeric *Curcuma longa* (Youn et al. 2006 [1]). Bromelain, a protease derived from pineapple stems, inhibits TLR4 signalling indirectly by reducing expression of co-receptor CD14 (Huang et al. 2008).

At the level of downstream signal inhibition, Youn et al. (2006 [2]) used RAW264.7 Mϕ and transfected HEK lines to show that (–)-epigallocatechin-3-gallate (EGCG), a flavonoid polyphenol found in green tea, inhibits TRIF-dependent TLR signalling of TLR4 and 3 by inhibiting the phosphorylation of interferon-regulating factor 3 (IRF3) by tank-binding kinase 1 (TBK1). Further along the signalling pathway Ahn et al. (2016) showed that an ethanolic extract of *Eupatorium makinoi* inhibits TLR signalling in RAW264.7 cells through suppression of IκBα degradation, while the widely-distributed plant flavonoid quercetin inhibits nuclear translocation of the NF-κB p65 subunit (Huang et al. 2010; Bhaskar et al. 2016). The plant alkaloid warifteine was found to interfere with both MyD88- and TRIF-dependent TLR signalling, implying that it inhibits a signalling process common to both pathways, possibly NF-κB activation (Rocha et al. 2010). Nicotine, another plant alkaloid, has been shown to suppress *in vitro* activation of transcription factors NF-κB and AP-1 (Sugano et al. 1998; Laan

et al. 2013). In another study, cystic fibrosis (CF) epithelial cells treated with nicotine displayed decreased TLR2-mediated CXCL8 production, key to the neutrophil accumulation which causes the majority of inflammatory damage in CF (Greene et al. 2010). While the harmful effects of smoking tobacco are well-documented, as well as the addictive nature of nicotine itself, it is possible that the development of non-addictive, safely-administered nicotine analogues could greatly improve quality of life for CF patients.

This broad array of TLR-modulatory plant extracts and derivatives (a selection of examples are presented in Table 1.3), operating via a multitude of mechanisms, serves to underline the diverse possibilities and great potential of plants as a source of TLR-modulatory compounds.

Table 1.3. Overview of known plant-derived TLR modulators.

Modulator	Category	Origin	Type	Target	Effect	Reference
THF	Polyphenol (flavonoid)	*Scutellaria baicalensis*	Inhib.	LPS	Binds LPS	Fu et al. 2008
PGG	Polyphenol	Red peony root	Inhib.	LPS	Binds LPS	Genfa et al. 2005
miR168	Micro RNA (miRNA)	*Fragaria vesca*	Inhib.	TLR3	Inhibits TRIF signalling	Cavalieri et al. 2016
6-shogaol	Shogaol	Ginger	Inhib.	TLR4	Inhibits dimerisation	Park & Youn 2010; Ahn et al. 2009
Isoliquiritigenin	Polyphenol	Liquorice root	Inhib.	TLR4	Inhibits dimerisation	Park & Youn 2010
Curcumin	Polyphenol	Turmeric	Inhib.	TLR4	Inhibits dimerisation	Youn et al. 2006 [1]
Bromelain	Protease	Pineapple stem	Inhib.	TLR4	Inhibits CD14 expresssion	Huang et al. 2008
EGCG	Polyphenol (flavonoid)	Green tea	Inhib.	Signalling	Inhibits phosphorylation of IFR3 and TBK1	Youn et al. 2006 [2]
EEM	Crude ethanolic extract	*Eupatorium makinoi*	Inhib.	Signalling	Suppresses IκBα degradation	Ahn et al. 2016
Quercetin	Polyphenol (flavonoid)	Wide range of plants	Inhib.	Signalling	Inhibits NF-κB p65 translocation	Bhaskar et al. 2016
Warifteine	Alkaloid	*Cissampelos sympodialis*	Inhib.	Signalling	Supresses MyD88- and TRIF-dependent signalling	Rocha et al. 2010
Nicotine	Alkaloid	*Solanaceae*, esp. *Nicotiana*	Inhib.	Signalling	Suppresses NF-κB and AP-1 activation	Sugano et al. 1998; Laan et al. 2013
Immulina	Polysaccharide	*Arthrospira spp.*	Stim.	TLR2/6	Stimulates IgA, Il-6 *ex vivo* and IFN-γ *in vivo* production	Balachandran et al. 2006
Ursolic acid	Triterpenoid	Fruit peels and waxes	Stim.	TLR2 & 4	Stimulates IFN-γ response	Jung et al. 2010
Levan	Polysaccharide	Soybean mucilage	Stim.	TLR4	IL-12 production, Th2 suppression	Xu et al. 2006

An illustrative selection of the diverse forms and mechanisms of known plant-derived TLR modulators. THF: 2',5,6',7-tetrahydroxyflavanonol; PGG: Beta-1,2,3,4,6-penta-O-galloyl-D-glucopyranose; EGCG: (–)-epigallocatechin-3-gallate; EEM: ethanolic *Eupatorium makinoi*; iNOS: inducible nitric oxide synthase; NO: nitric oxide.

1.5 Rationale and aims/objectives

1.5.1 Rationale

As evidenced in the published scientific literature, regulation of immunity by TLR modulation represents a promising tool for a variety of clinical applications. Plants have been shown to be a productive source of novel bioactive compounds, including those with TLR-mediated immunomodulatory properties. It is also the case that only a very small proportion of putatively immunomodulatory plant species have been scientifically examined for such compounds. If identified, investigated and refined, these substances could be used in a range of medical applications, depending on their activity and mode of action.

1.5.2 Aims/objectives

The aim of this study is to investigate potential TLR-mediated immunomodulatory activity of a range of extracts from Malaysian rainforest plants. We have approached this using a bottom-up approach, and our objectives are to:

- Screen plant extracts from a variety of species for TLR-modulatory activity in a transfected HEK-based system.
- Isolate and characterise the active components of extracts identified in the initial screen.
- Assess the activity of these components in primary B cells *in vitro*.

This approach is intended to provide us with a perspective of immunomodulatory activity from the receptor up to the cellular level.

Chapter 2. Materials and Methods

2.1 Plant extracts

2.1.1 Extracts from Crops for the Future research centre (CftF)

All samples will be referred to by their sample code throughout once initial description has been provided.

Lyophilised extracts were kindly provided by Dr. Kang Nee Ting at the University of Nottingham's Malaysia campus and redissolved in dimethyl sulphoxide (DMSO) at a stock concentration of 20mg/ml to ensure uniformity between ethanol and ethyl acetate extracts. All samples were sterilised through a 0.2µm filter (Sigma-Aldrich) before use.

Table 2.1. Plant extracts provided by Dr. Ting

Sample Code	Plant name	Plant part	Extraction solvent
87EtB	*Ficus schwarzii* Koord.	Bark	Ethanol
87EtL	*Ficus schwarzii* Koord.	Leaf	Ethanol
1402EtL	*Tristaniopsis merguensis*	Leaf	Ethanol
1403EtL	Unknown	Leaf	Ethanol
1404EtL	*Gironniera nervosa*	Leaf	Ethanol
1406EAL	*Elaeocarpus petiolatus*	Leaf	Ethyl acetate
1406EtL	*Elaeocarpus petiolatus*	Leaf	Ethanol
1407EtL	*Elaeocarpus griffithii*	Leaf	Ethanol
1409EtL	*Elaeocarpus robustus*	Leaf	Ethanol
1412EtB	*Ficus ribes*	Bark	Ethanol
1412EtL	*Ficus ribes*	Leaf	Ethanol
1413EtL	*Daphniphyllum scortechinii*	Leaf	Ethanol
1418EtL	*Ficus fistulosa var. tengerensis*	Leaf	Ethanol
1419EtB	*Ficus variegata*	Bark	Ethanol
1419EtL	*Ficus variegata*	Leaf	Ethanol

2.1.2 Extracts from Plant Sciences, University of Nottingham

Dr. Andrew Bottley of the Plant Sciences Department at the University of Nottingham is investigating the bioactivities of a particular plant extract, and kindly supplied samples of purified fractions of the extract for screening for TLR-mediated immunomodulatory properties. The plant of origin remains confidential under intellectual property rights protection, as such these extracts are referred to solely by their sample codes: AB21, AB46, AB48, AB57, AB62 and AB139. These were supplied in DMSO at a concentration of 20mM. Concentrations in mg/ml could not be calculated because the masses of the fractions are unknown.

2.1.3 Plant-based controls

Published work describes the TLR-dependent response to various ginseng species, including *Panax ginseng* (Byeon et al. 2012). *P. ginseng* extract was used as a plant-based positive control. The extract was obtained from Naturex, supplied as a lyophilised extract of root tissue. The extraction solvent was 75% ethanol, 25% water. Lyophilised material was redissolved in DMSO at a stock concentration of 20mg/ml to maximise comparability with experimental samples.

2.1.4 Dialysis

Extracts were dialysed against phosphate-buffered saline (PBS, Sigma) using Float-A-Lyzer G2 cellulose acetate dialysis cartridges (Spectrum) with a 100Da molecular weight cut-off (MWCO). Samples were dialysed overnight in 1 litre of endotoxin-free PBS at 4^{o}C on a magnetic stirrer, with two changes of PBS at 4 and 16 hours. Where sample volume increased due to intake of water to the dialysis cartridge, volumes used in cell culture were adjusted accordingly to ensure a constant final concentration of plant extract in culture medium.

2.1.5 Fluorescent Lectin Stain

A grid of 1x1cm squares was drawn onto a polyvinylidene fluoride (PVDF) membrane using a pencil (
Figure 2.1). The membrane was soaked in 100% methanol until translucent then equilibrated in PBS for 3 min. Treatments and controls were spotted onto the membrane in 15µl volumes, one per square, and incubated at RT until dry. For optimisation experiments, *Lactobacillus* lysate was used as a substrate. The PBS-only treatment served as a control for background fluorescence, the *Lactobacillus*-only control for inherent fluorescence of the bacterial lysate, and the PBS + GNL control for non-specific binding of lectin to the membrane. The membrane was blocked with 5% Marvel milk powder in PBS for 2h on a rocker at 45 cycles/min, then washed three times in PBST, three times in PBS and once in deionised water. 15µl of FITC-labelled *Galanthus nivalis* snowdrop lectin (FITC-GNL) was spotted onto the samples and the membrane was incubated at RT in the dark for 1h. After being washed as described previously the membrane was visualised on the Typhoon TRIO+ (GE Life Sciences).

PBS	PBS + 100µg/ml GNL	LL + 100µg/ml GNL	LL + 90µg/ml GNL	LL + 80µg/ml GNL	LL + 70µg/ml GNL
PBS	PBS + 100µg/ml GNL	LL + 100µg/ml GNL	LL + 90µg/ml GNL	LL + 80µg/ml GNL	LL + 70µg/ml GNL
PBS	PBS + 100µg/ml GNL	LL + 100µg/ml GNL	LL + 90µg/ml GNL	LL + 80µg/ml GNL	LL + 70µg/ml GNL
LL + 60µg/ml GNL	LL + 50µg/ml GNL	LL + 40µg/ml GNL	LL + 30µg/ml GNL	LL + 20µg/ml GNL	LL
LL + 60µg/ml GNL	LL + 50µg/ml GNL	LL + 40µg/ml GNL	LL + 30µg/ml GNL	LL + 20µg/ml GNL	LL
LL + 60µg/ml GNL	LL + 50µg/ml GNL	LL + 40µg/ml GNL	LL + 30µg/ml GNL	LL + 20µg/ml GNL	LL

Figure 2.1. Membrane layout for fluorescent lectin stain optimisation. Membrane was soaked in 100% methanol until translucent then equilibrated in PBS for 3 min. Treatments and controls were applied in 15µl amounts and incubated at RT until dry. Membrane was blocked with 5% Marvel milk powder in PBS for 2h on a rocker at 45 cycles/min, then washed three times in PBST, three times in PBS and once in deionised water. 15µl of FITC-labelled snowdrop lectin (FITC-GNL) was spotted onto the samples and the membrane was incubated at RT in the dark for 1h. After being washed as described previously the membrane was visualised on the Typhoon TRIO+ (GE Life Sciences). LL: *Lactobacillus* lysate; GNL: *Galanthus nivalis* lectin

2.1.6 Extract modification

2.1.6.1 Acid treatment

Extracts were treated with 20µl of 1M hydrochloric acid (HCl) per millilitre of extract and incubated for at least 1 hour at room temperature (RT). The extracts were then neutralised with 20µl/ml of 1M sodium hydroxide (NaOH) and sterilised through a 0.2µm filter (Sigma-Aldrich) before use.

2.1.6.2 Heat inactivation

1ml aliquots were heated to 100°C in a heat block for at least 1 hour, then allowed to cool at RT before storage.

2.1.6.3 Metaperiodate carbohydrate oxidation

Extracts were oxidised as described by Jenkins et al. (2005). 1ml aliquots were dialysed against 50mM sodium acetate buffer (pH 4.5) for 4 hours, then treated with sodium metaperiodate at a final concentration of 10mM in the dark for 45 minutes at RT. The reaction was stopped by adding sodium borohydride to a final concentration of 50mM for 30 minutes. The samples were then dialysed overnight against three changes of PBS at 4°C.

2.1.7 Sodium dodecyl sulphate polyacrylamide gel electrophoresis (SDS-PAGE)

Extracts were run on 4-12% Bis-Tris NuPAGE gradient gels (Thermo Fisher) according to manufacturer's instructions, with a 10-200kDa ladder (New England Biolabs). 2µl of sample was mixed with 2.5µl NuPage LDS Sample Buffer (Thermo Fisher), 1µl 2-mercaptoethanol (Thermo Fisher) and 4.5µl deionised water, and the mixture heated to 70°C for 10 minutes. Samples, ladder and BSA standard were loaded into wells, and the gel run using MOPS buffer for 45 min at 200V. The gels were stained either with Coomassie Blue (Bio-Rad) for proteins or periodic acid Schiff (PAS; Sigma Aldrich) staining for glycoproteins and visualised using an ImageQuant 300 (GE Life Sciences).

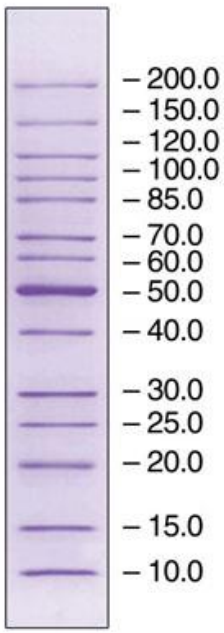


Figure 2.2 10-200kDa protein ladder used in SDS-PAGE. Increments are displayed in kDa. Taken from Colletti & Cruz (2001)

2.1.8 Size fractionation

Size fractionation was carried out using Spin-X UF centrifugal concentrators (Corning) with polyethersulphone membranes, which were sterilised with 70% ethanol and rinsed with sterile D-PBS prior to use. Samples were diluted 1:25 in sterile D-PBS to reduce the concentration of DMSO sufficiently to avoid membrane damage, then filtered through a concentrator with a 100kDa MWCO at 10^{o}C until the supernatant volume was decreased to 1/25 of the starting volume. The supernatant was retained and the eluent transferred to a 50kDa MWCO concentrator. The process was repeated for 30, 10 and 5kDa MWCO columns. This yielded six size fractions of >100kDa, 50-100kDa, 30-50kDa, 10-30kDa, 5-10kDa and <5kDa respectively (Figure 2.1).

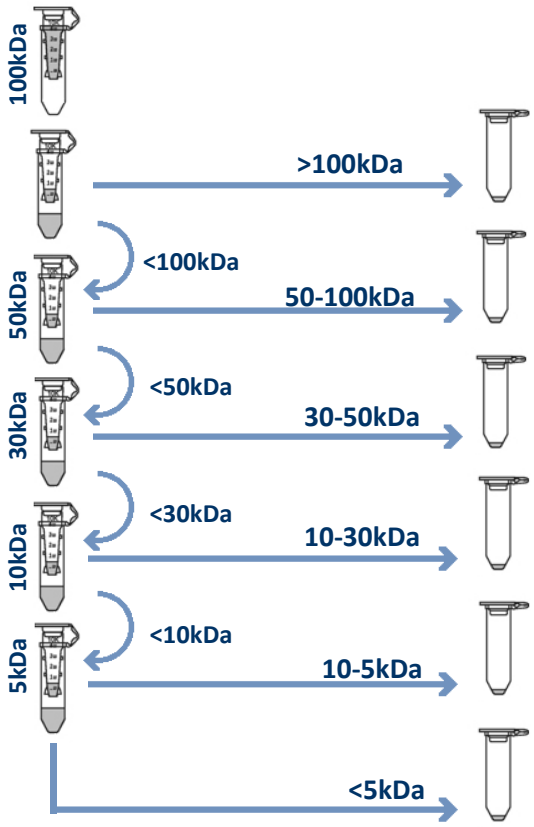


Figure 2.3. Method for sequential filtration through progressively-smaller molecular weight cut-off (MWCO) membranes. Samples were diluted 1:25 in sterile D-PBS to reduce the concentration of DMSO sufficiently to avoid membrane damage, then filtered through a concentrator with a 100kDa MWCO at 4°C until the supernatant volume was decreased to 1/25 of the starting volume. The supernatant was retained and the eluent transferred to a 50kDa MWCO concentrator. The process was repeated for 30, 10 and 5kDa MWCO columns. Fractions were then stored at -20°C.

2.2 Cells and culture techniques

2.2.1 Human embryonic kidney (HEK) cell lines

HEK cell lines were obtained from Invivogen expressing each of the following extracellular TLRs (see Table 2.2).

2.2.1.1 Growth media and conditions

HEK cells were grown in complete Dulbecco's modified Eagle's medium (DMEM, Sigma) (4500mg/l glucose, 110mg/L sodium pyruvate and 2mM L-glutamine, supplemented with 10% foetal calf serum (FCS, Sigma) and 1% penicillin/streptomycin (50 U/ml penicillin, 50 µg/ml streptomycin, Gibco)) according to supplier's instructions (Invivogen). Selective antibiotics were added as per Table 2.2 to ensure selective expression of the recombinant plasmid. Long-term storage of cells was in 1.8ml cryovials (Thermo) at 10^6 cells/ml in 50% DMEM, 40% FCS and 10% DMSO, frozen in liquid nitrogen. Upon thawing in a water bath at 37°C cells were washed in complete DMEM, the whole aliquot seeded in 5ml complete DMEM in 25cm^2 filter-capped tissue culture flasks (Greiner Bio-One) and maintained at 37°C and 5% CO_2. At 80% confluence they were harvested in DPBS using cell scrapers (Greiner), pelleted at 1200rpm for 5min and resuspended in complete DMEM before being split into two 75cm^2 filter-capped tissue culture flasks. Subsequent passages were carried out as before, but with one tenth of the confluent 75cm^2 flask's cells seeded into each of two new 75cm^2 flasks. After two passages in non-selective medium the cells were switched to their respective selection regimes as per supplier's instructions (outlined in Table 2.2). After 30 passages the cultures were discarded and fresh ones drawn from frozen stocks.

Table 2.2. HEK cell lines used in this study.

Cell line	TLRs	Selection	Notes	Positive control in culture
HEK293-mTLR1/2	Murine TLR2/1	Blasticidin 10µg/ml	Human TLR1-transfected cells were unavailable	10ng/ml Pam3CSK4 (Invivogen)
HEK293-hTLR2/6	Human TLR2/6	Blasticidin 10µg/ml	None	10ng/ml Pam2CSK4 (Invivogen)
HEK293-hTLR4A-MD2-CD14	Human TLR4 with co-receptors MD2 and CD14	Blasticidin 10µg/ml and Hygromycin 50µg/ml	None	200ng/ml LPS from *Escherichia coli* (Source Bioscience)
HEK293	None	None	Negative control for HEK293 lines	N/A
HEK-Blue hTLR5	Human TLR5	Blasticidin 10µg/ml and Zeocin 100µg/ml	Includes secreted embryonic alkaline phosphatase (SEAP) reporter system (not used in this study)	100ng/ml flagellin from *Salmonella typhimurium* (FLA-ST) (Source Bioscience)
HEK-Blue Null1	None	Zeocin 100µg/ml	Negative control for HEK-Blue hTLR5 line	N/A

HEK cell lines and culture conditions used in this study. All cell lines and selective antibiotics were obtained from Invivogen and grown in complete DMEM (4500mg/l glucose, 110mg/L sodium pyruvate and 2mM L-glutamine, supplemented with 10% foetal calf serum (Sigma) and 1% penicillin/streptomycin (50 U/ml penicillin, 50 µg/ml streptomycin, Gibco)) at 37°C and 5% CO_2. Selection regimes and positive controls were used according to supplier's instructions.

2.2.1.2 Cytotoxicity assay

Untransfected HEK cells were seeded at $1x10^5$/well in a flat-bottomed 96-well plate in 100ul of complete DMEM. After being allowed to adhere for two hours the media was aspirated and replaced and the cells were treated with either 100 or 50µg/ml of plant extracts, with final DMSO concentrations of 0.5% and 0.25% respectively. Negative controls were treated with complete DMEM; high-toxicity positive control with 70% ethanol; solvent control with 0.5% DMSO in complete DMEM. All treatments were carried out in triplicate. After incubation for 48h supernatant was collected for lactacte dehydrogenase (LDH) quantification (see section 2.3.1).

2.2.1.3 Stimulation experiments

Cells were seeded and adhered as in section 2.2.1.2. The medium was replaced and the cells were treated with 100µg/ml of plant extracts, serially diluted seven times to a minimum concentration of 78.125ng/ml. Negative controls were treated with complete DMEM; positive control with appropriate TLR ligand (Table 2.2) in complete DMEM; solvent control with 0.5% DMSO in complete DMEM. All treatments were carried out in triplicate. After incubation for 48h supernatant was collected for CXCL8 quantification (see section 2.3.2).

2.2.1.4 Inhibition experiments

Cells were seeded and adhered as in section 2.2.1.2, then medium was replaced with complete DMEM containing the appropriate TLR ligand as controls (Table 2.2). Cells were treated with 100µg/ml of plant extracts, serially diluted as in section 2.2.1.3. Negative controls were treated with ligand-free complete medium; ligand-only controls with ligand-containing medium; solvent controls with 0.5% DMSO in ligand-containing medium; inhibition controls with 40µM parthenolide (Sigma Aldrich) in ligand-containing medium. All treatments were carried out in triplicate. Incubation and CXCL8 quantification were carried out as in section 2.2.1.3.

2.2.2 Murine B lymphocytes

2.2.2.1 Isolation and culture conditions

Whole spleens of healthy adult female C57BL/6 mice were collected following schedule 1 euthanasia by cervical dislocation. They were homogenised to a single-cell suspension in complete Roswell Park Memorial Institute (RPMI, Sigma) medium (supplemented with 10% FCS and 1% penicillin/streptomycin (50 U/ml penicillin, 50 µg/ml streptomycin)).

$CD19^+$ (cluster of differentiation 19 positive) B lymphocytes were isolated by magnetic-activated cell sorting (MACS) using rat anti-mouse CD19 microbeads (Miltenyi Biotech). All

reagents were kept on ice throughout unless otherwise specified, and centrifugation was at 4°C. As per manufacturer's instructions (Miltenyi Biotech), cells were washed in complete RPMI and resuspended in 2ml sterile MACS running buffer (0.5% bovine serum albumin (BSA) and 2mM ethylenediaminetetraacetic acid (EDTA) in PBS). The cells were counted in a haemocytometer and pelleted by centrifugation at 300xg for 10min. They were then resuspended in 100µl of 4:1 running buffer:microbeads per 10^7 cells, with a minimum volume of 100µl, and incubated for 15min at 4°C in the dark. After incubation 2ml of running buffer was added per 10^7 cells, the mixture spun at 300xg for 10min, the supernatant discarded and the pellet resuspended in 500µl of running buffer. The suspension was applied to a MACS LS column (Miltenyi) in a MACS magnetic separator (Miltenyi) which had been pre-rinsed three times with 3ml sterile MACS rinsing buffer (2mM EDTA in PBS). Once the cell suspension had passed through the column it was rinsed three times with 3ml rinsing buffer, then the column was removed from the magnetic separator, placed over a 15ml tube and purged by filling with 5ml running buffer and the plunger firmly pushed down. The resulting cell suspension was counted in a haemocytometer and pelleted at 300xg for 10min, then resuspended in RPMI at $3x10^6$ cells/ml.

2.2.2.2 Stimulation

100µl of cell suspension was applied to each well of a 96-well U-bottomed plate (Thermo) and 100µl of the relevant treatment applied (see Table 2.3) in triplicate wells. Plates were incubated for 120h at 37°C before analysis of class switching and proliferation by flow cytometry.

Table 2.3. Treatments used in B cell stimulation experiments

Treatment	Notes
RPMI	Medium-only negative control
25µg/ml LPS + 10ng/ml IL-4	Positive control for IgG1 class switch (Zaheen & Martin 2010)
20ng/ml Pam2CSK4	Positive control for TLR2/6 activation
200µg/ml 1402EtL	Crude extract
100µg/ml 1402EtL	Crude extract
50µg/ml 1402EtL	Crude extract
200µg/ml 1412EtB	Crude extract
100µg/ml 1412EtB	Crude extract
50µg/ml 1412EtB	Crude extract
1412EtB (acid-treated)	Concentration equivalent to 100µg/ml crude extract
1412EtB (boiled)	Concentration equivalent to 100µg/ml crude extract
1412EtB (oxidised)	Concentration equivalent to 100µg/ml crude extract
1412EtB (>100kDa)	Concentration equivalent to 100µg/ml crude extract
1412EtB (50-100kDa)	Concentration equivalent to 100µg/ml crude extract
1412EtB (30-50kDa)	Concentration equivalent to 100µg/ml crude extract
1412EtB (5-30kDa)	Concentration equivalent to 100µg/ml crude extract
1412EtB (<5kDa)	Concentration equivalent to 100µg/ml crude extract

Cells were seeded in 96-well U-bottomed plates at a density of $3x10^5$ cells/well and treated in triplicate with the treatments listed. Plates were incubated for 120h at 37°C, then class switching and proliferation analysed by flow cytometry.

2.2.2.3 Flow cytometry

Class switching and proliferation were assessed using fluorescence-activated cell sorting (FACS). All reagents were kept on ice unless otherwise specified. Plates were centrifuged at 300xg for 10min and the supernatant removed for storage. The pellet was washed twice in FACS buffer (5% FCS in PBS) then resuspended in blocking buffer (0.5% BSA in PBS) and incubated on ice for 20min. After washing twice more with FACS buffer the cells were resuspended in fixation/permeabilisation buffer (BD Biosciences, catalogue #54-2090KZ) on ice for 20min, then washed twice in permeabilisation/wash buffer (perm/wash, BD, catalogue #51-2091KZ) before staining. Cells were stained with 1µg/ml of fluorochrome-conjugated antibody in perm/wash buffer on ice for 30min. Experimental treatments were stained with FITC rat anti-mouse IgM (IgG2a clone #R6-60.2), APC rat anti-mouse IgG1 (IgG1 clone #X56) and PE rat anti-mouse Ki-67 (IgG2a clone #16A8). Single-stained controls were

used to calibrate compensation between fluorochrome emission spectra. Isotype controls were treated with FITC rat anti-mouse (IgG2a clone #eBR2a), APC rat anti-mouse (IgG1 clone #R3-34) and PE rat anti-mouse (IgG2a clone #RTK2758). A non-stained treatment was included to control for fixation effects. Data were analysed using Kaluza Analysis v1.5 (Beckman Coulter).

2.3 Supernatant assays

2.3.1 LDH assay

Supernatant LDH was assayed using a commercial LDH cytotoxicity kit (Source BioScience). 10µl of cell culture supernatant was transferred to a 96-well flat-bottomed plate and 100µl of WSL substrate in kit reaction diluent was added. After 30min incubation at 25°C the plates were read on a Varioskan Flash plate reader (Thermo) at 450nm with 650nm as a reference wavelength.

2.3.2 CXCL8 ELISA

Supernatant CXCL8 was assayed using a commercial human CXCL8 ELISA kit (DuoSet, R&D Systems), all steps at RT. 96-well high-binding plates (Greiner Bio-One) were coated with 100µl 4µg/ml monoclonal mouse anti-human CXCL8 (IgG1 clone #6217) overnight at RT. They were then washed three times with 0.05% Tween 20 (Sigma) in PBS, followed by one wash with PBS alone. The plates were blocked with 100µl 1% BSA in PBS for at least one hour then washed as previously described. Samples were then added in 100ul volumes. Recombinant CXCL8 standard diluted in 0.1% BSA and 0.05% Tween20 in Tris-buffered saline (TBS) starting at 2000pg/ml and serially diluted twofold to a minimum concentration of 7.8125pg/ml, with a blank well containing diluent only. After two hours of incubation plates were washed and treated with 100µl 20ng/ml biotinylated polyclonal goat anti-human CXCL8 (IgG clone

#890805) for a further two hours then washed. Plates were then treated with streptavidin-HRP conjugate (R&D systems product #893975) diluted 40-fold in the same BSA-Tween-TBS diluent as the standards as per manufacturer's instructions (concentration of streptavidin-HRP not provided by supplier) for 20 minutes in the dark. After a final wash stage 100µl 3,3',5,5'-tetramethylbenzidine (TMB) substrate was added and the reaction monitored for colour change. When the colour had developed sufficiently to be read the reaction was stopped by adding 50µl 1M HCl and the plates were read on a Varioskan Flash plate reader (Thermo) at 450nm with 540nm as a reference wavelength. Plate layout is provided in Figure 2.4.

	1	2	3	4	5	6	7	8	9	10	11	12
A												
B		Extract 1 100 µg/ml	Extract 1 50 µg/ml	Extract 1 25 µg/ml	Extract 1 12.5 µg/ml	Extract 1 6.25 µg/ml	Extract 1 3.125 µg/ml	Extract 1 1.5625 µg/ml	Extract 1 0.78125 µg/ml	DMEM control	Ligand + parth. control	
C		Extract 1 100 µg/ml	Extract 1 50 µg/ml	Extract 1 25 µg/ml	Extract 1 12.5 µg/ml	Extract 1 6.25 µg/ml	Extract 1 3.125 µg/ml	Extract 1 1.5625 µg/ml	Extract 1 0.78125 µg/ml	DMEM control	Ligand + parth. control	
D		Extract 1 100 µg/ml	Extract 1 50 µg/ml	Extract 1 25 µg/ml	Extract 1 12.5 µg/ml	Extract 1 6.25 µg/ml	Extract 1 3.125 µg/ml	Extract 1 1.5625 µg/ml	Extract 1 0.78125 µg/ml	DMEM control	Ligand + parth. control	
E		Extract 2 100 µg/ml	Extract 2 50 µg/ml	Extract 2 25 µg/ml	Extract 2 12.5 µgml	Extract 2 6.25 µg/ml	Extract 2 3.125 µg/ml	Extract 2 1.5625 µg/ml	Extract 2 0.78125 µg/ml	Ligand control	DMSO control	
F		Extract 2 100 µg/ml	Extract 2 50 µg/ml	Extract 2 25 µg/ml	Extract 2 12.5 µgml	Extract 2 6.25 µg/ml	Extract 2 3.125 µg/ml	Extract 2 1.5625 µg/ml	Extract 2 0.78125 µg/ml	Ligand control	DMSO control	
G		Extract 2 100 µg/ml	Extract 2 50 µg/ml	Extract 2 25 µg/ml	Extract 2 12.5 µgml	Extract 2 6.25 µg/ml	Extract 2 3.125 µg/ml	Extract 2 1.5625 µg/ml	Extract 2 0.78125 µg/ml	Ligand control	DMSO control	
H		CXCL8 2000 pg/ml	CXCL8 1000 pg/ml	CXCL8 500 pg/ml	CXCL8 250 pg/ml	CXCL8 125 pg/ml	CXCL8 62.5 pg/ml	CXCL8 31.25 pg/ml	CXCL8 15.625pg/ml	CXCL8 7.8125 pg/ml	CXCL8 0 pg/ml	

Figure 2.4. Layout of CXCL8 ELISA plates. Plates were coated with 100µl 4µg/ml monoclonal mouse anti-human CXCL8 overnight at RT. They were then washed three times with 0.05% Tween 20 in PBS and once with PBS alone. Plates were blocked with 100µl 1% BSA in PBS for one hour then washed as previously described. Samples were added in 100ul volumes. Recombinant CXCL8 standard diluted in 0.1% BSA and 0.05% Tween20 in TBS starting at 2000pg/ml and serially diluted twofold to a minimum concentration of 7.8125pg/ml, with a blank well containing diluent only. After two hours of incubation plates were washed and treated with 100µl 20ng/ml biotinylated polyclonal goat anti-human CXCL8 for two hours then washed. Plates were treated with streptavidin-HRP conjugate diluted 40-fold in BSA-Tween-TBS diluent as per manufacturer's instructions for 20 minutes in the dark. After a final wash 100µl TMB substrate was added and the reaction monitored for colour change. When colour had developed sufficiently the reaction was stopped using 50µl/well 1M HCl. Plates were read on a Varioskan Flash plate reader at 450nm with 540nm as a reference wavelength. Extract 1: supernatant from cells treated with extract 1 at concentrations described; Extract 2: supernatant from cells treated with extract 2 at concentrations described; ligand control: supernatant from cells treated with TLR ligands described in Table 2.2; DMEM control: supernatant from cells treated with complete DMEM only; DMSO control: supernatant from cells treated with 0.5% DMSO; Ligand + parth control: supernatant from cells stimulated with TLR ligand and 40µM parthenolide (inhibition experiments only).

2.4 Statistical analysis

ELISA data were analysed using GraphPad Prism 6 software. A quadratic standard curve was drawn with R^2 values in the range of 0.9800 to 0.9999. Experimental concentrations were then interpolated from this curve. All treatments were carried out in triplicate and assays were tested using 2-way ANOVA. Experimental treatments were compared to solvent control treatments, with Dunnett's analysis for multiple comparisons. p-values of 0.05 or less were deemed significant. p-values of 0.05 or less are presented as *, 0.01 as **, 0.001 as *** and 0.0001 as ****. Data were tested for dose dependency using non-linear one phase decay, with R^2 values of 0.9 or greater deemed significant.

Chapter 3. Screening for modulation of extracellular TLRs by plant extracts

3.1 Introduction

Plants and their extracts have represented a bountiful source of novel drugs and candidate molecules throughout the history of medicine, and continue to do so (Newman & Cragg 2016). Many of our most effective medicines have botanical origins, such as aspirin from *Salix sp.* (and later *Filipendula ulmaria*) and morphine (as well as its many derivative opioids) from *P. somniferum* (Luch 2009; Mahdi et al. 2006). Half of the 2015 Nobel Prize for Physiology or Medicine was awarded to Tu Youyou, who developed the highly successful anti-malarial drug Artemisinin from sweet wormwood, *A. annua* (Van Voorhis et al. 2015; Tu 2011).

Among the many classes of bioactive compounds isolated from plants, a number of TLR-mediated immunomodulators have been characterised including proteins, polysaccharides, glycoproteins, flavonoids, fatty acids, phenols, nucleic acids and more (reviewed by Chahal et al. 2012; Cavalieri et al. 2016). Compounds from a wide range of plants have been found to stimulate or inhibit the activity of TLRs at various points in the signal transduction pathway, including receptor dimerisation, ligand binding and activation of cellular signalling molecules and transcription factors. For example, Xie et al. (2016) found that a polysaccharide from *D. huoshanense* bound and activated TLR4 in RAW264.7 Mϕ and primary peritoneal Mϕ, while a dextran control did not; upregulating phosphorylation of ERK, JNK Akt and p38. Three studies have identified separate plant-derived inhibitors of TLR4 homodimerisation (Ahn et al. 2009; Youn et al. 2006; Park & Youn 2010). Further along the signalling pathway, Youn et al. (2006) used RAW264.7 Mϕ and transfected HEK lines to show that EGCG, a flavonoid polyphenol found in green tea, inhibits TRIF-dependent TLR signalling of TLR4 and 3 by inhibiting the phosphorylation of IRF3 by TBK1. Ahn et al. (2016) showed that an ethanolic

extract of *E. makinoi* inhibits TLR signalling in RAW264.7 cells through suppression of IκBα degradation.

The majority of published studies on TLR modulators tend to stem from a highly directed rationale, either at the level of a single plant (Yang et al. 2007), traditional remedy (Youn et al. 2006) or family of related compounds (Oberg et al. 2009). There have been high-throughput screens of chemical libraries for NF-κB regulation (reviewed in Karin et al. 2004), e.g. (Palanki et al. 2000; Murata et al. 2003), but not using plant-derived candidates. However, plant compounds are often screened for other useful properties such as antimicrobial, anthelmintic or antioxidant properties (Othman et al. 2011; Katiki et al. 2013; Proestos et al. 2013).

Our approach involves screening extracts from 12 plant species representing six genera, and is directed prinicpally by the presence of two groups of chemicals. The plants in this study (Table 2.1) were selected because they contain cucurbitacins and/or alkaloids, diverse groups of chemicals previously described as possessing various immunomodulatory activities.

Cucurbitacins are triterpenoid phytochemicals primarily found in the family Cucurbitaceae, thought to function as a defence against herbivores (Zhou et al. 2016; Dinan et al. 1997). Their primary mode of action in this function is by inhibition of insect steroid hormone function (Sarker et al. 1999). Their structural diversity is a result of variation in the side chains attached to the central triterpenoid skeleton (Stuppner et al. 1991; Stuppner & Moller 1993). Cucurbitacin-containing plant products feature in several ethnomedicinal repertoires (Reguero et al. 1987; Chen et al. 2005; Delazar et al. 2006) and are subject to ongoing interest as potential sources of viable pharmacological compounds (Kaushik et al. 2015). For example, cucurbitacins A, B, E, I and Q have been shown to inhibit Janus kinase/signal transducer and activator of transcription 3 (JAK/STAT3) signalling via a range of mechanisms,

resulting in increased apoptosis and decreased angiogenesis in mouse tumours and human tumour allograft models (Sun et al. 2005; Dong et al. 2010).

With regards to their effects on immune and inflammatory functions, Jayaprakasam et al. (2003) found that cucurbitacins B, D, E and I isolated from *Cucurbita andreana* selectively inhibited cyclooxygenase 2 (COX-2) activity *in vitro*. Cucurbitacin B, found in a wide range of plant species, was shown by Kim et al. (2015) to inhibit the production of reactive oxygen species (ROS) and pro-inflammatory mediators such as nitric oxide (NO), tumour necrosis factor alpha (TNF-α) and interleukin 6 IL-6, IL-12 and IL-1β in murine peritoneal Mϕ. In addition, two cucurbitacins isolated from the roots of *Picrorhiza scrophulariaeflora* have been shown to inhibit mitogen-induced human T cell proliferation *in vitro* (Smit et al. 2000). Various studies in mice have also reported analgesic properties of some cucurbitacins in addition to anti-inflammatory effects (Peters et al. 1997; Marzouk et al. 2013).

Alkaloids are a diverse group of nitrogen-containing, mostly heterocyclic compounds found in a wide range of organisms, although plants remain the primary natural source with over 27,000 described so far (Dewick 2009; Kukula-Koch & Widelski 2016). Bioactive alkaloids include chemotherapy drugs such as vinblastine and paclitaxel, antimalarial compounds such as quinine and its derivatives, and analgesics such as morphine and capsaicin (World Health Organization 2017; De Lourdes Reyes-Escogido et al. 2011), as well as psychoactive drugs caffeine, cocaine, mescaline and lysergic acid diethylamine (LSD; Schwartz & David 1985; Wu & Wittick 1977; Lee 2009).

Greene et al. (2010) showed that nicotine, a plant-derived alkaloid, inhibits TLR2-mediated CXCL8 production in the human tracheal epithelial cell line CFTE29o-, a model for CF, via the α7-nAChR nicotine receptor. In a study by Rocha et al. (2010) warifteine, an alkaloid purified from *Cissampelos sympodialis*, inhibited B cell proliferation and immunoglobulin secretion by murine B lymphocytes both *in vitro* and *in vivo*.

Various *Ficus spp.* are used in traditional medicine, adding to the rationale for their inclusion here (Priyadi et al., 2010). Ethanol was used in the extraction procedure because of its amphiphilic nature, enabling it to solubilise both hydrophobic and hydrophilic molecules from the plant tissue. Ethyl acetate was the second preferred extraction solvent because it is highly effective at extracting polyphenols, a diverse group of chemicals with a wide range of bioactivities including TLR-mediated immunoregulation (Pekić et al. 1998; Liu et al. 2011).

The majority of the plants screened have been the subject of no published immunological investigation at the time of writing. Extracts from *F. fistulosa* have recently been shown to have antiproliferative effects on two human cancer cell lines (Yap et al. 2016) as well as antiviral (Hafid et al. 2016), antifungal (Subramaniam et al. 2009) and antiplasmodial (Zhang et al. 2002) activities. An ethanolic extract of *E. petiolatus* bark has been shown to inhibit COX-2 expresssion, phosphorylation of ERK, JNK and p38, and NF-κB p65 translocation in RAW264.7 (Kwon et al. 2012).

In addition to the plant extracts from Crops for the Future (CftF) provided by Dr. Ting, Dr. Andrew Bottley of the Plant Sciences Department at the University of Nottingham kindly supplied samples of purified fractions from another extract of interest (see section 2.1.2). These were screened for TLR-modulatory activity in the HEK293-TLR lines described in section 2.2.1.

Within this chapter we aimed to identify plant extracts with putative TLR-stimulatory and -inhibitory activity. The cell-surface TLRs (2/1, 2/6, 4 and 5) were selected because their ligands do not require transport to the endosome, therefore are more likely to be detected.

CXCL8 was selected as an indicative readout of TLR activity because it is produced in response to activation of all TLRs being investigated (TLR5: Means et al. 2003; TLR4: Bernatoniene et al. 2008; TLR2/1 and 2/6: Halperin et al. 2012), thus providing a unifying metric across experiments. CXCL8 is a chemokine primarily known as a chemotactic factor for

neutrophils (Yoshimura et al. 1987), but also involved in a range of other neutrophil functions including increased adhesion, shape change and generation of peroxides and superoxides (Paccaud et al. 1990; Thelen et al. 1988; Schröder et al. 1987). The neutrophil specificity of CXCL8 is due to the glutamic acid-leucine-arginine (ELR) motif immediately preceding the first cysteine residue of the cysteine-x-cysteine (CXC) motif. The ELR motif is critical to the binding of CXCL8 to the neutrophil C-X-C motif chemokine receptors 1 and 2 (CXCR1 and CXCR2; Clark-Lewis et al. 1991). The commercial CXCL8 ELISA kit (R&D systems) employed in this study has been used in multiple previous immunological studies (for example Tohyama et al. 2009; Iram et al. 2012; Wang et al. 2017).

3.2 Results

3.2.1 Cytotoxicity of plant extracts

Before investigating any potential biological activities of the extracts it was important to check for any effects on cell viability. Five extracts showed significant cytotoxicity at the highest concentration used, 100µg/ml (1402EtL, 1406EAL, 1406EtL, 1412EtB and 1418EtL; all $p \leq 0.0001$; Figure 3.1). Only 1406EAL and 1406EtL retained their cytotoxicity at 50µg/ml ($p \leq 0.0001$). This suggests that the cytotoxic effects observed at 100µg/ml only were related to high protein concentrations as opposed to specific effects of the extract.

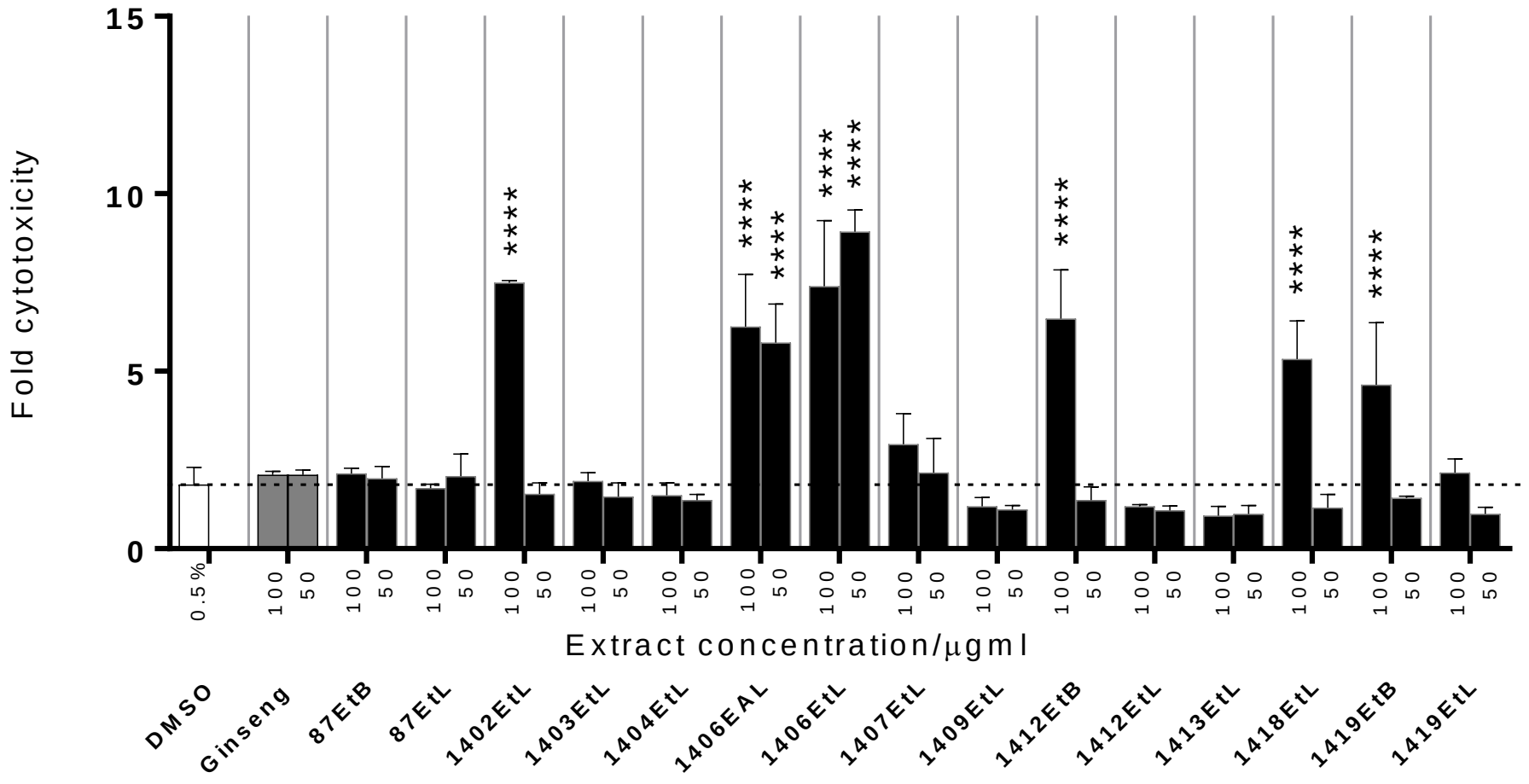


Figure 3.1. Lactate dehydrogenase (LDH) cytotoxicity assay. Untransfected HEK293 cells were incubated for 48h with the indicated extracts at either 100 or 50µg/ml. After 48h 10µl of supernatant was taken and LDH was measured by colourimetric assay kit (Source Biosciences) as described in section 2.3.1. Cytotoxicity of plant extracts is shown relative to untreated cells. Colours used are purely to aid distinction between data sets, and the dashed line indicates the LDH readings for the solvent-only control. Readings shown are means +/- standard deviation (SD) of triplicate wells. Results were tested for significant differences using ANOVA; **** $p \leq 0.0001$.

3.2.2 Stimulation of transfected HEK293 TLR cell lines.

To determine if any of the extracts had a TLR-activating effect we measured the production of CXCL8 48hrs post-stimulation in the supernatants of transfected cell lines. Of the extracts tested four showed statistically significant increases in CXCL8 production by HEK293-TLR1/2 cells, when compared with the DMEM control (1402EtL, 1406EAL, 1412EtB and 1418EtL; all $p \leq 0.0001$; Figure 3.1). Increased CXCL8 production was detected at a range of concentrations; both 100 and 50µg/ml of 1402EtL; 50µg/ml of 1406EAL; 100µg/ml of 1412EtB; and 50, 25, 12.5, 6.25 and 3.125µg/mL for 1418EtL. The effect of 1402EtL on CXCL8 output was dose-dependent ($R^2 = 0.9044$). Nine showed possible inhibitory effects (1404EtL, 1407EtL, 1409EtL, 1412EtL, 1413EtL, 1418EtL, 1419EtB and 1419EtL $p \leq 0.0001$; 1406EtL $p \leq 0.01$). These inhibitory effects were judged as a reduction in CXCL8 output relative to the DMEM control that appeared statistically significant. Putative inhibitors were further assayed for inhibitory activity in section 3.2.3.

A.

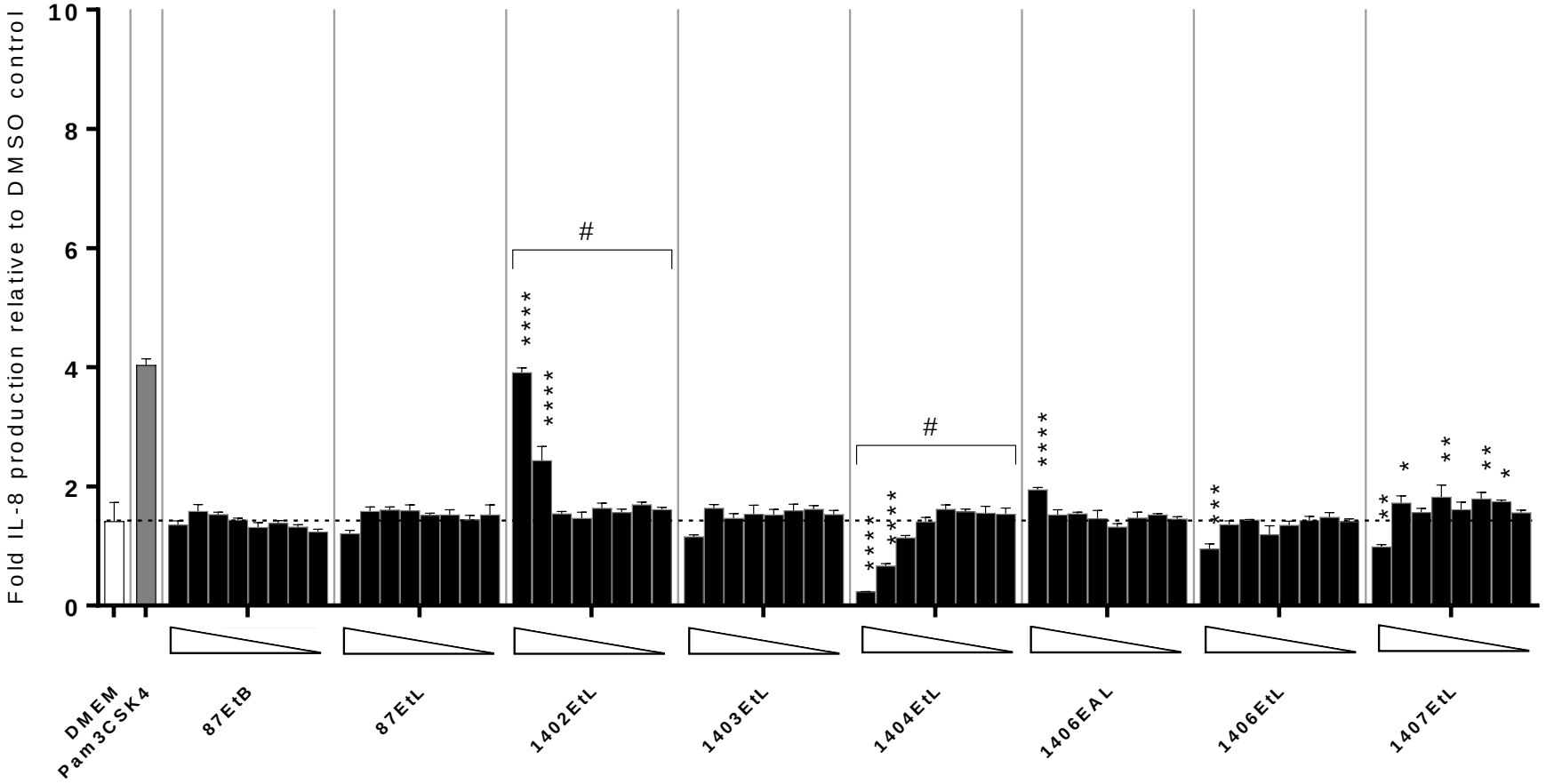


Figure 3.2.A. TLR2/1 screening results. HEK293-TLR1/2 cells were incubated for 48h with the extracts at twofold serial dilutions between 100 and 0.78125µg/ml. Ginseng extract was included as a plant-derived control at the same concentration as CftF extracts. Thereafter CXCL8 production was quantified by supernatant ELISA. CXCL8 production is shown relative to DMSO control. The dashed line indicates the CXCL8 readout for the negative control. Readings shown are means +/- SD of triplicate wells. Results were tested for significant differences using two-way ANOVA; * $p \leq 0.05$; ** $p \leq 0.01$; *** $p \leq 0.001$; **** $p \leq 0.0001$; tested for dose-dependency using non-linear one phase decay regression; # $R^2 \geq 0.9$

B.

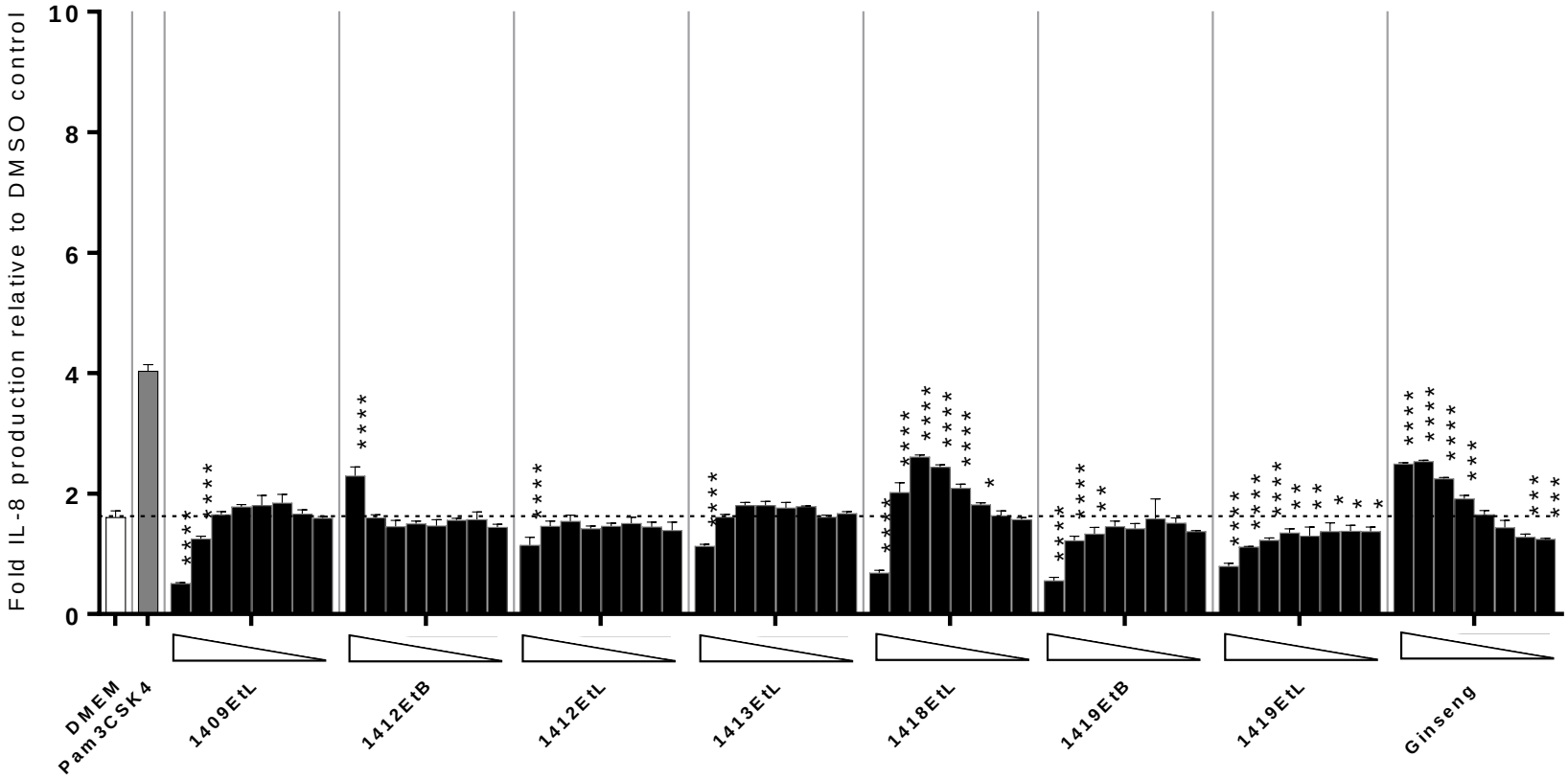


Figure 3.2.B. TLR2/1 screening results. HEK293-TLR1/2 cells were incubated for 48h with the extracts at twofold serial dilutions between 100 and 0.78125µg/ml. Ginseng extract was included as a plant-derived control at the same concentration as CftF extracts. Thereafter CXCL8 production was quantified by supernatant ELISA. CXCL8 production is shown relative to DMSO control. The dashed line indicates the CXCL8 readout for the negative control. Readings shown are means +/- SD of triplicate wells. Results were tested for significant differences using two-way ANOVA; * $p \leq 0.05$; ** $p \leq 0.01$; *** $p \leq 0.001$; **** $p \leq 0.0001$; tested for dose-dependency using non-linear one phase decay regression; # $R^2 \geq 0.9$

C.

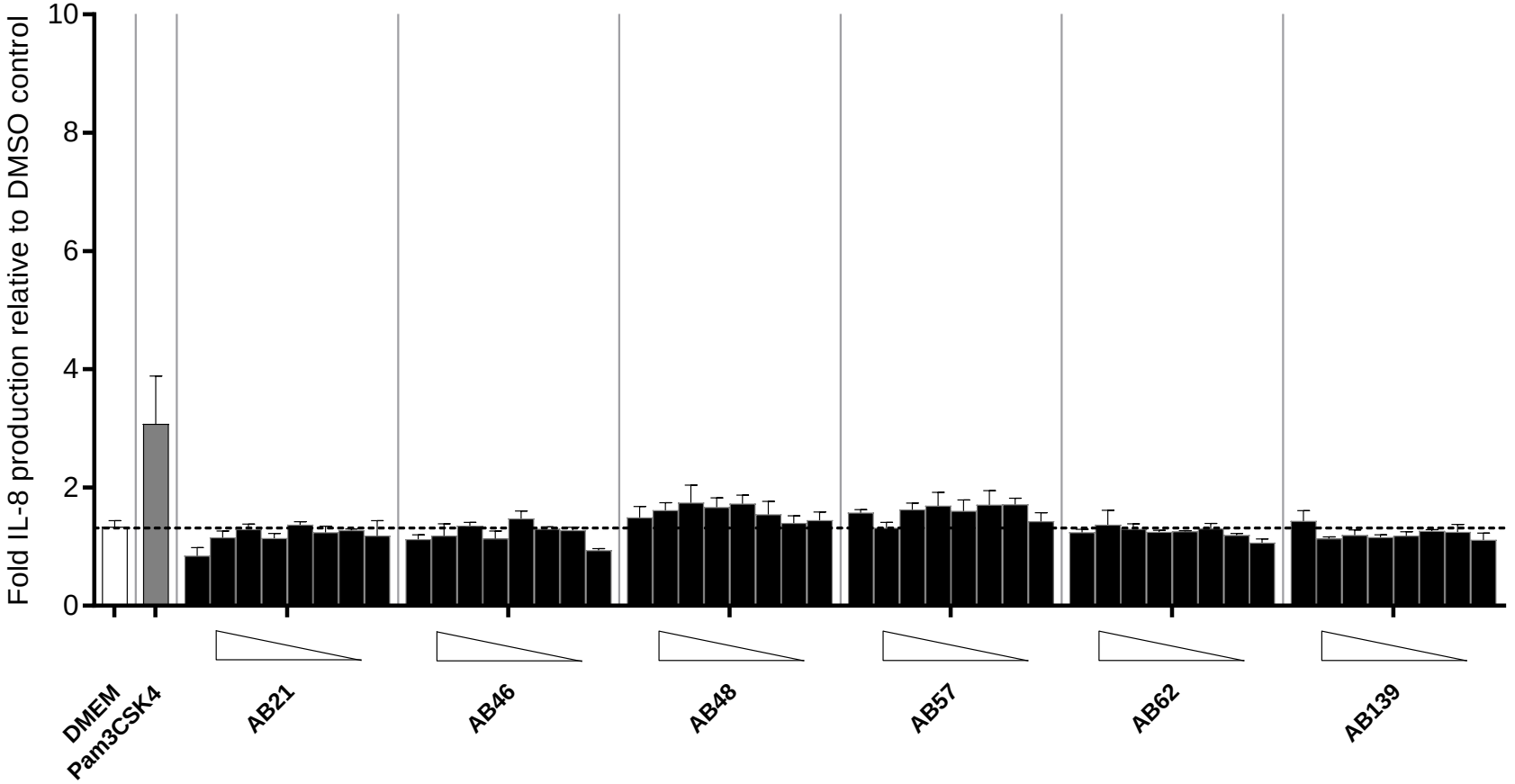


Figure 3.2.C. TLR2/1 screening results. HEK293-TLR1/2 cells were incubated for 48h with the extracts at twofold serial dilutions between 100 and 0.78125µg/ml for CftF extracts (panels A and B) or between 40µM and 312.5nM for Plant Sciences extracts (panel C). Ginseng extract was included as a plant-derived control at the same concentration as CftF extracts. Thereafter CXCL8 production was quantified by supernatant ELISA. CXCL8 production is shown relative to DMSO control. The dashed line indicates the CXCL8 readout for the negative control. Readings shown are means +/- SD of triplicate wells. Results were tested for significant differences using two-way ANOVA; * $p \leq 0.05$; ** $p \leq 0.01$; *** $p \leq 0.001$; **** $p \leq 0.0001$; tested for dose-dependency using non-linear one phase decay regression; # $R^2 \geq 0.9$

Three extracts showed statistically significant increases in CXCL8 production by HEK293-TLR2/6 cells when compared with the DMEM control (1402EtL, 1406EAL and 1412EtB; all $p \leq 0.0001$; Figure 3.3). Increased CXCL8 production was stimulated at both 100 and 50µg/ml of 1402EtL and 1412EtB, and 50µg/ml of 1406EAL. 1412EtB's activity was strongly dose dependent ($R^2 = 0.9114$). Nine of the extracts showed possible inhibitory effects (1404EtL, 1406EtL, 1407EtL, 1409EtL, 1413EtL, 1418EtL and $p \leq 0.0001$; 1419EtB $p \leq 0.01$; 87EtL, 1403EtL and 1413 EtL $p \leq 0.05$). These inhibitory effects were judged as a reduction in CXCL8 output relative to the DMEM control that appeared statistically significant. Putative inhibitors were further assayed for inhibitory activity in section 3.2.3.

A.

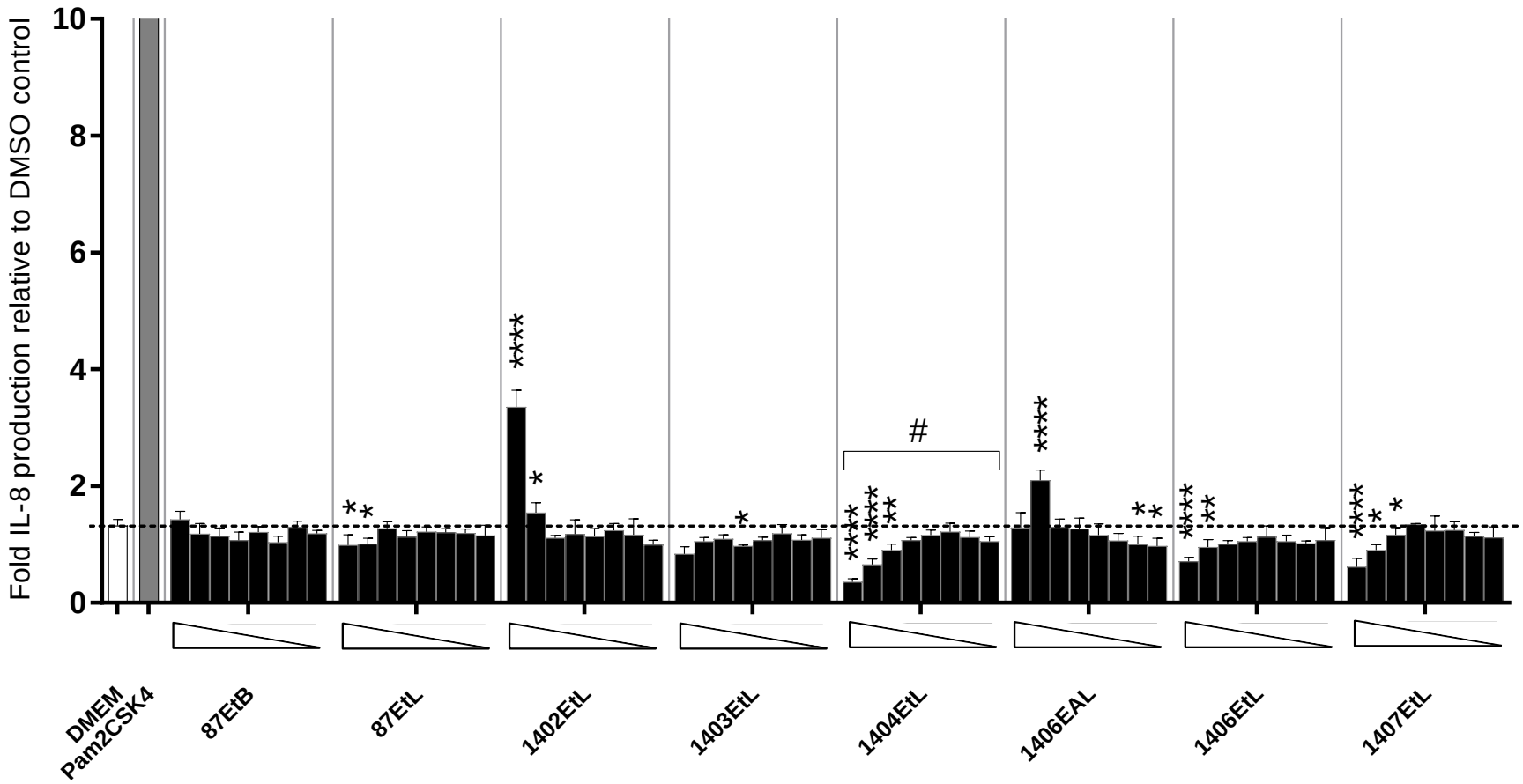


Figure 3.3.A. TLR2/6 screening results. HEK293-TLR2/6 cells were incubated for 48h with the extracts at twofold serial dilutions between 100 and 0.78125µg/ml for CftF extracts (panels A and B) or between 40µM and 312.5nM for Plant Sciences extracts (panel C). Ginseng extract was included as a plant-derived control at the same concentration as CftF extracts. Thereafter CXCL8 production was quantified by supernatant ELISA. CXCL8 production is shown relative to DMSO control. The dashed line indicates the CXCL8 readout for the negative control. Readings shown are means +/- SD of triplicate wells. Results were tested for significant differences using two-way ANOVA; * $p \leq 0.05$; ** $p \leq 0.01$; *** $p \leq 0.001$; **** $p \leq 0.0001$; tested for dose-dependency using non-linear one phase decay regression; # $R^2 \geq 0.9$

B.

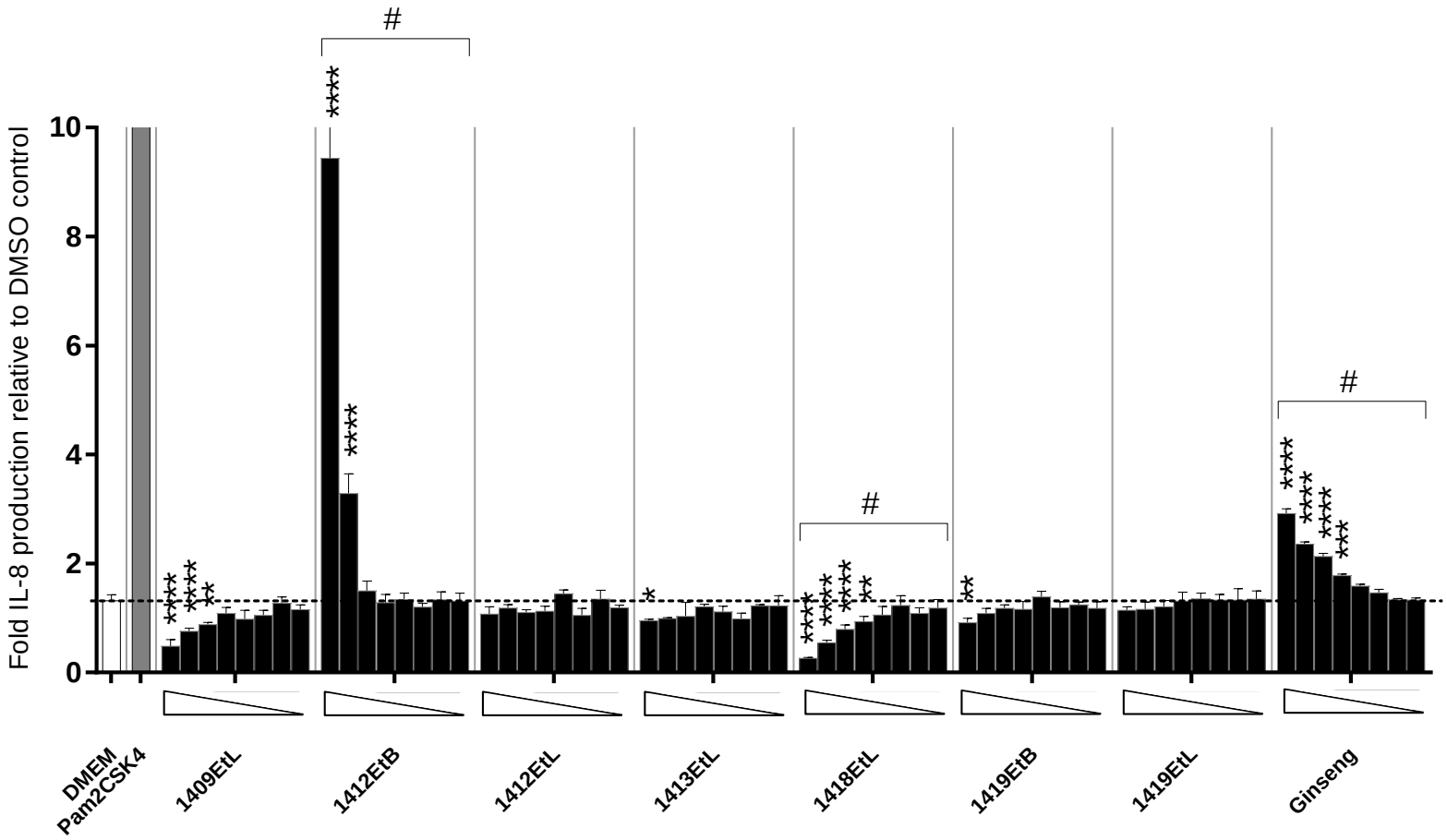


Figure 3.3.B. TLR2/6 screening results. HEK293-TLR2/6 cells were incubated for 48h with the extracts at twofold serial dilutions between 100 and 0.78125µg/ml for CftF extracts (panels A and B) or between 40µM and 312.5nM for Plant Sciences extracts (panel C). Ginseng extract was included as a plant-derived control at the same concentration as CftF extracts. Thereafter CXCL8 production was quantified by supernatant ELISA. CXCL8 production is shown relative to DMSO control. The dashed line indicates the CXCL8 readout for the negative control. Readings shown are means +/- SD of triplicate wells. Results were tested for significant differences using two-way ANOVA; * $p \leq 0.05$; ** $p \leq 0.01$; *** $p \leq 0.001$; **** $p \leq 0.0001$; tested for dose-dependency using non-linear one phase decay regression; # $R^2 \geq 0.9$

C.

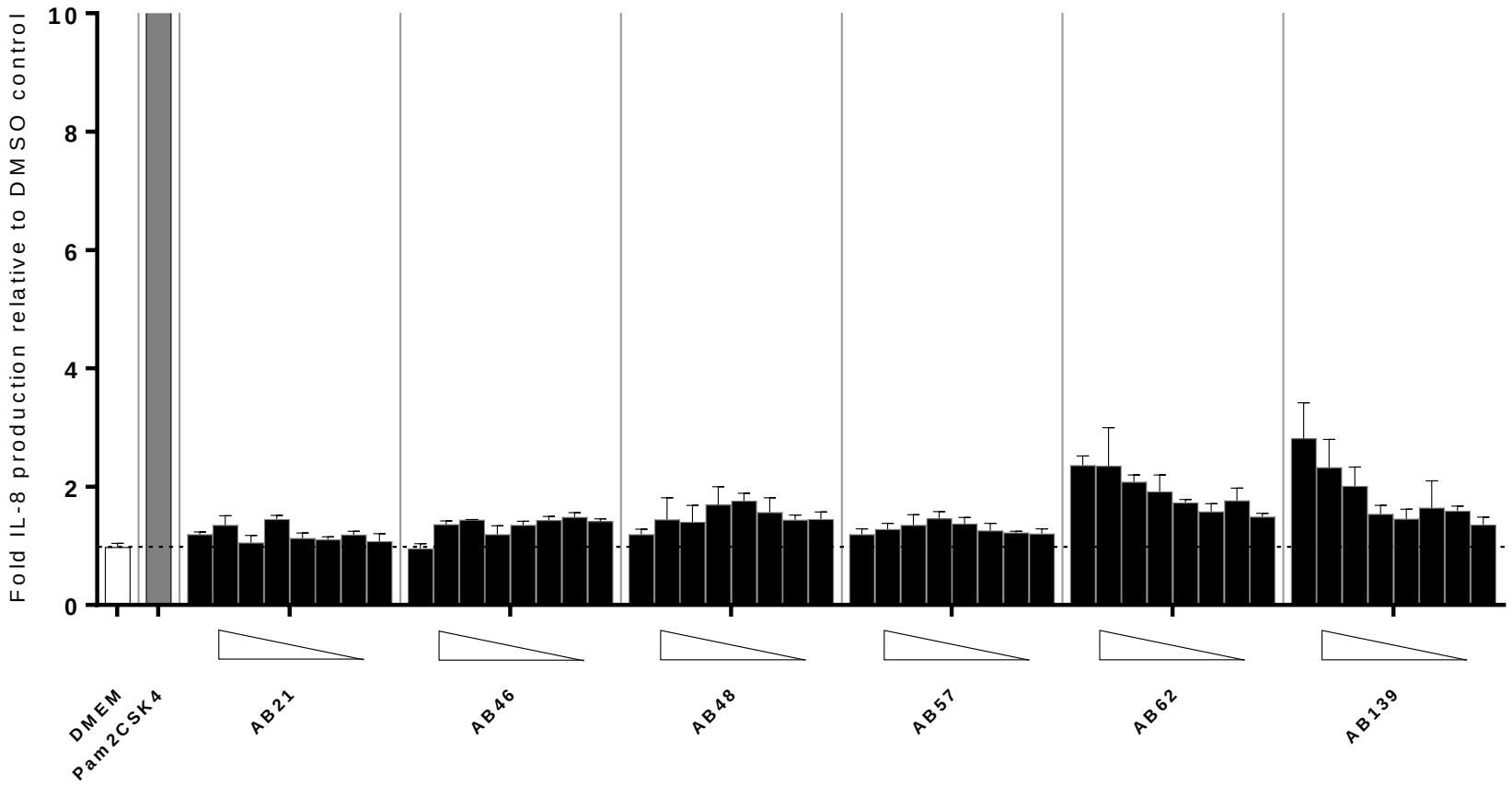


Figure 3.3.C. TLR2/6 screening results. HEK293-TLR2/6 cells were incubated for 48h with the extracts at twofold serial dilutions between 100 and 0.78125µg/ml for CftF extracts (panels A and B) or between 40µM and 312.5nM for Plant Sciences extracts (panel C). Ginseng extract was included as a plant-derived control at the same concentration as CftF extracts. Thereafter CXCL8 production was quantified by supernatant ELISA. CXCL8 production is shown relative to DMSO control. The dashed line indicates the CXCL8 readout for the negative control. Readings shown are means +/- SD of triplicate wells. Results were tested for significant differences using two-way ANOVA; * $p \leq 0.05$; ** $p \leq 0.01$; *** $p \leq 0.001$; **** $p \leq 0.0001$; tested for dose-dependency using non-linear one phase decay regression; # $R^2 \geq 0.9$

100µg/ml 1402EtL showed statistically significant dose-dependent TLR4 stimulatory activity when compared with the DMEM control ($p \leq 0.0001$; $R^2 = 0.9114$; Figure 3.4). Fourteen showed possible inhibitory effects (87EtL, 1404EtL, 1409EtL, 1418EtL, 1419EtL, AB139 $p \leq 0.0001$; 1407EtL, 1419EtB $p \leq 0.001$; 87EtB, 1413EtL, 1412EtL, 1413EtL $p \leq 0.01$; 1406EtL, 1412EtB $p \leq 0.05$). These inhibitory effects were judged as a reduction in CXCL8 output relative to the DMEM control that appeared statistically significant. Putative inhibitors were further assayed for inhibitory activity in section 3.2.3.

A.

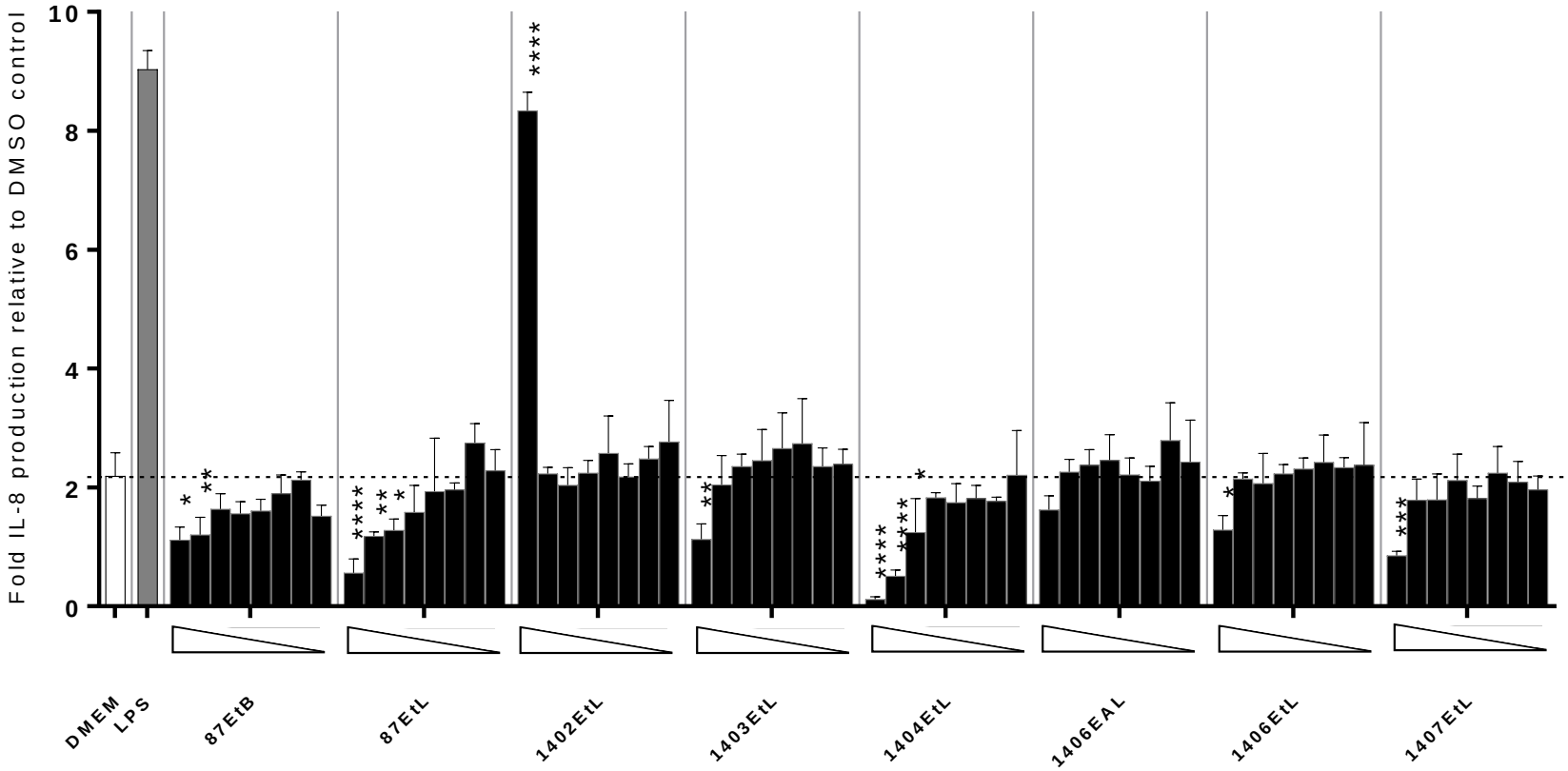


Figure 3.4.A. TLR4 screening results. HEK293-TLR4-MD2-CD14 cells were incubated for 48h with the extracts at twofold serial dilutions between 100 and 0.78125µg/ml for CftF extracts (panels A and B) or between 40µM and 312.5nM for Plant Sciences extracts (panel C). Ginseng extract was included as a plant-derived control at the same concentration as CftF extracts. Thereafter CXCL8 production was quantified by supernatant ELISA. CXCL8 production is shown relative to DMSO control. The dashed line indicates the CXCL8 readout for the negative control. Readings shown are means +/- SD of triplicate wells. Results were tested for significant differences using two-way ANOVA; * $p \leq 0.05$; ** $p \leq 0.01$; *** $p \leq 0.001$; **** $p \leq 0.0001$; tested for dose-dependency using non-linear one phase decay regression; # $R^2 \geq 0.9$

B.

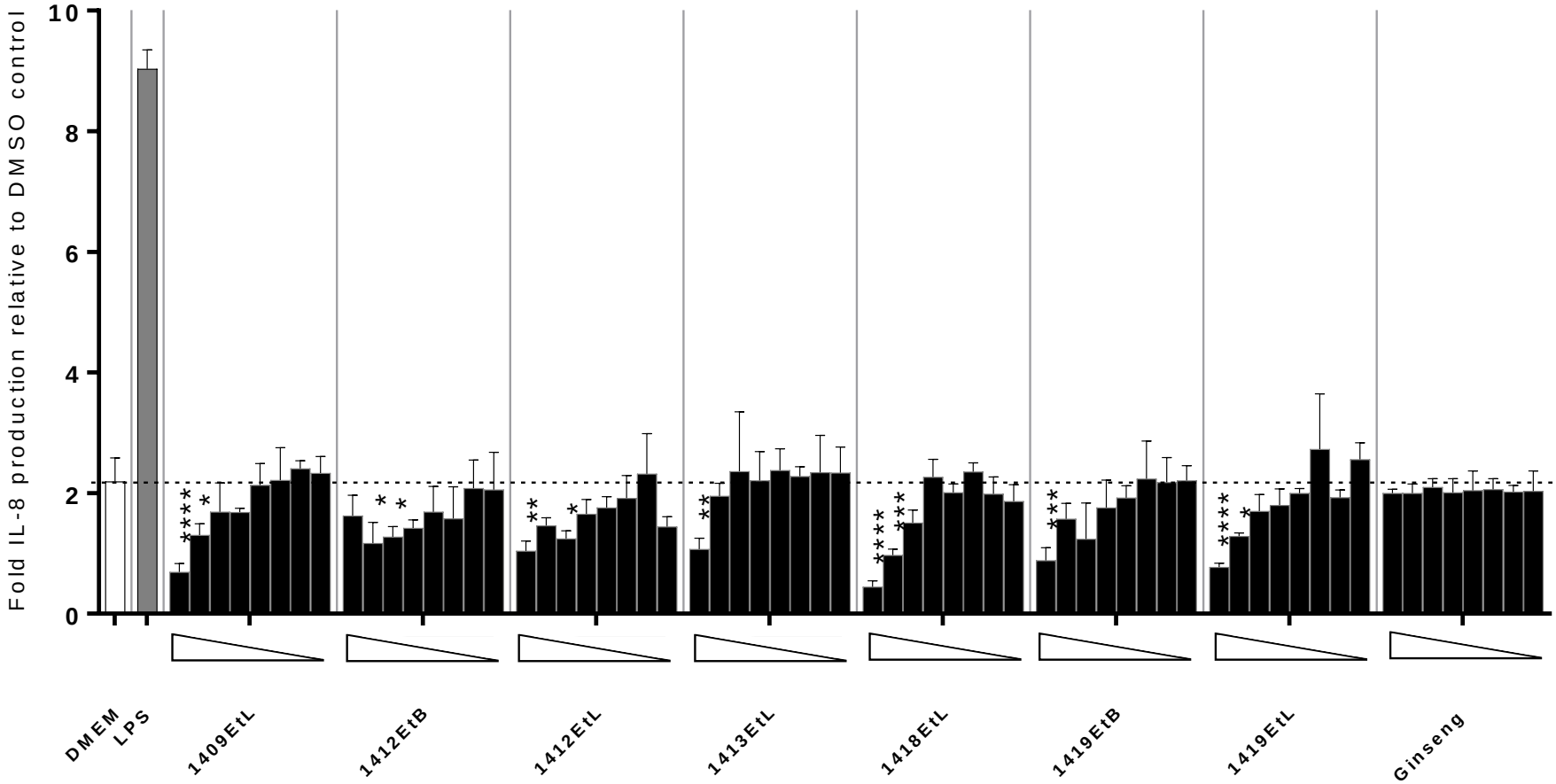


Figure 3.4.B. TLR4 screening results. HEK293-TLR4-MD2-CD14 cells were incubated for 48h with the extracts at twofold serial dilutions between 100 and 0.78125µg/ml for CftF extracts (panels A and B) or between 40µM and 312.5nM for Plant Sciences extracts (panel C). Ginseng extract was included as a plant-derived control at the same concentration as CftF extracts. Thereafter CXCL8 production was quantified by supernatant ELISA. CXCL8 production is shown relative to DMSO control. The dashed line indicates the CXCL8 readout for the negative control. Readings shown are means +/- SD of triplicate wells. Results were tested for significant differences using two-way ANOVA; * $p \leq 0.05$; ** $p \leq 0.01$; *** $p \leq 0.001$; **** $p \leq 0.0001$; tested for dose-dependency using non-linear one phase decay regression; # $R^2 \geq 0.9$

C.

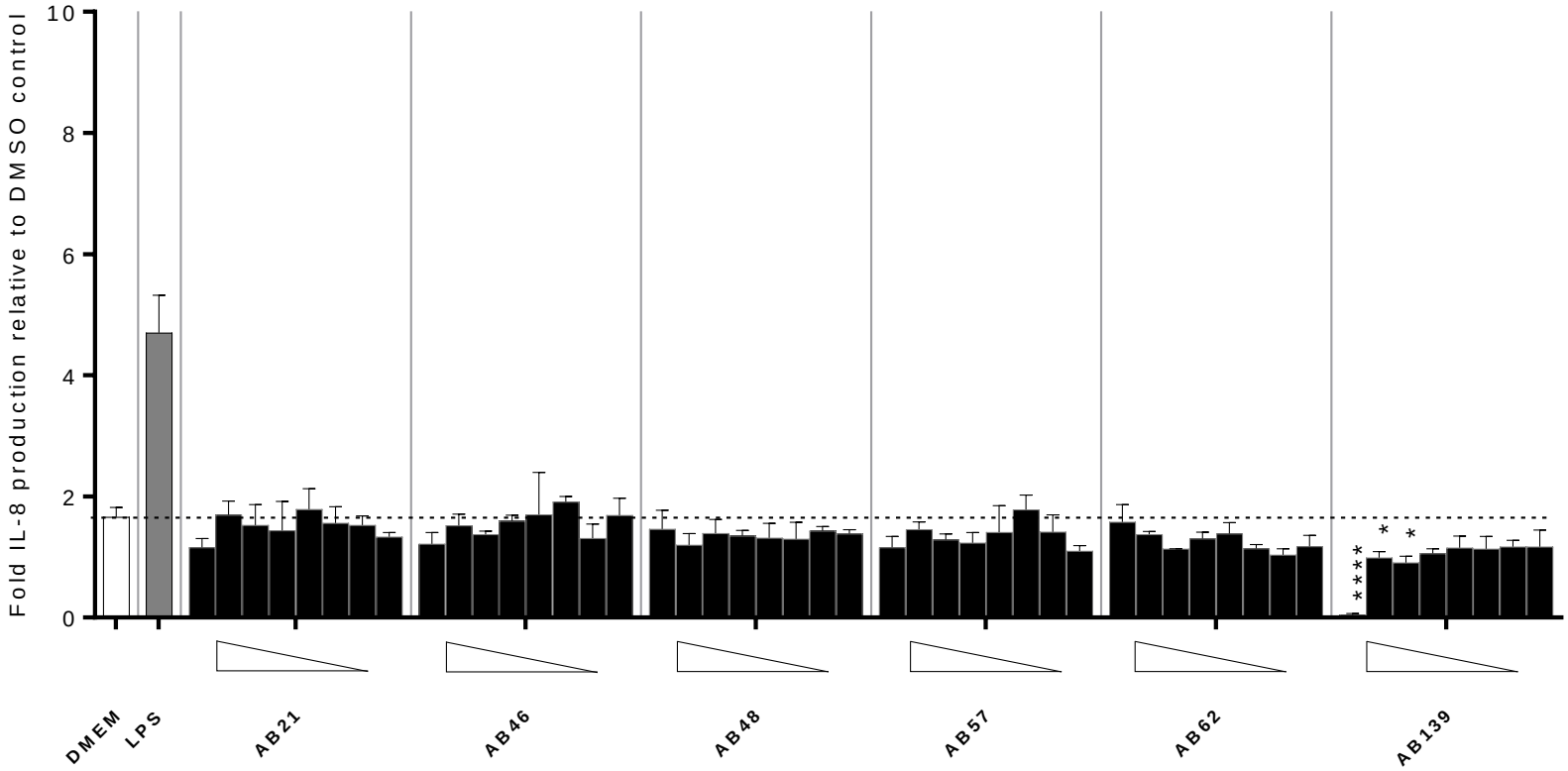


Figure 3.4.C. TLR4 screening results. HEK293-TLR4-MD2-CD14 cells were incubated for 48h with the extracts at twofold serial dilutions between 100 and 0.78125µg/ml for CftF extracts (panels A and B) or between 40µM and 312.5nM for Plant Sciences extracts (panel C). Ginseng extract was included as a plant-derived control at the same concentration as CftF extracts. Thereafter CXCL8 production was quantified by supernatant ELISA. CXCL8 production is shown relative to DMSO control. The dashed line indicates the CXCL8 readout for the negative control. Readings shown are means +/- SD of triplicate wells. Results were tested for significant differences using two-way ANOVA; * $p \leq 0.05$; ** $p \leq 0.01$; *** $p \leq 0.001$; **** $p \leq 0.0001$; tested for dose-dependency using non-linear one phase decay regression; # $R^2 \geq 0.9$

Screening using HEK393-TLR5 cells yielded highly inconsistent and unreliable data (Figure 3.5). Positive stimulation of TLR5 transfected cells with Fla-ST yielded significant induction of CXCL8 and the negative control treatment did not produce large quantities of CXCL8, however when treated with our plant extracts there was little dose pattern visible in terms of CXCL8 responses nor was there consistency in the levels produced by each dose of extract. Therefore we chose to conduct no further investigation using this cell line.

A.

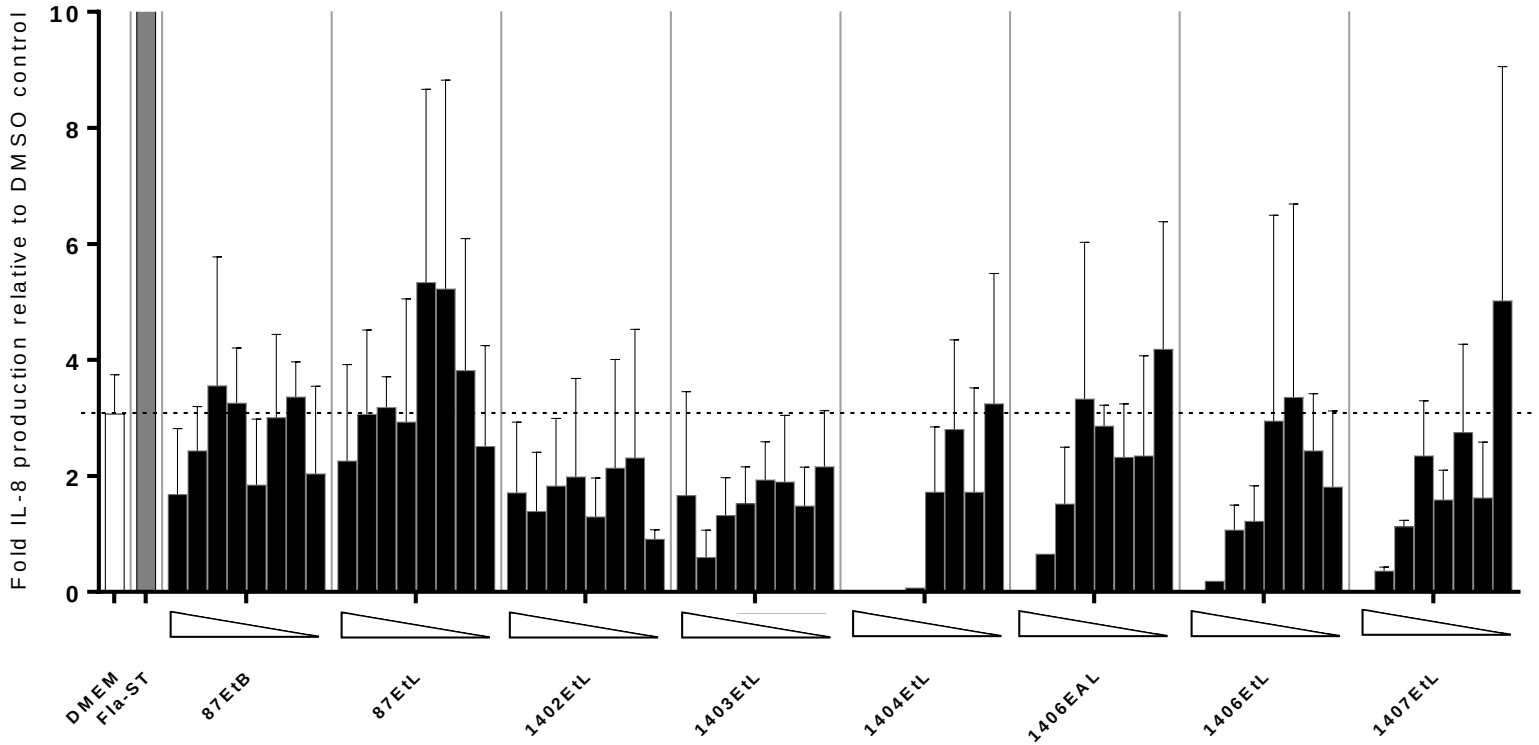


Figure 3.5.A. TLR5 screening results. HEKBlue-TLR5 cells were incubated for 48h with the extracts at twofold serial dilutions between 100 and 0.78125µg/ml. Thereafter CXCL8 production was quantified by supernatant ELISA. CXCL8 production is shown relative to DMSO control. The dashed line indicates the CXCL8 readout for the negative control. Readings shown are means +/- SD of triplicate wells. Results were tested for significant differences using two-way ANOVA; * $p \leq 0.05$; ** $p \leq 0.01$; *** $p \leq 0.001$; **** $p \leq 0.0001$; tested for dose-dependency using non-linear one phase decay regression; tested for dose-dependency using non-linear one phase decay regression; tested for dose-dependency using nonlinear one phase decay regression; # $R^2 \geq 0.9$

B.

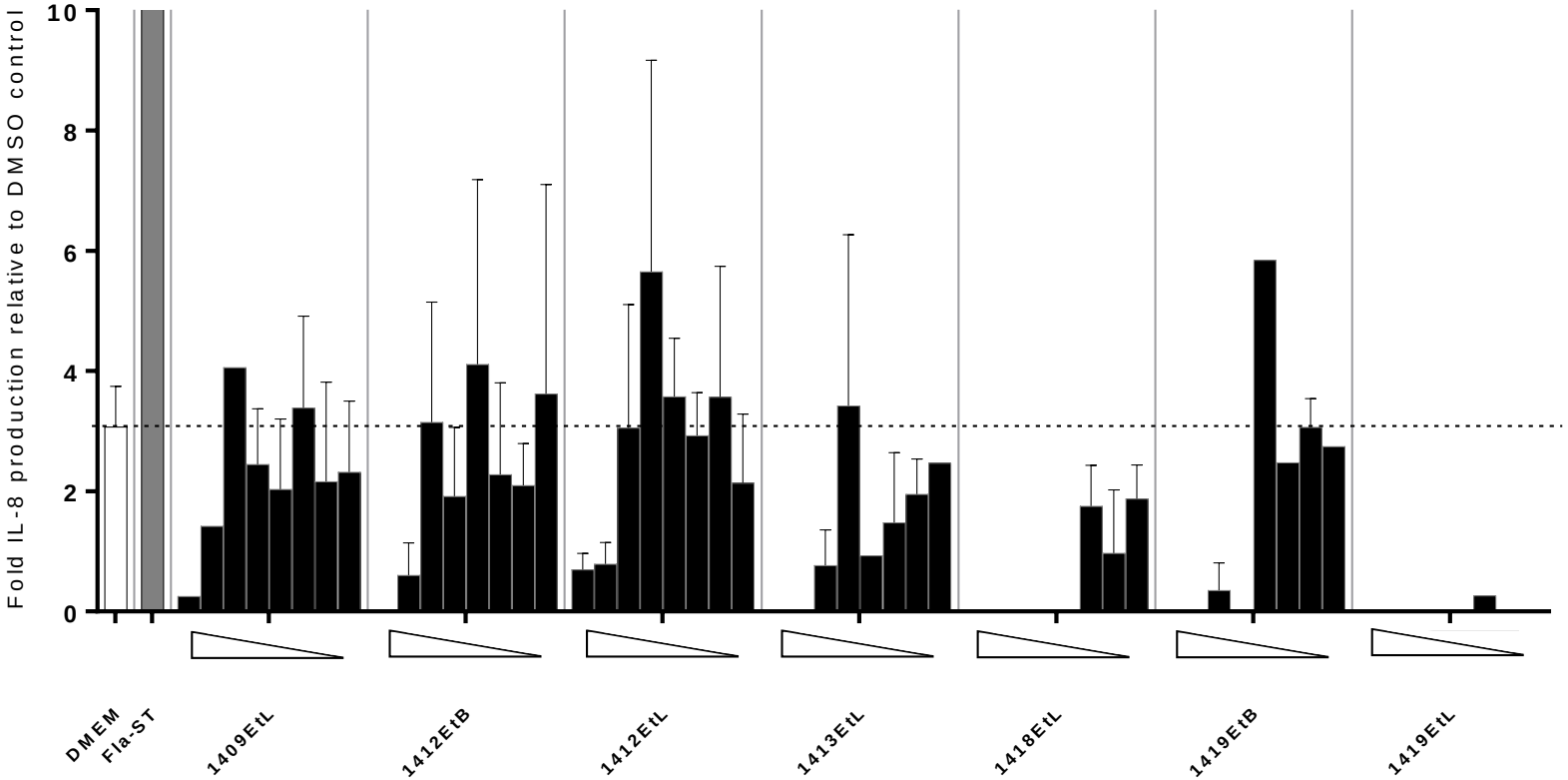


Figure 3.5.B. TLR5 screening results. HEKBlue-TLR5 cells were incubated for 48h with the extracts at twofold serial dilutions between 100 and 0.78125µg/ml. Thereafter CXCL8 production was quantified by supernatant ELISA. CXCL8 production is shown relative to DMSO control. The dashed line indicates the CXCL8 readout for the negative control. Readings shown are means +/- SD of triplicate wells. Results were tested for significant differences using two-way ANOVA; * $p \leq 0.05$; ** $p \leq 0.01$; *** $p \leq 0.001$; **** $p \leq 0.0001$; tested for dose-dependency using non-linear one phase decay regression; tested for dose-dependency using non-linear one phase decay regression; tested for dose-dependency using nonlinear one phase decay regression; # $R^2 \geq 0.9$

3.2.3 Inhibition of HEK293 TLR cells with plant extracts

Extracts which resulted in a reduced baseline CXCL8 output in stimulation assays were tested for inhibition of ligand-induced TLR activity, with 40μM parthenolide as an inhibition positive control. Five extracts showed statistically significant TLR2/6 inhibitory activity when compared with the Pam3CSK4 control (1404EtL, 1409EtL, and 1419EtB $p \leq 0.0001$; 1407EtL and 1413EtL $p \leq 0.01$; Figure 3.6). Inhibition was detected at both 100 and 50μg/ml of 1404EtL and 1419EtB, and 100μg/ml of 1407EtL, 1409EtL and 1413EtL.

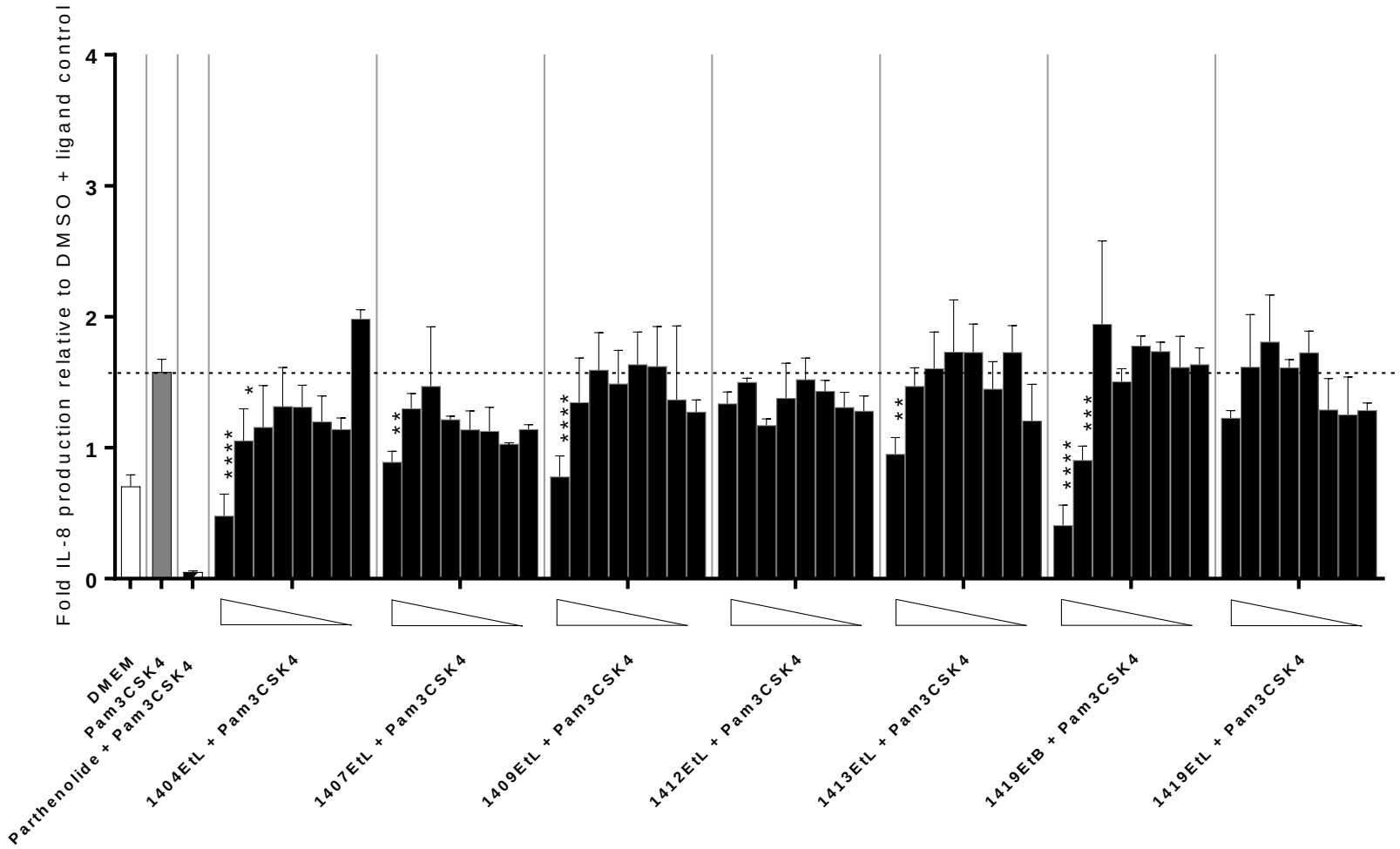


Figure 3.6. TLR2/1 inhibition screening results. HEK293-TLR1/2 cells were incubated for 48h the extracts at twofold serial dilutions between 100 and 0.78125µg/ml as well as with 10ng/ml Pam3CSK4. After 48h CXCL8 production was quantified by supernatant ELISA. CXCL8 production is shown relative to a Pam3CSK4 + DMSO solvent control. The dashed line indicates the CXCL8 readout for the Pam3CSK4 stimulation-only control. Parthenolide + Pam3CSK4 treatment was included to provide a strong inhibitory control. Readings shown are means +/- SD of triplicate wells. Results were tested for significant differences using two-way ANOVA; * $p \leq 0.05$; ** $p \leq 0.01$; *** $p \leq 0.001$; **** $p \leq 0.0001$; tested for dose-dependency using non-linear one phase decay regression; # $R^2 \geq 0.9$

All seven extracts showed statistically significant TLR2/6 inhibitory activity when compared with the Pam2CSK4 control (87EtL, 1403EtL, 1404EtL, 1407EtL, 1409EtL and 1419EtB $p \leq 0.0001$; 1418EtL $p \leq 0.01$; Figure 3.7). Inhibition was detected at 100, 50, 25, 12.5, 6.25, 3.125, 1.5625µg/ml of 1407EtL; 100, 50, 25 and 12,5µg/ml of 1403EtL; 100, 50 and 25µg/ml of 1409Etl and 1419EtB; 100 and 50µg/ml of 87EtL and 1404EtL and 100µg/ml of 1418EtL.

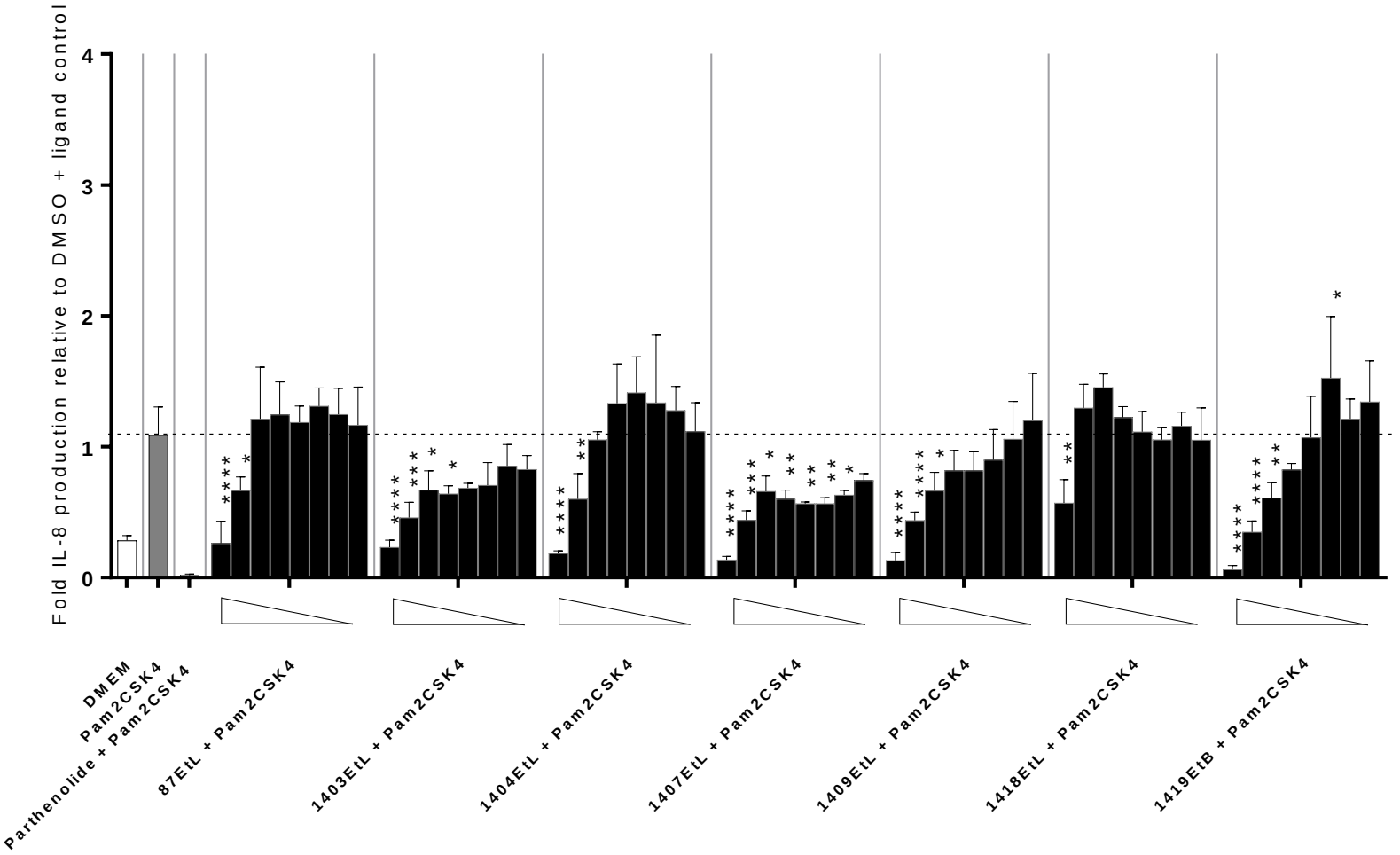


Figure 3.7. TLR2/6 inhibition screening results. HEK293-TLR2/6 cells were incubated for 48h with the extracts at twofold serial dilutions between 100 and 0.78125µg/ml as well as 10ng/ml Pam2CSK4. After 48h CXCL8 production was quantified by supernatant ELISA. CXCL8 production is shown relative to a Pam2CSK4 + DMSO solvent control. The dashed line indicates the CXCL8 readout for the Pam2CSK4 stimulation-only control. Parthenolide + Pam2CSK4 treatment was included to provide a strong inhibitory control. Readings shown are means +/- SD of triplicate wells. Results were tested for significant differences using two-way ANOVA; * $p \leq 0.05$; ** $p \leq 0.01$; *** $p \leq 0.001$; **** $p \leq 0.0001$; tested for dose-dependency using non-linear one phase decay regression; # $R^2 \geq 0$.

Seven extracts showed statistically significant TLR4 inhibitory activity when compared with the LPS control (87EtB, 1404EtL, 1409EtL, 1413EtL, 1418EtL and 1419EtB $p \leq 0.0001$; 1406EtL $p \leq 0.01$; Figure 3.8). Inhibition was detected at between 100 and 3.125µg/ml of 1409EtL; between 100 and 25µg/ml of 1404EtL; 100 and 50µg/ml of 1406EtL, 1418EtL and 1419EtL; and 100µg/ml of 87EtB and 1413EtL. The inhibitory effect of 1404EtL inhibitory effect was dose-dependent ($R^2 = 0.9686$).

A.

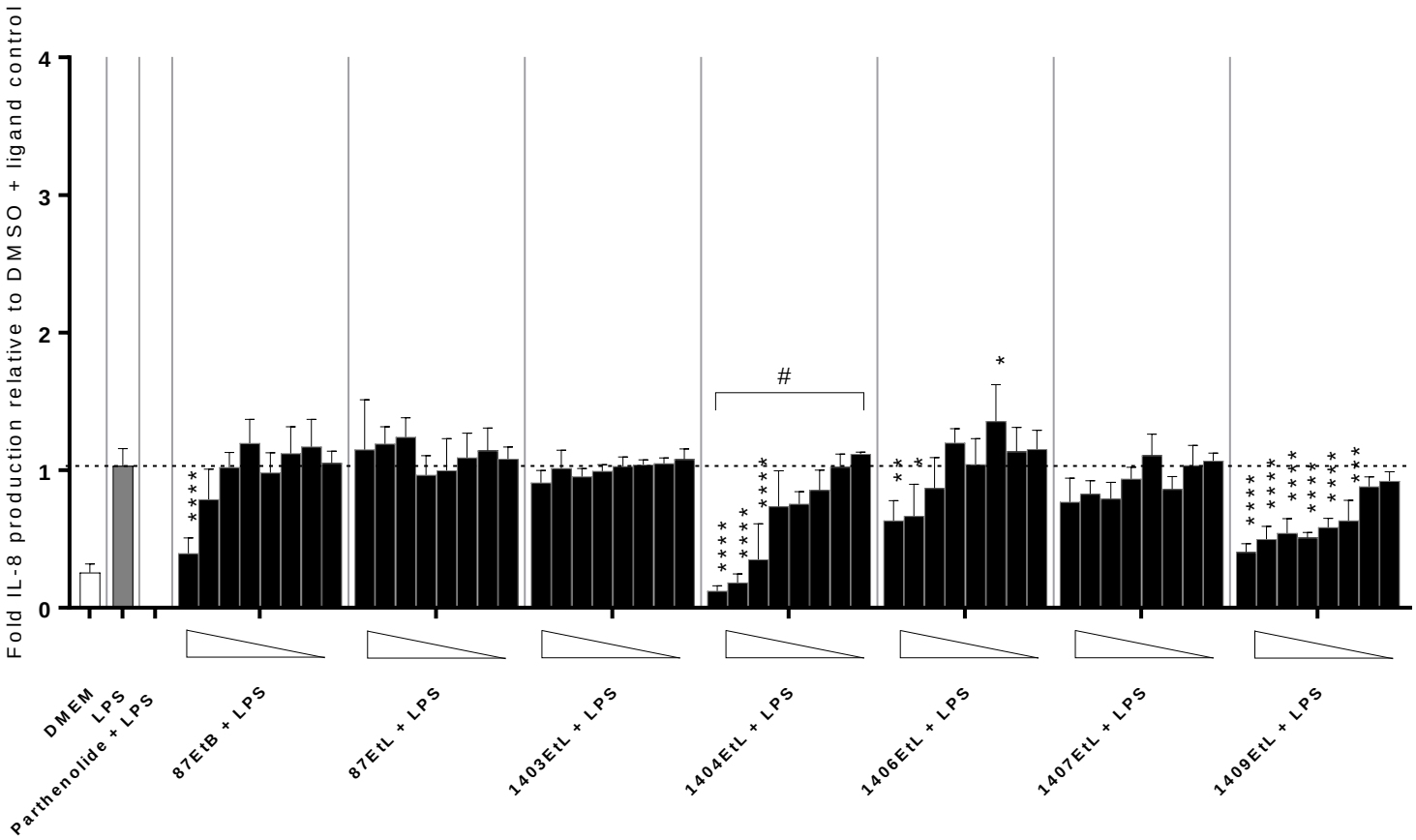


Figure 3.8.A. TLR4 inhibition screening results. HEK293-TLR4-MD2-CD14 cells were incubated for 48h with the extracts at twofold serial dilutions between 100 and 0.78125µg/ml as well as 200ng/ml LPS. After 48h CXCL8 production was quantified by supernatant ELISA. CXCL8 production is shown relative to a LPS + DMSO solvent control. The dashed line indicates the CXCL8 readout for the LPS stimulation-only control. Parthenolide + LPS treatment was included to provide a strong inhibitory control. Readings shown are means +/- SD of triplicate wells. Results were tested for significant differences using two-way ANOVA; * $p \leq 0.05$; ** $p \leq 0.01$; *** $p \leq 0.001$; **** $p \leq 0.0001$; tested for dose-dependency using non-linear one phase decay regression; # $R^2 \geq 0.9$

B.

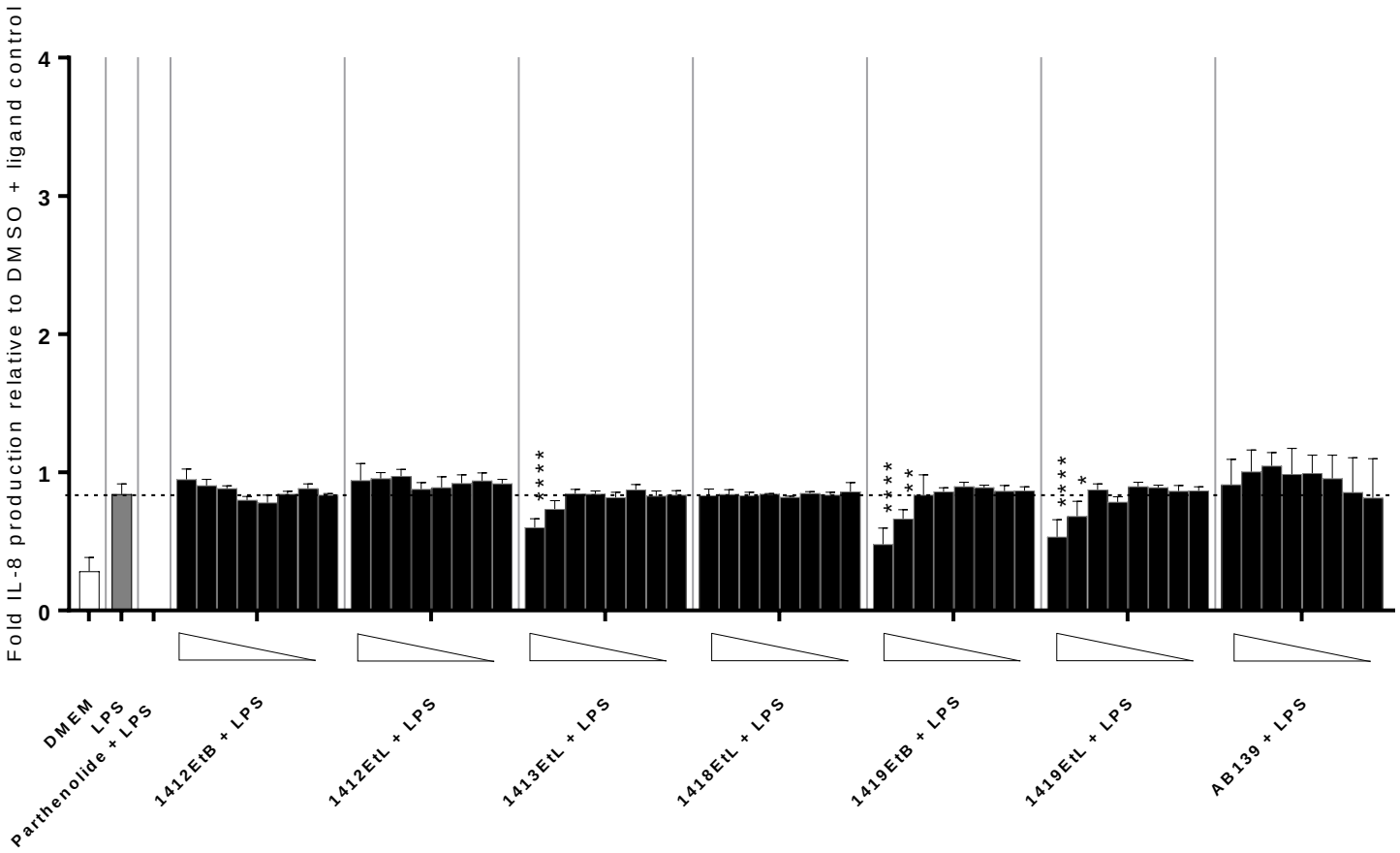


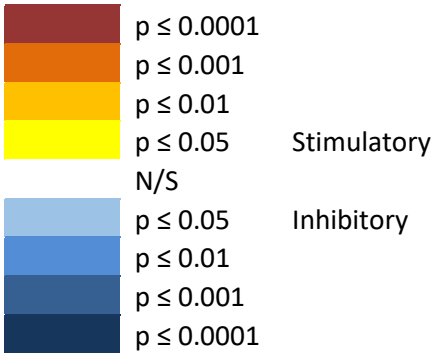
Figure 3.8.B. TLR4 inhibition screening results. HEK293-TLR4-MD2-CD14 cells were incubated for 48h with 200ng/ml LPS as well as either the CftF extracts at twofold serial dilutions between 100 and 0.78125µg/ml or Plant Sciences extract AB139 at dilutions between between 40µM and 312.5nM. After 48h CXCL8 production was quantified by supernatant ELISA. CXCL8 production is shown relative to a LPS + DMSO solvent control. The dashed line indicates the CXCL8 readout for the LPS stimulation-only control. Parthenolide + LPS treatment was included to provide a strong inhibitory control. Readings shown are means +/- SD of triplicate wells. Results were tested for significant differences using two-way ANOVA; * $p \leq 0.05$; ** $p \leq 0.01$; *** $p \leq 0.001$; **** $p \leq 0.0001$; tested for dose-dependency using non-linear one phase decay regression; # $R^2 \geq 0.9$

3.2.4 Summary

The extracts screened were found to have a variety of inhibitory and stimulatory effects on CXCL8 production in the HEK293-TLR cell lines tested. A summary heat map of screening results is provided below (Table 3.1).

Table 3.1. Summary heat map of screening results.

	Toxicity	TLR2/1	TLR2/6	TLR4
Ginseng	-	#	#	
87 EtB	-			
87 EtL	-			
1402 EtL	100ug/ml	#		
1403 EtL	-			
1404 EtL	-			#
1406 EAL	50ug/ml		50µg/ml	
1406 EtL	50ug/ml			
1407 EtL	-			
1409 EtL	-			
1412 EtB	100ug/ml		#	
1412 EtL	-			
1413 EtL	-			
1418 EtL	100ug/ml			
1419 EtB	100ug/ml			
1419 EtL	-			
AB21	-			
AB46	-			
AB48	-			
AB57	-			
AB62	-			
AB139	-			



Summary of stimulatory and inhibitory effects of the extracts tested on each cell line. Toxicity = minimum dose at which significant cytotoxicity is observed. # = dose-dependent effect ($R^2 \geq 0.9$). The lack of TLR4 stimulatory activity by the ginseng control can be accounted for by the fact that *P. ginseng* has been shown to reduce TLR4 activity (Peng et al. 2015; Nguyen & Rhee 2016).

3.3 Discussion

3.3.1 Cytotoxicity of plant extracts

Using LDH as a measure of cytotoxicity we first examined the extracts for any evidence of induced cell death/damage. The LDH assay was chosen because its colourimetric readout allows for rapid and accurate assessment of cell death without the time-consuming and subjective nature of assessing cell confluence and plaque formation by microscopy. A top concentration of 100µg/ml of plant extract was chosen because it provided a high maximum from which to dilute down through a wide range of concentrations. This also gave a final DMSO concentration of no more than 0.5% in the culture medium, which minimises cytotoxic effects from the solvent (Timm et al. 2013).

The results show that the majority of extracts from CftF are not cytotoxic at 100 or 50µg/ml. 1402EtL, 1412EtB, 1418EtL and 1419EtB are cytotoxic at 100 but not 50µg/ml, while 1406EAL and 1406EtL were toxic at both 100 and 50µg/ml. This will need to be taken into account later when interpreting and discussing the TLR modulation data.

The cause of the toxicity is unknown, but it could be due to metabolic choking of cells by high concentrations of exogenous molecules as 100µg/ml is a considerable level of foreign material. Upon fractionation and refinement it is possible that this effect could be alleviated.

Another possibility is that some of the extracts themselves may contain actively cytotoxic or antiproliferative compounds. This hypothesis is supported by the fact that 1406EAL and 1406EtL, both extracts from the leaves of *E. petiolatus*, were toxic at both 100 and 50µg/ml. It is possible that *E. petiolatus* leaves contain a cytotoxic agent, as both alkaloids and saponins have been detected in chloroform extracts of *E. petiolatus* stem and leaf (Carrick et al. 1968). Both of these groups of compounds have the potential for cytotoxicity by a range of means, including disruption of membrane integrity, inhibition of cytoskeletal components,

DNA intercalation and inhibition of ribosomal protein synthesis (Wink 2007; Podolak et al. 2010). However, Kwon et al. (2012) tested the viability of RAW264.7 cells in the presence of an ethanolic extract of *E. petiolatus* bark at concentrations of up to 50µg/ml and found no significant reduction in viability at that concentration. The discrepancy between Kwon's results and ours could be due to differences between HEK293 and RAW264.7 cells, or between the chemical compositions of the leaves and bark of *E. petiolatus*.

Another extract, 1418EtL, is derived from *F. fistulosa*. Extracts derived from the bark of this species were shown to have antiproliferative effects on two human cancer cell lines (Yap et al. 2016), which could explain the reduced cell number observed here.

3.3.2 TLR5 data

The data from the TLR5 screen (Figure 3.5) were highly inconsistent and deemed unreliable, therefore no further investigation was carried out on this cell line. This could be due to the additional plasmid included in the HEKBlue TLR5 line not present in the HEK293 TLR lines, namely a SEAP reporter gene under the control of an NF-κB- and AP-1-inducible promoter. It is possible that this system interacted with the endogenous signalling pathways and confounded the CXCL8 response to TLR activity. The effects of exogenous plasmid DNA on TLR responses has been reported previously (Tamassia et al. 2012). It would be possible to use the SEAP reporter system found in the HEKBlue cell line to assess TLR activity, but this would not be directly comparable with the results from the HEK293 TLR cells. There was insufficient time and resources to obtain and re-screen a HEK293 TLR5 cell line. This could prove a worthwhile avenue of investigation in future.

3.3.3 Extracts from CftF

Several of the extracts screened were found to stimulate or inhibit CXCL8 production in HEK293-TLR cells. A summary heat map of screening results is provided in the previous section (Table 3.1).

1402EtL was found to be cytotoxic at 100µg/ml but not at 50µg/ml, which could explain the increased TLR4 activity detected at 100µg/ml due to the release of TLR4-activating DAMPs rather than direct stimulation of the receptor by the plant extract. However, Erridge (2010) suggests that many of the endogenous compounds currently purported to directly activate TLR4 and TLR2 might actually be better described as PAMP-sensitising molecules (PSM). As the cells were cultured without LPS present this suggests that the observed effect is likely to be caused by the plant extract rather than PSM-PAMP synergy. The low CXCL8 output from the DMEM control supports this assertion. 1402EtL also strongly activated TLR2/1 and 2/6 at 100 and 50µg/ml. This effect is unlikely to be caused by cytotoxicity as the stimulatory effect was retained at non-cytotoxic concentrations, and the TLR2/1-stimulatory effect was dose-dependent. Given that the extract stimulated all three receptors under investigation it is conceivable that the same mode of action is responsible for all three effects. This could be due to promiscuous ligand-receptor binding, or the extract acting on the signalling pathway at a point downstream of the receptors themselves such as TIRAP. TIRAP is an adaptor molecule shared by TLR2/1, 2/6 and 4 due to homology in their TIR domains (Toshchakov et al. 2007) but no other TLRs. However, this is purely speculatory as we have not examined whether the extracts are able to cross the plasma membrane to reach signalling molecules such as TIRAP. It is also possible that the extract contains multiple distinct TLR modulators.

1412EtB showed strong dose-dependent TLR2/6 stimulatory activity, weak TLR2/1 stimulation and no effect on 4. TLR2/1 stimulation was only observed at 100µg/ml, a concentration found to be cytotoxic, so, as with 1402EtL's TLR4 activity, it is not entirely clear

whether this effect was due to or in spite of cytotoxic effects. By contrast, 1412EtL showed neither cytotoxicity nor TLR-modulatory activity.

1418EtL was cytotoxic at 100µg/ml but not at 50µg/ml. In the TLR2/1 cell line CXCL8 output was reduced at 100µg/ml but increased between 50 and 3.125µg/ml. This is likely to be the result of an interaction between a stimulatory effect and the cytotoxicity seen at 100µg/ml. TLR2/6 activity was inhibited at 100µg/ml and TLR4 at 100 and 50µg/ml. This could be due to cytotoxicity, although the effect on TLR4 was detectable at concentrations lower than those determined to be cytotoxic. These contrasting effects, combined with reported antiviral (Hafid et al. 2016), antifungal (Subramaniam et al. 2009) and antiplasmodial (Zhang et al. 2002) activities suggest that *F. fistulosa* has a range of bioactive components and would be a promising candidate for further investigation.

1404EtL demonstrated strong dose-dependent inhibitory effects on TLR2/1 and 2/6 inhibition at 100 and 50µg/ml, and dose-dependent TLR4 between 100 and 25µg/ml. As with the stimulatory effects of 1402EtL, it is possible that the same mechanism underlies all three inhibitory effects. It is possible that 1404EtL contains a general TLR ligand binding competitor, or that it inhibits a common downstream link in the signalling pathway such as MyD88 or NF-κB. Alternatively, the extract could contain multiple distinct inhibitors of TLR function. No cytotoxicity was detected so this can be disregarded as a cause of reduced CXCL8 output in response to 1404EtL.

No cytotoxicity was detected in response to 1409EtL either, and this extract inhibited TLR2/1 at 100µg/ml, TLR2/6 between 100 and 25µg/ml and TLR4 between 100 and 3.125µg/ml. As with 1404EtL, it is unknown whether these effects share a common mechanism or are caused by distinct components of the crude extract.

1407EtL inhibited TLR2/1 at 100µg/ml, and strongly inhibited TLR2/6 between 100 and 1.5625µg/ml. It is possible that the same component is responsible for both effects, with the presence TLR1 or 6 in the heterodimer influencing the degree of inhibition exerted.

Both 1406EAL and 1406EtL showed cytotoxic effects at both 100 and 50µg/ml. Stimulatory effects of 1406EAL on TLR2/1 at 100µg/ml and TLR2/6 at 50µg/ml could possibly be due to cytotoxicity and release of DAMPs. However, it is also possible that the effects detected were in spite of cell death, rather than because of it. 1406EtL inhibited TLR2/1 at 100µg/ml and TLR2/6 and 4 at 100 and 50µg/ml. As 1406EtL is cytotoxic at those doses it is possible that the reduction in CXCL8 output is purely due to reduction in cell population. It could, however, be a genuine inhibitory effect as an ethanolic extract of *E. petiolatus* bark has, as previously mentioned, been shown to inhibit COX-2 expresssion, phosphorylation of extracellular signal-ERK, JNK and p38, and NF-κB p65 translocation in RAW264.7 Mϕ (Kwon et al. 2012).

87EtB inhibited TLR4-dependent CXCL8 production at 100µg/ml, and 87EtL inhibited TLR2/6 activity at 100 and 50µg/ml. 87EtB and 87EtL are both derived from *Ficus schwarzii*, from the bark and leaves respectively. That each extract exhibited a different profile of activity suggests that there are distinct bioactive compounds present in each tissue.

Cytotoxic effects of 1419EtB were observed at 100µg/ml but not 50µg/ml. 1419EtB inhibited TLR2/1 and TLR4 at 100 and 50µg/ml, and TLR2/6 between 100 and 25µg/ml. These effects are unlikely to be purely due to cytotoxicity as they were detected at concentrations below cytotoxic levels. 1419EtL retained the TLR4 inhibitory effects but did not modulate TLR2/1 or 2/6 function. This suggests that different bioactive compounds are responsible for the TLR2- and TLR4-modulatory effects, and that the TLR2 modulator is found in the bark but not in the leaves of *Ficus variegata*.

1403EtL specifically inhibited TLR2/6-mediated CXCL8 production between 100 and 12.5µg/ml.

1413EtL weakly inhibited all three cell lines at 100µg/ml. No cytotoxicity was detected, so it is possible that this is a genuine inhibitory effect. However, even at 100µg/ml the effect is so small that its biological relevance is questionable; extensive purification would be required prior to any further testing.

3.3.4 Extracts from Plant Sciences Dept., Nottingham

Dr. Bottley confirmed that the extract fractions provided were not cytotoxic at the doses used. No statistically significant TLR-modulatory activity was detected in any of the HEK293 TLR cell lines. This was reported to Dr. Bottley for use in his study, and no further work was carried out on these extracts in this study.

3.3.5 Conclusions

We have identified a number of candidates which display either stimulatory or inhibitory activity, however at this stage discussion of any possible mechanism for the observed effects is largely speculatory, as there are no data concerning the exact chemical composition of the extracts. In the following chapter we attempt to characterise some of these extracts to identify their active components. Due to time restrictions it was decided that hereafter the analysis should focus on one TLR only. TLR2/6 was selected for several reasons. Firstly, it exhibited a range of strong stimulatory and inhibitory responses to various extracts which were reliably repeatable. Secondly, it is expressed in both human and murine B lymphocytes (Bekeredjian-Ding & Jego 2009) and stimulation of TLR2/6 leads to proliferation and increased frequency of IgM+ and IgG+ cells independently of any accessory cells (Borsutzky et al. 2005). B cells are a useful target *in vivo* for applications such as vaccine adjuvants and in treatment of various autoimmune disorders (Blüml et al. 2013; Chan et al. 2013), and compared to other TLR-expressing populations such as dendritic cells are relatively simple to isolate for *in vitro* experimentation. In addition, there has been demonstrable success in the use of TLR agonists such as CpG ODN as B cell-mediated vaccine adjuvants (Vollmer 2005).

Of the extracts found to stimulate TLR2/6, 1406EAL was not selected because of its cytotoxicity at 50µg/ml. The remaining two stimulatory extracts, 1402EtL (*Tristaniopsis merguensis* ethanolic leaf extract) and 1412EtB (*Ficus ribes* ethanolic bark extract), were carried forward. For contrast, one inhibitory extract was selected as well. 1404EtL (*Gironniera nervosa* ethanolic leaf extract) was selected because its wide range of TLR inhibition means that, if successful, it could potentially have a variety of therapeutic applications.

There remain a number of promising candidates within this screen with either stimulatory or inhibitory effects on TLR2/1, 2/6 or 4. These would certainly merit further investigation, given time, as they could possibly contain valuable immunomodulatory compounds. It would also be illuminating to re-screen the extracts against a singly-transfected HEK293 TLR5 line, as well as investigating the effects on the intracellular TLRs TLR3, 7, 8 and 9.

Chapter 4. Chemical and size characterisation of putative TLR ligands in three plant extracts

4.1 Introduction

Having identified and selected three crude plant extracts with TLR2/6-modulatory activity, our subsequent step should be to characterise the active component or components responsible for the observed effects. This is important because if these products are to have a clinical *in vivo* use the precise compositions of which compounds are eliciting the effects observed must be known, and by what mechanisms they operate. If the active component can be isolated and characterised entirely this would enable structural analysis to be carried out. This could possibly identify alternative or *de novo* synthesis pathways so that the ligand can be obtained without the need to deplete wild populations of the plants of origin or occupy valuable land resources for their sylviculture. One example of this is the Kolbe-Schmitt synthesis of salicylic acid (Lindsey & Jeskey 1957), the chemical precursor to aspirin which was originally obtained directly from the bark of the willow *S. alba*. Isolation of the active component also allows for modifications to be made to the molecule, enhancing its efficacy, safety or other desirable attributes. Such an approach led to the development of the Nobel Prize-winning broad-spectrum antiparasitic drug Ivermectin from the *Streptomyces avermitilis*-derived avermectin B_1 (Campbell et al. 1984; Van Voorhis et al. 2015).

The characterised PAMPs which bind TLR2/6 are mostly bacterial or fungal cell wall components, such as zymosan (Sato et al. 2003) lipomannan and phospholipomannan (LM; Dao et al. 2004; PLM; Jouault et al. 2003), lipoteichoic acid (LTA; von Aulock et al. 2003), peptidoglycan (PGN; Ozinsky et al. 2000) and mycoplasmal diacylated membrane lipopeptides such as macrophage-activating lipopeptide 2 (MALP-2; Takeuchi et al. 2001). A number of protozoan glycosylphosphatidylinositol (GPI) anchor molecules are also bound by

TLR2/6 (Gazzinelli & Denkers 2006). There are compositional commonalities between some TLR2/6 ligands, but none shared by all. For example LM, LTA, PGN and GPI all contain carbohydrate moieties (and zymosan is itself a carbohydrate), however the membrane lipopeptides do not. LM, LTA, lipopeptides and GPI all feature lipid components, but PGN does not. PGN and lipopeptides both contain peptide components, whereas LM, LTA and GPI do not. LTA and diacylated lipopeptides both have two lipid chains attached to a glycerol centre, which is in turn connected to a hydrophilic polymer (Jin et al. 2007). Uniquely among pathogenic microbes, many mycobacteria express glycopeptolipids on their surface, which feature carbohydrate, lipid and peptide components (Chatterjee & Khoo 2001). Glycopeptolipids have not been investigated in relation to TLRs but mycobacterial glycolipids such as LM are known to bind TLR2/6 (Dao et al. 2004) so it is conceivable that glycopeptolipids could do so too. These studies serve to demonstrate the compositional diversity of TLR2/6 ligands.

Sugawara et al. (2003) found that TLR6 knockout mice showed no significant difference from wild type individuals in their resistance to *M. tuberculosis* infection, whereas TLR2 knockout individuals showed decreased mRNA levels for genes encoding iNOS, TNF-α, TGF-β, IL-1β, and IL-2 as well as increased bacterial loads recovered from lung tissue three weeks after infection. This indicates that in the absence of TLR6, TLR2 is able to bind the mycobacterial ligand. It was not made clear in that study whether the TLR2/1 heterodimer or TLR2/2 homodimer is responsible. It is, however, important to note that the homodimeric form is so far only theoretical, to account for TLR2-dependent signalling in the absence of both TLR1 and 6. Efforts by Jin et al. (2007) to elucidate the crystal structures of the TLR2/1, 2/6 and 2/2 dimers were unsuccessful in producing a TLR2/2 homodimer *in vitro*.

A review of published research into plant-based TLR modulators by Chahal et al. (2013) found that the majority fell into four chemical families: proteins, polysaccharides, glycoproteins and polyphenols (including flavonoids). Plant-derived TLR2/6 ligands in particular have largely

been found to be polysaccharides. For example, a polysaccharide fraction extracted from edible microalga *Sprulina platensis* was found to activate NF-κB in human THP-1 monocytes and increase mRNA levels of IL-1B and TNF-α (Pugh et al. 2001) via TLR2/6 (Balachandran et al. 2006).

Several plant polysaccharides have been found to stimulate immune responses in a manner dependent on both TLR2 and TLR4. For example, polysaccharides from *Acanthopanax koreanum* and *Acanthopanax senticosus* activate B cells via TLR2 and 4 (Han, Park, et al. 2003; Han, Yoon, et al. 2003), a polysaccharide extracted from *Larix leptolepis* also stimulates TLR2 and 4 activity (Koizumi et al. 2012), and a <100kDa polysaccharide from *E. purpurea* elicited TLR2- and TLR4-dependent IL-6 secretion from BALB/c-derived Mϕ *in vitro* (Sullivan et al. 2008). TLR2 and 4 share TIRAP as a common signalling molecule, which other TLRs do not recruit, due to homology in their TIR domains (Toshchakov et al. 2007). It is possible that compounds which modulate both TLR2 and TLR4 activity do so via this shared intermediary.

Non-polysaccharide plant-derived TLR2/6 ligands have also been found. The lectin concanavalin A (ConA) from the jack-bean *Canavalia ensiformis* specifically stimulated TLR2/6-mediated NF-κB activation in transfected HEK cells, while other TLRs were not activated (Unitt & Hornigold 2011). The mechanism of activation is not clear at this stage, but as ConA is a protein which binds carbohydrates, particularly those rich in mannose, it is possible that poly- or oligosaccharides bound to ConA play a role in its TLR activation. The study in question investigated the binding of various lectins to TLR2/6, 3, 4, 5, 7, 8 and 9 but did not investigate TLR2/1, for reasons that remain unclear. Ursolic acid, a triterpenoid widely found in fruit peels and waxes, and many herbs, was found to activate human dendritic cells *in vitro* and induce a Th1-type IFN-γ response in $CD4^+$ naïve T cells via TLR2 and 4 (Jung et al. 2010). As mentioned previously, as these receptors share the signalling molecule TIRAP, it is possible that this is the target of ursolic acid.

In this series of experiments, to learn more about the chemical structures critical to the extracts' TLR-modulatory properties we subjected our extracts of interest to treatments designed to interfere with different aspects of their structure. Acid treatment would disrupt hydrogen bonding and interfere with protein tertiary structure. Boiling would denature the secondary, tertiary and quaternary structures of proteins and the primary and secondary structures of polysaccharides (Franz & Feuerstein 1997; Bischof & He 2005). Metaperiodate oxidation converts carbohydrate moieties into aldehydes, disrupting their structure and function. Periodate has also, however, been found to oxidise the amino acids cysteine, methionine, tryptophan, tyrosine and histidine in both proteins and glycoproteins (Clamp & Hough 1965; Yamasaki et al. 1982).

Another approach to elucidating the chemical composition of the active components would be to use fluorescent lectin staining. Lectins bind to specific carbohydrate moieties, and as such can be used to detect molecules of interest. For example, given that some known TLR ligands include mannan chains (LM and PLM; Dao et al. 2004; Jouault et al. 2003), and that plants are known to produce endogenous mannans such as glucomannan and galactoglucomannan (Moreira & Filho 2008), *G. nivalis* lectin could be a useful candidate due to its affinity for mannose-rich structures (Hester et al. 1995).

Size fractionation is another important tool in characterisation of active extract components, as it allows a large swathe of irrelevant compounds to be eliminated. This is especially important when dealing with crude biological extracts as they are likely to be highly diverse mixtures so any reduction in the number of potential candidate molecules is desirable. A less varied mixture is also more readily fed into further analytical techniques such as liquid chromatography-mass spectrometry (LC-MS). Electrophoretic separation by SDS-PAGE would provide the additional benefit of information regarding the size distribution of compounds in the extracts, assisting in targeting further analysis.

TLR2 ligands are highly variable in size. MALP-2 has a mass of 2kDa (Mühlradt et al. 1997), there is also a 19kDa *M. tuberculosis* lipoprotein (Brightbill et al. 1999), a <100kDa polysaccharide from *E. purpurea* (Sullivan et al. 2008), a >100kDa polysaccharide extract of *S. platensis* (Balachandran et al. 2006) and *J. scopolorum* polysaccharides of 200 and 680kDa (Schepetkin et al. 2005). Therefore it is desirable to separate the extract into several fractions to more precisely ascertain the molecular weight of the active component.

One potential obstacle to the fractionation and modification of the extracts is the DMSO in which they were resuspended. DMSO is a highly polar solvent which is incompatible with the polyethersulphone membranes of the centrifugal concentrators used *(Mfg Polysulfone Chemical Compatibility Chart*, 2014). DMSO also prevents treatment with HCl, as the combination directly evolves dimethyl sulphide, destroying the DMSO in the process (Savige & Fontana 1977). DMSO does not preclude heat-inactivation as its boiling point at atmospheric pressure is 189^{o}C (*The Merck Index,* 2013), and periodate oxidation is also still possible in DMSO (Malinin 1977).

To enable thorough characterisation it was necessary for the extracts to be dialysed into PBS and re-screened for TLR2/6 activity before proceeding. In addition, if these plant-derived TLR modulators are to be used in a therapeutic context it is desirable that they be soluble in aqueous conditions without requiring the presence of DMSO or other exogenous solvent.

4.2 Results

4.2.1 Solubility of plant extracts in PBS

The DMSO in which the extracts had been resuspended could interfere with the fractionation and modification processes, so to facilitate further characterisation the extracts were dialysed into PBS and re-screened for TLR2/6-modulatory activity (Figure 4.1 A-C). After dialysis there was some precipitation observed in all three extracts, suggesting that some DMSO-soluble components were insoluble in PBS. 1402EtL did not retain its stimulatory effect, in fact it decreased baseline CXCL8 production at the highest dose (Figure 4.1 A, $p \leq 0.05$). This effect, although small, was repeated in several iterations of the experiment. The loss of stimulatory activity suggests that the compound responsible is insoluble in PBS. In contrast, 1404EtL did retain its dose-dependent inhibitory effect in PBS (Figure 4.1 B, $p \leq 0.0001$, $R^2 = 0.963$), and 1412EtB retained its dose-dependent stimulatory effect (Figure 4.1 C, $p \leq 0.0001$, $R^2 = 0.9259$).

The loss of activity of 1402EtL in PBS limits the extent of characterisation possible, so we chose to focus further characterisation efforts on 1404EtL and 1412EtB.

A.

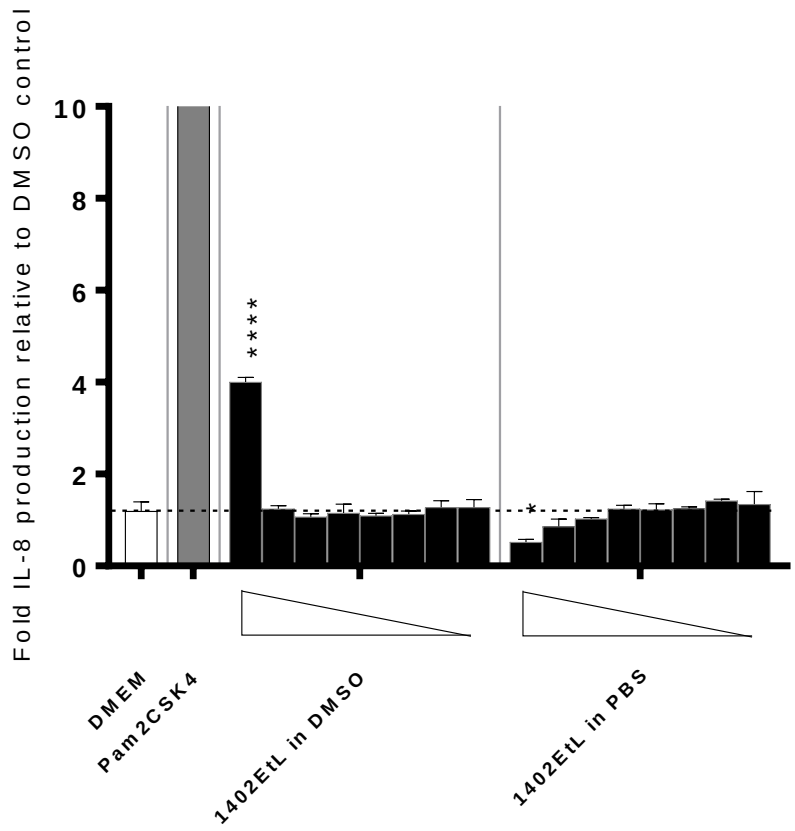


Figure 4.1. Stimulation of CXCL8 production by HEK293-TLR2/6 cells in response to 1402EtL in aqueous or DMSO solution. HEK293-TLR2/6 cells were incubated for 48h with the extracts at twofold serial dilutions between 100 and 0.78125µg/ml. Thereafter CXCL8 production was quantified by supernatant ELISA. CXCL8 production is shown relative to DMSO solvent control. The dashed line indicates the CXCL8 readout for DMEM medium-only negative control. Readings shown are means +/- SD of triplicate wells. Results were tested for significant difference from medium-only control using two-way ANOVA; * $p \leq 0.05$; ** $p \leq 0.01$; *** $p \leq 0.001$; **** $p \leq 0.0001$; tested for dose-dependency using non-linear one phase decay regression; # $R^2 \geq 0.9$

B.

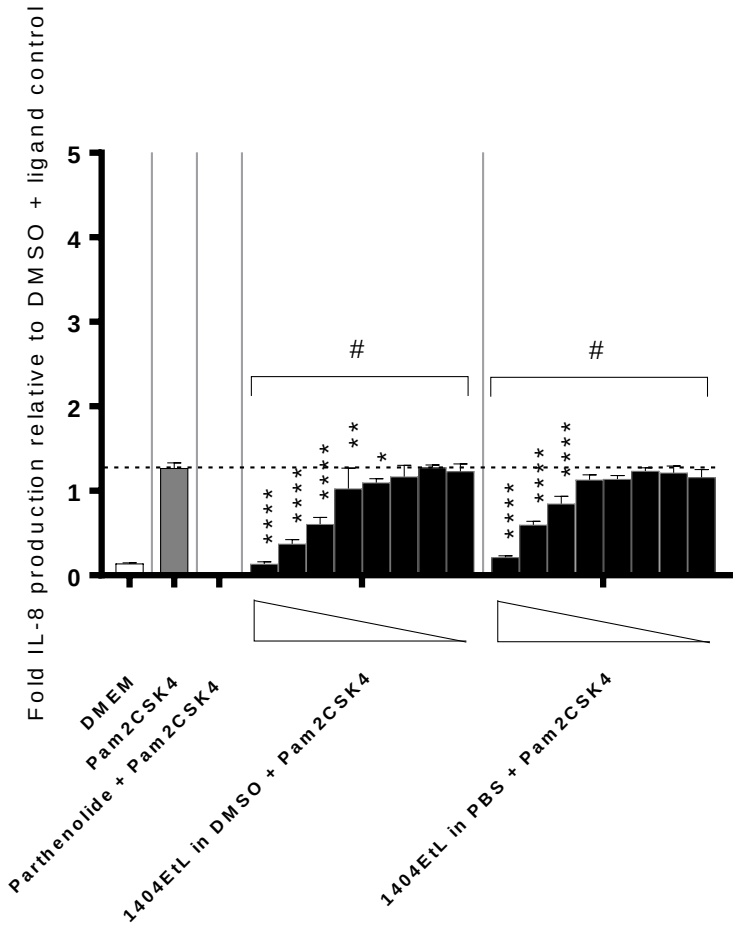


Figure 4.2. Inhibition of CXCL8 production by HEK293-TLR2/6 cells in response to 1404EtL in aqueous or DMSO solution. HEK293-TLR2/6 cells were incubated for 48h with the extracts at twofold serial dilutions between 100 and 0.78125µg/ml. Thereafter CXCL8 production was quantified by supernatant ELISA. CXCL8 production is shown relative to DMSO solvent control. The dashed line indicates the CXCL8 readout for the Pam2CSK4 ligand-only control. Readings shown are means +/- SD of triplicate wells. Results were tested for significant difference from ligand-only control using two-way ANOVA; * $p \leq 0.05$; ** $p \leq 0.01$; *** $p \leq 0.001$; **** $p \leq 0.0001$; tested for dose-dependency using non-linear one phase decay regression; # $R^2 \geq 0.9$

C.

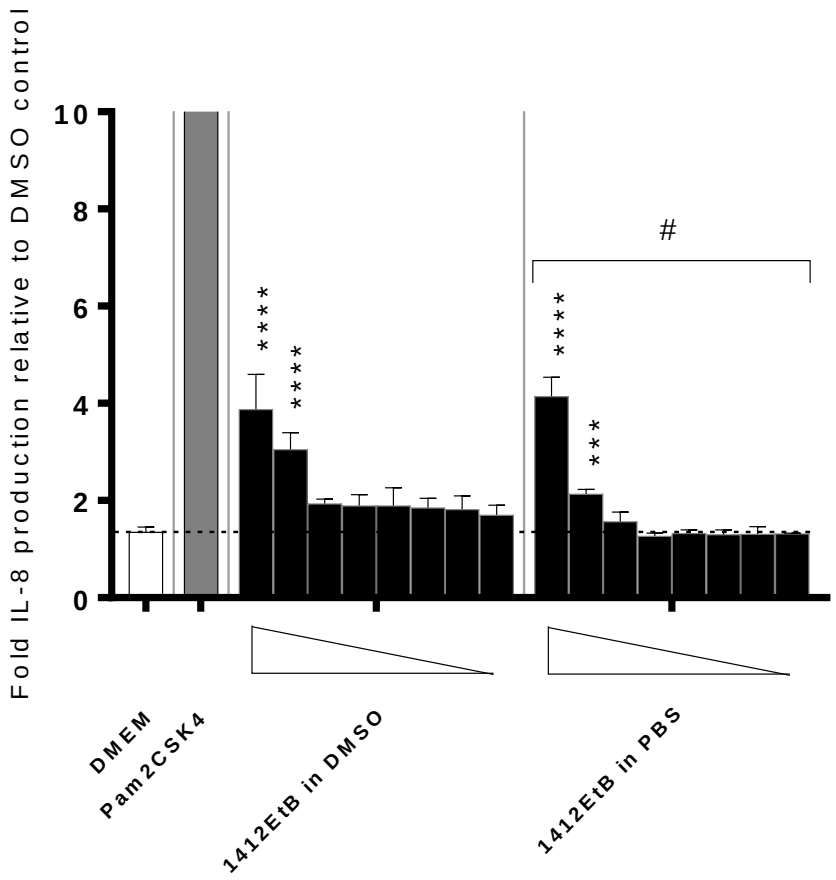


Figure 4.3. Stimulation of CXCL8 production by HEK293-TLR2/6 cells in response to 1412EtB in aqueous or DMSO solution. HEK293-TLR2/6 cells were incubated for 48h with the extracts at twofold serial dilutions between 100 and 0.78125µg/ml. Thereafter CXCL8 production was quantified by supernatant ELISA. CXCL8 production is shown relative to DMSO solvent control. The dashed line indicates the CXCL8 readout for the DMEM medium-only negative control. Readings shown are means +/- SD of triplicate wells. Results were tested for significant difference from medium-only control using two-way ANOVA; * $p \leq 0.05$; ** $p \leq 0.01$; *** $p \leq 0.001$; **** $p \leq 0.0001$; tested for dose-dependency using non-linear one phase decay regression; # $R^2 \geq 0.9$

4.2.2 Fluorescent Lectin Stain

It was not possible to generate meaningful data using the method described in section 2.1.5 **Figure 4.4** shows an example membrane image from an optimisation experiment using *Lactobacillus* lysate. After several repeats the problems of persistent background staining on the PBS + GNL control and generally weak signal were not solved. Instead of dedicating further time to optimising this protocol, it was decided that research time would be more effectively allocated to exploring other methods which could provide more information.

PBS	PBS + 100µg/ml GNL	LL + 100µg/ml GNL	LL + 90µg/ml GNL	LL + 80µg/ml GNL	LL + 70µg/ml GNL
PBS	PBS + 100µg/ml GNL	LL + 100µg/ml GNL	LL + 90µg/ml GNL	LL + 80µg/ml GNL	LL + 70µg/ml GNL
PBS	PBS + 100µg/ml GNL	LL + 100µg/ml GNL	LL + 90µg/ml GNL	LL + 80µg/ml GNL	LL + 70µg/ml GNL
LL + 60µg/ml GNL	LL + 50µg/ml GNL	LL + 40µg/ml GNL	LL + 30µg/ml GNL	LL + 20µg/ml GNL	LL
LL + 60µg/ml GNL	LL + 50µg/ml GNL	LL + 40µg/ml GNL	LL + 30µg/ml GNL	LL + 20µg/ml GNL	LL
LL + 60µg/ml GNL	LL + 50µg/ml GNL	LL + 40µg/ml GNL	LL + 30µg/ml GNL	LL + 20µg/ml GNL	LL

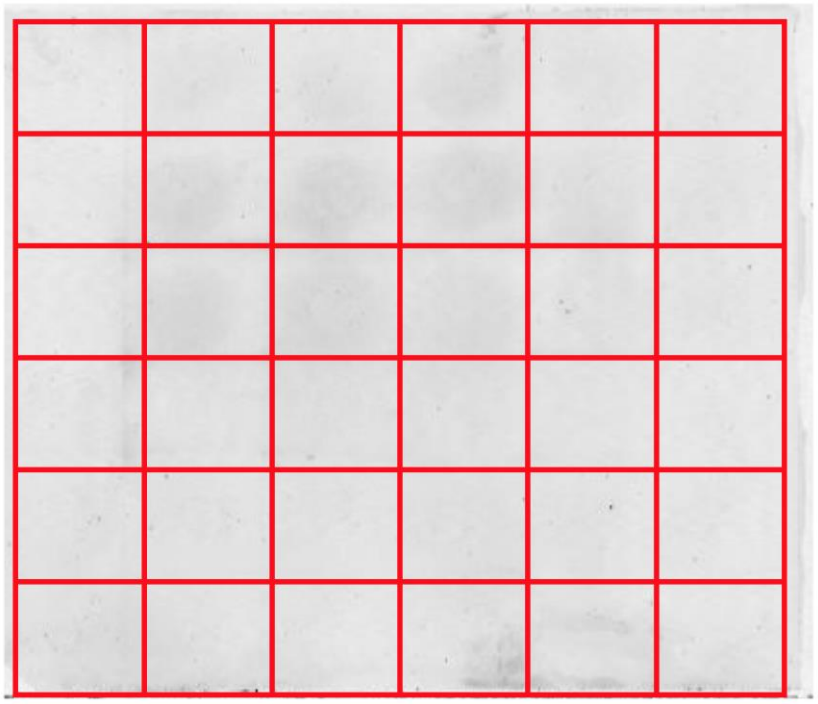


Figure 4.4. Membrane layout and image of fluorescent lectin stain optimisation. Membrane was soaked in 100% methanol until translucent then equilibrated in PBS for 3 min. Treatments and controls were applied in 15µl amounts and incubated at RT until dry. Membrane was blocked with 5% Marvel milk powder in PBS for 2h on a rocker at 45 cycles/min, then washed three times in PBST, three times in PBS and once in deionised water. 15µl of FITC-labelled snowdrop lectin (FITC-GNL) was spotted onto the samples at the concentrations indicated and the membrane was incubated at RT in the dark for 1h. After being washed as described previously the membrane was visualised on the Typhoon TRIO+ (GE Life Sciences). LL = *Lactobacillus* lysate; GNL = FITC-GNL

4.2.3 Chemical modification of plant extracts

In an effort to determine the chemical nature of the active ingredients, aliquots of the extracts were acid-treated (and then neutralised), boiled or oxidised with sodium metaperiodate. All treatments of 1404EtL retained their TLR2/6-inhibitory activity between 100 and 25µg/ml (all $p \leq 0.0001$; Figure 4.2). The dose response was also retained between 100 and 3.125µg/ml of acid-treated and oxidised extract, and between 100 and 6.25µg/ml of boiled extract (all $R^2 \geq 0.9$). When tested for significant difference in CXCL8 output compared to the crude extract, acid-treated extract showed significantly lower CXCL8 production at 1.5625µg/ml ($p \leq 0.01$) and boiled extract showed lower production at 3.125 ($p \leq 0.05$) and 1.5625µg/ml ($p \leq 0.001$).

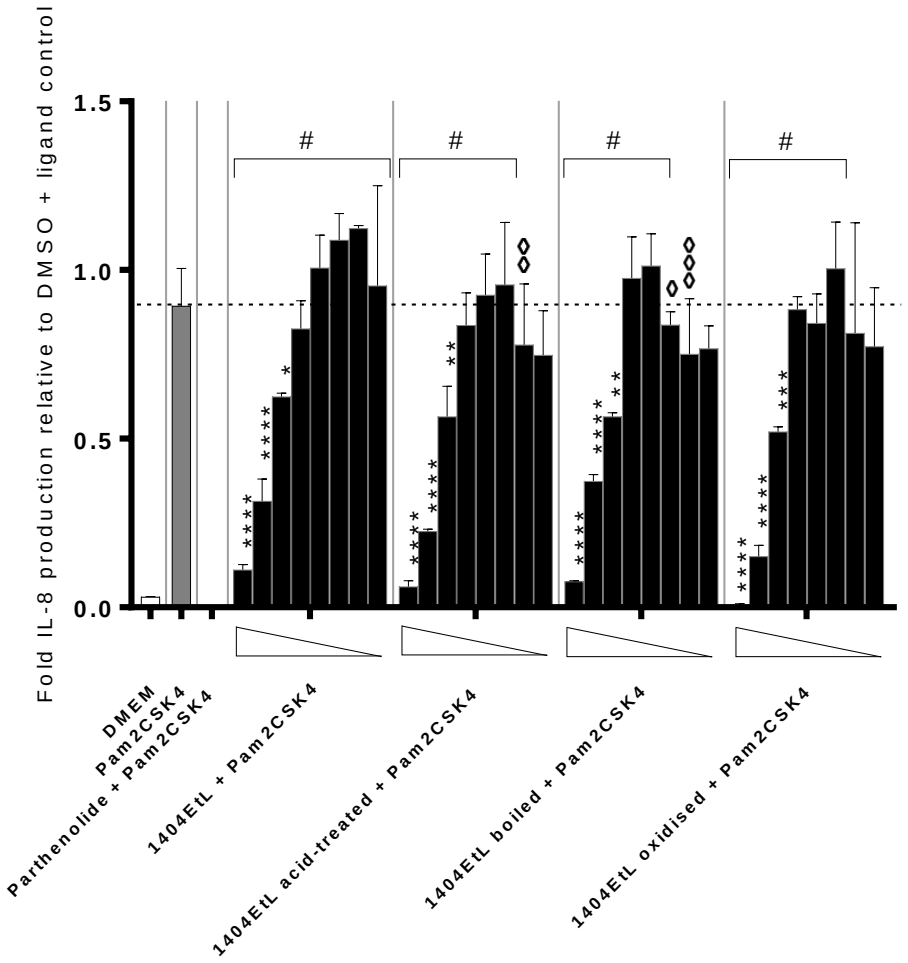


Figure 4.5. Inhibition of TLR2/6-mediated CXCL8 production by 1404EtL and its chemically modified variants. HEK293-TLR2/6 cells were incubated for 48h with the crude and modified extracts at twofold serial dilutions between 100 and 0.78125µg/ml and 10ng/ml Pam2CSK4. Thereafter CXCL8 production was quantified by supernatant ELISA. CXCL8 production is shown relative to DMSO + Pam2CSK4 solvent control. The dashed line indicates the CXCL8 readout for the Pam2CSK4 ligand-only control. Readings shown are means +/- SD of triplicate wells. Results were tested for significant differences using two-way ANOVA; vs. ligand-only control: * $p \leq 0.05$; ** $p \leq 0.01$; *** $p \leq 0.001$; **** $p \leq 0.0001$; vs. crude extract: ◊ $p \leq 0.05$; ◊◊ $p \leq 0.01$; ◊◊◊ $p \leq 0.001$; ◊◊◊◊ $p \leq 0.0001$; tested for dose-dependency using non-linear one phase decay regression; # $R^2 \geq 0.9$

The acid-treated and boiled aliquots of 1412EtB both retained their dose-dependent TLR2/6-stimulatory effects (Figure 4.3; both $p \leq 0.0001$, both $R^2 \geq 0.9$). The oxidised extract lost its stimulatory activity and in fact significantly reduced baseline CXCL8 output at 100 and 50µg/ml ($p \leq 0.0001$ and 0.01 respectively). A reddish-brown precipitate was observed in the oxidised extract, suggesting that the active component is insoluble when oxidised. The boiled extract showed significantly decreased CXCL8 production relative to the crude extract at 100 and 50µg/ml ($p \leq 0.0001$) and 25µg/ml ($p \leq 0.01$).

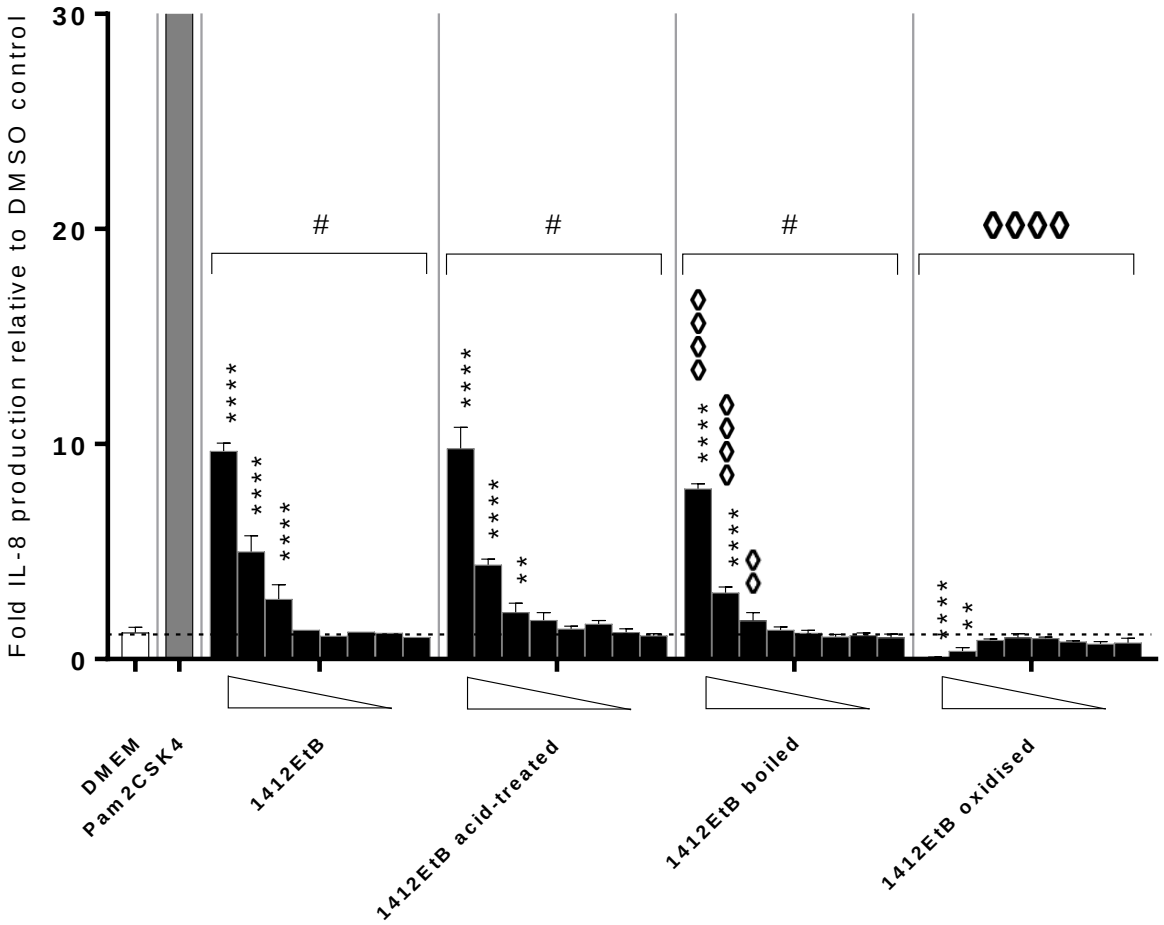


Figure 4.6. Stimulation of TLR2/6-mediated CXCL8 production by 1412EtB and its chemically modified variants. HEK293-TLR2/6 cells were incubated for 48h with the crude and modified extracts at twofold serial dilutions between 100 and 0.78125µg/ml. Thereafter CXCL8 production was quantified by supernatant ELISA. CXCL8 production is shown relative to DMSO solvent control. The dashed line indicates the CXCL8 readout for the DMEM medium-only negative control. Readings shown are means +/- SD of triplicate wells. Results were tested for significant differences using two-way ANOVA; vs. medium-only control: * $p \leq 0.05$; ** $p \leq 0.01$; *** $p \leq 0.001$; **** $p \leq 0.0001$; vs. crude extract: ◊ $p \leq 0.05$; ◊◊ $p \leq 0.01$; ◊◊◊ $p \leq 0.001$; ◊◊◊◊ $p \leq 0.0001$; tested for dose-dependency using non-linear one phase decay regression; # $R^2 \geq 0.9$

4.2.4 Fractionation of plant extracts

The plant extracts with which the cells have been treated so far are unrefined, and as such are likely to contain a multitude of different compounds. Here we used size fractionation to identify a size range for the active component and exclude many of the inactive compounds.

4.2.4.1 SDS-PAGE

There were persistent difficulties in obtaining distinct bands from any of the extracts tested (Figure 4.7). The darker areas of the smears observed suggest a greater abundance of proteins in the 30-150kDa range for 1402EtL in DMSO, although this shifts to 20-50kDa in PBS. 1404EtL appears to consist mainly of sub-20kDa molecules in both DMSO and PBS. 1412EtB appears to show greatest staining in the 40-150kDa range in DMSO, and 30-120kDa in PBS. However, these data are merely suggestive due to the smearing observed.

After several repeats and various methodological permutations we were unable to obtain any greater resolution than the smears observed in Figure 4.7. As this was insufficient to further characterise the extracts, SDS-PAGE was abandoned in favour of fractionation by sequential filtration.

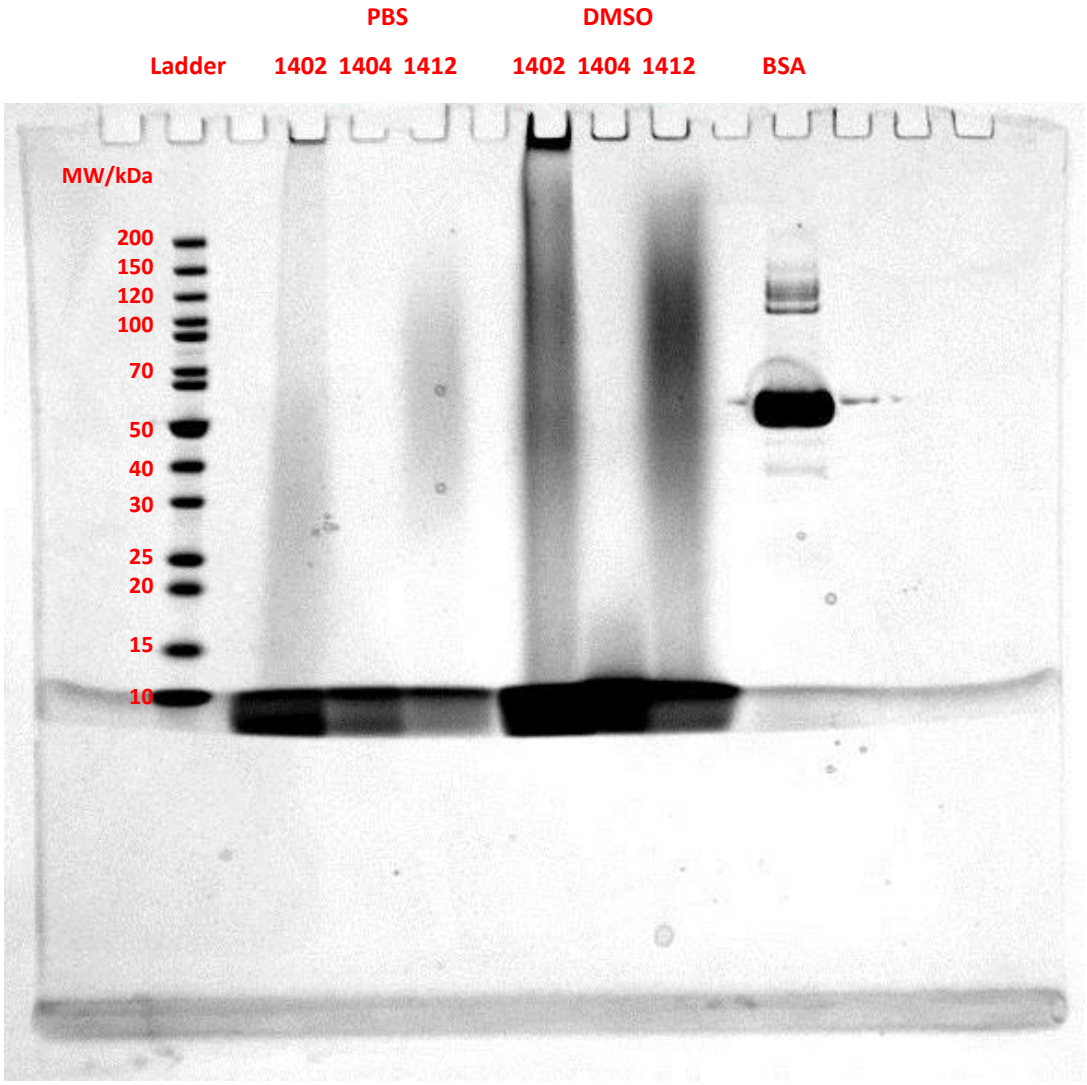


Figure 4.7 Polyacrylamide gel electrophoresis (PAGE) of crude extracts in PBS and in DMSO. Extracts were run on 4-12% Bis-Tris NuPAGE gradient gels (Thermo Fisher) according to manufacturer's instructions, with a 10-200kDa ladder (New England Biolabs). 2µl of sample was mixed with 2.5µl NuPage LDS Sample Buffer (Thermo Fisher), 1µl 2-mercaptoethanol (Thermo Fisher) and 4.5µl deionised water, and the mixture heated to 70°C for 10 minutes. Samples, ladder and BSA standard were loaded into wells, and the gel run using MOPS buffer for 45 min at 200V. The gels were stained either with Coomassie Blue (Bio-Rad) for proteins or periodic acid Schiff (PAS; Sigma Aldrich) staining for glycoproteins and visualised using an ImageQuant 300 (GE Life Sciences). MW/kDA: molecular weight in kilodaltons; BSA: bovine serum albumin control.

4.2.4.2 Sequential filtration

The extracts were successfully separated into six distinct fractions by sequential filtration as described in section 0.

In 1404EtL inhibition was detected at between 100 and 25µg/ml of the 10-30kDa fraction, at 100 and 50µg/ml of the 50-100kDa and <5kDa fractions, 100µg/ml of the 30-50kDa fraction (Figure 4.4; all $p \leq 0.0001$). The 10-30kDa fraction produced the greatest decrease in CXCL8 production as well as retaining the strong dose response observed in the crude extract ($R^2 \geq 0.9$).

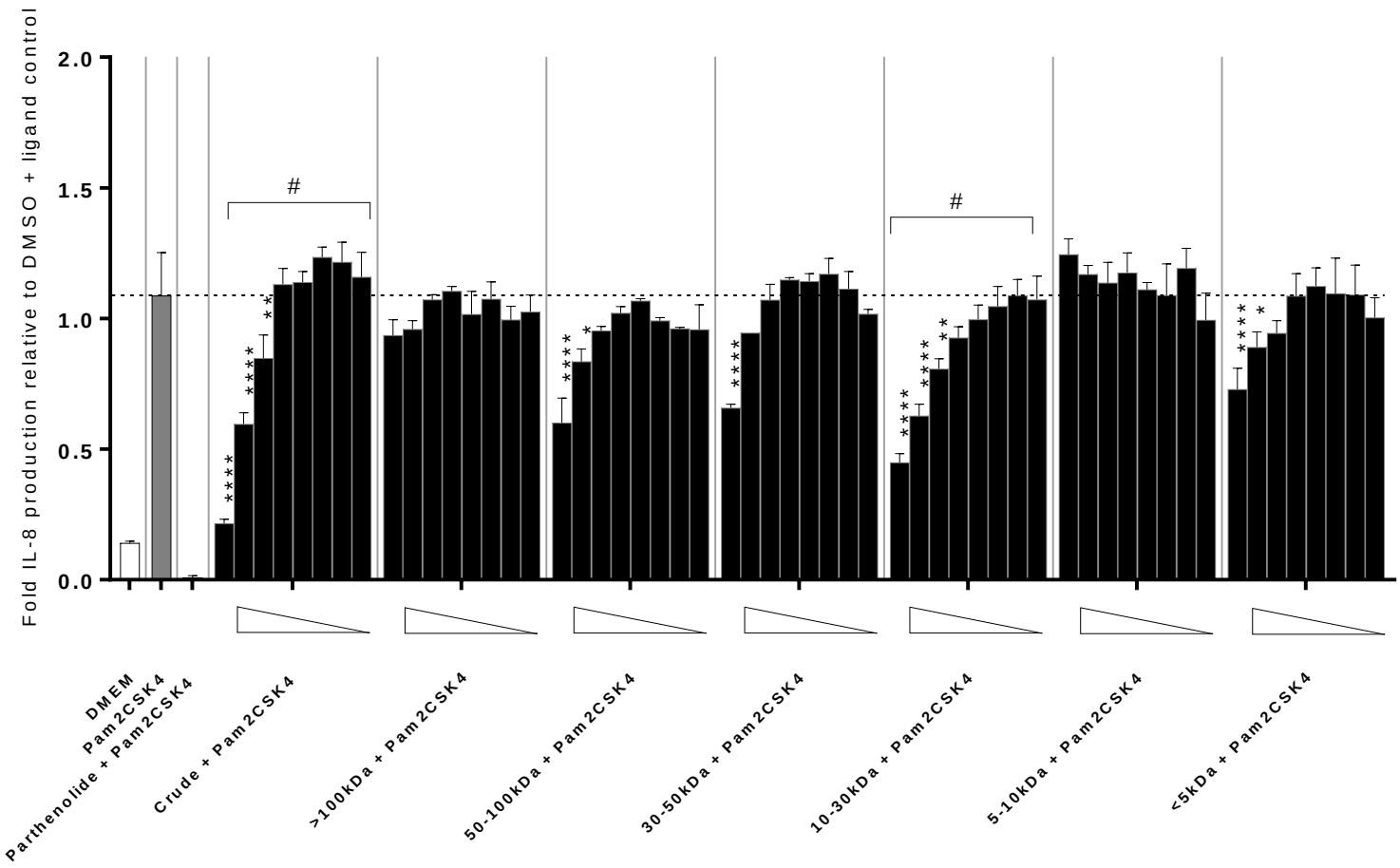


Figure 4.8. Inhibition of TLR2/6-mediated CXCL8 production by 1404EtL and size fractions thereof. HEK293-TLR2/6 cells were incubated for 48h with crude and size-fractionated extracts at twofold serial dilutions between 100 and 0.78125µg/ml and 10ng/ml Pam2CSK4. Thereafter CXCL8 production was quantified by supernatant ELISA. CXCL8 production is shown relative to DMSO + Pam2CSK4 solvent control. The dashed line indicates the CXCL8 readout for the Pam2CSK4 ligand-only control. Readings shown are means +/- SD of triplicate wells. Results were tested for significant differences using two-way ANOVA; vs. ligand-only control: * $p \leq 0.05$; ** $p \leq 0.01$; *** $p \leq 0.001$; **** $p \leq 0.0001$; vs. crude extract: ◊ $p \leq 0.05$; ◊◊ $p \leq 0.01$; ◊◊◊ $p \leq 0.001$; ◊◊◊◊ $p \leq 0.0001$; tested for dose-dependency using non-linear one phase decay regression; # $R^2 \geq 0.9$

The >100kDa fraction of 1412EtB retained the strong dose-dependent effect of the crude extract (Figure 4.5; $p \leq 0.0001$, $R^2 \geq 0.9$). There were small increases in CXCL8 at 25 and 12.5µg/ml of the 50-100kDa fraction ($p \leq 0.001$), 50 and 25µg/ml of the 30-50kDa fraction ($p \leq 0.001$), 100 and 50µg/ml of the 5-30kDa fraction ($p \leq 0.01$) and 50µg/ml of the <5kDa fraction ($p \leq 0.01$). No effects of fractions below 100kDa were dose-dependent (all $R^2 < 0.9$).

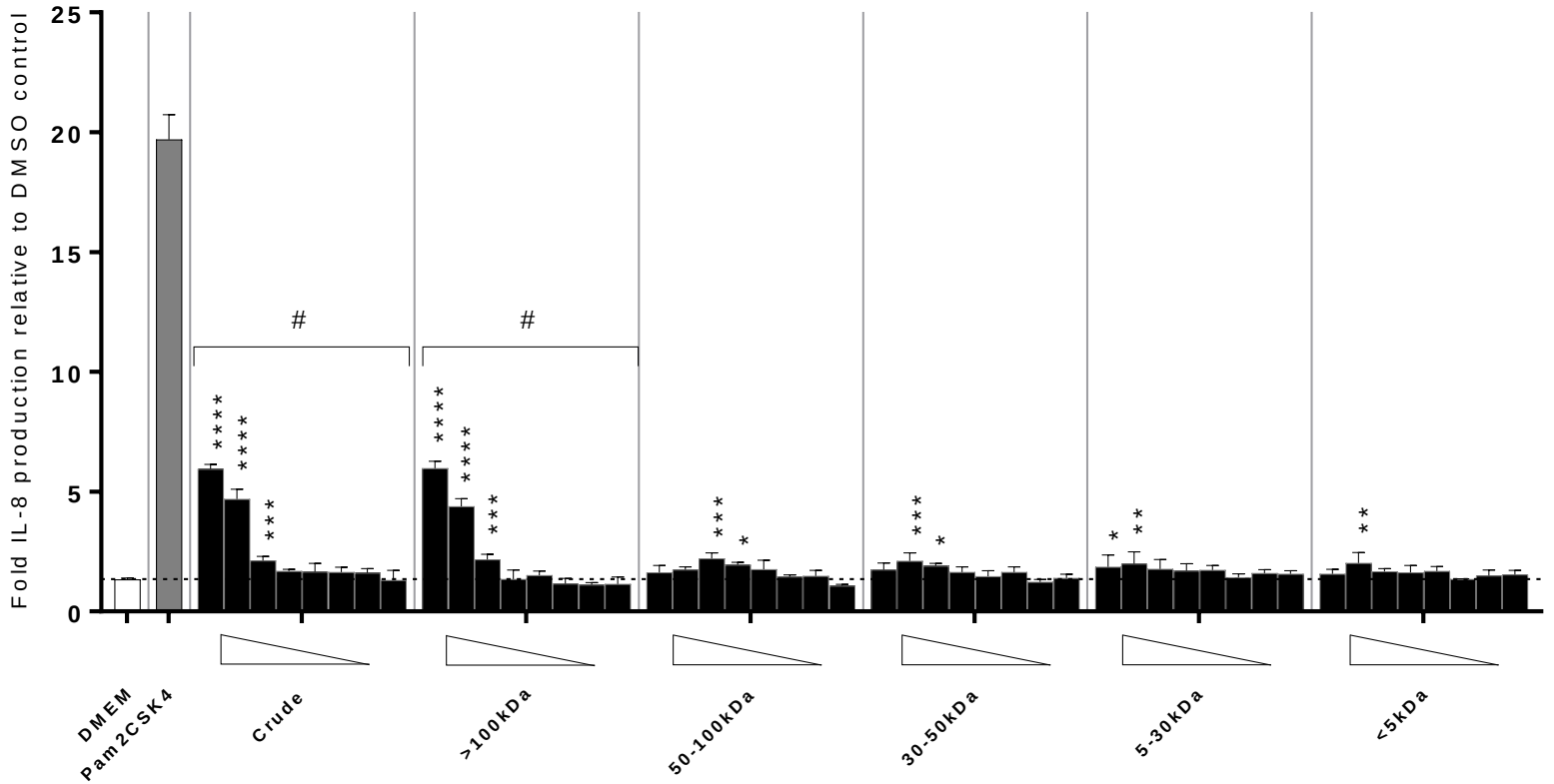


Figure 4.9. Stimulation of TLR2/6-mediated CXCL8 production by 1412EtB and size fractions thereof. HEK293-TLR2/6 cells were incubated for 48h with the crude and size-fractionated extracts at twofold serial dilutions between 100 and 0.78125µg/ml. Thereafter CXCL8 production was quantified by supernatant ELISA. CXCL8 production is shown relative to DMSO solvent control. The dashed line indicates the CXCL8 readout for the DMEM medium-only negative control. Readings shown are means +/- SD of triplicate wells. Results were tested for significant differences using two-way ANOVA; vs. medium-only control: * $p \leq 0.05$; ** $p \leq 0.01$; *** $p \leq 0.001$; **** $p \leq 0.0001$; vs. crude extract: ◊ $p \leq 0.05$; ◊◊ $p \leq 0.01$; ◊◊◊ $p \leq 0.001$; ◊◊◊◊ $p \leq 0.0001$; tested for dose-dependency using non-linear one phase decay regression; # $R^2 \geq 0.9$

4.2.5 Summary

The extracts under investigation were found to have a variety of inhibitory and stimulatory effects on CXCL8 production whend modified and fractionated. A summary heat map of screening results is provided below (Table 4.1).

Table 4.1. Summary heat map of characterisation results.

	1402EtL	1404EtL	1412EtB
Crude in DMSO	#	#	#
Crude in PBS		#	#
Acid-treated		#	#
Boiled		#	#
Oxidised		#	
>100kDa			#
50-100kDa			
30-50kDa			
10-30kDa		#	
5-10kDa			
<5kDa			

	p ≤ 0.0001	
	p ≤ 0.001	
	p ≤ 0.01	
	p ≤ 0.05	Stimulatory
	N/S	
	p ≤ 0.05	Inhibitory
	p ≤ 0.01	
	p ≤ 0.001	
	p ≤ 0.0001	

Summary of stimulatory and inhibitory effects of the extracts on HEK293-TLR2/6 cells. All three extracts were tested in their crude forms in both DMSO and PBS solutions. The stimulatory effect of 1402EtL was not retained in aqueous solution so no further characterisation was carried out. 1404EtL and 1412EtB were chemically modified (acid-treated, boiled or oxidised) or size-fractionated (molecular weight cut-offs described in table) for further investigation; # = dose-dependent effect ($R^2 \geq 0.9$).

4.3 Discussion

Several of the modified and fractionated extracts screened were found to stimulate or inhibit CXCL8 production in HEK293-TLR cells. A summary heat map of the results is provided in the previous section (Table 4.1).

1402EtL lost its stimulatory activity when dialysed into PBS (Figure 4.1 A), which precludes acid treatment due to a reaction between HCl and DMSO (Savige & Fontana 1977), and fractionation because of disruption to the polyethersulphone membranes of the centrifugal concentrators used *(Mfg Polysulfone Chemical Compatibility Chart*, 2014). For this reason we decided to focus further characterisation efforts on 1404EtL and 1412EtB. However, it would still be possible to boil or oxidise 1402EtL. Information regarding thermostability and presence of carbohydrate residues could be gained from such investigation. For fractionation purposes it could be possible to use nylon rather than polyethersulphone membranes, due to their greater resistance to damage by DMSO (*Corning Filtration Guide* 2011). However, nylon has a greater tendency to bind proteins and other macromolecules from solution so loss of active ingredients due to retention on the filtration membrane is a potential problem with this method.

1404EtL retained its dose-dependent inhibitory effect in PBS, which allowed further characterisation (Figure 4.1 B). It also retained its inhibitory effect after all three chemical modifications, with no significant difference in activity between crude and modified extracts at any except the lowest two concentrations (Figure 4.2), at which point the data became much more variable with larger SD values. It is not clear what caused this effect at low concentrations rather than a plateau. Upon size fractionation an active 10-30kDa fraction was identified, which retained the strong dose-dependent inhibition of TLR2/6 shown by the parent crude extract (Figure 4.4). There was some inhibition of CXCL8 secretion detected at the highest concentrations of some of the larger molecular weight fractions, which could be

attributed to the fractionation method. Due to the fact that a small volume of solution was retained, unfiltered, in the upper part of the centrifugal concentrator, it is possible that the fractions drawn from those contained small amounts of compounds with molecular weights lower than the MWCO of the concentrator membrane. Some reduction in CXCL8 secretion was also detected at the highest concentrations of the <5kDa fraction. There are several possible explanations for this. It is possible that a second, weaker inhibitor of TLR2/6 can be found in this size fraction. This is still within a feasible size range for TLR modulators as the TLR2/6 ligand MALP-2 has a molar mass of 2kDa (Mühlradt et al. 1997), and TLR4 inhibitor TAK-242 has a mass of only 361.8Da (Matsunaga et al. 2011; Cayman Chemical 2015). Another possibility is that some of the 10-30kDa active component has degraded and a <5kDa fragment of it either accumulated to toxic levels or retains some activity, albeit reduced.

The stimulatory effect of 1412EtB on TLR2/6 was retained in PBS (Figure 4.1 C) and unaffected by acid treatment, but boiling significantly reduced its effectiveness (Figure 4.3). This suggests that the active component is at least somewhat heat labile. This could be due to disruption of various degrees of structure in protein and/or polysaccharide components (Franz & Feuerstein 1997; Bischof & He 2005). Metaperiodate oxidation completely negated its stimulatory activity, suggesting that a polysaccharide or carbohydrate-containing molecule is responsible for the effect observed. As noted in the introduction to this chapter, however, periodate has also been found to oxidise the amino acids cysteine, methionine, tryptophan, tyrosine and histidine (Clamp & Hough 1965; Yamasaki et al. 1982), so it is possible that a functional peptide residue is the target of oxidation here. Zeng et al. (2010) investigated the structural requirements for the lipopeptide TLR2/6 ligand Pam2Cys (structurally identical to Pam2CSK4 minus a serine and four lysine residues) and found that removal of the amino group reduced the DC-activating effect of Pam2Cys, although other parts of the molecule were found to have a greater influence on immunogenicity such as the 2,3-dihydroxypropyl

group and the cysteine sulphur atom. The active compound is a large molecule (>100kDa; Figure 4.5), as evidenced by the fact that this fraction retained the strong dose-dependent stimulatory effect whereas only small dose-independent effects were detected in response to other fractions. This is well within the wide size range of plant-derived immunomodulatory polysaccharides already discovered, as a 3-10kDa polysaccharide extract from *D. huoshanense* found to activate Mϕ via TLR4 (Xie et al. 2016) and a 680kDa macrophage-activating polysaccharide from *J. scopolorum* (Schepetkin et al. 2005) have shown.

It is interesting to note that when 1402EtL and 1412EtB lost their stimulatory activity (1402EtL after dialysis into PBS, Figure 4.1 A; 1412EtB after oxidation, Figure 4.3), the products both had significant inhibitory effects on CXCL8 production from our HEK293 TLR2/6 cells. These treatments also resulted in the formation of an insoluble precipitate, which could provide a clue to the cause of the observed effect. Changes in the solvent or oxidation of glycan residues could affect the folding of proteins, glycoproteins or lipoproteins, decreasing their solubility leading to aggregation, and protein aggregates have been shown to be inherently cytotoxic (Bucciantini et al. 2002; Stefani & Dobson 2003). Assaying the cytotoxicity (as in Chapter 3) of 1402EtL in PBS and oxidised 1412EtB would test this hypothesis. Conversely, if found to be non-cytotoxic, investigation of their inhibitory effects could prove informative.

As discussed in the introduction to this chapter, existing TLR2/6 modulators come in a range of shapes and sizes including polysaccharides, proteins, glycoproteins, lipoproteins, glycolipids and polyphenols with masses as variable as 2 and 680kDa. For use *in vivo* however, sometimes chemical modifications are needed to enhance the molecule's efficacy, safety or other property. For example, a PEGylated (covalently bound to polyethylene glycol (PEG)) form of TLR2/6 ligand Pam2Cys has been shown to provide laboratory mice with effective short-term protection from mouse-adapted H1N1 avian influenza (Tan et al. 2012).

The PEG was incorporated to increase solubility and allow for administration via intranasal spray, an example of the potential utility of modified TLR ligands in clinical applications.

The modification and size fractionation described here have allowed valuable inferences to be drawn regarding the active components of the extracts under investigation, despite the unsuccessful attempts at fluorescent lectin staining and SDS-PAGE. Had the lectin stain been successful the results could have complemented the data from the modification experiments and given a more complete picture of the compounds present. It is possible that the SDS-PAGE was hindered by the diversity of solutes in the crude extracts. A similar experiment using the active fractions identified by sequential filtration could assist in further isolating and identifying the active component.

In this chapter we have had varying success in characterising the extracts under investigation. However, so far experiments have focused on CXCL8 production by transfected HEK293 cells over-expressing a single receptor or pair of functional heterodimeric receptors. This reductionist approach has allowed us to examine the relationships between these extracts and individual TLRs, but we do not yet know how the extracts will perform in a more complex signalling environment such as is found *in vivo*. The next step towards *in vivo* testing is the *in vitro* use of primary immune cells. Their varied signalling pathways with complex cross-talk will provide a clearer picture of how these extracts work at a cellular, rather than receptor, level. Primary cells also provide us with more varied readouts with which to assess the effects elicited. Murine splenic B lymphocytes were selected because both they and their human counterparts express TLR2/6 (Bekeredjian-Ding & Jego 2009). Stimulation of TLR2/6 has been found to increase proliferation and frequency of IgM^+ and IgG^+ cells without the need for accessory cells (Borsutzky et al. 2005), so proliferation and antibody profile are two potential readouts, both with biological relevance to therapeutic applications such as vaccine adjuvants and in treatment of autoimmune disorders (Blüml et al. 2013; Chan et al. 2013).

Other TLR-mediated vaccine adjuvants have also been investigated, such as CpG ODN (Vollmer 2005).

Experiments to further characterise the extracts could include LC-MS, a powerful tool for differentiating components of mixtures. The effectiveness of LC-MS would be aided by the identification in this chapter of active fractions of 1404EtL and 1412EtB, discarding many irrelevant fractions before undertaking the process.

Chapter 5. Effects of plant extracts on proliferation and immunoglobulin class-switching in primary B cells

5.1 Introduction

Having characterised active fractions of both 1404EtL and 1412EtB, as well as an inactivated oxidised aliquot of 1412EtB, we next sought to determine if the functional effects of our extracts were maintained in primary lymphocytes. Murine splenic B cells were chosen for this purpose because they express TLR2/6 (Bekeredjian-Ding & Jego 2009), as do human B cells. Moreover B cells are a clinically relevant target due to their importance in antibody based vaccine strategies and their role in immune disorders including systemic lupus erythematosus and myasthenia gravis (Murphy 2012).

Vaccine adjuvants currently licensed for use in human vaccines operate via a range of mechanisms. Oil/water emulsions such as Freund's adjuvant, or squalene-based emulsions such as Novartis' MF59 and GlaxoSmithKline's adjuvant system 3 (AS03), potentiate immune responses to vaccination by creating a *depot effect* which releases antigen slowly. This prolongs the stimulatory effect and increases uptake of antigen by APCs such as DC (Dupuis et al. 1998). Formulations based on alum activate the PRR NOD-like receptor P3 (NLRP3) in the inflammasome (Li et al. 2008). Liposome vaccines mimic the membrane of envelope viruses, combining antigen delivery and adjuvancy in one (Moser et al. 2013; Zhao et al. 2014; Perrie et al. 2016). Some existing veterinary vaccines use a plant-derived adjuvant; the saponin-based class of adjuvants known as immunostimulatory complexes (ISCOM) are nanoparticles composed of saponins derived from *Quillaja saponaria* (Morein et al. 1995).

As key mediators of innate and adaptive immune activation, TLRs represent a promising target for use in vaccine adjuvants. There is already one TLR-stimulating vaccine adjuvant licensed for use in human vaccines; the TLR4 ligand monophosphoryl lipid A (MPL), a non-

toxic derivative of LPS, is a constituent of GSK's AS04 in combination with alum (Didierlaurent et al. 2009) currently used in vaccines both for hepatitis B and human papilloma virus (Casella & Mitchell 2008) and AS01 where MPL is combined with a liposomal adjuvant. MPL is also under investigation as a potential component of conjugated vaccines (Schülke et al. 2016). Several other adjuvants based on TLR ligands are currently in clinical trials (Lee & Nguyen 2015). The TLR9-stimulating synthetic ODN called immunostimulatory sequence 1018 (1018 ISS) is currently awaiting an FDA review of phase III trial safety data for use in a hepatitis B vaccine called HEPLISAV (Sablan et al. 2012; Halperin et al. 2012; Eng et al. 2013; Dynavax press release 18th April 2016). Previous trials have shown the formulation to be highly effective at producing more rapid protection than the current leading vaccine, GSK's Engerix-B. Rintatolimod (trade name Ampligen) is another TLR-mediated adjuvant awaiting approval for use in human vaccines; it is a polyI:C synthetic double-stranded RNA which binds TLR3 and has been shown to be effective in a murine H5N1 influenza vaccine model (Ichinohe et al. 2009). Ampligen was originally formulated as a therapy for chronic fatigue syndrome (CFS), and has already been shown to be safe in phase 3 clinical trials for this application (Strayer et al. 2012). Conjugated vaccines incorporating flagellin, the TLR5 PAMP ligand, have completed phase I clinical trials for protection from influenza (Turley et al. 2011; Taylor et al. 2012) and malaria (Camacho et al. 2011).

At the time of writing no specific TLR2/6 ligands have entered clinical trials for use as vaccine adjuvants. An adjuvant derived from *M. bovis* called SMP-105 is undergoing clinical trials, but its receptor specificity has only been determined to the level of TLR2 specificity (Miyauchi et al. 2012; Uenishi et al. 2007). Similarly, a polysaccharide derived from the shrub *A. senticosus* has been shown by Han, Yoon et al. (2003) to activate mouse B cells *in vitro* via TLR2 and TLR4. TLR2/6 ligands have, however, been shown to be effective in mouse models. As mentioned in the previous chapter, the TLR2/6 ligand Pam2Cys has been shown to be an effective adjuvant in a mouse influenza vaccine model (Tan et al. 2012). In addition,

Pam2CSK4, a TLR2/6 ligand which is structurally very similar to Pam2Cys, has been shown to drive a Th2 response and reduce parasite burden in a mouse *Brugia malayi* vaccine model (Halliday et al. 2016).

TLR ligands have several advantages over conventional adjuvants. Due to their direct modulation of both innate and adaptive immune effectors a wide range of mechanisms can be enlisted in the immune response. Tan et al. (2012) showed that the rapid onset of the innate immune response allows Pam2Cys to act not only as a vaccine adjuvant but also provide short-term prophylactic protection against influenza infection in mice while adaptive immunity is activated. Subsequently, Mifsud et al. (2016) found that the protective effect extended to protection against secondary pneumococcal infections. Another advantage is the ability to tailor the Th1/Th2 balance of the response induced. This is due to the varied signalling pathways and outcomes of the TLRs. For example, the TLR9 ligand 1018 ISS produces a mainly Th1 type response (Eng et al. 2013), whereas Pam2CSK4 leads to a Th2-skewed response in mice (Halliday et al. 2016). TLR ligands can also be incorporated into other adjuvants such as alum or liposomal adjuvants to synergise their effects; the MPL used in GSK's AS01 and AS04 are examples of this.

In this chapter we investigate the potential adjuvant effects of the TLR2/6-stimulatory extracts 1402EtL and 1412EtB on proliferation and antibody production in primary murine splenic B cells. As IgG1 predominates in vaccine responses (Siegrist 2008) switching expression of IgM to IgG1 was selected as the readout of class switching. The nuclear protein Ki-67 is strongly associated with cell proliferation (Duchrow et al. 1996), and as such was chosen as the readout for measuring induction of proliferation by the extracts. As the positive control a method outlined by Zaheen & Martin (2010) was chosen, using LPS and IL-4 to induce proliferation and class-switching from IgM to IgG1. A Pam2CSK4 treatment was included as an additional positive control for TLR2/6. The top concentration of plant extract and Pam2CSK4 was increased to account for the fact that primary cells are likely to have

lower constitutive expression of TLR2/6 than the transfected cell line used previously, and are also more likely to exhibit confounding cross-talk between varied signalling pathways.

5.2 Results

Results of flow cytometric analysis of cultured $CD19^+$ B cells are summarised in Figures 5.1 - 5.3, representative raw data are supplied in Appendix A.

5.2.1 Cell proliferation (Ki-67 expression)

When analysed, our positive controls failed to produce a significant increase in Ki-67 expression (Figure 5.5), neither did any concentration of 1402EtL. 1412EtB produced a strong dose-dependent increase in Ki-67 expression ($p \leq 0.0001$; # $R^2 \geq 0.9$). Acid-treated and boiled 1412EtB both retained the potential to elicit strong Ki-67 responses (both $p \leq 0.0001$), whereas the oxidised form of the extract produced a much-reduced effect ($p \leq 0.0001$). The >100kDa fraction of 1412EtB also produced a strong increase in Ki-67 expression ($p \leq 0.0001$) whereas the other fractions did not. Levels of Ki-67 produced in response to acid-treated and boiled extract, as well as the >100kDa fraction, were all significantly higher than those produced in response to 100µg/ml crude extract (all $p \leq 0.0001$).

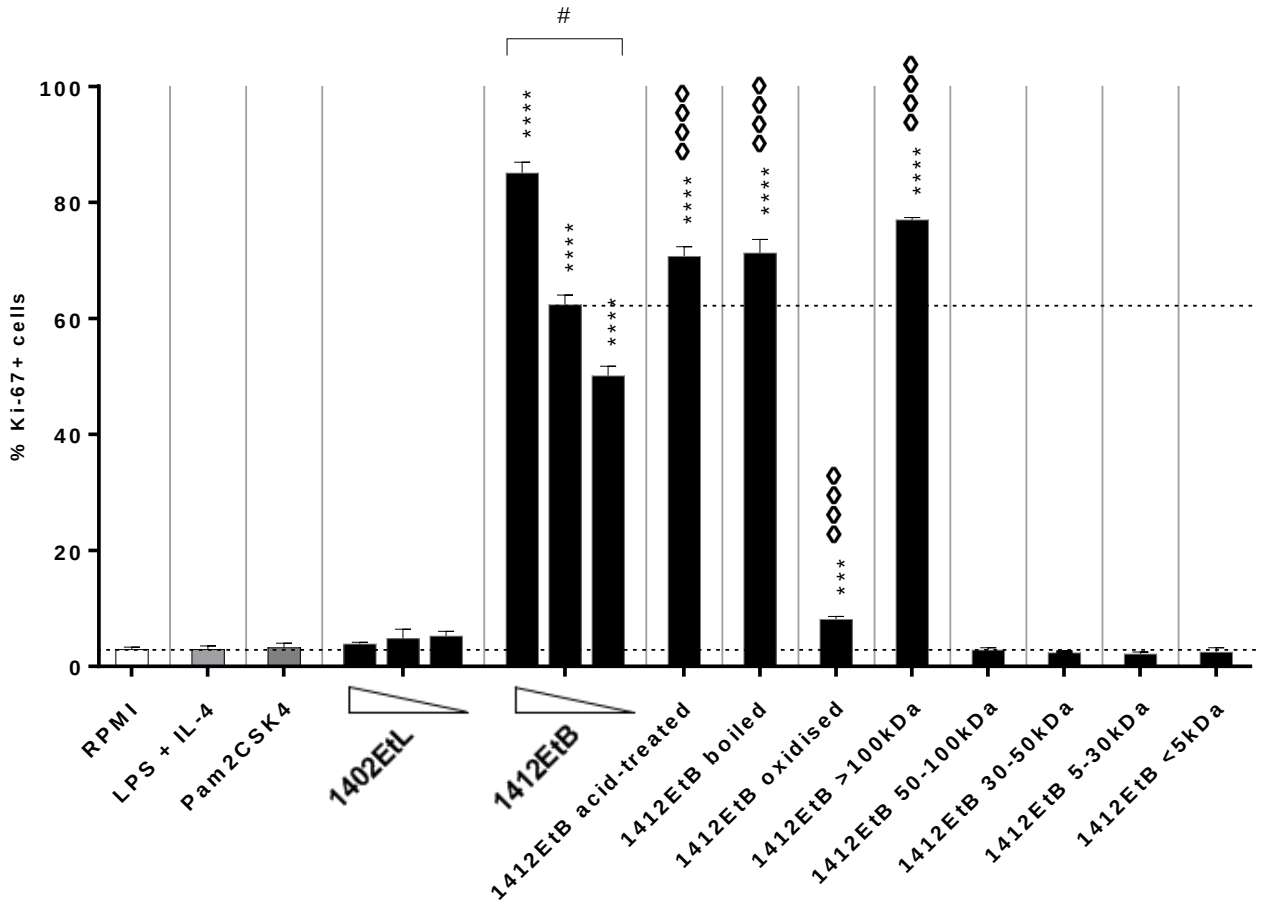


Figure 5.1. Summary of the effects of crude, modified and fractionated plant extracts on Ki-67 expression. Murine primary splenic B cells were incubated for 120h with crude 1402EtL or 1412EtB, modified (acid-treated, boiled or oxidised) or size-fractionated treatments of 1412EtB. Crude extracts were used at 200, 100 and 50µg/ml, modified and fractionated extracts at concentrations equivalent to 100µg/ml crude extract. Thereafter Ki-67 expression was assayed by FACS as described in section 2.2.2.3. Readings shown are means +/- SD of triplicate wells. The dashed lines indicate the percentages of Ki-67+ cells for the RPMI control and 100µg/ml crude extract. Results were tested for significant difference from RPMI control using two-way ANOVA; * $p \leq 0.05$; ** $p \leq 0.01$; *** $p \leq 0.001$; **** $p \leq 0.0001$; and from 100µg/ml crude extract: ◊ $p \leq 0.05$; ◊◊ $p \leq 0.01$; ◊◊◊ $p \leq 0.001$; ◊◊◊◊ $p \leq 0.0001$; responses to crude extracts tested for dose-dependency using non-linear one phase decay regression; # $R^2 \geq 0.9$

5.2.2 IgM expression

1402EtL produced a dose-dependent significant increase in IgM expression (Figure 5.6; 200 and 100µg/ml $p \leq 0.0001$; 50µg/ml $p \leq 0.05$; $R^2 \geq 0.9$), however 1412EtB produced a larger dose-dependent increase ($p \leq 0.0001$; # $R^2 \geq 0.9$). Acid-treated and boiled 1412EtB both elicited strong IgM responses (both $p \leq 0.0001$), whereas oxidised extract produced a reduced effect ($p \leq 0.0001$). The >100kDa fraction of 1412EtB also produced a strong increase in IgM expression ($p \leq 0.0001$) whereas the other fractions did not. Levels of IgM produced in response to acid-treated and boiled extract, as well as the >100kDa fraction, were all significantly higher than those produced in response to 100µg/ml crude extract (all $p \leq 0.0001$).

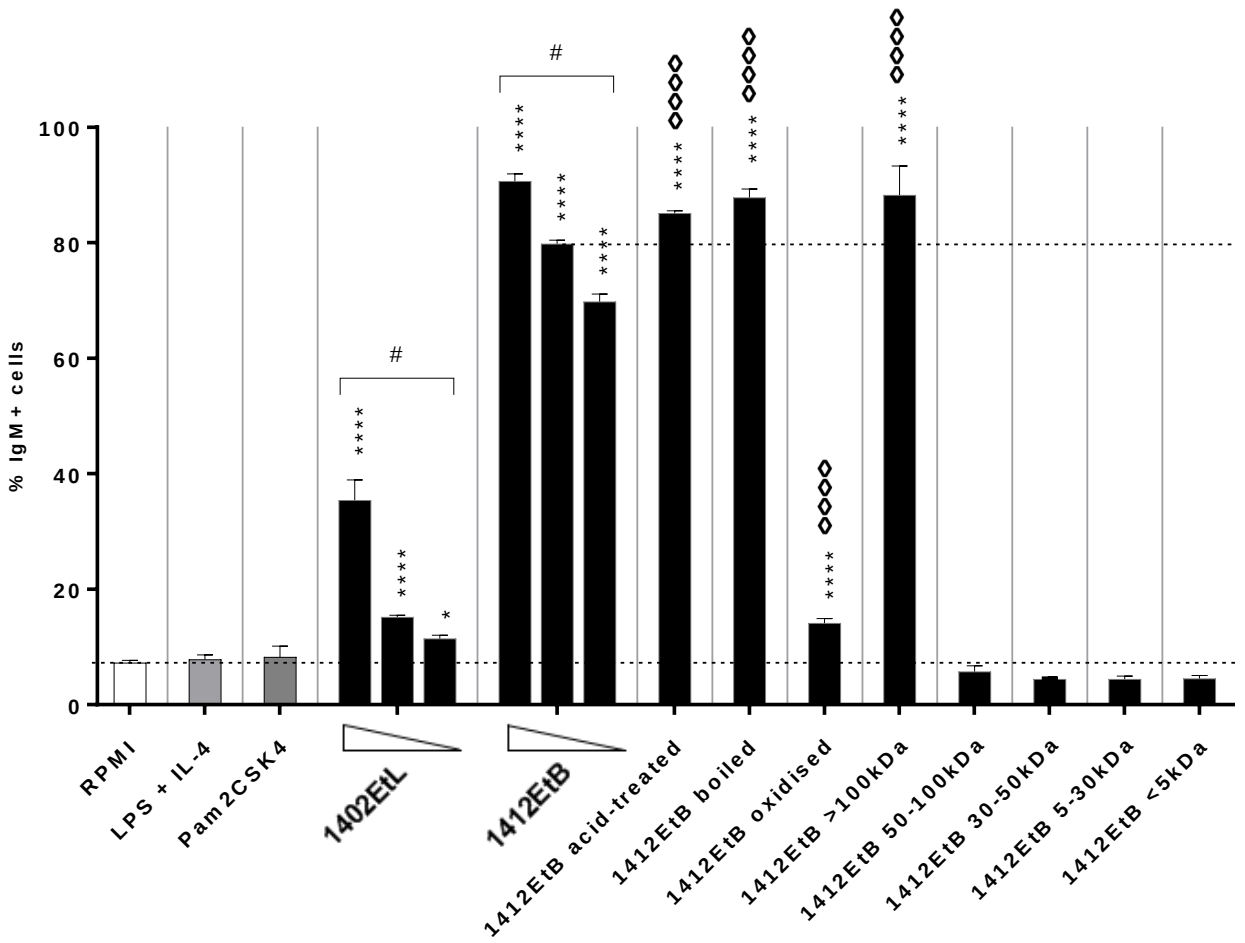


Figure 5.2. Summary of the effects of crude, modified and fractionated plant extracts on IgM expression. Murine primary splenic B cells were incubated for 120h with crude 1402EtL or 1412EtB, modified (acid-treated, boiled or oxidised) or size-fractionated treatments of 1412EtB. Crude extracts were used at 200, 100 and 50µg/ml, modified and fractionated extracts at concentrations equivalent to 100µg/ml crude extract. Thereafter IgM expression was assayed by FACS as described in section 2.2.2.3. Readings shown are means +/- SD of triplicate wells. The dashed lines indicate the percentages of IgM+ cells for the RPMI control and 100µg/ml crude extract. Results were tested for significant difference from RPMI control using two-way ANOVA; * $p \leq 0.05$; ** $p \leq 0.01$; *** $p \leq 0.001$; **** $p \leq 0.0001$; and from 100µg/ml crude extract: ◊ $p \leq 0.05$; ◊◊ $p \leq 0.01$; ◊◊◊ $p \leq 0.001$; ◊◊◊◊ $p \leq 0.0001$; responses to crude extracts tested for dose-dependency using non-linear one phase decay regression; # $R^2 \geq 0.9$

5.2.3 Antibody class switching - IgG1 expression

Neither of the positive controls produced a significant increase in IgG1 expression, although the mean percentage of $IgG1^+$ cells was 1.3-fold higher in response to LPS/IL-4 than RPMI, and 2-fold higher in response to Pam2CSK4 (Figure 5.7). 1402EtL produced a significant increase at 200µg/ml ($p \leq 0.0001$). Crude 1412EtB had no effect, however both acid-treated and boiled 1412EtB both elicited significant increases in IgG1 expression ($p \leq 0.001$), whereas the oxidised form of the extract did not. The >100kDa fraction of 1412EtB also produced an increase in IgG1 expression ($p \leq 0.0001$) whereas the other fractions did not.

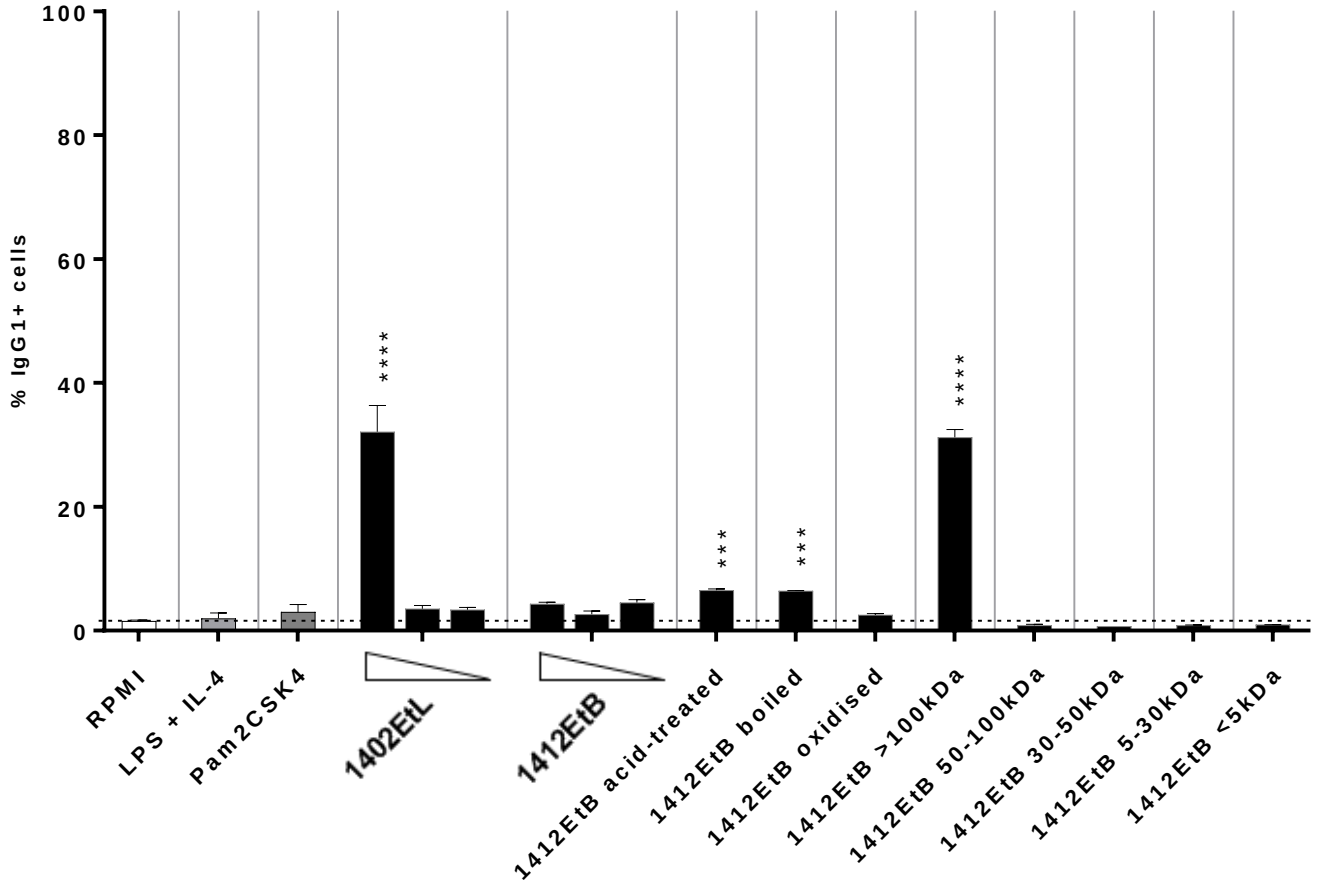


Figure 5.3. Summary of the effects of treatments on IgG1 expression. Bar chart summarising the effects of crude, modified and fractionated plant extracts on IgG1 expression. Murine primary splenic B cells were incubated for 120h with crude 1402EtL or 1412EtB, modified (acid-treated, boiled or oxidised) or size-fractionated treatments of 1412EtB. Crude extracts were used at 200, 100 and 50µg/ml, modified and fractionated extracts at concentrations equivalent to 100µg/ml crude extract. Thereafter IgG1 expression was assayed by FACS as described in section 2.2.2.3. Readings shown are means +/- SD of triplicate wells. The dashed lines indicate the percentages of IgG1+ cells for the RPMI control and 100µg/ml crude extract. Results were tested for significant difference from RPMI control using two-way ANOVA; * $p \leq 0.05$; ** $p \leq 0.01$; *** $p \leq 0.001$; **** $p \leq 0.0001$; and from 100µg/ml crude extract: ◊ $p \leq 0.05$; ◊◊ $p \leq 0.01$; ◊◊◊ $p \leq 0.001$; ◊◊◊◊ $p \leq 0.0001$; responses to crude extracts tested for dose-dependency using non-linear one phase decay regression; # $R^2 \geq 0.9$

5.3 Discussion

Our data would suggest that the two extracts tested have markedly different effects on B cell activity.

1402EtL did not affect proliferation, whereas the crude form of 1412EtB produced a strong, dose-dependent proliferative effect with between 85% and 50% Ki-67^{+} cells (Figure 5.5). In line with the findings from Chapter 4, this effect was much reduced in the oxidised extract and retained in the acid-treated and boiled extracts as well as the >100kDa fraction. An effect not observed in the HEK cell experiments was that the mean responses to the acid-treated, boiled and active fractionated extracts were 1.13, 1.14 and 1.24 times greater, respectively, than that of the equivalent dose of crude extract. It is possible that these procedures have denatured or removed competitor molecules from the crude extract or changed the presentation of the native ligand, allowing for increased ligand-receptor binding. It is also possible that the cytotoxicity observed in the initial screen is reduced or absent in the fractionated extract as the total concentration of exogenous chemicals in the growth medium is reduced. Through further purification and characterisation it might be possible to further amplify the proliferative effect, further reducing cytotoxicity and minimising the dose required to have a functional effect.

Both crude extracts elicited significant dose-dependent upregulation of IgM production, although the effect of 1412EtB was more than twice as large as that of 1402EtL at all concentrations tested (Figure 5.6). In a similar trend to the one observed in Ki-67 responses, the oxidised extract had a much-reduced effect and the acid-treated, boiled and >100kDa treatments all produced significantly higher levels of IgM than the equivalent dose of crude 1412EtB, suggesting that the same element of 1412EtB was responsible for both proliferation and IgM expression. In treatments expressing both IgM and Ki-67, they appear to be

coexpressed due to the predominance of $IgM^+/Ki\text{-}67^+$ over cells positive for Ki-67 or IgM alone (Figure 5.4 D, E, F, G, H, J).

As shown in Figure 5.7, 1402EtL caused a significant increase in IgG1 production at 200µg/ml, but not at 100 or 50µg/ml. There appear to be three distinct populations expressing varying levels of IgG1, as evidenced by three distinct peaks visible in histograms as represented in Figure 5.3 F (one large $IgG1^-$ population (circa 68% of gated cells) one large $IgG1^+$ (c. 27%) and one smaller $IgG1^+$ but with a greater fluorescence intensity (c. 5%)) and corresponding clusters in Figure 5.4 A. Within the two $IgG1^+$ clusters IgG1 appears to increase with Ki-67/IgM. Crude 1412EtB did not affect IgG1 production, but the acid-treated, boiled and >100kDa extracts did. The response to the >100kDa fraction was particularly strong, comparable in amplitude to that of 200µg/ml crude 1402EtL. The scatter plots of Figure 5.4 J appear to show two distinct populations of cells: one $IgG1^-$ population with very high Ki-67/IgM expression, and an $IgG1^+$ population with somewhat lower Ki-67/IgM expression. This suggests that some cells are proliferating strongly and others are class-switching while still expressing higher levels of Ki-67 and IgM than untreated cells. As with the 200µg/ml 1402EtL treatment, within the $IgG1^+$ population IgG1 appears to increase with Ki-67. The acid-treated and boiled 1412EtB treatments both elicited modest IgG1 responses (Figure 5.3 L and M). The scatter plots in Figure 5.4 G and H show that $IgG1^+$ cells were mostly IgM^+ and $Ki\text{-}67^+$ as well.

One notable feature of this experiment is the weak response in all parameters to both of the positive control treatments used. The parameter with the greatest difference in mean percentage of positive cells was IgG1, with LPS/IL-4 and Pam2CSK4 producing a 1.3-fold and 2-fold increase, respectively. This is consistent across all of our previous experiments which have produced between 1.2- and 2-fold increases in IgG1. It is possible that a greater number of replicates would increase the power of the analysis. Other studies have successfully used IL-4 and LPS to induce class IgG1 class switching *in vitro*, although often under different

conditions to those used here. For example, Mahata et al. (2014) attained 15% $IgG1^+$ cells after five days, however that study used 40μg/ml LPS and 25ng/ml IL-4 as opposed to the 25μg/ml LPS and 10ng/ml IL-4 used here. Dingler et al. (2014) managed in excess of 40% $IgG1^+$ cells using 40μg/ml LPS, 25ng/ml IL-4 and 20ng/ml B cell activating factor (BAFF). However, neither of the aforementioned studies state the percentage of $IgG1^+$ cells in untreated controls, so the relative increase in IgG1 cannot be calculated.

It has previously been shown that isotype switching to IgG1 is highly dependent on how many divisions the cell has undergone (Hodgkin et al. 1996; Hasbold et al. 1999). In the study by Hodgkin et al. $IgG1^+$ cells made up less than 3% of the population after two divisions, rising to more than 30% after six cycles. Given that none of the positive control treatments induced B cell proliferation this could have been a factor in their negligible IgG1 production. However, 200μg/ml 1402EtL produced a strong IgG1 response, with no corresponding increase in Ki-67. It is possible that the effect would have been even stronger in the presence of a proliferative effect. It is not clear why neither LPS/IL-4 nor Pam2CSK4 provided this mitogenic effect, as Hoffmann et al. (1977) found that either LPS or gram-negative lipoproteins induced proliferation in B cells *in vitro*, and more recently Borsutzky et al. (2005) found that the TLR2/6 ligand MALP-2 also induced proliferation in B cells as well as increasing the proportion of IgM- and IgG-secreting cells. Using carboxyfluorescein succinimidyl ester (CFSE) staining rather than Ki-67 expression as a measure of proliferation would have enabled us to discern and examine discrete generations of cells, which could help resolve this problem. An alternative to using LPS/IL-4 to activate B cells could be to replace the LPS with an anti-CD40 monoclonal antibody, as used by Rush & Hodgkin (2001). They found a similar pattern of cell generation-dependent IgG1 isotype switching to that observed by Hodgkin et al. (1996). Snapper et al. (1993) found that anti-TGF-β monoclonal antibody increased proliferation twofold, although it decreased production of IgG isotypes.

Another possibility is that the cells could have undergone sequential class switching from IgM to IgG1, then switching again to IgE. Mandler et al. (1993) found that only a very small proportion of B cells activated *in vitro* using LPS/IL-4 co-expressed IgG1 and IgE. In fact, of the IgM^+/IgE^+ cells analysed, only 3% were also $IgG1^+$. It could also be possible that IFN-γ-producing innate B cells are being induced by TLR ligand stimulation, as found by (Bao et al. 2014), given that IFN-γ is known to inhibit B cell differentiation (Abed et al. 1994).

Despite the weak responses to the intended positive controls, the validity of our results is supported by their low variability and by our previous experiments. Several conclusions can be drawn from the varied responses of murine splenic B cells to *in vitro* stimulation by the TLR2/6-stimulating extracts under investigation. Crude 1402EtL increased both IgM and IgG1 production, however previous experiments have shown that it loses its activity in the absence of the DMSO solvent. Further investigation could identify a method of retaining the solubility of the active component in aqueous solution, enabling purification and characterisation of the compound responsible for the class-switching effect. The strong, dose-dependent increase in proliferation and IgM production observed in response to 1412EtB, as well as the retention of activity in acid-treated, boiled and >100kDa fractions corroborates the findings of our previous findings with the transfected-HEK cell experiments. The increased Ki-67 and IgM response to these fractions, along with the added class-switching effect, makes 1412EtB a highly promising candidate for sourcing a novel TLR-mediated B cell adjuvant.

Further *in vitro* work to confirm or expand upon these findings could include a kinetic analysis of the full range of antibody isotypes to more completely understand the effects of >100kDa 1412EtB on the B cell response. Moreover, examining the effects on subpopulations of B cells would also help to direct the potential clinical uses of 1412EtB, such as enhancing the antibody-presenting capacity of B cells or restoration of antibody synthesis to regulatory B cells. Also worth investigation would be the antigen presenting capacity of B cells and

whether this could be modified by the use of 1412EtB for further optimisation of adjuvancy. Ultimately, with sufficient purification, characterisation and *in vitro* experimentation, the use of *in vivo* animal models to study these extracts' effects on infection, vaccination, cancer or autoimmunity would all be possible due to the wide range of immune and disease pathways influenced by TLRs.

Chapter 6. General Discussion

Over the course of this study we have investigated possible TLR-mediated immunomodulatory activity of a range of Malaysian plant extracts, with the aim of identifying candidates for development into novel immunomodulatory drugs or adjuvant components. Our bottom-up approach of progressing from an initial screen to TLR-specific characterisation to a primary cell-based assay system has provided us with valuable insight into possible candidates.

6.1 TLR-modulatory properties of plant extracts tested

From an initial screen of 21 extracts from 12 plant species, 14 were found to either stimulate or inhibit CXCL8 production mediated by TLR2/1, 2/6 or 4 in stably-transfected HEK293 cell lines (Table 3.1). Three TLR2/6-modulatory extracts were selected for characterisation by chemical modification and size fractionation. These were two stimulatory extracts (1402EtL, an ethanolic extract of the leaves of *Tristaniopsis merguensis* and 1412EtB, an ethanolic extract of the bark of *Ficus ribes*) and one inhibitory extract (1404EtL, an ethanolic extract of the leaves of *Gironniera nervosa*).

These plants have not yet been the subject of any published immunological investigation, but two are reported as being used in traditional medicine in their native habitats. Various products of *F. ribes* are used in Javan traditional medicine (Priyadi et al. 2010). In particular the bark, from which 1412EtB is derived, is used for the treatment of malaria. A tea brewed from the leaves of *T. merguensis* is also used in some Indonesian communities to treat fever (Weihreter 2014). *Tree Flora of Sabah and Sarawak* (2002) lists *G. nervosa* as possessing edible fruits and timber of construction quality, but no purported medicinal uses. While it is important to note that the therapeutic efficacies of these traditional remedies have not yet been verified or refuted in published scientific literature, it is possible to hypothesise on their

effectiveness in the context of available immunological knowledge and the additional understanding gained in this study. In light of its stimulatory effects on TLR2/1 and TLR2/6, it is possible that the bark of *F. ribes* does affect the host response to malaria infection. Activation of monocytes has been shown by several studies to play an array of important roles during malaria infection (Ing et al. 2005; Leisewitz et al. 2004), and TLR stimulation could boost the response of monocytes to *Plasmodium* infection. On the other hand, controlling the pathology of malaria infection is the product of a trade-off between resistance and tolerance; excessive activation can lead to increased risk of dangerous complications such as cerebral malaria, lung injury or placental malaria (Perkins et al. 2011; Chua et al. 2013). Glycosylphosphatidylinositols (GPIs) from *Plasmodium falciparum* have been shown to act as ligands for both TLR2/1 and TLR2/6 (Durai et al. 2013), so synergistic activation of innate immune effectors by a combination of protozoal PAMPs and *F. ribes* exract could result in increased immunopathology. The role of TLRs in malaria is complex and still not fully understood, with indications that they are likely involved in both protection and immunopathogenesis (M Eriksson et al. 2014; Chua et al. 2013). The efficacy of a TLR-activating plant such as *T. merguensis* to treat fever symptoms is dubious as the NF-κB pathway is known to play a role in the onset of pyrexia (Ryan & Levy 2003; Shao et al. 2004; Lee et al. 2003). If the remedy is indeed effective at reducing fever, it is likely that other signalling pathways are involved which might mitigate pyrogenetic NF-κB signalling. One possibility is inhibition of cyclooxygenases, a known mechanism of plant-derived NSAIDS such as aspirin (Hinz & Brune 2007).

6.2 Characterisation of selected extracts

When we attempted to characterise the three selected extracts, 1402EtL was found to be insoluble in the absence of DMSO, which precluded further characterisation. However, 1404EtL and 1412EtB could both be dialysed into PBS without precipitation formation and so

were successfully modified and fractionated, with a 10-30kDa active fraction of 1404EtL and >100kDa active fraction of 1412EtB identified. As discussed in Chapter 5, these are both well within the size range of known TLR stimulators and inhibitors. 1412EtB was found to lose its stimulatory activity when oxidised by sodium metaperiodate, but retained activity when boiled or acid-treated. This suggests that a carbohydrate-containing molecule is critical to the extract's TLR2/6-stimulatory activity. Many existing TLR2/6 ligands contain glycan components, such as lipomannan (Dao et al. 2004), lipoteichoic acid (von Aulock et al. 2003) and peptidoglycan (Ozinsky et al. 2000) as well as the plasmodial GPIs mentioned above (Durai et al. 2013). 1404EtL retained activity after all three treatments, suggesting that the active component is resistant to acid, thermal and oxidative degradation. This stability could be caused by any of a range of factors, depending on what type of molecule the active component is. For example, in peptides β-pleated sheets are known be highly stable secondary structures (Perczel et al. 2005), and motifs such as positively-charged hairpins decrease pH stability (García-Mayoral et al. 2006; Talley & Alexov 2010). Whatever the cause, such stability would be an extremely beneficial trait for any product potentially developed from this extract.

6.3 B-cell *in vitro* modulation by selected extracts

Finally, we investigated the *in vitro* effects of the stimulatory extracts 1402EtL and 1412EtB on primary murine splenic B lymphocytes. 1402EtL was found to increase IgM expression and, at 200µg/ml, induce antibody class switching to IgG1 (Figure 5.6 and Figure 5.7). This is the dominant isotype in human vaccine responses (Siegrist 2008), suggesting that 1402EtL has promise as a potential vaccine adjuvant, however the insolubility of its active component in the absence of DMSO presents a major obstacle to further investigation and any clinical application. If it could somehow be solubilised then its properties could potentially be improved, as seen in the active fraction of 1412EtB when compared to crude extract (Figures

5.5 - 5.7). There are a number of possible approaches to this, such as conjugation of a polyethylene glycol (PEG) chain (PEGylation). PEGylation is known to increase solubility and stability of a range of biological molecules (Harris & Chess 2003). For example, Tan et al. (2012) PEGylated Pam2Cys to increase its solubility for intranasal administration. Another use of polymers to increase solubility is in nanoparticulate delivery systems, as used by Chen et al. (2014) to package curcumin in a polymeric nanoparticle to overcome its hydrophobic nature in aqueous conditions.

Crude 1412EtB increased B cell proliferation (as measured by Ki-67 expression) and upregulated IgM expression. In addition, the acid-treated, boiled and >100kDa forms of the extract produced even greater Ki-67 and IgM responses and also induced IgG1 class switching (Figures 5.5 - 5.7). The isotype switching response was particularly strong in the fractionated extract, suggesting that removal rather than denaturation of non-target molecules better improves the efficacy of the extract. The combination of proliferative and class switching responses observed in response to the >100kDa fraction of 1412EtB suggest that further investigation and characterisation of the active component could yield an effective vaccine adjuvant. The difference in B cell responses to 1402EtL and 1412EtB suggest that pathways other than solely TLR2/6 signalling are being affected by one or both of these extracts. For example, in the initial screen 1402EtL was found to stimulate TLR4 at 100µg/ml, whereas 1412EtB had no effect (Figure 3.4).

6.4 Evaluation of 1412EtB, ethanolic extract of bark of *F. ribes*

The inactivation of 1412EtB by periodate oxidation suggests that a carbohydrate or glycan-containing molecule is involved in the extract's TLR-modulatory activity. Carbohydrate-based PRR ligands represent an attractive avenue of investigation because they are able to bind a wide variety of receptor targets, including TLRs, CLRs and NLRs (Petrovsky & Cooper 2011). PRR-binding carbohydrates include glucans such as dextran (Houston et al. 1976; Choi et al.

2010) and zymosan (Sato et al. 2003), mannans such as lipomannan (Dao et al. 2004) and phospholipomannan (Jouault et al. 2003) as well as a range of saponins, fructans and other carbohydrate groups (Petrovsky & Cooper 2011). For example, Berner et al. (2008) proposed the use of a β-glucan derived from *Saccharomyces cerevisiae* as a dual-purpose delivery system and adjuvant in conjugant vaccines, increasing phagocytosis and IgG response to BSA immunisation. Another advantage of carbohydrate-based adjuvants is that they avoid the rare cases of problems occasionally caused by long-term accumulation of aluminium salts associated with alum-based adjuvants in susceptible individuals such as macrophagic myofasciitis (Exley et al. 2009; Gherardi et al. 2016).

6.5 Contextual considerations

Our findings concerning the structure and adjuvant activity of 1412EtB can be viewed in the context of an increased interest in the development of PRR-mediated adjuvants and immunomodulatory drugs (Kumar et al. 2012; Steinhagen et al. 2011). Innate immune receptors such as PRRs represent promising immunological targets because of their central role in coordination of both innate and adaptive immune responses and the wide range of immune effectors brought to bear by their activation. This is exemplified by the demonstration by Mifsud et al. (2016) that TLR2/6 ligand Pam2Cys not only acted as a potent adjuvant in a mouse-adapted H1N1 avian influenza vaccine model, but also provided short-term prophylactic protection from both viral infection and bacterial coinfection. The role of PRRs such as TLRs in directing the immune response also allows the Th1/Th2 balance to be adjusted as desired, as exemplified by the Th2-polarised adjuvant effect of Pam2CSK4 in a murine *Brugia malayi* vaccine model (Halliday et al. 2016). Another use of TLR-mediated Th1/Th2 modulation would be to shift the equilibrium away from a pathological Th2 response in a range of allergic and autoimmune disorders. The TLR9 agonist CYT003 (also known as QbG10), made up of a CpG ODN packaged in a virus-like particle, was found by

Beeh et al. (2013) to reduce symptoms of allergic asthma in a proof-of-concept clinical trial, however a subsequent phase IIb trial by Casale et al. (2015) did not find such an effect. TLRs are thought to play varied roles in multiple sclerosis (Miranda-Hernandez & Baxter 2013), suggesting that they might be useful targets for the development of future treatments (Gooshe et al. 2014).

The fact that the candidates under investigation in this study are all plant extracts, and that some in particular are used in traditional medicine for conditions such as fever and infection, highlights the value of these pools as sources of novel therapeutics. There are many examples of traditional medicinal plants which, following rigorous investigation and review, have yielded drugs which are now approved for a diverse range of clinical uses in humans. Colchicine, derived from the autumn crocus *Colchicum autumnale*, is the gold standard drug for the treatment of the inherited autoimmune disorder known as familial Mediterranean fever (Zadeh et al. 2011). Capsaicin, from *Capiscum spp.* chilli peppers, is approved for topical use to alleviate neuropathic pain (Haanpää & Treede 2012). Indeed, Tu Youyou was awarded half of the 2015 Nobel Prize for Physiology or Medicine for the development of the anti-malarial drug Artemisinin from sweet wormwood, *Artemisia annua* (Tu 2011; Van Voorhis et al. 2015). In 2015 Harrison et al. reconstructed a salve recipe found in a medieval textbook and found that it significantly inhibited the growth of methicillin-resistant *Staphylococcus aureus* (MRSA), despite the fact that the text predated germ theory by several hundred years. Many of these global botanical and cultural resources are under threat due to changing land use, as ecosystem destruction and cultural assimilation lead to loss of undiscovered or unstudied species (Giam et al. 2010; Ceballos et al. 2015) and local knowledge (Reddy 2004; Sudeesh 2012). Increasing efforts to protect biodiversity and preserve cultural and human knowledge banks would have both financial and societal benefits (Mendelsohn & Balick 1995; Baker et al. 2007).

While there have been many important successes in the isolation of scientifically verifiable medicines from the extensive catalogue of enthnopharmacological remedies accumulated throughout human history, it is important to retain a healthy scepticism when addressing any such claims (Talalay 2001; Rates 2001). There is a growing pseudo-scientific "wellness" industry which does not demand the same burden of evidence as medical science, and risks harm to patients with unproven claims about efficacy and safety of a wide variety of treatments, both plant-based and otherwise, for various conditions. Nevertheless, in the future plants will almost certainly continue to be a source of novel bioactive compounds, and TLRs are likely to play an increasingly important role in the management of immune-related conditions as our understanding of them and their roles in various diseases and disorders improves.

6.6 Study limitations and further work

Several limitations were encountered during the course of this study, which there were insufficient time and resources to overcome here.

Firstly, it was not possible to obtain a reliable CXCL8 readout from the HEKBlue TLR5 cells used in the screening experiments. Using a HEK293 cell line without the HEKBlue reporter plasmid would allow for assessment of TLR5-modulatory properties of the extracts under investigation, in a manner comparable to the other HEK293 TLR lines.

If the fluorescent lectin staining experiment could be optimised, a battery of lectins could be used to probe for a range of glycan moieties. Glycan arrays would potentially provide a more precise, higher-throughput method than the dot blotting employed in this study (Liang & Wu 2009). The data gathered would be particularly helpful in characterising the active component of 1412EtB, as our data suggest that a carbohydrate structure involved in its TLR2/6 modulatory activity.

The crude extracts produced smears when subjected to SDS-PAGE, possibly due to their diverse composition. Running the active fractions of those extracts could provide improved resolution and assist in identifying the active molecule. In addition, assessing the cytotoxicity of separate fragments rather than crude extracts would reduce the likelihood of metabolic choking by high concentrations of endogenous solutes and provide more salient information on the toxicity of the active components.

A major limitation of the primary B lymphocyte experiments was the difficulty in achieving a strong positive control for proliferation, IgM expression or IgG1 class switching. As outlined in the discussion of that chapter, an anti-CD40 monoclonal antibody could be used as an alternative to LPS to activate B cells (Rush & Hodgkin 2001). Using CFSE staining rather than Ki-67 expression as a proliferation metric would offer the possibility of separately analysing discrete generations of cells, to examine Ig profile in relation to cell division.

The promising results regarding the TLR-modulatory and B cell stimulatory properties of 1412EtB extract present several possible avenues for further research. Expanding the investigation to include other primary TLR2/6-expressing cell types such as dendritic cells (Nakao et al. 2005) and epithelial cells (Huhta et al. 2016) could yield valuable insight into the effects of 1412EtB within distinct intracellular signalling environments found at the sites of a wide range of infections and immunopathologies. *In vitro* co-culture tissue modelling could be used to mimic *in vivo* cellular communities to investigate the effects of 1412EtB on interactions between relevant cell types. Once this is more fully understood investigation into use of the active extract *in vitro*, and later *in vivo*, disease and vaccination models would guide the formulation of potential clinical applications.

Further investigation of 1402EtL would be best served by first finding a way to maintain its solubility in aqueous solution. This would both enable a wider range of tests to be carried out and increase the feasibility of its clinical use. In this study we were unable to investigate

potential inhibition of TLR-mediated B cell activity by 1404EtL. Once a strong positive control has been optimised, it will be possible to assess inhibitory as well as stimulatory effects. In addition, there were several other putatively active extract/TLR combinations identified in the initial screen which there was insufficient time to investigate further (Table 3.1). These merit further investigation, because any of them might potentially contain valuable bioactive compounds.

6.7 Concluding remarks

In summary, the study of TLRs and other PRRs continues to be one of the most exciting and fruitful areas in modern immunology, providing the opportunity to modulate and coordinate immunity more finely than ever before. A >100kDa glycan-containing molecule found in the ethanolic extract of the bark of *F. ribes* stimulates TLR2/1 and 2/6, and induces proliferation and class-switching in murine B cells, providing a promising candidate for development of a novel TLR-mediated vaccine adjuvant. Other extracts screened were also found to stimulate or inhibit TLR2/1, 2/6 or 4, and further investigation of these could yield more pharmaceutical candidates. As our understanding grows, TLR-mediated medicine has the capacity to bring about changes in vaccination and the treatment of conditions such as immune disorders, infection and cancer. Plants, particularly those used in traditional medicine around the world, continue to be promising sources of new drugs. We must, however, remain vigilant against both destruction and misrepresentation of these resources. If utilised appropriately, there are untold pharmacological treasures which could be harnessed to improve the health of people the world over.

Bibilography

Abed, N.S. et al., 1994. Interferon-gamma regulation of B lymphocyte differentiation: activation of B cells is a prerequisite for IFN-gamma-mediated inhibition of B cell differentiation. *Cellular immunology*, 153(2), pp.356–66. Available at: http://www.sciencedirect.com/science/article/pii/S0008874984710343.

Ahn, S.-I. et al., 2016. *Eupatorium makinoi* suppresses toll-like receptor signaling pathways. *Food and Agricultural Immunology*, 27(2), pp.242–250. Available at: http://www.tandfonline.com/doi/full/10.1080/09540105.2015.1086315.

Ahn, S.-I., Lee, J.-K. & Youn, H.-S., 2009. Inhibition of homodimerization of toll-like receptor 4 by 6-shogaol. *Molecules and cells*, 27(2), pp.211–5. Available at: http://www.ncbi.nlm.nih.gov/pubmed/19277504 [Accessed August 20, 2013].

Anon, 2011. Corning Filtration Guide: Innovative Products for Filtration and Ultrafiltration. , p.2. Available at: https://www.corning.com/media/worldwide/cls/documents/CLS-FIL-004 REV4 DL.pdf.

Anon, 2016. Dynavax press release. Available at: http://investors.dynavax.com/releasedetail.cfm?ReleaseID=965615 [Accessed July 8, 2016].

Anon, 2014. Mfg Polysulfone Chemical Compatibility Chart. , p.2. Available at: http://www.industrialspec.com/pdf/polysulfone-chemical-compatibility-chart-from-ism.pdf.

Anon, 2013. *The Merck Index* 15th ed., The Royal Society of Chemistry.

von Aulock, S. et al., 2003. Lipoteichoic acid from Staphylococcus aureus is a potent stimulus for neutrophil recruitment. *Immunobiology*, 208(4), pp.413–22. Available at: http://www.ncbi.nlm.nih.gov/pubmed/14748514.

Awate, S., Babiuk, L.A. & Mutwiri, G., 2013. Mechanisms of action of adjuvants. *Frontiers in Immunology*, 4(MAY), pp.1–10.

Baker, D.D. et al., 2007. The value of natural products to future pharmaceutical discovery. *Natural product reports*, 24(6), pp.1225–1244.

Balachandran, P. et al., 2006. Toll-like receptor 2-dependent activation of monocytes by Spirulina polysaccharide and its immune enhancing action in mice. *International Immunopharmacology*, 6(12), pp.1808–1814.

Balzola, F. et al., 2013. Andrographis paniculata extract (HMPL-004) for active ulcerative colitis. *Inflammatory Bowel Disease Monitor*, 13(2), p.70. Available at: http://dx.doi.org/10.1038/ajg.2012.340.

Bao, Y. et al., 2014. Identification of IFN-γ-producing innate B cells. *Cell research*, 24(2), pp.161–76. Available at: http://dx.doi.org/10.1038/cr.2013.155.

Barton, G.M. & Kagan, J.C., 2009. A cell biological view of Toll-like receptor function: regulation through compartmentalization. *Nature reviews. Immunology*, 9(8), pp.535–42. Available at: http://www.ncbi.nlm.nih.gov/pubmed/19556980 [Accessed May 31, 2013].

Beeh, K.M. et al., 2013. The novel TLR-9 agonist QbG10 shows clinical efficacy in persistent allergic asthma. *Journal of Allergy and Clinical Immunology*, 131(3), pp.866–874. Available at: http://dx.doi.org/10.1016/j.jaci.2012.12.1561.

Behboudi, S., Morein, B. & Villacres-Eriksson, M., 1996. In vitro activation of antigen-presenting cells (APC) by defined composition of Quillaja saponaria Molina triterpenoids. *Clinical and experimental immunology*, 105(1), pp.26–30. Available at: http://www.pubmedcentral.nih.gov/articlerender.fcgi?artid=2200485&tool=pmcentrez&rendertype=abstract.

Bekeredjian-Ding, I. & Jego, G., 2009. Toll-like receptors - Sentries in the B-cell response. *Immunology*, 128(3), pp.311–323.

Bell, J.K. et al., 2003. Leucine-rich repeats and pathogen recognition in Toll-like receptors. *Trends in Immunology*, 24(10), pp.528–533.

Berger, M. et al., 2015. Mutagenetix Phenotypic Mutation “TLR13rev1.” *Mutagenix*, 17, pp.1–17.

Bergstrom-Mollaoglu, M. et al., 1992. Antigen-specific increases in the number of splenocytes expressing MHC class II molecules following restimulation with antigen in various physical forms. *Scandinavian Journal of Immunology*, 36(4), pp.565–574.

Bernatoniene, J. et al., 2008. Induction of CC and CXC Chemokines in Human Antigen-Presenting Dendritic Cells by the Pneumococcal Proteins Pneumolysin and CbpA, and the Role Played by Toll-Like Receptor 4, NF-κB, and Mitogen-Activated Protein Kinases. *The Journal of Infectious Diseases*, 198(12), pp.1823–1833. Available at: https://academic.oup.com/jid/article-lookup/doi/10.1086/593177.

Berner, V.K., Sura, M.E. & Hunter, K.W., 2008. Conjugation of protein antigen to microparticulate beta-glucan from Saccharomyces cerevisiae: A new adjuvant for intradermal and oral immunizations. *Applied Microbiology and Biotechnology*, 80(6), pp.1053–1061.

Bertoglio, J.C. et al., 2016. Andrographis paniculata decreases fatigue in patients with relapsing-remitting multiple sclerosis: a 12-month double-blind placebo-controlled pilot study. *BMC Neurology*, 16(1), p.77. Available at: http://bmcneurol.biomedcentral.com/articles/10.1186/s12883-016-0595-2.

Bhaskar, S., Sudhakaran, P.R. & Helen, A., 2016. Quercetin attenuates atherosclerotic inflammation and adhesion molecule expression by modulating TLR-NF-κB signaling pathway. *Cellular Immunology*, 1. Available at: http://linkinghub.elsevier.com/retrieve/pii/S0008874916300843.

Bischof, J.C. & He, X., 2005. Thermal stability of proteins. *Annals of the New York Academy of Sciences*, 1066, pp.12–33.

Biswas, S.K. et al., 2006. A distinct and unique transcriptional program expressed by A distinct and unique transcriptional program expressed by tumor-associated macrophages (defective NF- B and enhanced IRF-3 / STAT1 activation). *Blood*, 107(5), pp.2112–22. Available at: http://www.ncbi.nlm.nih.gov/pubmed/16269622.

Blüml, S. et al., 2013. B-cell targeted therapeutics in clinical development. *Arthritis research & therapy*, 15 Suppl 1(Suppl 1), p.S4. Available at: http://arthritis-research.com/content/15/S1/S4.

Borsutzky, S. et al., 2005. The Mucosal Adjuvant Macrophage-Activating Lipopeptide-2 Directly Stimulates B Lymphocytes via the TLR2 without the Need of Accessory Cells. *The Journal of Immunology*, 174(10), pp.6308–6313. Available at: http://www.jimmunol.org/content/174/10/6308.full.

Botos, I., Segal, D.M. & Davies, D.R., 2011. The structural biology of Toll-like receptors. *Structure*, 19(4), pp.447–459. Available at: http://dx.doi.org/10.1016/j.str.2011.02.004.

Brightbill, H.D. et al., 1999. Host Defense Mechanisms Triggered by Microbial Lipoproteins Through Toll-Like Receptors. *Science*, 285(5428), pp.732–736. Available at: http://www.sciencemag.org/cgi/doi/10.1126/science.285.5428.732.

Bucciantini, M. et al., 2002. Inherent toxicity of aggregates implies a common mechanism for protein misfolding diseases. *Nature*, 416(6880), pp.507–511.

Byeon, S.E. et al., 2012. Molecular mechanism of macrophage activation by red ginseng acidic polysaccharide from Korean red ginseng. *Mediators of inflammation*, 2012, p.732860. Available at: http://www.pubmedcentral.nih.gov/articlerender.fcgi?artid=3306998&tool=pmcentrez&rendertype=abstract [Accessed March 26, 2014].

Camacho, A.G.A. et al., 2011. TLR5-dependent immunogenicity of a recombinant fusion protein containing an immunodominant epitope of malarial circumsporozoite protein and the Flic flagellin of Salmonella Typhimurium. *Memorias do Instituto Oswaldo Cruz*, 106(SUPPL. 1), pp.167–171.

Campbell, W.C. et al., 1984. The discovery of ivermectin and other avermectins. *Pesticide synthesis through rational approaches*, pp.5–20.

Carrick, J., Chan, K. & Cheung, H., 1968. A new phytochemical survey of Malaya - Chemical screening. *Chem. Pharm. Bull.*, 16(12), pp.2436–2441.

Casale, T.B. et al., 2015. CYT003, a TLR9 agonist, in persistent allergic asthma - A randomized placebo-controlled Phase 2b study. *Allergy: European Journal of Allergy and Clinical Immunology*, 70(9), pp.1160–1168.

Casella, C.R. & Mitchell, T.C., 2008. Putting endotoxin to work for us: MPLA as clinical adjuvant. *Cell Mol Life Sci*, 65(20), pp.3231–3240.

Cavalieri, D. et al., 2016. Plant microRNAs as novel immunomodulatory agents. *Scientific Reports*, 6(April), p.25761. Available at: http://www.nature.com/articles/srep25761.

CaymanChemical, 2015. TAK-242. Available at: https://www.caymanchem.com/pdfs/13871.pdf.

Ceballos, G. et al., 2015. Accelerated modern human – induced species losses: entering the sixth mass extinction. *Sciences Advances*, 1(e1400253), pp.1–5.

Chahal, D.S. et al., 2013. Plant-Based Modulation of Toll-like Receptors: An Emerging Therapeutic Model. *Phytotherapy research : PTR*, 27(10), pp.1423–1438. Available at: http://www.ncbi.nlm.nih.gov/pubmed/23147906.

Chan, V.S. et al., 2013. B-cell-targeted therapies in systemic lupus erythematosus. *Cellular & Molecular Immunology*, 10(2), pp.133–142. Available at: http://ovidsp.ovid.com/ovidweb.cgi?T=JS&CSC=Y&NEWS=N&PAGE=fulltext&D=medl&AN=23455017.

Chatterjee, D. & Khoo, K., 2001. The surface glycopeptidolipids of mycobacteria: structures and biological properties. *Cellular and Molecular Life Sciences*, 58, pp.2018–2042.

Chen, J.C. et al., 2005. Cucurbitacins and cucurbitane glycosides: structures and biological activities. *Natural product reports*, 22, pp.386–399.

Chen, X. et al., 2014. Nanocurcumin attenuates inflammation by decreasing Toll-like receptor 2 and 4 expression and activity and promoting an anti-inflammatory macrophage phenotype (830.22). *The FASEB Journal* , 28(1 Supplement). Available at: http://www.fasebj.org/content/28/1_Supplement/830.22.abstract.

Choi, H.J. et al., 2010. A pattern recognition receptor, SIGN-R1, mediates ROS generation against polysaccharide dextran, resulting in increase of peroxiredoxin-1 and its interaction to SIGN-R1. *Biomolecules and Therapeutics*, 18(3), pp.271–279.

Chua, C.L.L. et al., 2013. Monocytes and macrophages in malaria: Protection or pathology? *Trends in Parasitology*, 29(1), pp.26–34. Available at: http://dx.doi.org/10.1016/j.pt.2012.10.002.

Clamp, J.R. & Hough, L., 1965. The Periodate Oxidation of Amino Acids With Reference To Studies on Glycoproteins. *The Biochemical journal*, 94, pp.17–24. Available at: http://www.pubmedcentral.nih.gov/articlerender.fcgi?artid=1206400&tool=pmcentrez&rendertype=abstract.

Clark-Lewis, I. et al., 1991. Structure-activity relationships of interleukin-8 determined using chemically synthesized analogs. Critical role of NH2-terminal residues and evidence for uncoupling of neutrophil chemotaxis, exocytosis, and receptor binding activities. *The*

Journal of biological chemistry, 266(34), pp.23128–23134.

Colletti, M. & Cruz, M., 2001. New England Biolabs. , (201213716), p.67789228. Available at: http://discovery.ucl.ac.uk/239013/ [Accessed September 11, 2016].

Czeslick, E. et al., 2006. E5564 (Eritoran) inhibits lipopolysaccharide-induced cytokine production in human blood monocytes. *Inflamm.Res.*, 55(11), pp.511–515.

Dange, R.B. et al., 2015. Toll-like receptor 4 inhibition within the paraventricular nucleus attenuates blood pressure and inflammatory response in a genetic model of hypertension. *Journal of neuroinflammation*, 12(1), p.31. Available at: http://www.pubmedcentral.nih.gov/articlerender.fcgi?artid=4337244&tool=pmcentrez&rendertype=abstract.

Dao, D.N. et al., 2004. Mycobacterium tuberculosis Lipomannan Induces Apoptosis and Interleukin-12 Production in Macrophages Mycobacterium tuberculosis Lipomannan Induces Apoptosis and Interleukin-12 Production in Macrophages. *Infect. Immun.*, 72(4), pp.2067–2074.

Dekruyff, R.H. et al., 2014. Innate immunity in the lung regulates the development of asthma. *Immunological Reviews*, 260(1), pp.235–248.

Delazar, A. et al., 2006. Flavone C-glycosides and cucurbitacin glycosides from Citrullus colocynthis. *Daru*, 14(3), pp.109–114. Available at: http://www.scopus.com/inward/record.url?eid=2-s2.0-33751335866&partnerID=tZOtx3y1.

Dewick, P.M., 2009. Medicinal natural products. A biosynthetic approach. In *Medicinal natural products. A biosynthetic approach. 3rd ed.* John Wiley & Sons Ltd, pp. 311–481.

Didierlaurent, A.M. et al., 2009. AS04, an aluminum salt- and TLR4 agonist-based adjuvant system, induces a transient localized innate immune response leading to enhanced adaptive immunity. *Journal of immunology*, 183(10), pp.6186–97. Available at: http://www.jimmunol.org/cgi/doi/10.4049/jimmunol.0901474%5Cnhttp://www.ncbi.nlm.nih.gov/pubmed/19864596%5Cnhttp://www.ncbi.nlm.nih.gov/pubmed/19864596.

Dinan, L. et al., 1997. Cucurbitacins are insect steroid hormone antagonists acting at the ecdysteroid receptor. *The Biochemical journal*, 327 (Pt 3, pp.643–650.

Dingler, F.A. et al., 2014. Uracil excision by endogenous SMUG1 glycosylase promotes efficient Ig class switching and impacts on A:T substitutions during somatic mutation. *European Journal of Immunology*, 44(7), pp.1925–1935.

Dong, Y. et al., 2010. Cucurbitacin E, a tetracyclic triterpenes compound from Chinese medicine, inhibits tumor angiogenesis through VEGFR2-mediated Jak2-STAT3 signaling pathway. *Carcinogenesis*, 31(12), pp.2097–2104.

Dowling, J.K. & Mansell, A., 2016. Toll-like receptors: the swiss army knife of immunity and vaccine development. *Clinical & Translational Immunology*, 5(5), p.e85. Available at: http://www.nature.com/doifinder/10.1038/cti.2016.22.

Duchrow, M. et al., 1996. Molecular characterization of the gene locus of the human cell proliferation-associated nuclear protein defined by monoclonal antibody Ki-67. *Cell proliferation*, 29(1), pp.1–12. Available at: http://www.ncbi.nlm.nih.gov/pubmed/8603106.

Dupuis, M. et al., 1998. Dendritic cells internalize vaccine adjuvant after intramuscular injection. *Cellular immunology*, 186(1), pp.18–27. Available at: http://www.sciencedirect.com/science/article/pii/S0008874998912837.

Durai, P., Govindaraj, R.G. & Choi, S., 2013. Structure and dynamic behavior of Toll-like receptor 2 subfamily triggered by malarial glycosylphosphatidylinositols of Plasmodium falciparum. *FEBS Journal*, 280(23), pp.6196–6212.

Eng, N.F. et al., 2013. The potential of 1018 ISS adjuvant in hepatitis B vaccines: HEPLISAV" review. *Human Vaccines and Immunotherapeutics*, 9(8), pp.1661–1672.

Erridge, C., 2010. Endogenous ligands of TLR2 and TLR4: agonists or assistants? *J. Leukoc. Biol*, 87(June), pp.989–999.

Exley, C. et al., 2009. A role for the body burden of aluminium in vaccine-associated macrophagic myofasciitis and chronic fatigue syndrome. *Medical Hypotheses*, 72(2), pp.135–139. Available at: http://dx.doi.org/10.1016/j.mehy.2008.09.040.

Fox, R.J. et al., 2016. Design, rationale, and baseline characteristics of the randomized double-blind phase II clinical trial of ibudilast in progressive multiple sclerosis. *Contemporary Clinical Trials*, 50(August), pp.166–177. Available at: http://dx.doi.org/10.1016/j.cct.2016.08.009.

Franz, G. & Feuerstein, U., 1997. Chemical stability of some model polysaccharides. *Macromolecular Symposia*, 120(1), pp.169–181.

Fu, J. et al., 2008. An anti-sepsis monomer, 2',5,6',7-tetrahydroxyflavanonol (THF), identified from Scutellaria baicalensis Georgi neutralizes lipopolysaccharide in vitro and in vivo. *International immunopharmacology*, 8(12), pp.1652–7. Available at: http://www.ncbi.nlm.nih.gov/pubmed/18755299 [Accessed September 5, 2013].

Fukuzawa, N. et al., 2011. A TLR5 agonist inhibits acute renal ischemic failure. *Journal of immunology (Baltimore, Md. : 1950)*, 187(7), pp.3831–9. Available at: http://www.pubmedcentral.nih.gov/articlerender.fcgi?artid=3178726&tool=pmcentrez&rendertype=abstract.

Gao, D. & Li, W., 2017. Structures and recognition modes of toll-like receptors. *Proteins: Structure, Function, and Bioinformatics*, 85(1), pp.3–9. Available at: http://doi.wiley.com/10.1002/prot.25179 [Accessed February 28, 2018].

García-Mayoral, M.F. et al., 2006. pH-dependent conformational stability of the ribotoxin alpha-sarcin and four active site charge substitution variants. *Biochemistry*, 45(46), pp.13705–13718.

Garçon, N., Chomez, P. & Van Mechelen, M., 2007. GlaxoSmithKline Adjuvant Systems in vaccines: concepts, achievements and perspectives. *Expert Review of Vaccines*, 6(5), pp.723–739. Available at: http://dx.doi.org/10.1586/14760584.6.5.723.

Gazzinelli, R.T. & Denkers, E.Y., 2006. Protozoan encounters with Toll-like receptor signalling pathways: implications for host parasitism. *Nature reviews. Immunology*, 6(12), pp.895–906.

Genfa, L. et al., 2005. The screening and isolation of an effective anti-endotoxin monomer from Radix Paeoniae Rubra using affinity biosensor technology. *International immunopharmacology*, 5(6), pp.1007–17. Available at: http://www.ncbi.nlm.nih.gov/pubmed/15829416 [Accessed September 5, 2013].

Gherardi, R.K.K. et al., 2016. Aluminum adjuvants of vaccines injected into the muscle: Normal fate, pathology and associated disease. *Morphologie*, 100(329), pp.85–94. Available at: http://dx.doi.org/10.1016/j.morpho.2016.01.002.

Giam, X. et al., 2010. The extent of undiscovered species in Southeast Asia. *Biodiversity and*

Conservation, 19(4), pp.943–954.

Gooshe, M. et al., 2014. Toll like receptors: a new hope on the horizon to treat multiple sclerosis. *Expert review of clinical immunology*, 10(10), pp.1277–9. Available at: http://www.ncbi.nlm.nih.gov/pubmed/25161080.

Greene, C.M. et al., 2010. Inhibition of Toll-like receptor 2-mediated interleukin-8 production in Cystic Fibrosis airway epithelial cells via the alpha7-nicotinic acetylcholine receptor. *Mediators of inflammation*, 2010, p.423241. Available at: http://www.pubmedcentral.nih.gov/articlerender.fcgi?artid=2850130&tool=pmcentrez&rendertype=abstract [Accessed September 5, 2013].

Grivennikov, S.I., Greten, F.R. & Karin, M., 2010. Immunity, inflammation, and cancer. *Cell*, 140(6), pp.883–99. Available at: http://www.pubmedcentral.nih.gov/articlerender.fcgi?artid=2866629&tool=pmcentrez&rendertype=abstract [Accessed July 10, 2014].

Haanpää, M. & Treede, R.D., 2012. Capsaicin for neuropathic pain: Linking traditional medicine and molecular biology. *European Neurology*, 68(5), pp.264–275.

Hafid, A.F. et al., 2016. Activities of Ficus fistulosa Leave Extract and Fractions against Hepatitis C Virus. *Procedia Chemistry*, 18(Mcls 2015), pp.179–184. Available at: http://www.sciencedirect.com/science/article/pii/S1876619616000292.

Halliday, A. et al., 2016. The TLR2/6 ligand PAM2CSK4 is a Th2 polarizing adjuvant in Leishmania major and Brugia malayi murine vaccine models. *Parasites & Vectors*, 9(1), pp.1–9. Available at: http://dx.doi.org/10.1186/s13071-016-1381-0.

Halperin, S.A. et al., 2012. Comparison of safety and immunogenicity of two doses of investigational hepatitis B virus surface antigen co-administered with an immunostimulatory phosphorothioate oligodeoxyribonucleotide and three doses of a licensed hepatitis B vaccine in healthy adul. *Vaccine*, 30(15), pp.2556–2563. Available at: http://dx.doi.org/10.1016/j.vaccine.2012.01.087.

Han, S.B., Park, S.K., et al., 2003. Characterization of B cell membrane receptors of polysaccharide isolated from the root of Acanthopanax koreanum. *International Immunopharmacology*, 3(5), pp.683–691.

Han, S.B., Yoon, Y.D., et al., 2003. Toll-like receptor-mediated activation of B cells and

macrophages by polysaccharide isolated from cell culture of Acanthopanax senticosus. *International Immunopharmacology*, 3(9), pp.1301–1312.

Harris, J.M. & Chess, R.B., 2003. Effect of pegylation on pharmaceuticals. *Nature reviews. Drug discovery*, 2(3), pp.214–221.

Harrison, F. et al., 2015. A 1,000-Year-Old Antimicrobial Remedy with Antistaphylococcal Activity. *American Society of Microbiology*, 6(4), pp.1–7.

Hasan, U. et al., 2005. Human TLR10 is a functional receptor, expressed by B cells and plasmacytoid dendritic cells, which activates gene transcription through MyD88. *Journal of immunology (Baltimore, Md. : 1950)*, 174(5), pp.2942–50. Available at: http://www.ncbi.nlm.nih.gov/pubmed/15728506.

Hasbold, J. et al., 1999. Cell division number regulates IgG1 and IgE switching of B cells following stimulation by CD40 ligand and IL-4. *European Journal of Immunology*, 28(3), pp.1040–1051.

Heneka, M.T., Kummer, M.P. & Latz, E., 2014. Innate immune activation in neurodegenerative disease. *Nature reviews. Immunology*, 14(7), pp.463–77. Available at: http://www.ncbi.nlm.nih.gov/pubmed/24962261.

Henriksen-Lacey, M. et al., 2010. Liposomes based on dimethyldioctadecylammonium promote a depot effect and enhance immunogenicity of soluble antigen. *Journal of Controlled Release*, 142(2), pp.180–186. Available at: http://dx.doi.org/10.1016/j.jconrel.2009.10.022.

Hester, G. et al., 1995. Structure of mannose-specific snowdrop (Galanthus nivalis) lectin is representative of a new plant lectin family. *Nature Structural Biology*, 2, p.472. Available at: http://dx.doi.org/10.1038/nsb0695-472.

Hinz, B. & Brune, K., 2007. Antipyretic Analgesics: Nonsteroidal Antiinflammatory Drugs, Selective COX-2 Inhibitors, Paracetamol and Pyrazolinones. In C. Stein, ed. *Analgesia*. Berlin, Heidelberg: Springer Berlin Heidelberg, pp. 65–93. Available at: http://dx.doi.org/10.1007/978-3-540-33823-9_3.

Hodgkin, P.D., Lee, J.H. & Lyons, a B., 1996. B cell differentiation and isotype switching is related to division cycle number. *The Journal of experimental medicine*, 184(July), pp.277–281.

Hoffmann, B.Y.M.K. et al., 1977. B-cell Activation by Lipopolysaccharide: Distinct Pathways for Induction of Mitosis and Antibody Production. *Journal of Experimental Medicine*, 146, pp.1640–1647.

Holst, J. et al., 2009. Properties and clinical performance of vaccines containing outer membrane vesicles from Neisseria meningitidis. *Vaccine*, 27(SUPPL. 2), pp.3–12.

Holten-Andersen, L. et al., 2004. Combination of the Cationic Surfactant Dimethyl Dioctadecyl Ammonium Bromide and Synthetic Mycobacterial Cord Factor as an Efficient Adjuvant for Tuberculosis Subunit Vaccines. *Infection and Immunity*, 72(3), pp.1608–1617.

Hon, H. et al., 2005. B Lymphocytes Participate in Cross-Presentation of Antigen following Gene Gun Vaccination. *The Journal of Immunology*, 174(9), pp.5233–5242. Available at: http://www.jimmunol.org/cgi/doi/10.4049/jimmunol.174.9.5233.

Hornung, V. et al., 2002. Quantitative expression of toll-like receptor 1-10 mRNA in cellular subsets of human peripheral blood mononuclear cells and sensitivity to CpG oligodeoxynucleotides. *Journal of immunology (Baltimore, Md. : 1950)*, 168(9), pp.4531–4537.

Houston, W.E. et al., 1976. Adjuvant effects of diethylaminoethyl-dextran. *Infection and immunity*, 13(6), pp.1559–62. Available at: http://www.pubmedcentral.nih.gov/articlerender.fcgi?artid=420800&tool=pmcentrez&rendertype=abstract.

Huang, J.-R. et al., 2008. Bromelain inhibits lipopolysaccharide-induced cytokine production in human THP-1 monocytes via the removal of CD14. *Immunological investigations*, 37(4), pp.263–277.

Huang, Q., 2001. The plasticity of dendritic cell responses to pathogens and their contents. *Science*, 294(October), pp.870–875.

Huang, R.-Y. et al., 2010. Immunosuppressive effect of quercetin on dendritic cell activation and function. *Journal of immunology (Baltimore, Md. : 1950)*, 184(12), pp.6815–21. Available at: http://www.ncbi.nlm.nih.gov/pubmed/20483746.

Huhta, H. et al., 2016. Toll-like receptors 1, 2, 4 and 6 in esophageal epithelium, Barrett's esophagus, dysplasia and adenocarcinoma. *Oncotarget*, 7(17), pp.1–10.

Ichinohe, T. et al., 2009. PolyI:polyC12U adjuvant-combined intranasal vaccine protects mice against highly pathogenic H5N1 influenza virus variants. *Vaccine*, 27(45), pp.6276–6279.

Ing, R. et al., 2005. Interaction of Mouse Dendritic Cells and Malaria-Infected Erythrocytes: Uptake, Maturation, and Antigen Presentation. *The Journal of Immunology*, 176(1), pp.441–450. Available at: http://www.jimmunol.org/content/176/1/441.full.

Iram, N. et al., 2012. Age-related changes in expression and function of Toll-like receptors in human skin. *Development (Cambridge, England)*, 139(22), pp.4210–4219.

Iribarren, K. et al., 2015. Trial Watch - Immunostimulation with Toll-like receptor agonists in cancer therapy. *OncoImmunology*, (September), pp.00–00. Available at: http://www.tandfonline.com/doi/abs/10.1080/2162402X.2015.1088631.

Janakiram, M. et al., 2015. Expression, clinical significance, and receptor identification of the newest B7 family member HHLA2 protein. *Clinical Cancer Research*, 21(10), pp.2359–2366.

Jantan, I., Ahmad, W. & Bukhari, S.N.A., 2015. Plant-derived immunomodulators: an insight on their preclinical evaluation and clinical trials. *Frontiers in Plant Science*, 6(August), p.655. Available at: http://www.pubmedcentral.nih.gov/articlerender.fcgi?artid=4548092&tool=pmcentrez&rendertype=abstract.

Jayaprakasam, B., Seeram, N.P. & Nair, M.G., 2003. Anticancer and antiinflammatory activities of cucurbitacins from Cucurbita andreana. *Cancer letters*, 189(1), pp.11–16.

Jenkins, S.J. et al., 2005. Schistosome larvae stimulate macrophage cytokine production through TLR4-dependent and -independent pathways. *International Immunology*, 17(11), pp.1409–1418.

Jiang, S. et al., 2016. TLR10 Is a Negative Regulator of Both MyD88-Dependent and -Independent TLR Signaling. *Journal of Immunology*, 196(9), pp.3834–3841. Available at: http://www.jimmunol.org/cgi/doi/10.4049/jimmunol.1502599.

Jin, M.S. et al., 2007. Crystal Structure of the TLR1-TLR2 Heterodimer Induced by Binding of a Tri-Acylated Lipopeptide. *Cell*, 130(6), pp.1071–1082.

Jin, M.S. & Lee, J.O., 2008. Structures of the Toll-like Receptor Family and Its Ligand

Complexes. *Immunity*, 29(2), pp.182–191.

Jouault, T. et al., 2003. *Candida albicans* Phospholipomannan Is Sensed through Toll-Like Receptors. *The Journal of Infectious Diseases*, 188(1), pp.165–172. Available at: http://jid.oxfordjournals.org/lookup/doi/10.1086/375784.

Jung, T.Y. et al., 2010. Ursolic acid isolated from Uncaria rhynchophylla activates human dendritic cells via TLR2 and/or TLR4 and induces the production of IFN-?? by CD4+ na??ve T cells. *European Journal of Pharmacology*, 643(2–3), pp.297–303. Available at: http://dx.doi.org/10.1016/j.ejphar.2010.06.030.

Kang, J.Y. et al., 2009. Recognition of Lipopeptide Patterns by Toll-like Receptor 2-Toll-like Receptor 6 Heterodimer. *Immunity*, 31(6), pp.873–884. Available at: https://www.sciencedirect.com/science/article/pii/S1074761309004920 [Accessed February 28, 2018].

Karin, M., Yamamoto, Y. & Wang, Q.M., 2004. The IKK NF-kappa B system: a treasure trove for drug development. *Nature reviews. Drug discovery*, 3(1), pp.17–26.

Katiki, L.M. et al., 2013. Anthelmintic effect of plant extracts containing condensed and hydrolyzable tannins on Caenorhabditis elegans, and their antioxidant capacity. *Veterinary Parasitology*, 192(1–3), pp.218–227. Available at: http://dx.doi.org/10.1016/j.vetpar.2012.09.030.

Kaushik, U., Aeri, V. & Mir, S.R., 2015. Cucurbitacins – An insight into medicinal leads from nature. *Pharmacognosy Reviews*, 9(17), pp.12–18. Available at: http://www.ncbi.nlm.nih.gov/pmc/articles/PMC4441156/.

Kawai, T. & Akira, S., 2010. The role of pattern-recognition receptors in innate immunity: update on Toll-like receptors. *Nature immunology*, 11(5), pp.373–84. Available at: http://www.ncbi.nlm.nih.gov/pubmed/20404851 [Accessed May 25, 2013].

Kay, E., Scotland, R.S. & Whiteford, J.R., 2014. Toll-like receptors: Role in inflammation and therapeutic potential. *BioFactors*, 40(3), pp.284–294.

Kersten, G.F. a et al., 1988. Incorporation of the Major Outer-Membrane Protein of Neisseria-Gonorrhoeae in Saponin-Lipid Complexes (Iscoms) - Chemical-Analysis, Some Structural Features, and Comparison of Their Immunogenicity with 3 Other Antigen Delivery Systems. *Infection and Immunity*, 56(2), pp.432–438.

Kim, H.M. et al., 2007. Crystal Structure of the TLR4-MD-2 Complex with Bound Endotoxin Antagonist Eritoran. *Cell*, 130(5), pp.906–917.

Kim, M. et al., 2015. Cucurbitacin B inhibits immunomodulatory function and the inflammatory response in macrophages. *Immunopharmacology and Immunotoxicology*, 37(5), pp.473–480. Available at: http://www.tandfonline.com/doi/full/10.3109/08923973.2015.1085065.

Koizumi, S. ichi et al., 2012. Extracts of Larix Leptolepis effectively augments the generation of tumor antigen-specific cytotoxic T lymphocytes via activation of dendritic cells in TLR-2 and TLR-4-dependent manner. *Cellular Immunology*, 276(1–2), pp.153–161. Available at: http://dx.doi.org/10.1016/j.cellimm.2012.05.002.

Kroemer, G. et al., 2013. Immunogenic Cell Death in Cancer Therapy ICD: immunogenic cell death. *Annu. Rev. Immunol*, 31(March), pp.51–72. Available at: www.annualreviews.org.

Krysko, O. et al., 2013. Many faces of DAMPs in cancer therapy. *Cell death & disease*, 4, p.e631. Available at: http://www.pubmedcentral.nih.gov/articlerender.fcgi?artid=3674363&tool=pmcentrez&rendertype=abstract [Accessed September 2, 2013].

Kukula-Koch, W.A. & Widelski, J., 2016. *Alkaloids*, Elsevier Inc. Available at: http://dx.doi.org/10.1016/B978-0-12-802104-0.00009-3.

Kumar, H.M.S., Hyder, I. & Singh, P.P., 2012. Pattern Recognition Receptors Based Immune Adjuvants : Their Role and Importance in Vaccine Design. In D. Ekinci, ed. *Medicinal Chemistry and Drug Design*. InTech.

Kwon, O.K. et al., 2012. Ethanol extract of Elaeocarpus petiolatus inhibits lipopolysaccharide-induced inflammation in macrophage cells. *Inflammation*, 35(2), pp.535–544.

Laan, M., Bozinovski, S. & Anderson, G.P., 2013. Cigarette smoke inhibits lipopolysaccharide-induced production of inflammatory cytokines by suppressing the activation of activator protein-1 in bronchial epithelial cells. *Journal of Immunology*, 173(6), pp.4164–70.

Lafon, M. et al., 2006. The Innate Immune Facet of Brain. *Journal of Molecular Neuroscience*, 29, pp.185–194.

Latz, E. et al., 2004. Haemophilus influenzae type b-outer membrane protein complex glycoconjugate vaccine induces cytokine production by engaging human toll-like receptor 2 (TLR2) and requires the presence of TLR2 for optimal immunogenicity. *Journal of immunology (Baltimore, Md. : 1950)*, 172(4), pp.2431–8. Available at: http://www.ncbi.nlm.nih.gov/pubmed/14764714.

Lee, J.-J. et al., 2003. Blocking NF-kappaB activation may be an effective strategy in the fever therapy. *The Japanese journal of physiology*, 53(5), pp.367–375.

Lee, M.R., 2009. The history of ergot of rye (Claviceps purpurea) II: 1900-1940. *The journal of the Royal College of Physicians of Edinburgh*, 39(4), pp.365–369.

Lee, S. & Nguyen, M.T., 2015. Recent advances of vaccine adjuvants for infectious diseases. *Immune network*, 15(2), pp.51–7.

Leemans, J.C. et al., 2005. Renal-associated TLR2 mediates ischemia/reperfusion injury in the kidney. *Journal of Clinical Investigation*, 115(10), pp.2894–2903.

Leisewitz, A.L. et al., 2004. Response of the splenic dendritic cell population to malaria infection. *Infection and Immunity*, 72(7), pp.4233–4239.

Li, H. et al., 2008. Cutting edge: inflammasome activation by alum and alum's adjuvant effect are mediated by NLRP3. *Journal of immunology*, 181(1), pp.17–21. Available at: http://www.ncbi.nlm.nih.gov/pubmed/18566365%5Cnhttp://www.pubmedcentral.nih.gov/articlerender.fcgi?artid=PMC2587213.

Liang, C.-H. & Wu, C.-Y., 2009. Glycan array: a powerful tool for glycomics studies. *Expert Review of Proteomics*, 6(6), pp.631–645. Available at: https://doi.org/10.1586/epr.09.82.

Lindsey, A.S. & Jeskey, H., 1957. The Kolbe-Schmitt Reaction. *Chemical Reviews*, 57(4), pp.583–620. Available at: http://pubs.acs.org/doi/abs/10.1021/cr50016a001.

Liu, L. et al., 2008. Structural basis of toll-like receptor 3 signaling with double-stranded RNA. *Science (New York, N.Y.)*, 320(5874), pp.379–381.

Liu, X., Zheng, J. & Zhou, H., 2011. TLRs as pharmacological targets for plant-derived compounds in infectious and inflammatory diseases. *International immunopharmacology*, 11(10), pp.1451–6. Available at:

http://www.ncbi.nlm.nih.gov/pubmed/21586344 [Accessed September 2, 2013].

De Lourdes Reyes-Escogido, M., Gonzalez-Mondragon, E.G. & Vazquez-Tzompantzi, E., 2011. Chemical and pharmacological aspects of capsaicin. *Molecules*, 16(2), pp.1253–1270.

Luch, A., 2009. *Molecular, clinical and environmental toxicology*, Springer.

Lysakova-Devine, T. et al., 2010. Viral inhibitory peptide of TLR4, a peptide derived from vaccinia protein A46, specifically inhibits TLR4 by directly targeting MyD88 adaptor-like and TRIF-related adaptor molecule. *Journal of immunology (Baltimore, Md. : 1950)*, 185(7), pp.4261–4271.

M Eriksson, E., N, G.S. & Schofield, L., 2014. Toll-Like Receptors and Malaria – Sensing and Susceptibility. *Journal of Tropical Diseases*, 2(1), pp.1–7. Available at: http://www.esciencecentral.org/journals/tolllike-receptors-and-malaria-sensing-and-susceptibility-2329-891X.1000126.php?aid=21977.

Mahata, B. et al., 2014. Single-cell RNA sequencing reveals T helper cells synthesizing steroids De Novo to contribute to immune homeostasis. *Cell Reports*, 7(4), pp.1130–1142.

Mahdi, J.G. et al., 2006. The historical analysis of aspirin discovery, its relation to the willow tree and antiproliferative and anticancer potential. *Cell Proliferation*, 39(2), pp.147–155.

Malinin, G.I., 1977. Oxidation of tissue polysaccharides by periodic acid in dimethyl sulfoxide and its anhydrous and aqueous mixtures. *J Histochem Cytochem*, 25(3), pp.188–192.

Maloy, K.J., Donachie, A.M. & Mowat, A.M., 1995. Induction of Th1 and Th2 CD4+ T cell responses by oral or parenteral immunization with ISCOMS. *European Journal of Immunology*, 25(10), pp.2835–2841.

Mandler, R. et al., 1993. IL-4 induction of IgE class switching by lipopolysaccharide-activated murine B cells occurs predominantly through sequential switching. *Journal of immunology*, 150(2), pp.407–418.

Mandrekar, P., 2012. Toll-like receptor signaling. *Cell Signaling Technology, Inc.*, (May 2006). Available at: http://www.cellsignal.com/reference/pathway/Toll_Like.html#describe [Accessed August 27, 2013].

Marzouk, B. et al., 2013. Anti-inflammatory and analgesic activities of a new cucurbitacin

isolated from Citrullus colocynthis seeds. *Medicinal Chemistry Research*, 22(8), pp.3984–3990.

Matsunaga, N. et al., 2011. TAK-242 (resatorvid), a small-molecule inhibitor of Toll-like receptor (TLR) 4 signaling, binds selectively to TLR4 and interferes with interactions between TLR4 and its adaptor molecules. *Molecular pharmacology*, 79(1), pp.34–41.

Means, T.K. et al., 2003. The Toll-like receptor 5 stimulus bacterial flagellin induces maturation and chemokine production in human dendritic cells. *Journal of immunology (Baltimore, Md. : 1950)*, 170(10), pp.5165–75. Available at: http://www.ncbi.nlm.nih.gov/pubmed/12734364.

Medzhitov, R., Schneider, D.S. & Soares, M.P., 2012. Disease Tolerance as a Defense Strategy. *Science*, 335(February), pp.936–942.

Mendelsohn, R. & Balick, M.J., 1995. The value of undiscovered pharmaceuticals in tropical forests. *Economic Botany*, 49(2), pp.223–228.

Mifsud, E.J. et al., 2016. Reducing the impact of influenza-associated secondary pneumococcal infections. *Immunology and Cell Biology*, 94(May), pp.1–8. Available at: http://www.ncbi.nlm.nih.gov/pubmed/26134269.

Miltenyi, CD19 MicroBeads mouse. Available at: file:///Users/khalilthirlway/Downloads/DS130-052-201.pdf [Accessed January 3, 2018].

Miranda-Hernandez, S. & Baxter, A.G., 2013. Role of toll-like receptors in multiple sclerosis. *American journal of clinical and experimental immunology*, 2(1), pp.75–93. Available at: http://www.pubmedcentral.nih.gov/articlerender.fcgi?artid=3714200&tool=pmcentrez&rendertype=abstract.

Miyauchi, M., 2011. Arabino-mycolates derived from cell-wall skeleton of Mycobacterium bovis BCG as a prominent structure for recognition by host immunity. *Drug Discoveries & Therapeutics*, 5(3), pp.130–135.

Miyauchi, M. et al., 2012. Optimization of cell-wall skeleton derived from Mycobacterium bovis BCG Tokyo 172 (SMP-105) emulsion in delayed-type hypersensitivity and antitumor models. *Drug Discoveries & Therapeutics*, 6(4), pp.218–225.

Mogensen, T.H., 2009. Pathogen recognition and inflammatory signaling in innate immune

defenses. *Clinical Microbiology Reviews*, 22(2), pp.240–273.

Morein, B. et al., 1995. Immunostimulating Complexes: Clinical Potential in Vaccine Development. *Clinical Immunotherapeutics*, 3(6), pp.461–475.

Moreira, L.R.S. & Filho, E.X.F., 2008. An overview of mannan structure and mannan-degrading enzyme systems. *Applied Microbiology and Biotechnology*, 79(2), pp.165–178.

Moser, C. et al., 2013. Influenza virosomes as vaccine adjuvant and carrier system. *Expert review of vaccines*, 12(7).

Mrabet-Dahbi, S. et al., 2009. Murine mast cells secrete a unique profile of cytokines and prostaglandins in response to distinct TLR2 ligands. *Experimental Dermatology*, 18(5), pp.437–444.

Mühlradt, P.F. et al., 1997. Isolation, structure elucidation, and synthesis of a macrophage stimulatory lipopeptide from Mycoplasma fermentans acting at picomolar concentration. *The Journal of experimental medicine*, 185(11), pp.1951–1958.

Murata, M., 2008. Activation of Toll-like receptor 2 by a novel preparation of cell wall skeleton from Mycobacterium bovis BCG Tokyo (SMP-105) sufficiently enhances immune responses against tumors. *Cancer Science*, 99(7), pp.1435–1440.

Murata, T. et al., 2003. Discovery of novel and selective IKK-β serine-threonine protein kinase inhibitors. Part 1. *Bioorganic and Medicinal Chemistry Letters*, 13(5), pp.913–918. Available at: http://www.scopus.com/scopus/inward/record.url?eid=2-s2.0-0037430545&partnerID=40&rel=R8.0.0.

Murphy, K., 2012. *Janeway's Immunobiology* 8th Editio., Garland Science.

Muzes, G., Tulassay, Z. & Sipos, F., 2013. Interplay of autophagy and innate immunity in Crohn's disease: A key immunobiologic feature. *World Journal of Gastroenterology*, 19(28), pp.4447–4454.

Nakao, Y. et al., 2005. Surface-expressed TLR6 participates in the recognition of diacylated lipopeptide and peptidoglycan in human cells. *Journal of immunology (Baltimore, Md. : 1950)*, 174(3), pp.1566–73. Available at: http://www.ncbi.nlm.nih.gov/pubmed/15661917.

Newman, D.J. & Cragg, G.M., 2016. Natural products as sources of new drugs from 1981 to 2014. *Journal of Natural Products*, 79, pp.629–661.

Nguyen, C.T. & Rhee, D., 2016. Panax ginseng as a potential modulator of macrophages. , 1, pp.3–7.

Oberg, F. et al., 2009. Herbal melanin activates TLR4/NF-kappaB signaling pathway. *Phytomedicine : international journal of phytotherapy and phytopharmacology*, 16(5), pp.477–84. Available at: http://www.ncbi.nlm.nih.gov/pubmed/19103478 [Accessed September 26, 2013].

Okamura, Y. et al., 2001. The Extra Domain A of Fibronectin Activates Toll-like Receptor 4. *Journal of Biological Chemistry*, 276(13), pp.10229–10233.

Oosting, M. et al., 2014. Human TLR10 is an anti-inflammatory pattern-recognition receptor. *Proceedings of the National Academy of Sciences of the United States of America*, 111(42), pp.E4478-84. Available at: http://www.pubmedcentral.nih.gov/articlerender.fcgi?artid=4210319&tool=pmcentrez&rendertype=abstract.

Othman, M. et al., 2011. Optimal methods for evaluating antimicrobial activities from plant extracts. *Journal of Microbiological Methods*, 84(2), pp.161–166. Available at: http://dx.doi.org/10.1016/j.mimet.2010.11.008.

Ozinsky, a et al., 2000. The repertoire for pattern recognition of pathogens by the innate immune system is defined by cooperation between toll-like receptors. *Proceedings of the National Academy of Sciences of the United States of America*, 97(25), pp.13766–71. Available at: http://www.pubmedcentral.nih.gov/articlerender.fcgi?artid=17650&tool=pmcentrez&rendertype=abstract.

Paccaud, J.-P., Schifferli, J.A. & Baggiolini, M., 1990. NAP-1IL-8 induces up-regulation of CR1 receptors in human neutrophil leukocytes. *Biochemical and Biophysical Research Communications*, 166(1), pp.187–192. Available at: http://www.sciencedirect.com/science/article/pii/0006291X9091929M.

Palanki, M.S.S. et al., 2000. Novel Inhibitors of AP-1 and NF- B Mediated Gene Expression : Structure ± Activity Relationship Studies of Ethyl 4- [(3-Methyl-. *Bioorganic & Medicinal*

Chemistry Letters, 10, pp.1645–1648.

Pannicke, U. et al., 2013. Deficiency of innate and acquired immunity caused by an IKBKB mutation. *The New England journal of medicine*, 369(26), pp.2504–2514. Available at: http://www.nejm.org/doi/abs/10.1056/NEJMoa1309199%5Cnhttp://www.ncbi.nlm.nih.gov/pubmed/24369075.

Park, S.-J. & Youn, H.-S., 2010. Suppression of homodimerization of toll-like receptor 4 by isoliquiritigenin. *Phytochemistry*, 71(14–15), pp.1736–40. Available at: http://www.ncbi.nlm.nih.gov/pubmed/20701936 [Accessed September 5, 2013].

De Pasquale, A., 1984. Pharmacognosy: The oldest modern science. *Journal of Ethnopharmacology*, 11(1), pp.1–16.

Pekić, B. et al., 1998. Study of the extraction of proanthocyanidins from grape seeds. *Food Chemistry*, 61(1–2), pp.201–206.

Peng, X.-X. et al., 2015. Panax Notoginseng flower saponins (PNFS) inhibit LPS-stimulated NO overproduction and iNOS gene overexpression via the suppression of TLR4-mediated MAPK/NF-kappa B signaling pathways in RAW264.7 macrophages. *Chinese medicine*, 10, p.15. Available at: http://www.pubmedcentral.nih.gov/articlerender.fcgi?artid=4493833&tool=pmcentrez&rendertype=abstract.

Perczel, A., Gáspári, Z. & Csizmadia, I.G., 2005. Structure and stability of beta-pleated sheets. *Journal of Computational Chemistry*, 26(11), pp.1155–1168.

Perkins, D.J. et al., 2011. Severe malarial anemia: Innate immunity and pathogenesis. *International Journal of Biological Sciences*, 7(9), pp.1427–1442.

Perrie, Y. et al., 2016. Designing liposomal adjuvants for the next generation of vaccines. *Advanced Drug Delivery Reviews*, 99, pp.85–96.

Peters, R.R., Farias, M.R. & Ribeiro-do-Valle, R.M., 1997. Anti-inflammatory and analgesic effects of cucurbitacins from Wilbrandia ebracteata. *Planta Medica*, 63(6), pp.525–528.

Petrovsky, N. & Cooper, P.D., 2011. Carbohydrate-based immune adjuvants. *Expert review of vaccines*, 4(164), pp.523–537.

Podolak, I., Galanty, A. & Sobolewska, D., 2010. Saponins as cytotoxic agents: A review. *Phytochemistry Reviews*, 9(3), pp.425–474.

Priyadi, H. et al., 2010. *Five hundred plant species in Gunung Halimun Salak National Park , West Java: A checklist including Sundanese names, distribution and use*,

Proestos, C. et al., 2013. Antioxidant Capacity of Selected Plant Extracts and Their Essential Oils. *Antioxidants* , 2(1).

Pugh, N. et al., 2001. Isolation of Three High Molecular Weight Polysaccharide Preparations with Potent Immunostimulatory Activity from Spirulina platensis, Aphanizomenon flos-aquae and Chlorella pyrenoidosa. *Planta Medica*, 67(8), pp.737–742.

Quail, D.F. & Joyce, J.A., 2013. Microenvironmental regulation of tumor progression and metastasis. *Nature medicine*, 19(11), pp.1423–1437. Available at: http://www.nature.com/nm/journal/v19/n11/abs/nm.3394.html.

Qureshi, N., Takayama, K. & Ribi, E., 1982. Purification and structural determination of nontoxic lipid A obtained from the lipopolysaccharide of Salmonella typhimurium. *Journal of Biological Chemistry*, 257(19), pp.11808–11815.

Rates, S.M., 2001. Plants as source of drugs. *Toxicon : official journal of the International Society on Toxinology*, 39(5), pp.603–13. Available at: http://www.ncbi.nlm.nih.gov/pubmed/11072038.

Reddy, S., 2004. Ecosystems approach to human health: a case of Konda Reddi tribes and women's health. *Journal of Human Ecology*, 16(4), pp.271–282.

Reguero, M.T. et al., 1987. Chemical studies on Mexican plants used in traditional medicine II: Cucurbitacins from Hintonia Latiflora. *Journal of natural products*, 50(2), pp.315–316.

Reilly, M. et al., 2013. Randomized, double-blind, placebo-controlled, dose-escalating phase I, healthy subjects study of intravenous OPN-305, a humanized anti-TLR2 antibody. *Clinical pharmacology and therapeutics*, 94(5), pp.593–600. Available at: http://www.pubmedcentral.nih.gov/articlerender.fcgi?artid=3805945&tool=pmcentrez&rendertype=abstract.

Rocha, J.D.B. et al., 2010. Inhibitory effect of the alkaloid warifteine purified from Cissampelos sympodialis on B lymphocyte function in vitro and in vivo. *Planta medica*,

76(4), pp.325–30. Available at: http://www.ncbi.nlm.nih.gov/pubmed/19787569 [Accessed September 5, 2013].

Rodríguez-Pinto, D., 2005. B cells as antigen presenting cells. *Cellular Immunology*, 238(2), pp.67–75.

Rush, J.S. & Hodgkin, P.D., 2001. B cells activated via CD40 and IL-4 undergo a division burst but require continued stimulation to maintain division, survival and differentiation. *European Journal of Immunology*, 31(4), pp.1150–1159.

Ryan, M. & Levy, M.M., 2003. Clinical review: fever in intensive care unit patients. *Crit Care*, 7(1364–8535 (Print)), pp.221–225. Available at: c:%5CKarsten%5CPDFs%5CInfektiologie-PDFs%5CInfekt-2003%5CRyan - Levy-Clinical review- fever in intensive care unit patients.pdf.

Sablan, B.P. et al., 2012. Demonstration of safety and enhanced seroprotection against hepatitis B with investigational HBsAg-1018 ISS vaccine compared to a licensed hepatitis B vaccine. *Vaccine*, 30(16), pp.2689–2696. Available at: http://dx.doi.org/10.1016/j.vaccine.2012.02.001.

Saklani, A. & Kutty, S.K., 2008. Plant-derived compounds in clinical trials. *Drug discovery today*, 13(3–4), pp.161–71. Available at: http://www.ncbi.nlm.nih.gov/pubmed/18275914 [Accessed August 26, 2013].

Sarker, S.D. et al., 1999. Identification and ecdysteroid antagonist activity of three resveratrol trimers (suffruticosols A, B and C) from Paeonia suffruticosa. *Tetrahedron*, 55(2), pp.513–524. Available at: http://www.sciencedirect.com/science/article/pii/S0040402098010497.

Saslis-Lagoudakis, C.H. et al., 2012. Phylogenies reveal predictive power of traditional medicine in bioprospecting. *Proceedings of the National Academy of Sciences of the United States of America*, 109(39), pp.15835–40. Available at: http://www.pubmedcentral.nih.gov/articlerender.fcgi?artid=3465383&tool=pmcentrez&rendertype=abstract.

Sato, M. et al., 2003. Direct Binding of Toll-Like Receptor 2 to Zymosan, and Zymosan-Induced NF- B Activation and TNF- Secretion Are Down-Regulated by Lung Collectin Surfactant Protein A. *The Journal of Immunology*, 171(1), pp.417–425.

Savige, W.E. & Fontana, A., 1977. Modification of tryptophan to oxindolylalanine by dimethyl sulfoxide-hydrochloric acid. *Methods in Enzymology*, 47(C), pp.442–453.

Scheel, B. et al., 2006. Therapeutic anti-tumor immunity triggered by injections of immunostimulating single-stranded RNA. *European Journal of Immunology*, 36(10), pp.2807–2816.

Schepetkin, I. a et al., 2005. Macrophage immunomodulatory activity of polysaccharides isolated from Juniperus scopolorum. *International immunopharmacology*, 5(13–14), pp.1783–99. Available at: http://www.ncbi.nlm.nih.gov/pubmed/16275615 [Accessed September 6, 2013].

Schröder, J.M. et al., 1987. Purification and partial biochemical characterization of a human monocyte-derived, neutrophil-activating peptide that lacks interleukin 1 activity. *The Journal of Immunology*, 139(10), p.3474 LP-3483. Available at: http://www.jimmunol.org/content/139/10/3474.abstract.

Schülke, S., Vogel, L. & Junker, A., 2016. A Fusion Protein Consisting of the Vaccine Adjuvant Monophosphoryl Lipid A and the Allergen Ovalbumin Boosts Allergen-Specific Th1, Th2, and Th17 Responses In. *Journal of Immunology*, 2016. Available at: http://www.hindawi.com/journals/jir/2016/4156456/abs/.

Schwartz, R.S. & David, K.O., 1985. Liquid chromatography of opium alkaloids, heroin, cocaine, and related compounds using electrochemical detection. *Analytical Chemistry*, 57(7), pp.1362–1366. Available at: http://dx.doi.org/10.1021/ac00284a041.

Shao, D.Z. et al., 2004. Inhibition of nuclear factor-kappa B prevents staphylococcal enterotoxin A-induced fever. *Molecular and Cellular Biochemistry*, 262(1–2), pp.177–185.

Siegrist, C., 2008. Vaccine Immunology. *Vaccines*, 22, pp.17–36. Available at: http://www.ncbi.nlm.nih.gov/entrez/query.fcgi?cmd=Retrieve&db=PubMed&dopt=Citation&list_uids=19335722.

Smit, H.F. et al., 2000. Inhibition of T-Lymphocyte Proliferation by Cucurbitacins from Picrorhiza scrophulariaeflora. *J. Nat. Prod*, 9(63), pp.1300–1302.

Snapper, C. et al., 1993. Transforming growth factor-β1 is required for secretion of IgG of all subclasses by LPS-activated murine B cells in vitro. *The Journal of Immunology*, 151(9),

pp.4625–36.

Soejarto, D.D. et al., 2005. Ethnobotany/ethnopharmacology and mass bioprospecting: Issues on intellectual property and benefit-sharing. *Journal of Ethnopharmacology*, 100(1–2), pp.15–22.

Soepadmo, E., Saw, L.G. & Chung, R.C.K., 2002. *Tree Flora of Sabah and Sarawak*, Kuala Lumpur: Forest Research Institute Malaysia.

Springer, T.A., 1990. Adhesion receptors of the immune system. *Nature*, 346, pp.425–434.

Stefani, M. & Dobson, C.M., 2003. Protein aggregation and aggregate toxicity: New insights into protein folding, misfolding diseases and biological evolution. *Journal of Molecular Medicine*, 81(11), pp.678–699.

Steinhagen, F. et al., 2011. TLR-based immune adjuvants. *Vaccine*, 29(17), pp.3341–3355. Available at: http://dx.doi.org/10.1016/j.vaccine.2010.08.002.

Strayer, D.R. et al., 2012. A double-blind, placebo-controlled, randomized, clinical trial of the TLR-3 agonist rintatolimod in severe cases of chronic fatigue syndrome. *PLoS ONE*, 7(3), pp.1–9.

Stuppner, H. & Moller, E.P., 1993. Cucurbitacins with unusual side chains from Picrorhiza kurroa. *Phytochemistry*, 33(5), pp.1139–1145. Available at: http://www.sciencedirect.com/science/article/pii/003194229385038S.

Stuppner, H., Müller, E.P. & Wagner, H., 1991. Cucurbitacins from Picrorhiza kurrooa. *Phytochemistry*, 30(1), pp.305–310.

Subramaniam, G. et al., 2009. A benzopyrroloisoquinoline alkaloid from Ficus fistulosa. *Phytochemistry Letters*, 2(2), pp.88–90.

Sudeesh, S., 2012. Ethnomedicinal Plants Used By Malayaraya Tribes of Vannapuram Village in Idukki , Kerala , India. , 1(1), pp.7–11.

Sugano, N. et al., 1998. Nicotine inhibits the production of inflammatory mediators in U937 cells through modulation of nuclear factor-kappaB activation. *Biochemical and biophysical research communications*, 252(1), pp.25–8. Available at: http://www.ncbi.nlm.nih.gov/pubmed/9813140.

Sugawara, I. et al., 2003. Mycobacterial infection in TLR2 and TLR6 knockout mice. *Microbiology and immunology*, 47(5), pp.327–336.

Sullivan, A.M. et al., 2008. *Echinacea* -Induced Macrophage Activation. *Immunopharmacology and Immunotoxicology*, 30(3), pp.553–574. Available at: http://www.tandfonline.com/doi/full/10.1080/08923970802135534.

Sun, J. et al., 2005. Cucurbitacin Q: a selective STAT3 activation inhibitor with potent antitumor activity. *Oncogene*, 24(20), pp.3236–3245.

Suzuki, M. et al., 2012. CD8+ CD45RA+ CCR7+ FOXP3+ T cells with immunosuppressive properties: a novel subset of inducible human regulatory T cells. *J Immunol*, 189(5), pp.2118–1230.

Takahashi, H. et al., 1990. Induction of CD8+ cytotoxic T cells by immunization with purified HIV-1 envelope protein in ISCOMs. *Nature*, 344(6269), pp.873–5. Available at: http://dx.doi.org/10.1038/344873a0.

Takeuchi, O. et al., 2001. Discrimination of bacterial lipoproteins by Toll-like receptor 6. *International immunology*, 13(7), pp.933–940.

Talalay, P., 2001. The importance of using scientific principles in the development of medicinal agents from plants. *Academic medicine : journal of the Association of American Medical Colleges*, 76(3), pp.238–47. Available at: http://www.ncbi.nlm.nih.gov/pubmed/11242573.

Talley, K. & Alexov, E., 2010. On the pH-optimum of activity and stability of proteins. *Proteins*, 78(12), pp.2699–2706.

Tamassia, N. et al., 2012. IFN- Expression Is Directly Activated in Human Neutrophils Transfected with Plasmid DNA and Is Further Increased via TLR-4-Mediated Signaling. *The Journal of Immunology*, 189(3), pp.1500–1509. Available at: http://www.jimmunol.org/cgi/doi/10.4049/jimmunol.1102985.

Tan, A.C.L. et al., 2012. Intranasal administration of the TLR2 agonist pam2Cys provides rapid protection against influenza in mice. *Molecular Pharmaceutics*, 9(9), pp.2710–2718.

Taylor, D.N. et al., 2012. Development of VAX128, a recombinant hemagglutinin (HA) influenza-flagellin fusion vaccine with improved safety and immune response. *Vaccine*,

30(39), pp.5761–5769.

Thelen, M. et al., 1988. Mechanism of neutrophil activation by NAF, a novel monocyte-derived peptide agonist. *FASEB journal : official publication of the Federation of American Societies for Experimental Biology*, 2(11), pp.2702–2706.

Timm, M. et al., 2013. Considerations regarding use of solvents in in vitro cell based assays. *Cytotechnology*, 65(5), pp.887–894.

Tohyama, M. et al., 2009. IL-17 and IL-22 mediate IL-20 subfamily cytokine production in cultured keratinocytes via increased IL-22 receptor expression. *European journal of immunology*, 39(10), pp.2779–2788.

Toshchakov, V.Y., Fenton, M.J. & Vogel, S.N., 2007. Cutting Edge: Differential inhibition of TLR signaling pathways by cell-permeable peptides representing BB loops of TLRs. *J Immunol*, 178(5), pp.2655–2660. Available at: http://www.jimmunol.org/cgi/content/abstract/178/5/2655.

Toussi, D.N. & Massari, P., 2014. Immune Adjuvant Effect of Molecularly-defined Toll-Like Receptor Ligands. *Vaccines*, 2, pp.323–353. Available at: www.mdpi.com/journal/vaccines.

Tu, Y., 2011. The discovery of artemisinin (qinghaosu) and gifts from Chinese medicine. *Nature Medicine*, 17(10), pp.1217–1220. Available at: http://dx.doi.org/10.1038/nm.2471%5Cnhttp://www.nature.com/doifinder/10.1038/nm.2471.

Turley, C.B. et al., 2011. Safety and immunogenicity of a recombinant M2e-flagellin influenza vaccine (STF2.4xM2e) in healthy adults. *Vaccine*, 29(32), pp.5145–5152.

Uenishi, Y. et al., 2007. Study on the cell wall skeleton derived from Mycobacterium bovis BCG Tokyo 172 (SMP-105): establishment of preparation and analytical methods. *Chemical & pharmaceutical bulletin*, 55(6), pp.843–52. Available at: http://www.ncbi.nlm.nih.gov/pubmed/17541180.

Unitt, J. & Hornigold, D., 2011. Plant lectins are novel Toll-like receptor agonists. *Biochemical Pharmacology*, 81(11), pp.1324–1328. Available at: http://dx.doi.org/10.1016/j.bcp.2011.03.010.

Vollmer, J., 2005. Progress in drug development of immunostimulatory CpG oligodeoxynucleotide ligands for TLR9. *Expert opinion on biological therapy*, 5(5), pp.673–682.

Van Voorhis, W.C., Hooft van Huijsduijnen, R. & Wells, T.N.C., 2015. Profile of William C. Campbell, Satoshi Ōmura, and Youyou Tu, 2015 Nobel Laureates in Physiology or Medicine. *Proceedings of the National Academy of Sciences*, 112(52), p.201520952. Available at: http://www.pnas.org/lookup/doi/10.1073/pnas.1520952112.

Wallin, R.P.A. et al., 2002. Heat-shock proteins as activators of the innate immune system. *Trends in Immunology*, 23(3), pp.130–135.

Waltenbaugh, C. et al., 2008. *Immunology*, Lippincott Williams & Wilkins.

Walter, A. et al., 2013. Aldara activates TLR7-independent immune defence. *Nature communications*, 4, p.1560. Available at: http://dx.doi.org/10.1038/ncomms2566.

Wang, Y. et al., 2017. Chlamydial Lipoproteins Stimulate Toll-Like Receptors 1/2 Mediated Inflammatory Responses through MyD88-Dependent Pathway. *Frontiers in microbiology*, 8, p.78.

Waring, P. & Müllbacher, A., 1999. Cell death induced by the Fas/Fas ligand pathway and its role in pathology. *Immunology and Cell Biology*, 77(4), pp.312–317.

Weihreter, E., 2014. *Traditional Knowledge, Perceptions and Forest Conditions in a Dayak Mentebah Community, West Kalimantan, Indonesia*, Bogor, Indonesia.

Wink, M., 2007. Ecological Roles of Alkaloids. In E. Fattorusso & O. Taglialatela-Scafati, eds. *Modern Alkaloids: Structure, Isolation, Synthesis and Biology*. Wiley-VCH Verlag GmbH & Co. KGaA, pp. 1–24.

Witwer, K.W. & Hirschi, K.D., 2014. Transfer and functional consequences of dietary microRNAs in vertebrates: Concepts in search of corroboration. *BioEssays*, 36(4), pp.394–406.

World Health Organization, 2017. WHO Model List of Essential Medicines. *Essential medicines and health products*, (August), pp.1–39. Available at: http://www.who.int/entity/medicines/publications/essentialmedicines/20th_EML2017_FINAL_amendedAug2017.pdf?ua=1.

Worley, M.J. et al., 2016. Ibudilast attenuates subjective effects of methamphetamine in a placebo-controlled inpatient study. *Drug and alcohol dependence*, 162, pp.245–50. Available at: http://www.sciencedirect.com/science/article/pii/S0376871616001204.

Wu, C.Y. & Wittick, J.J., 1977. Separation of five major alkaloids in gum opium and quantitation of morphine, codeine, and thebaine by isocratic reverse phase high performance liquid chromatography. *Analytical Chemistry*, 49(3), pp.359–363. Available at: http://dx.doi.org/10.1021/ac50011a009.

Xie, S. et al., 2016. Polysaccharide of Dendrobium huoshanense activates macrophages via toll-like receptor 4-mediated signaling pathways. *Carbohydrate polymers*, 146, pp.292–300. Available at: http://www.sciencedirect.com/science/article/pii/S0144861716302880.

Xu, Q. et al., 2006. Levan (β-2, 6-fructan), a major fraction of fermented soybean mucilage, displays immunostimulating properties via Toll-like receptor 4 signalling : induction of interleukin-12 production and suppression of T-helper type 2 response and immunoglobulin E pro. *Clinical and Experimental Allergy*, 36, pp.94–101.

Yamasaki, R.B., Osuga, D.T. & Feeney, R.E., 1982. Periodate oxidation of methionine in proteins. *Analytical Biochemistry*, 126(1), pp.183–189.

Yang, J. et al., 2015. Detection of dietary plant-based small RNAs in animals. *Cell research*, 25(4), pp.517–20. Available at: http://dx.doi.org/10.1038/cr.2015.26.

Yang, X. et al., 2007. Macrophage activation by an acidic polysaccharide isolated from Angelica sinensis (Oliv.) Diels. *Journal of biochemistry and molecular biology*, 40(5), pp.636–43. Available at: http://www.ncbi.nlm.nih.gov/pubmed/17927894.

Yap, V.A. et al., 2016. Fistulopsines A and B antiproliferative septicine-type alkaloids from Ficus fistulosa. *Phytochemistry Letters*, 15(July), pp.136–141. Available at: http://dx.doi.org/10.1016/j.phytol.2015.12.007.

Yarmarkovich, M. & Hirschi, K.D., 2015. Digesting dietary miRNA therapeutics. *Oncotarget*, 6(16), pp.13848–9. Available at: http://www.ncbi.nlm.nih.gov/pubmed/26116837%5Cnhttp://www.pubmedcentral.nih.gov/articlerender.fcgi?artid=PMC4546433.

Yoshimura, S. et al., 2001. Effective antigen presentation by dendritic cells is NF-kappaB

dependent: coordinate regulation of MHC, co-stimulatory molecules and cytokines. *Int Immunol*, 13(5), pp.675–683. Available at: http://www.ncbi.nlm.nih.gov/entrez/query.fcgi?cmd=Retrieve&db=PubMed&dopt=Citation&list_uids=11312255.

Yoshimura, T. et al., 1987. Purification of a human monocyte-derived neutrophil chemotactic factor that has peptide sequence similarity to other host defense cytokines. *Proceedings of the National Academy of Sciences of the United States of America*, 84(24), pp.9233–9237.

Youn, H.S. et al., 2006. Inhibition of homodimerization of Toll-like receptor 4 by curcumin. *Biochemical pharmacology*, 72(1), pp.62–9. Available at: http://www.ncbi.nlm.nih.gov/pubmed/16678799 [Accessed September 5, 2013].

Youn, H.S. et al., 2006. Suppression of MyD88- and TRIF-dependent signaling pathways of toll-like receptor by (-)-epigallocatechin-3-gallate, a polyphenol component of green tea. *Biochemical Pharmacology*, 72(7), pp.850–859.

Zadeh, N., Getzug, T. & Grody, W.W., 2011. Diagnosis and management of familial Mediterranean fever: integrating medical genetics in a dedicated interdisciplinary clinic. *Genetics in medicine : official journal of the American College of Medical Genetics*, 13(3), pp.263–269.

Zaheen, A. & Martin, A., 2010. Induction and assessment of class switch recombination in purified murine B cells. *Journal of visualized experiments : JoVE*, (42), pp.6–8.

Zeng, W. et al., 2010. Structural requirement for the agonist activity of the TLR2 ligand Pam2Cys. *Amino Acids*, 39(2), pp.471–480.

Zhang, H.J. et al., 2002. Antimalarial agents from plants. III. Trichothecenes from Ficus fistulosa and Rhaphidophora decursiva. *Planta Medica*, 68(12), pp.1088–1091.

Zhang, L. et al., 2012. Exogenous plant MIR168a specifically targets mammalian LDLRAP1: evidence of cross-kingdom regulation by microRNA. *Cell research*, 22(1), pp.107–26. Available at: http://www.pubmedcentral.nih.gov/articlerender.fcgi?artid=3351925&tool=pmcentrez&rendertype=abstract%5Cnhttp://www.ncbi.nlm.nih.gov/pubmed/21931358.

Zhao, L. et al., 2014. Nanoparticle vaccines. *Vaccine*, 32(3), pp.327–337. Available at:

http://dx.doi.org/10.1016/j.vaccine.2013.11.069.

Zhou, Y. et al., 2016. Convergence and divergence of cucurbitacin biosynthesis and regulation in Cucurbitaceae. *Nature plants*, 2, p.16183. Available at: http://www.ncbi.nlm.nih.gov/pmc/articles/PMC5449191/.

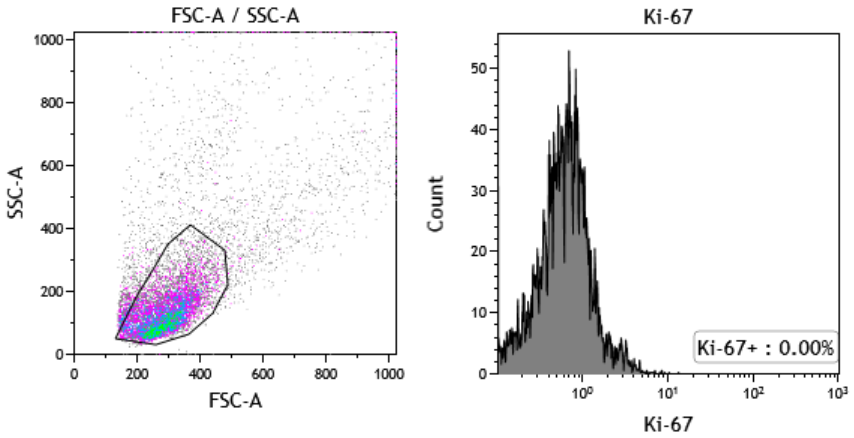
Zhou, Z. et al., 2014. Honeysuckle-encoded atypical microRNA2911 directly targets influenza A viruses. *Cell research*, 25(1), pp.1–11. Available at: http://www.ncbi.nlm.nih.gov/pubmed/25287280%5Cnhttp://www.nature.com/doifinder/10.1038/cr.2014.130.

Appendix A Flow cytometry data

A.1 Proliferation - Ki-67

A separate experiment was carried out to control for non-specific binding (Figure 5.1 A and B). No non-specific binding was detected in the isotype control (Figure 5.1 B).

A. Unstained



B. Isotype

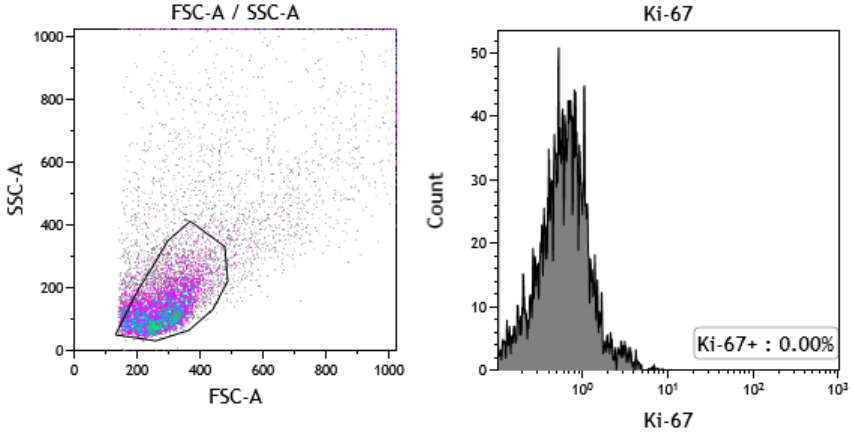
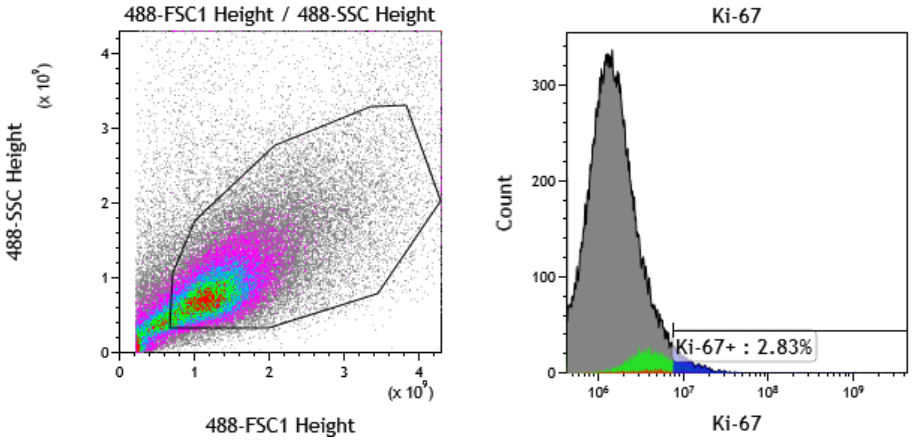
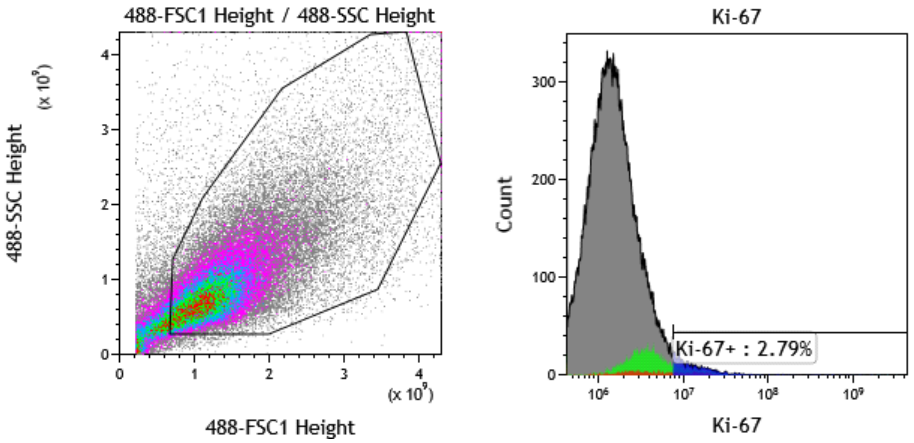


Figure 0.1. FACS readouts for Ki-67 in murine splenic B-cells. Events were gated for size by forward scatter (FSC) and granularity by side scatter (SSC). Events outside this gate were excluded from further analysis. Percentage = % Ki-67^{+} cells. Blue histograms: Ki-67+ cells; green histograms: IgM+ cells; red histograms: IgG1+ cells; grey histograms: unstained cells.

C. RPMI



D. LPS/IL-4



E. Pam2CSK4

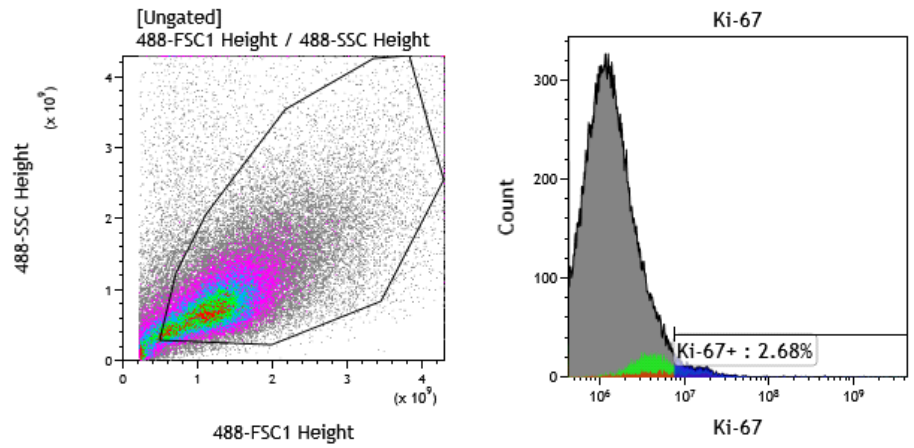
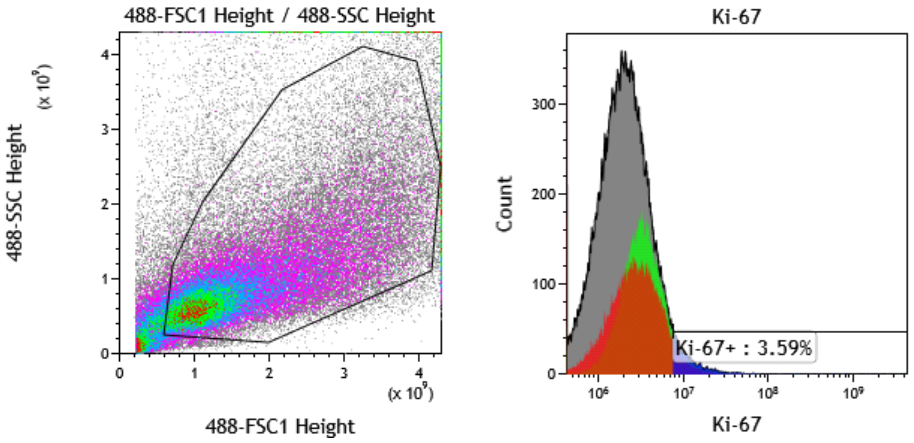
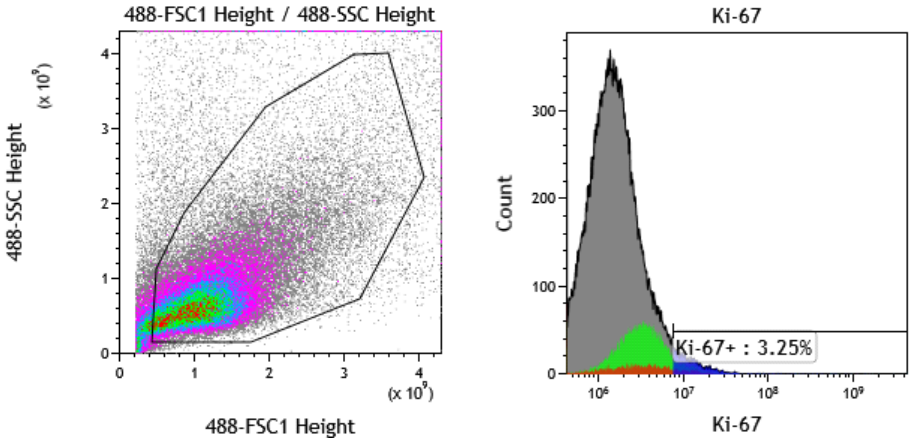


Figure 0.1 (continued). FACS readouts for Ki-67 in murine splenic B-cells. Events were gated for size by forward scatter (FSC) and granularity by side scatter (SSC). Events outside this gate were excluded from further analysis. Percentage = % Ki-67^{+} cells. Blue histograms: Ki-67+ cells; green histograms: IgM+ cells; red histograms: IgG1+ cells; grey histograms: unstained cells.

F. 200µg/ml 1402EtL



G. 100µg/ml 1402EtL



H. 50µg/ml 1402EtL

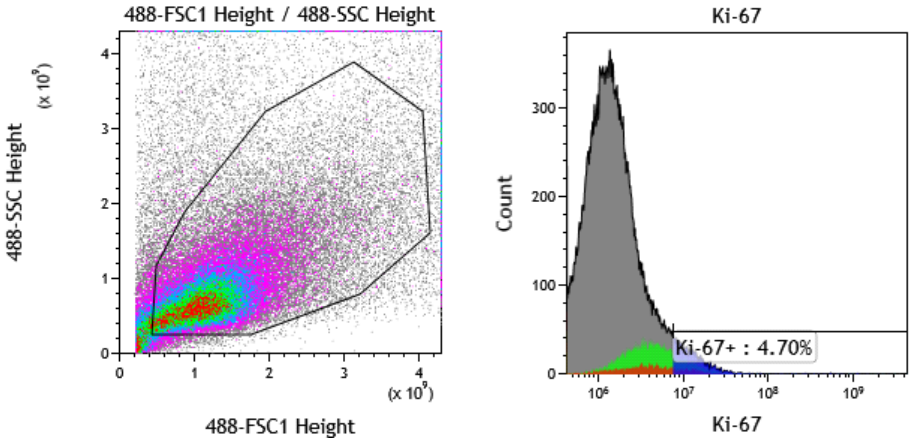
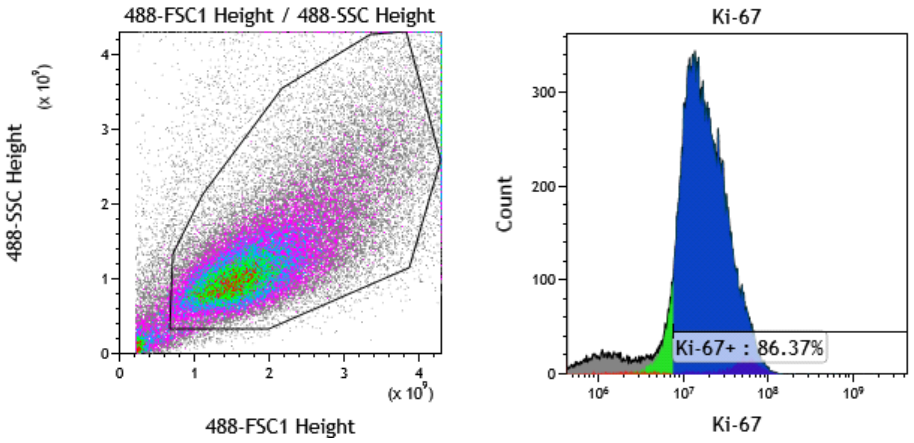
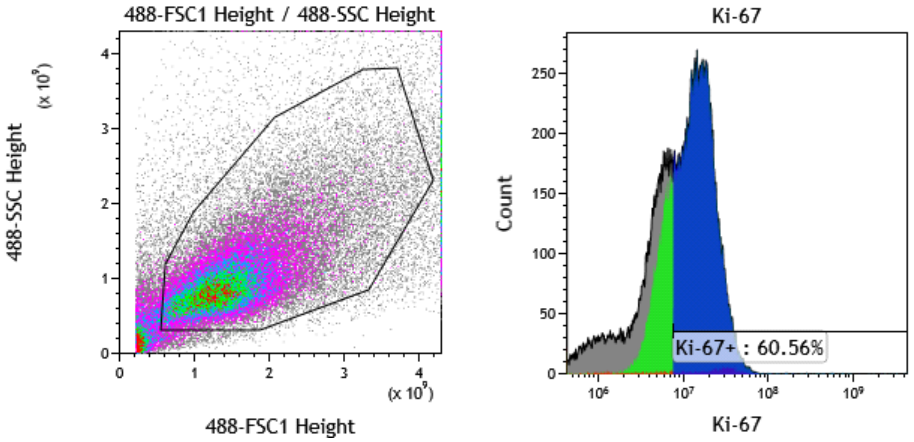


Figure 0.1 (continued). FACS readouts for Ki-67 in murine splenic B-cells. Events were gated for size by forward scatter (FSC) and granularity by side scatter (SSC). Events outside this gate were excluded from further analysis. Percentage = % Ki-67^{+} cells. Blue histograms: Ki-67+ cells; green histograms: IgM+ cells; red histograms: IgG1+ cells; grey histograms: unstained cells.

I. 200µg/ml 1412EtB



J. 100µg/ml 1412EtB



K. 50µg/ml 1412EtB

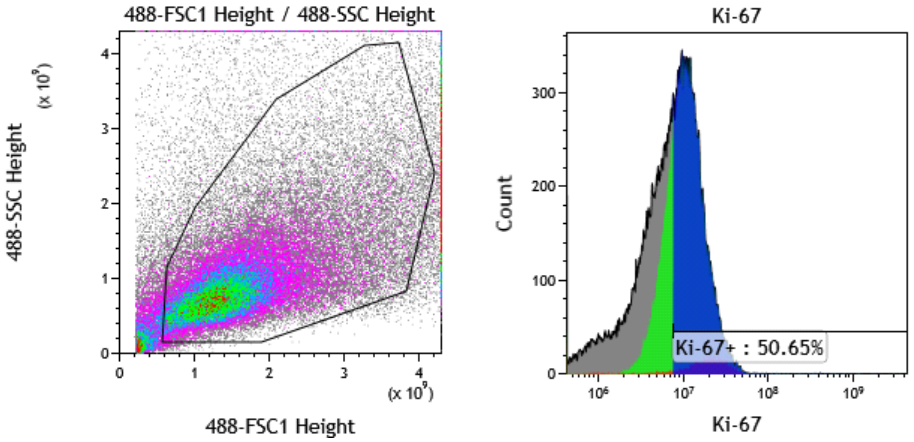
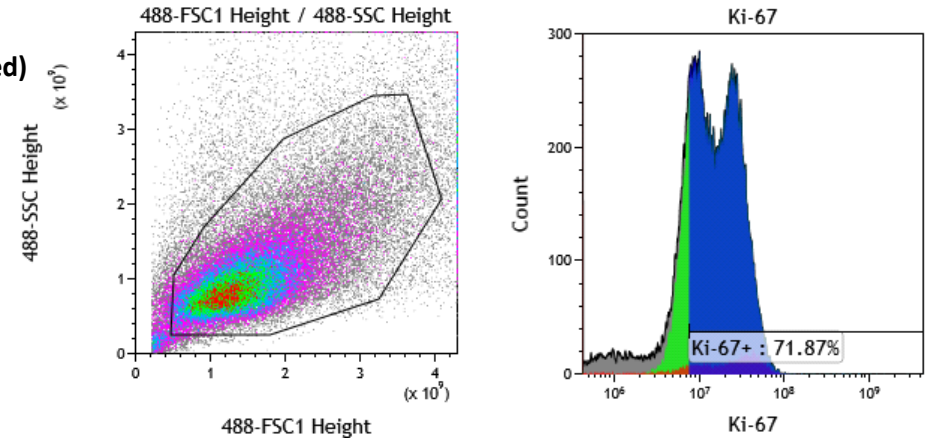
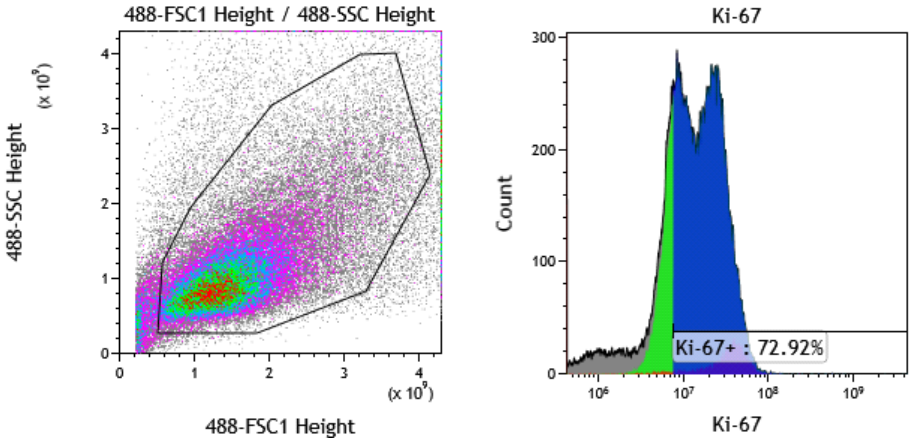


Figure 0.1 (continued). FACS readouts for Ki-67 in murine splenic B-cells. Events were gated for size by forward scatter (FSC) and granularity by side scatter (SSC). Events outside this gate were excluded from further analysis. Percentage = % Ki-67^{+} cells. Blue histograms: Ki-67+ cells; green histograms: IgM+ cells; red histograms: IgG1+ cells; grey histograms: unstained cells.

L. 1412EtB (acid-treated)



M. 1412EtB (boiled)



N. 1412EtB (oxidised)

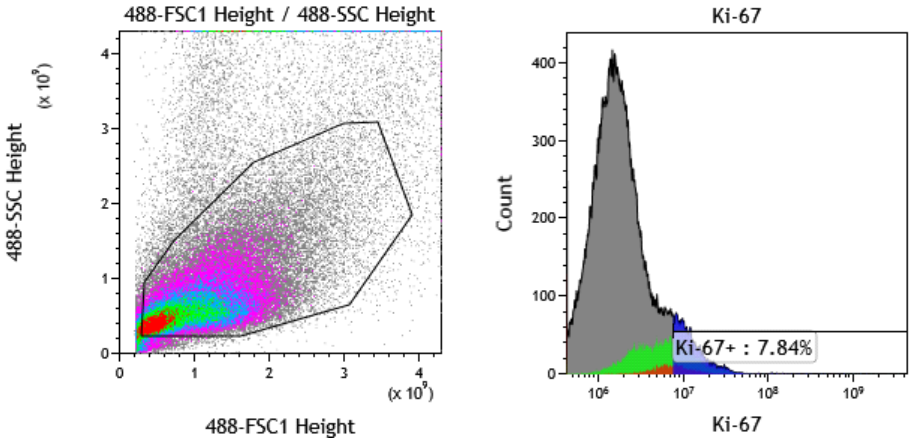
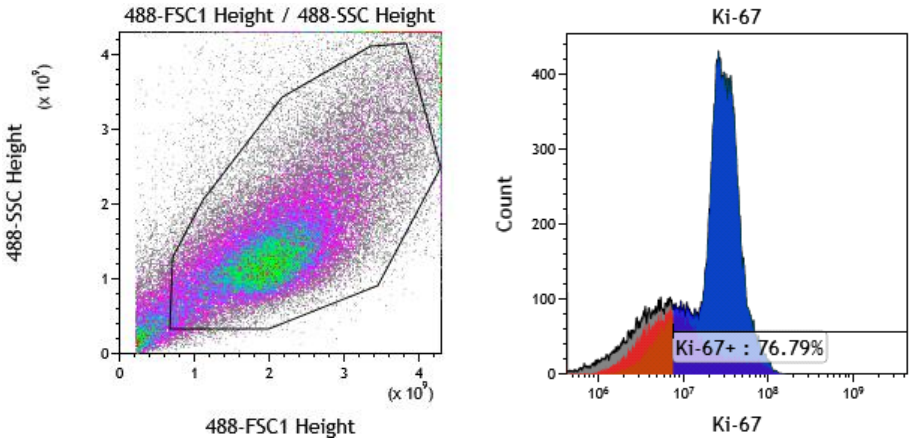
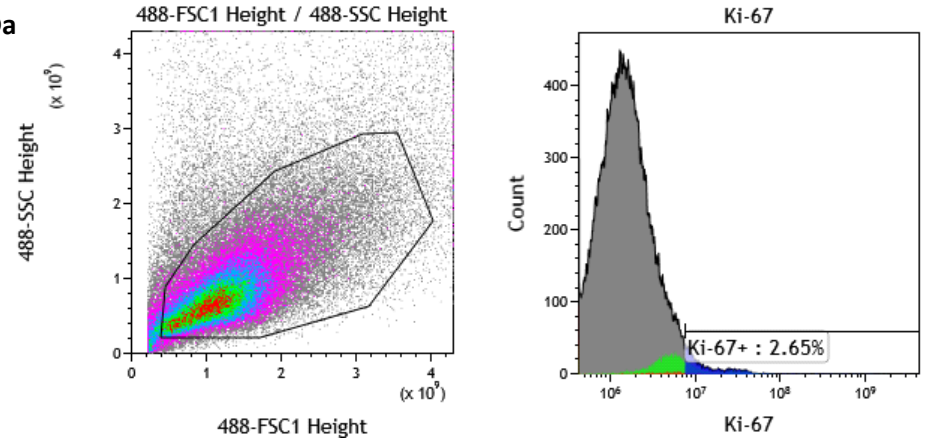


Figure 0.1 (continued). FACS readouts for Ki-67 in murine splenic B-cells. Events were gated for size by forward scatter (FSC) and granularity by side scatter (SSC). Events outside this gate were excluded from further analysis. Percentage = % Ki-67^{+} cells. Blue histograms: Ki-67+ cells; green histograms: IgM+ cells; red histograms: IgG1+ cells; grey histograms: unstained cells.

O. >100kDa
1412EtB



P. 50-100kDa
1412EtB



Q. 30-50kDa
1412EtB

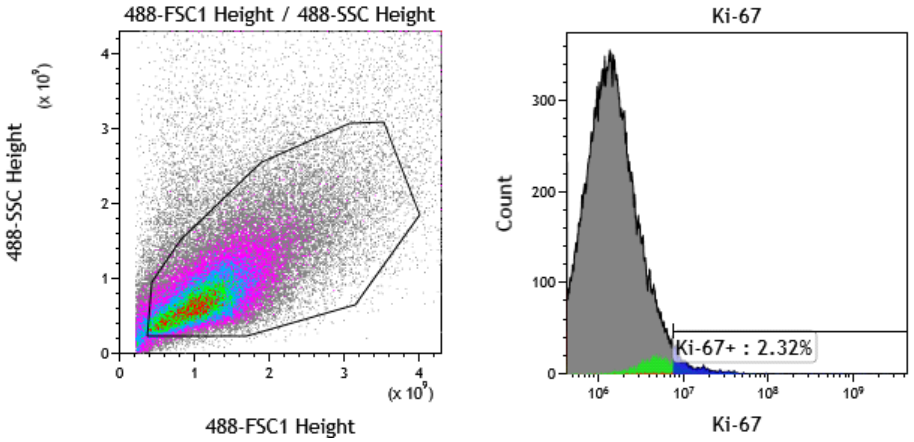
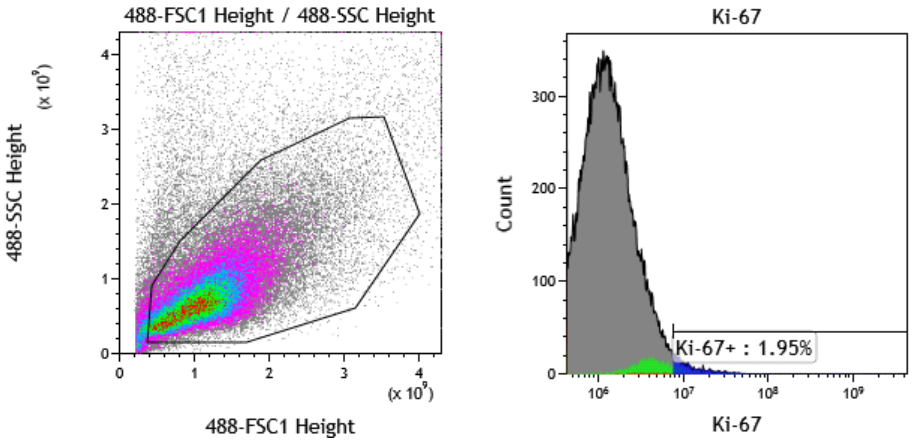


Figure 0.1 (continued). FACS readouts for Ki-67 in murine splenic B-cells. Events were gated for size by forward scatter (FSC) and granularity by side scatter (SSC). Events outside this gate were excluded from further analysis. Percentage = % Ki-67^{+} cells. Blue histograms: Ki-67+ cells; green histograms: IgM+ cells; red histograms: IgG1+ cells; grey histograms: unstained cells.

R. 5-30kDa
1412EtB



S. <5kDa
1412EtB

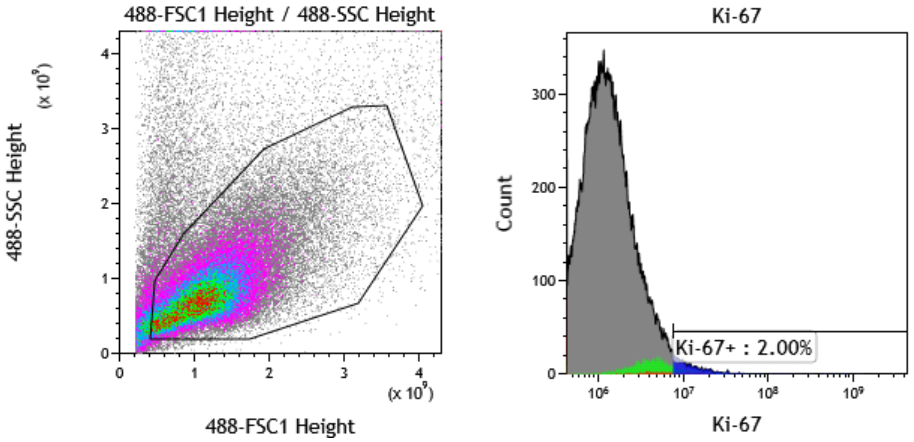


Figure 0.1 (continued). FACS readouts for Ki-67 in murine splenic B-cells. Events were gated for size by forward scatter (FSC) and granularity by side scatter (SSC). Events outside this gate were excluded from further analysis. Percentage = % Ki-67^{+} cells. Blue histograms: Ki-67+ cells; green histograms: IgM+ cells; red histograms: IgG1+ cells; grey histograms: unstained cells.

A.2 IgM

A separate experiment was carried out to control for non-specific binding (Figure 5.2 A and B). No non-specific binding was detected in the isotype control (Figure 5.2 B).

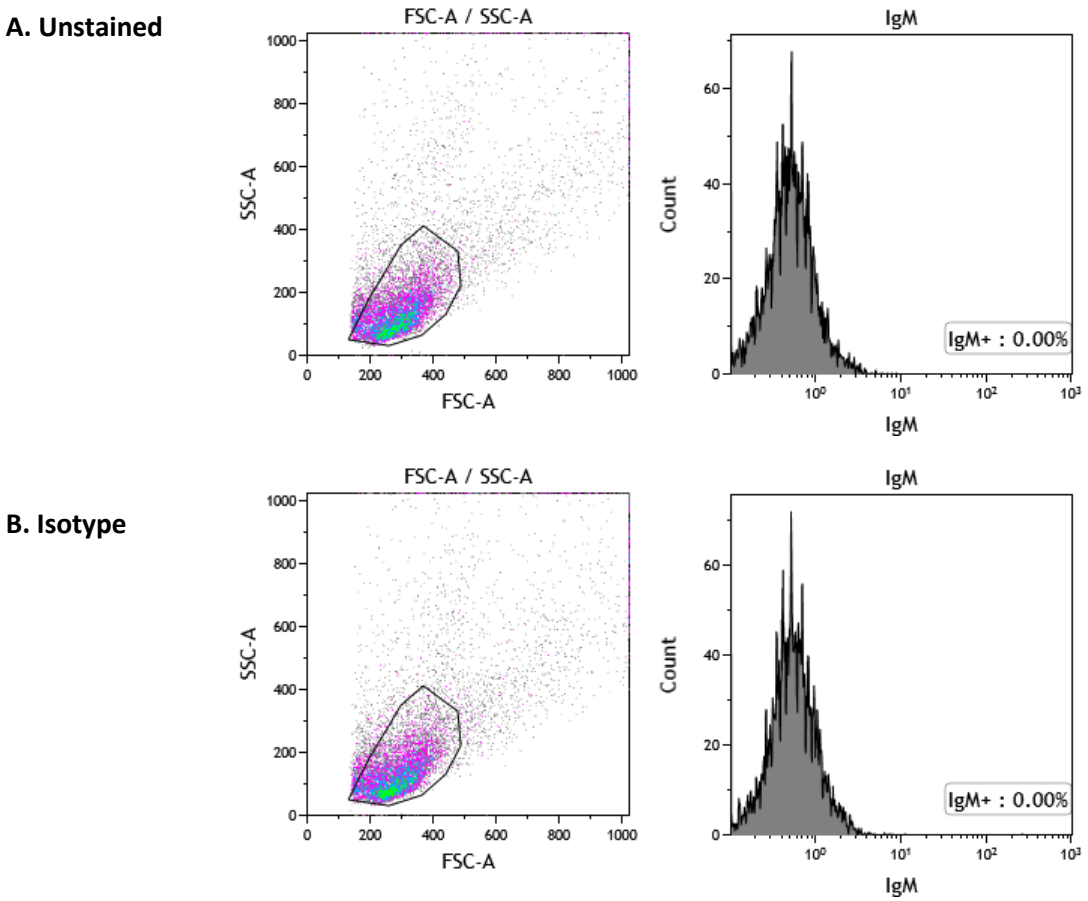
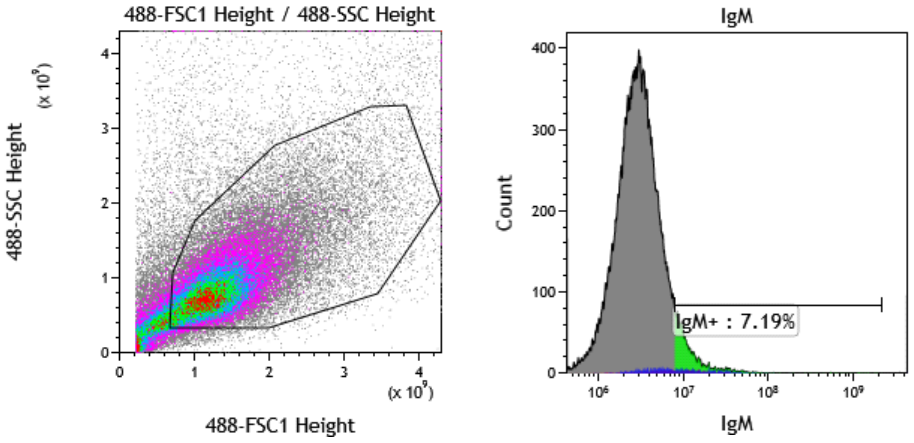
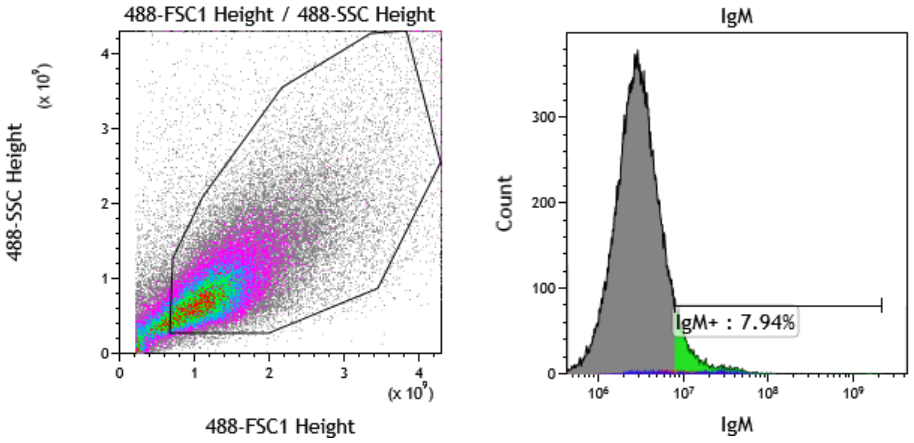


Figure 0.2. FACS readouts for IgM in murine splenic B-cells. Events were gated for size by forward scatter (FSC) and granularity by side scatter (SSC). Events outside this gate were excluded from further analysis. Percentage = % IgM^+ cells. Blue histograms: Ki-67+ cells; green histograms: IgM+ cells; red histograms: IgG1+ cells; grey histograms: unstained cells.

C. RPMI



D. LPS/IL-4



E. Pam2CSK4

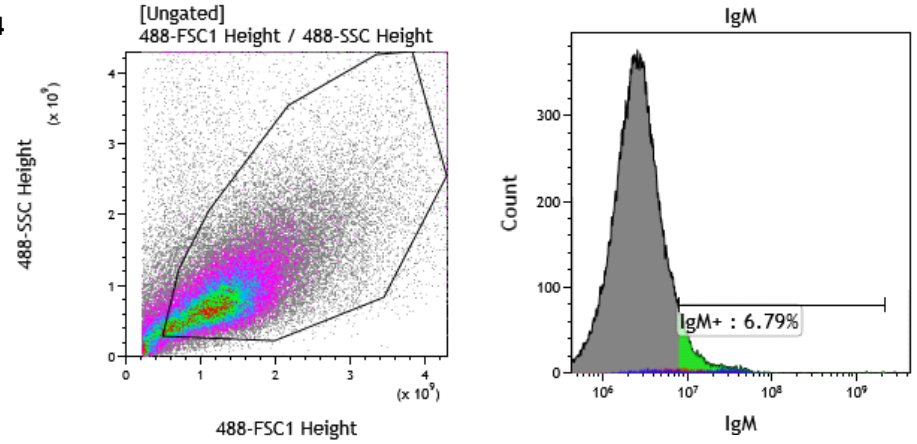
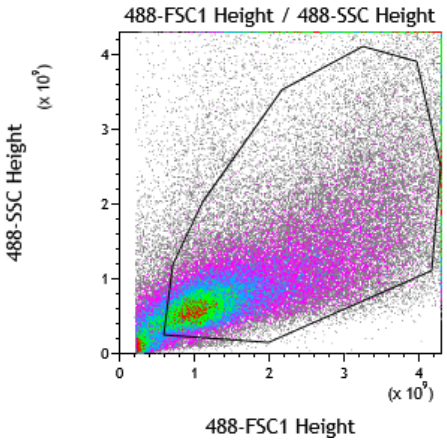
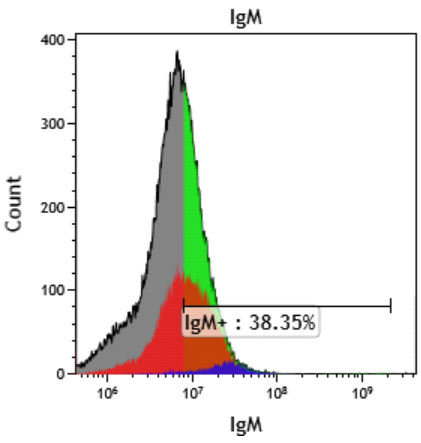


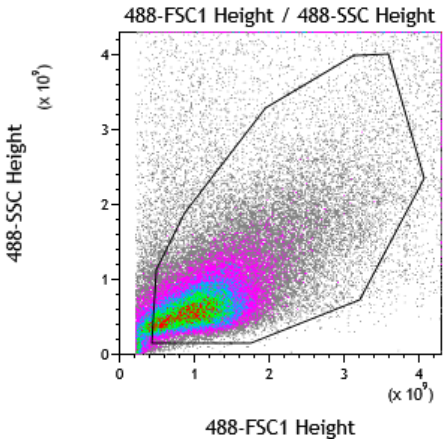
Figure 0.2 (continued). FACS readouts for IgM in murine splenic B-cells. Events were gated for size by forward scatter (FSC) and granularity by side scatter (SSC). Events outside this gate were excluded from further analysis. Percentage = % IgM^+ cells. Blue histograms: Ki-67+ cells; green histograms: IgM+ cells; red histograms: IgG1+ cells; grey histograms: unstained cells.

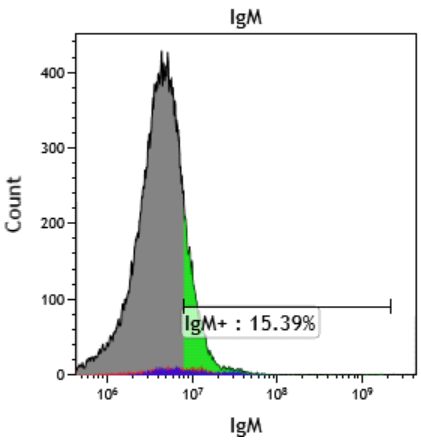
F. 200µg/ml 1402EtL



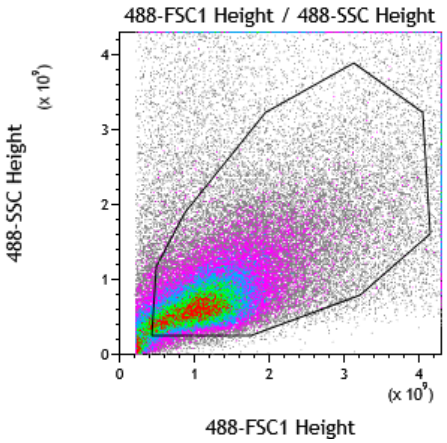


G. 100µg/ml 1402EtL





H. 50µg/ml 1402EtL



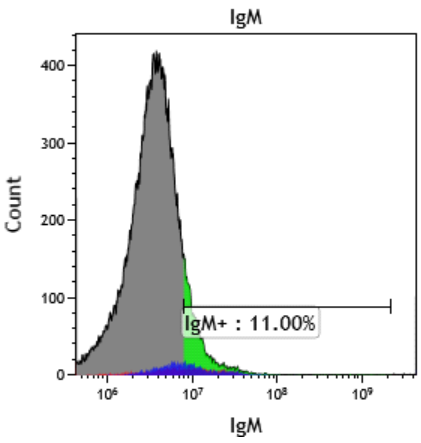
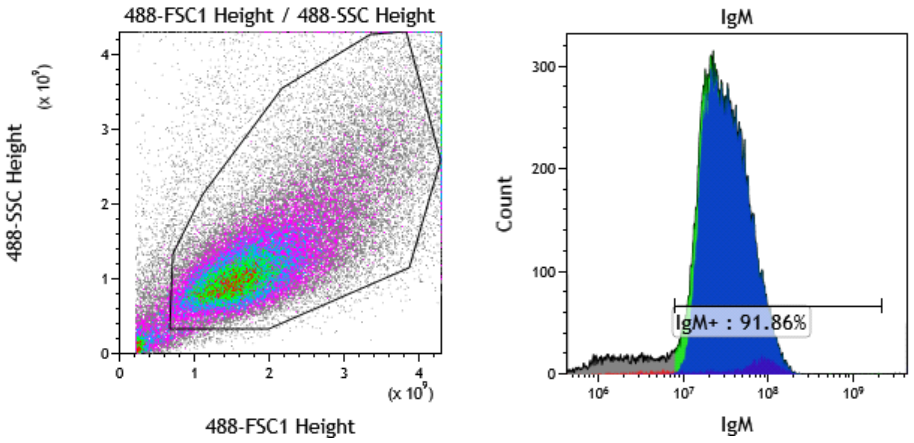
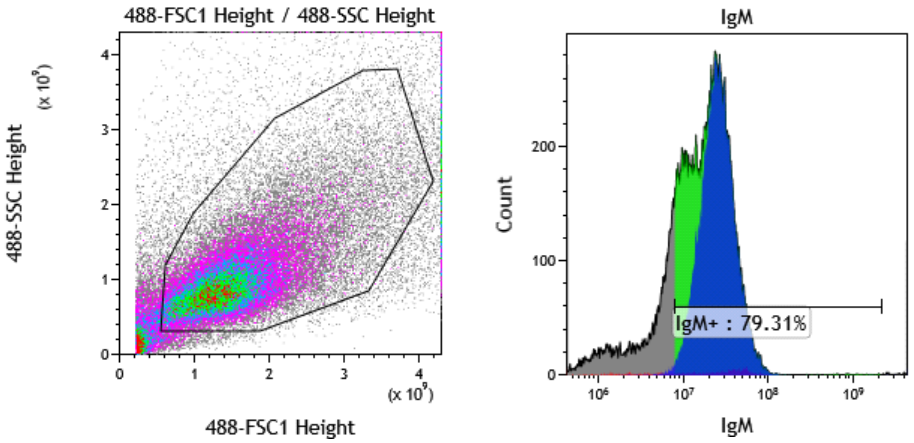


Figure 0.2 (continued). FACS readouts for IgM in murine splenic B-cells. Events were gated for size by forward scatter (FSC) and granularity by side scatter (SSC). Events outside this gate were excluded from further analysis. Percentage = % IgM^+ cells. Blue histograms: Ki-67+ cells; green histograms: IgM+ cells; red histograms: IgG1+ cells; grey histograms: unstained cells.

I. 200µg/ml 1412EtB



J. 100µg/ml 1412EtB



K. 50µg/ml 1412EtB

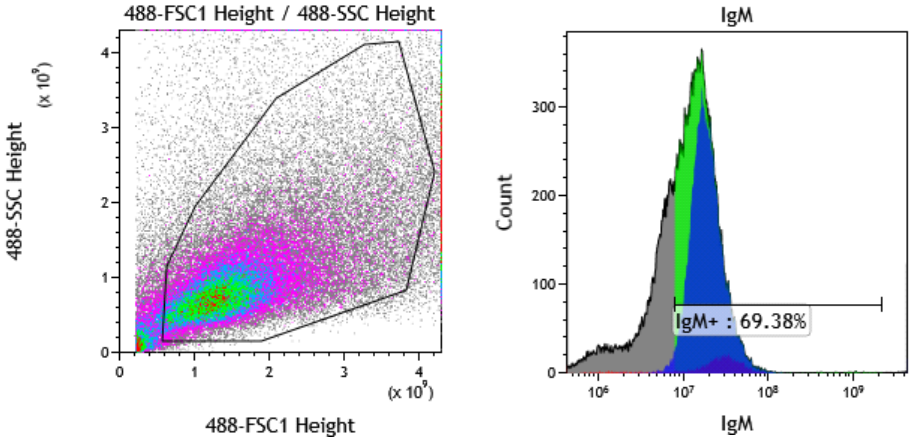
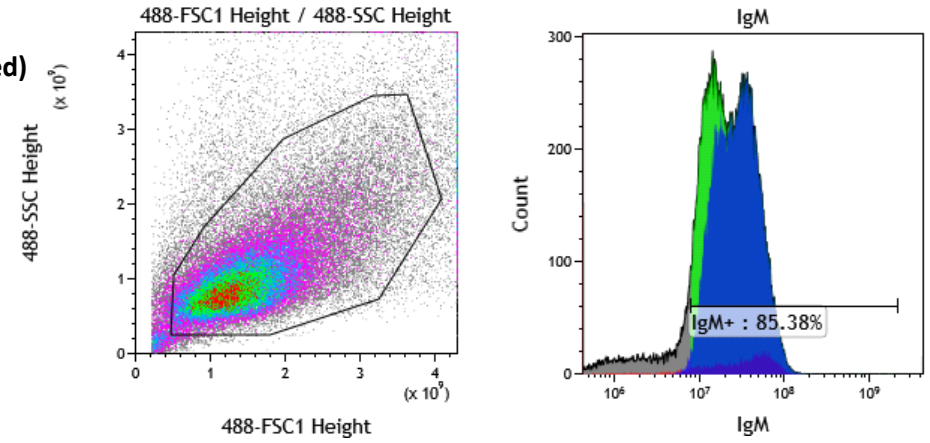
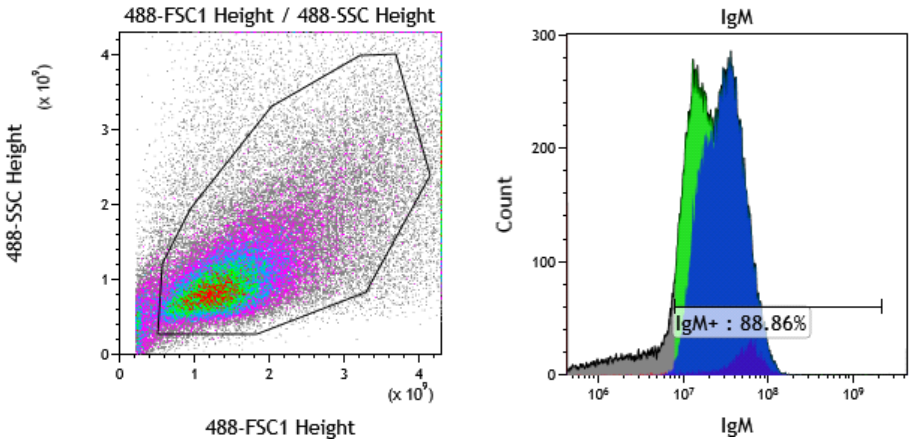


Figure 0.2 (continued). FACS readouts for IgM in murine splenic B-cells. Events were gated for size by forward scatter (FSC) and granularity by side scatter (SSC). Events outside this gate were excluded from further analysis. Percentage = % IgM^+ cells. Blue histograms: Ki-67+ cells; green histograms: IgM+ cells; red histograms: IgG1+ cells; grey histograms: unstained cells.

L. 1412EtB (acid-treated)



M. 1412EtB (boiled)



N. 1412EtB (acid-treated)

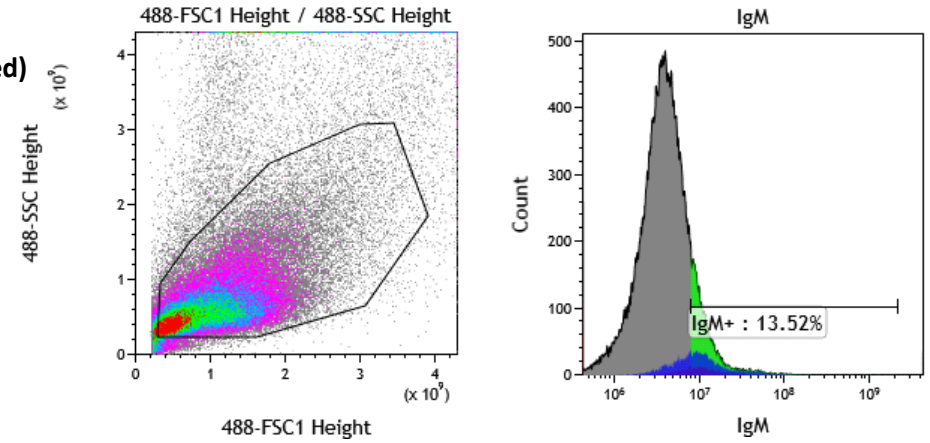
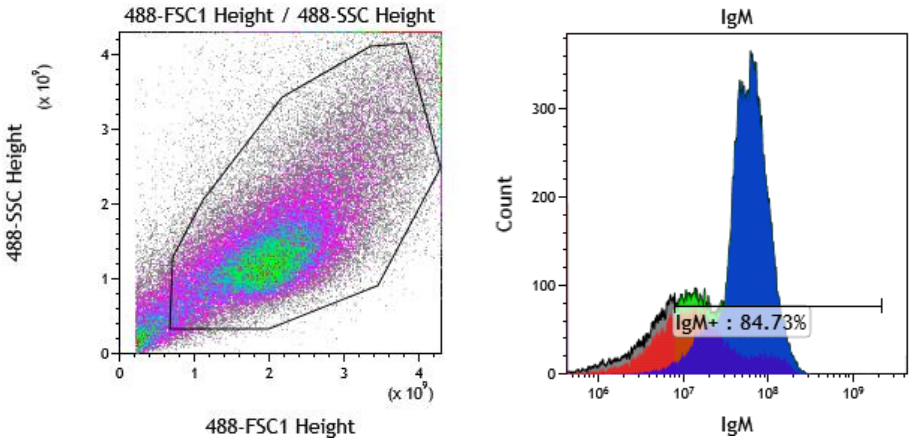
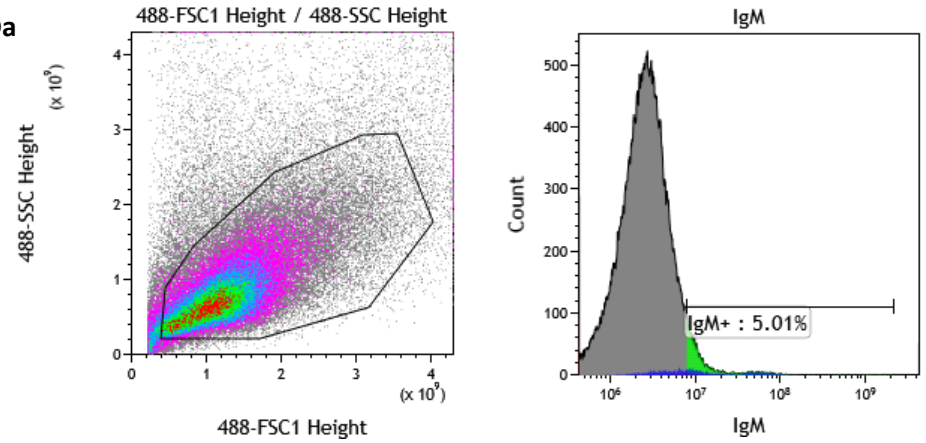


Figure 0.2 (continued). FACS readouts for IgM in murine splenic B-cells. Events were gated for size by forward scatter (FSC) and granularity by side scatter (SSC). Events outside this gate were excluded from further analysis. Percentage = % IgM^+ cells. Blue histograms: Ki-67+ cells; green histograms: IgM+ cells; red histograms: IgG1+ cells; grey histograms: unstained cells.

O. >100kDa
1412EtB



P. 50-100kDa
1412EtB



Q. 30-50kDa
1412EtB

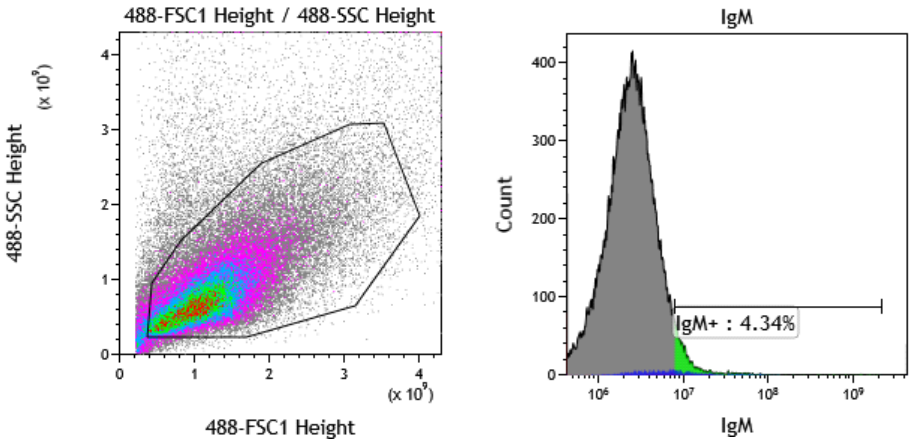
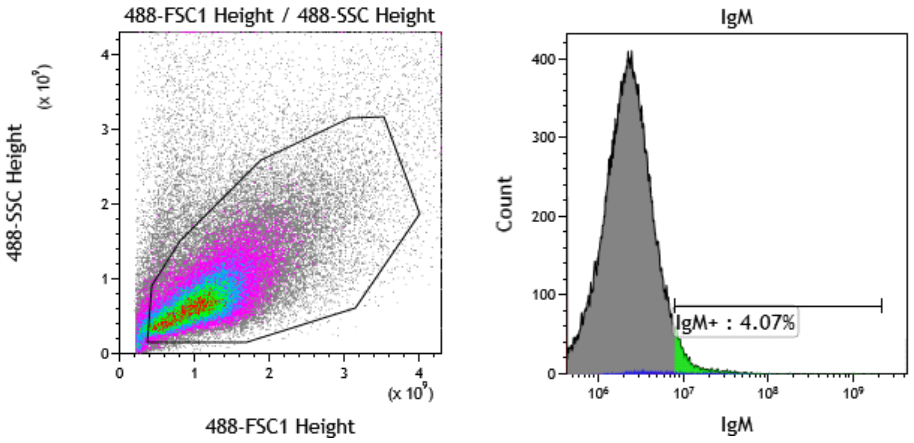


Figure 0.2 (continued). FACS readouts for IgM in murine splenic B-cells. Events were gated for size by forward scatter (FSC) and granularity by side scatter (SSC). Events outside this gate were excluded from further analysis. Percentage = % IgM^+ cells. Blue histograms: Ki-67+ cells; green histograms: IgM+ cells; red histograms: IgG1+ cells; grey histograms: unstained cells.

R. 5-30kDa
1412EtB



S. <5kDa
1412EtB

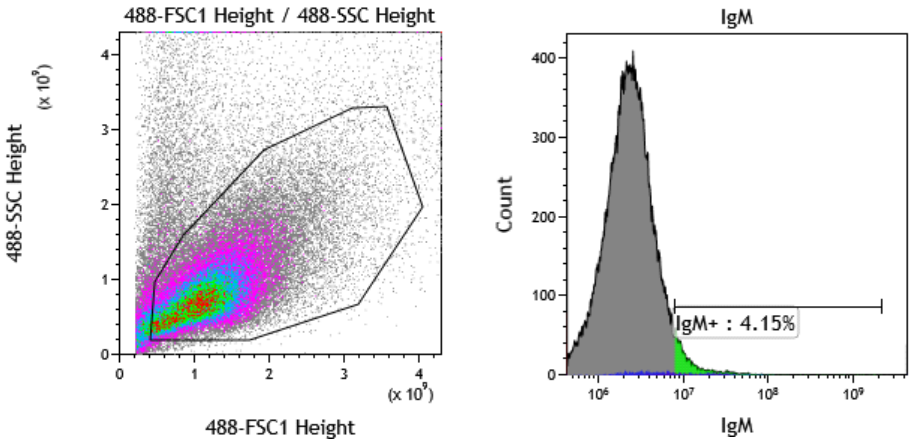


Figure 0.2 (continued). FACS readouts for IgM in murine splenic B-cells. Events were gated for size by forward scatter (FSC) and granularity by side scatter (SSC). Events outside this gate were excluded from further analysis. Percentage = % IgM^+ cells. Blue histograms: Ki-67+ cells; green histograms: IgM+ cells; red histograms: IgG1+ cells; grey histograms: unstained cells.

A.3 IgG1

A separate experiment was carried out to control for non-specific binding (Figure 5.3 A and B). No non-specific binding was detected in the isotype control (Figure 5.3 B).

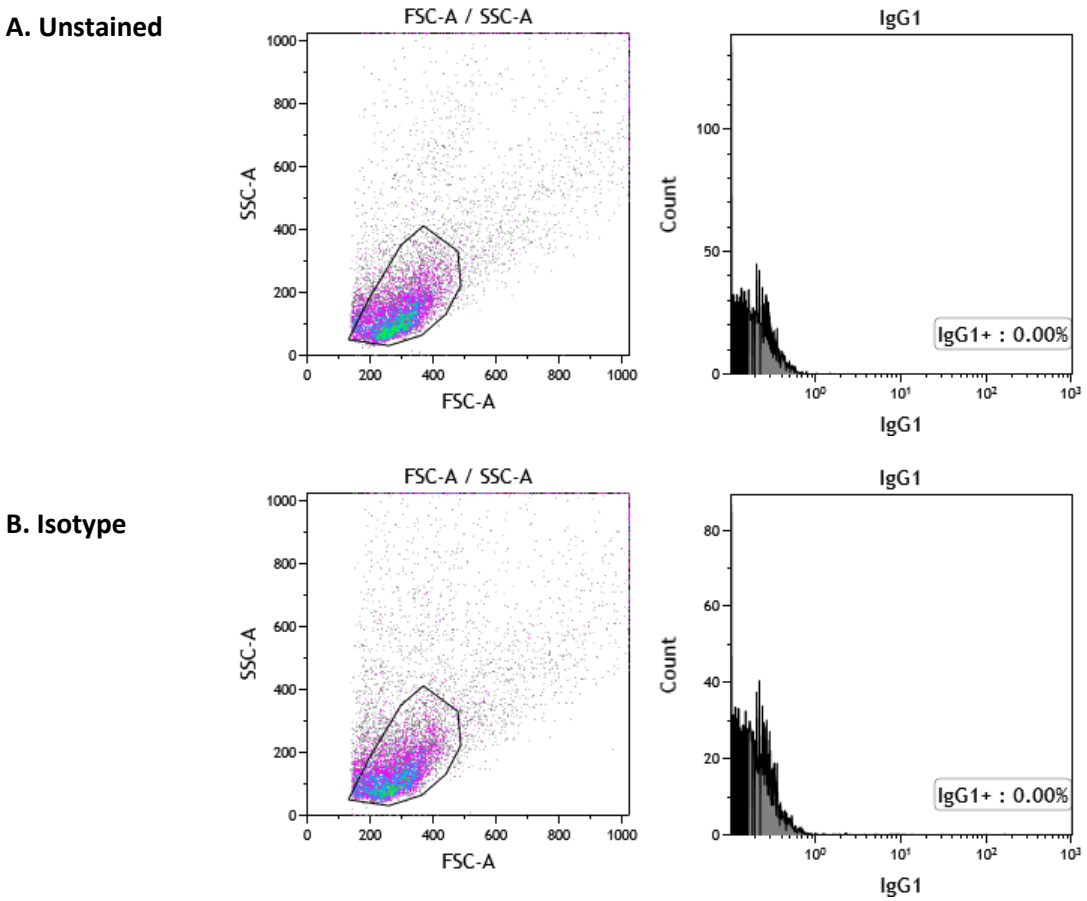
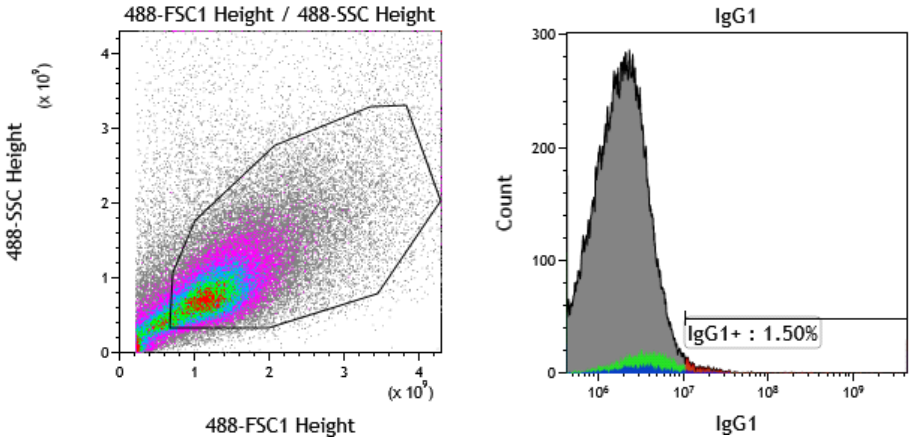
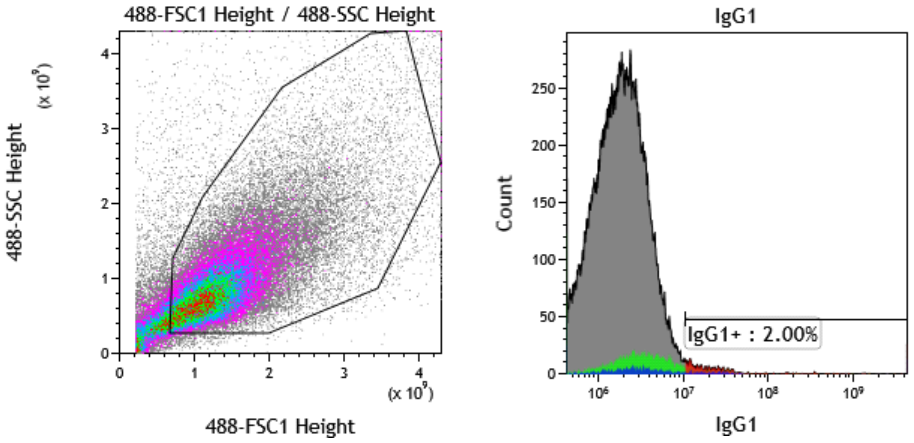


Figure 0.3. FACS readouts for IgG1 in murine splenic B-cells. Events were gated for size by forward scatter (FSC) and granularity by side scatter (SSC). Events outside this gate were excluded from further analysis. Percentage = % IgG1^{+} cells. Blue histograms: Ki-67+ cells; green histograms: IgM+ cells; red histograms: IgG1+ cells; grey histograms: unstained cells.

C. RPMI



D. LPS/IL-4



E. Pam2CSK4

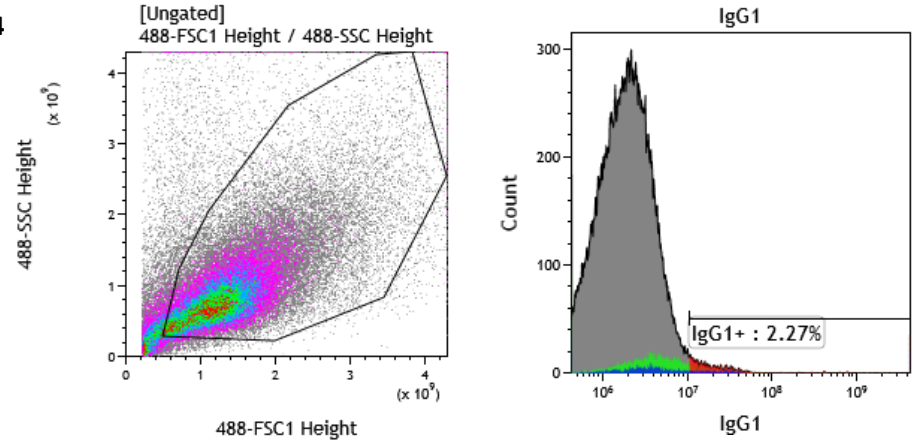
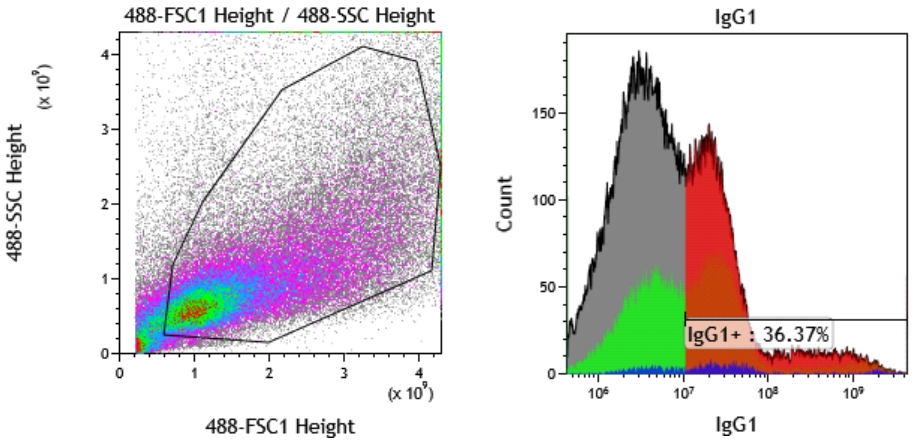
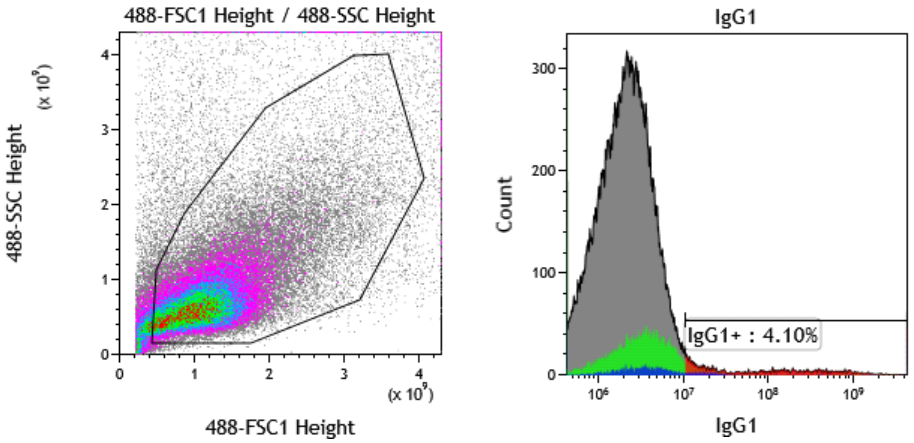


Figure 0.3 (continued). FACS readouts for IgG1 in murine splenic B-cells. Events were gated for size by forward scatter (FSC) and granularity by side scatter (SSC). Events outside this gate were excluded from further analysis. Percentage = % $IgG1^+$ cells. Blue histograms: Ki-67+ cells; green histograms: IgM+ cells; red histograms: IgG1+ cells; grey histograms: unstained cells.

F. 200µg/ml 1402EtL



G. 100µg/ml 1402EtL



H. 50µg/ml 1402EtL

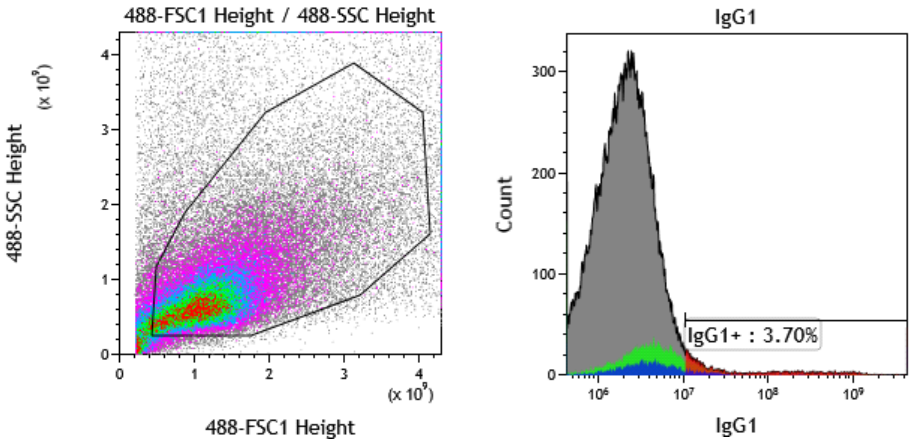
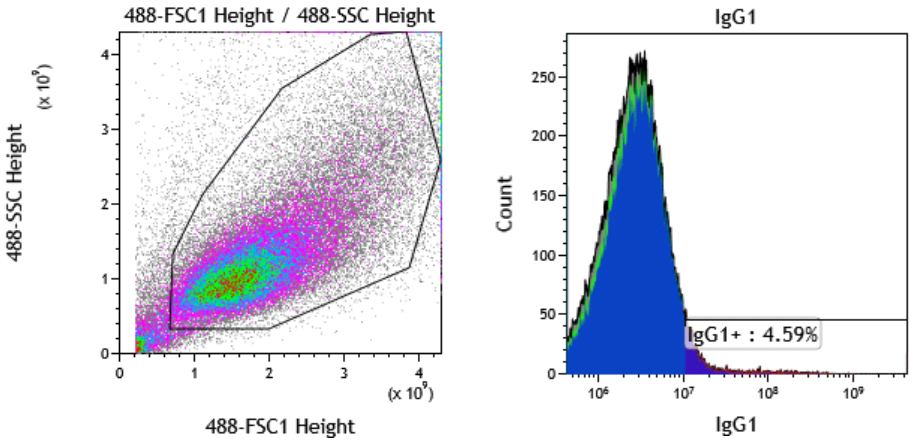
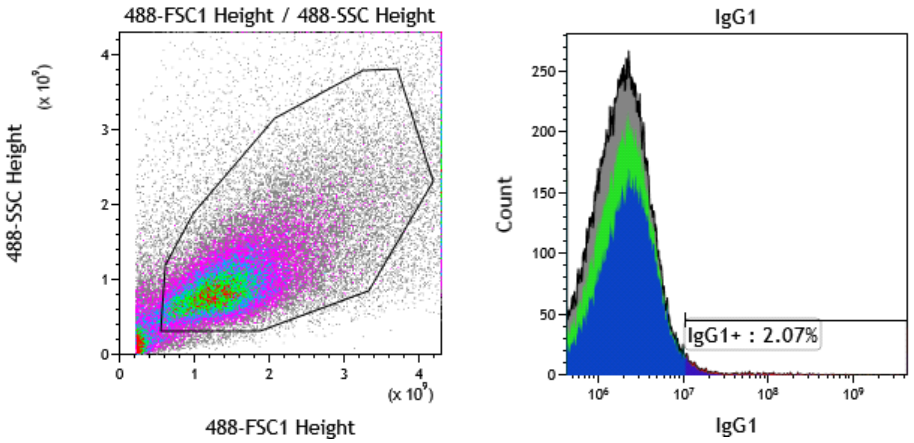


Figure 0.3 (continued). FACS readouts for IgG1 in murine splenic B-cells. Events were gated for size by forward scatter (FSC) and granularity by side scatter (SSC). Events outside this gate were excluded from further analysis. Percentage = % $IgG1^+$ cells. Blue histograms: Ki-67+ cells; green histograms: IgM+ cells; red histograms: IgG1+ cells; grey histograms: unstained cells.

I. 200µg/ml 1412EtB



J. 100µg/ml 1412EtB



K. 50µg/ml 1412EtB

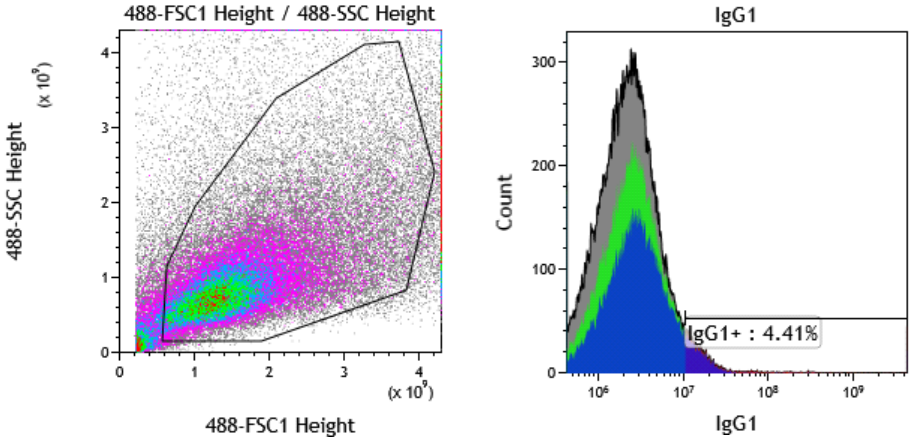
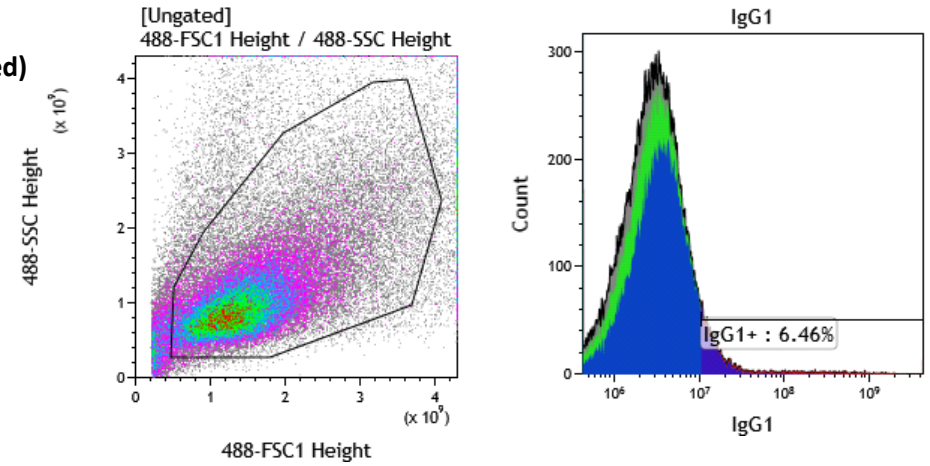
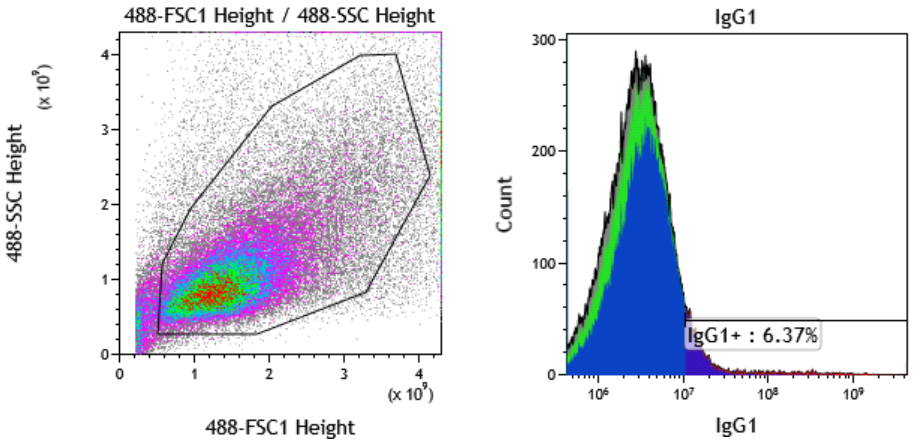


Figure 0.3 (continued). FACS readouts for IgG1 in murine splenic B-cells. Events were gated for size by forward scatter (FSC) and granularity by side scatter (SSC). Events outside this gate were excluded from further analysis. Percentage = % $IgG1^+$ cells. Blue histograms: Ki-67+ cells; green histograms: IgM+ cells; red histograms: IgG1+ cells; grey histograms: unstained cells.

L. 1412EtB (acid-treated)



M. 1412EtB (boiled)



N. 1412EtB (oxidised)

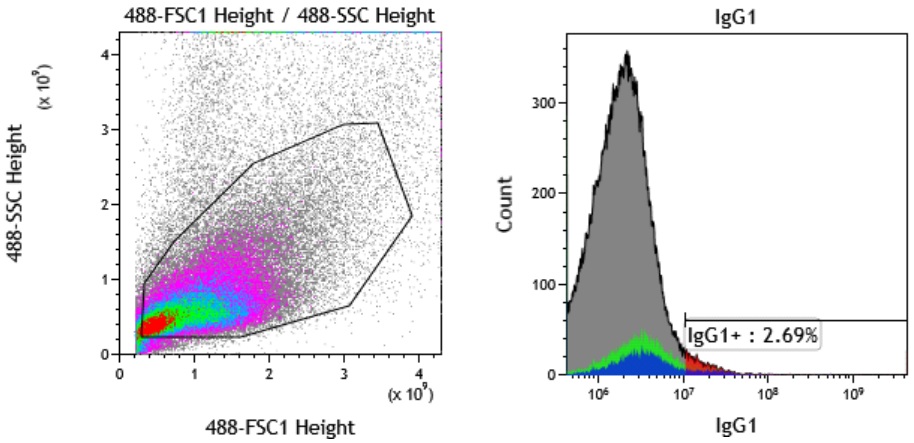
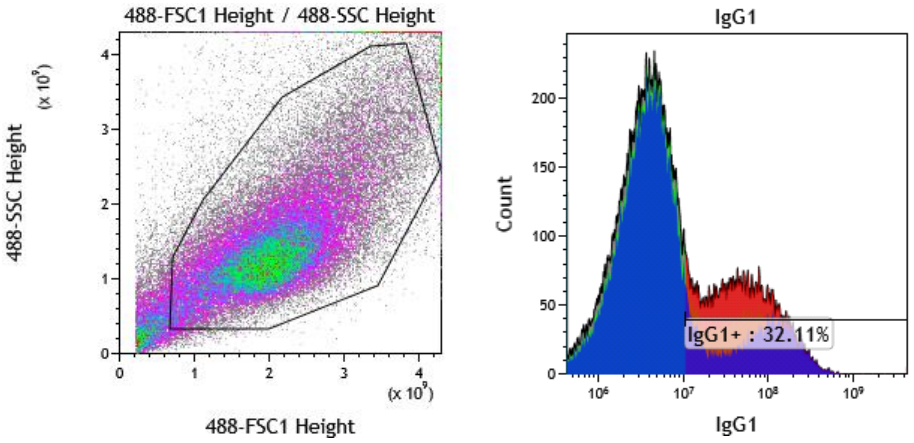
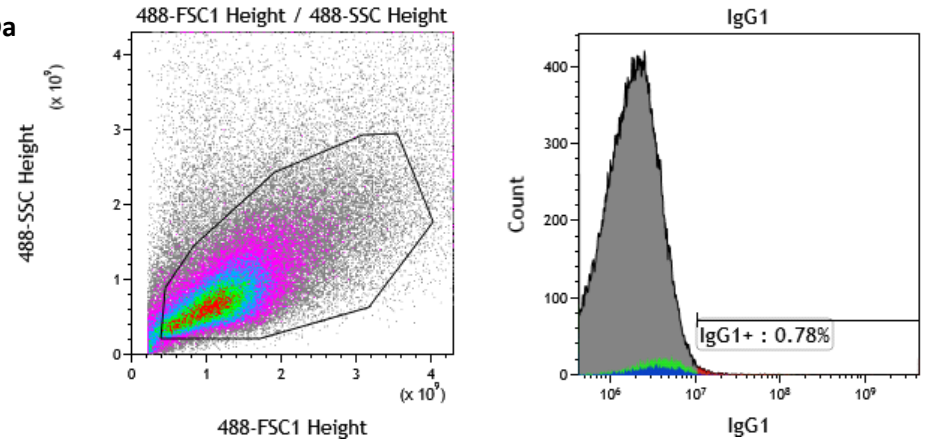


Figure 0.3 (continued). FACS readouts for IgG1 in murine splenic B-cells. Events were gated for size by forward scatter (FSC) and granularity by side scatter (SSC). Events outside this gate were excluded from further analysis. Percentage = % IgG1$^+$ cells. Blue histograms: Ki-67+ cells; green histograms: IgM+ cells; red histograms: IgG1+ cells; grey histograms: unstained cells.

O. >100kDa
1412EtB



P. 50-100kDa
1412EtB



Q. 30-50kDa
1412EtB

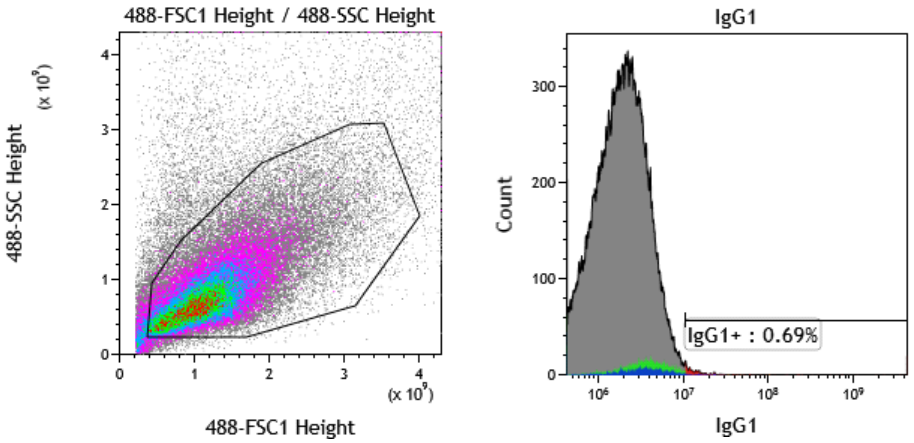
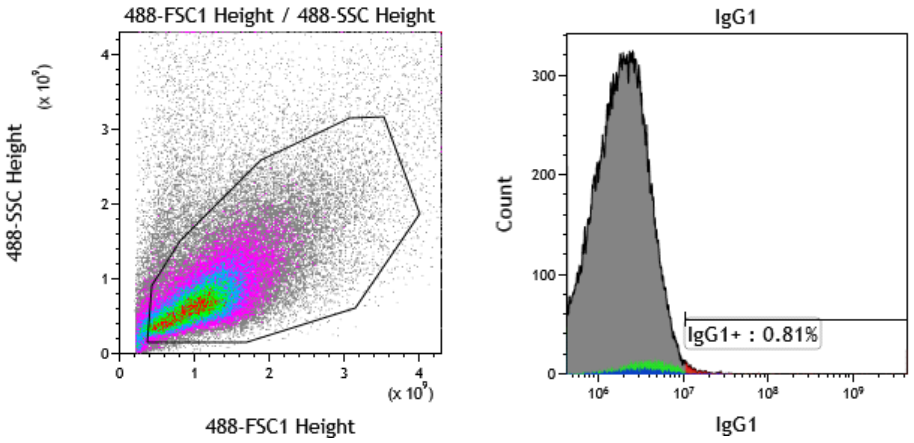


Figure 0.3 (continued). FACS readouts for IgG1 in murine splenic B-cells. Events were gated for size by forward scatter (FSC) and granularity by side scatter (SSC). Events outside this gate were excluded from further analysis. Percentage = % IgG1^{+} cells. Blue histograms: Ki-67+ cells; green histograms: IgM+ cells; red histograms: IgG1+ cells; grey histograms: unstained cells.

R. 5-30kDa
1412EtB



S. <5kDa
1412EtB

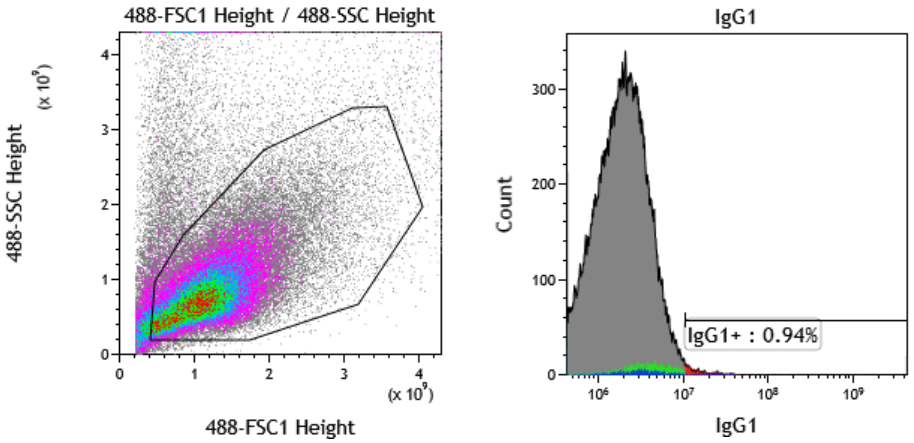


Figure 0.3 (continued). FACS readouts for IgG1 in murine splenic B-cells. Events were gated for size by forward scatter (FSC) and granularity by side scatter (SSC). Events outside this gate were excluded from further analysis. Percentage = % IgG1^{+} cells. Blue histograms: Ki-67+ cells; green histograms: IgM+ cells; red histograms: IgG1+ cells; grey histograms: unstained cells.

A.4 Proliferation and antibody expression analysis

200µg/ml 1402EtL

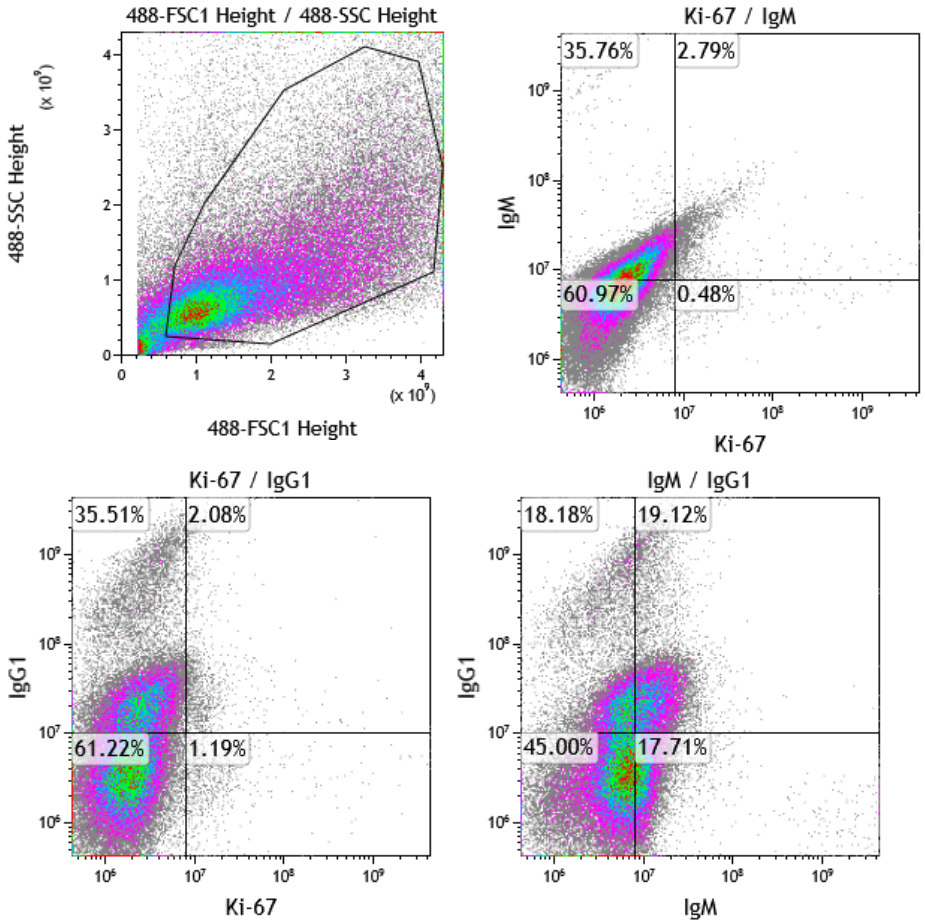


Figure 0.4 A. FACS scatter plots for Ki67, IgM and IgG1 in murine splenic B-cells treated with 200µg/ml 1402EtL. Events were gated for size by forward scatter (FSC) and granularity by side scatter (SSC). Events outside this gate were excluded from further analysis. Quadrant gates are set to the same values as the gates in Figures 5.1 - 5.3. Percentage shown = % positive cells.

100µg/ml 1402EtL

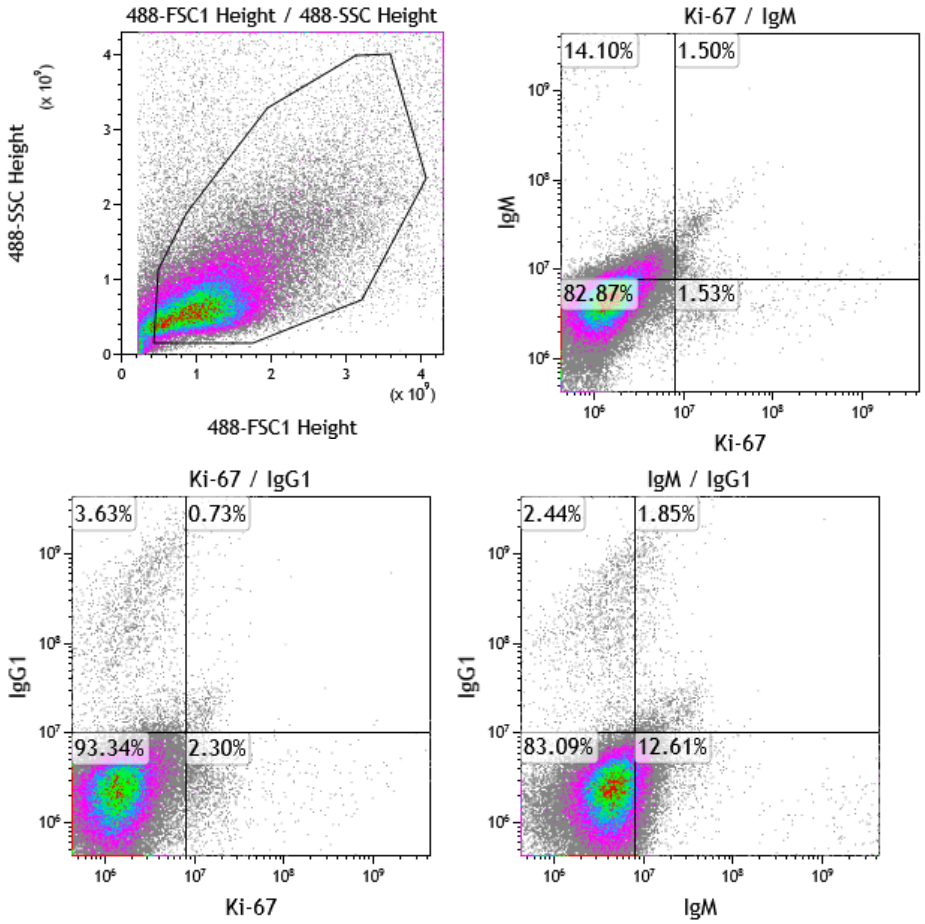


Figure 0.4.B. FACS scatter plots for Ki67, IgM and IgG1 in murine splenic B-cells treated with 100µg/ml 1402EtL. Events were gated for size by forward scatter (FSC) and granularity by side scatter (SSC). Events outside this gate were excluded from further analysis. Quadrant gates are set to the same values as the gates in Figures 5.1 - 5.3. Percentage shown = % positive cells.

50µg/ml 1402EtL

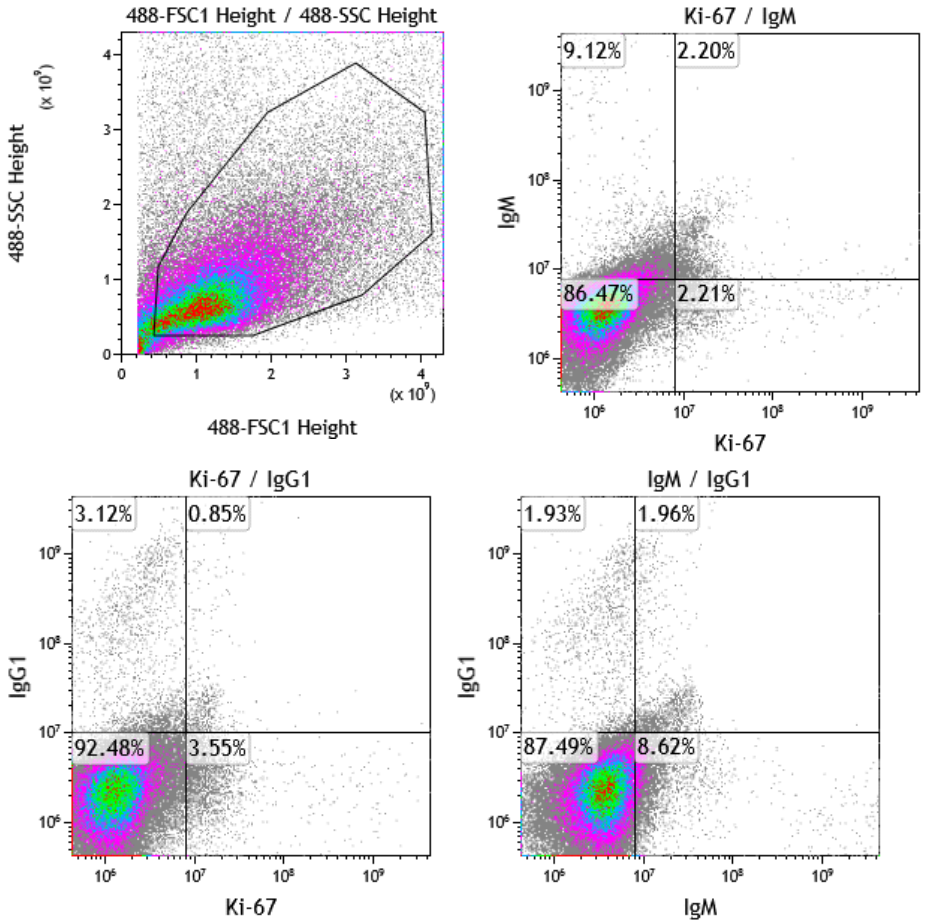


Figure 0.4.C. FACS scatter plots for Ki67, IgM and IgG1 in murine splenic B-cells treated with 50µg/ml 1402EtL. Events were gated for size by forward scatter (FSC) and granularity by side scatter (SSC). Events outside this gate were excluded from further analysis. Quadrant gates are set to the same values as the gates in Figures 5.1 - 5.3. Percentage shown = % positive cells.

200µg/ml 1412EtB

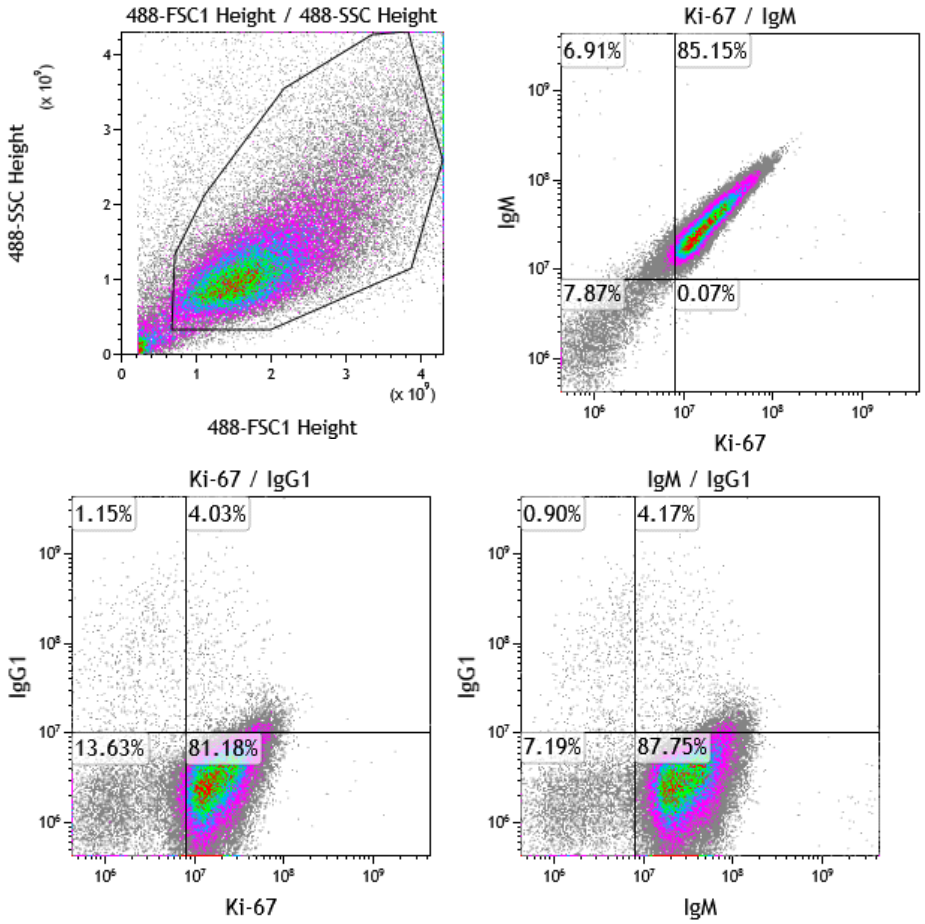


Figure 0.4.D. FACS scatter plots for Ki67, IgM and IgG1 in murine splenic B-cells treated with 200µg/ml 1412EtB. Events were gated for size by forward scatter (FSC) and granularity by side scatter (SSC). Events outside this gate were excluded from further analysis. Quadrant gates are set to the same values as the gates in Figures 5.1 - 5.3. Percentage shown = % positive cells.

100µg/ml 1412EtB

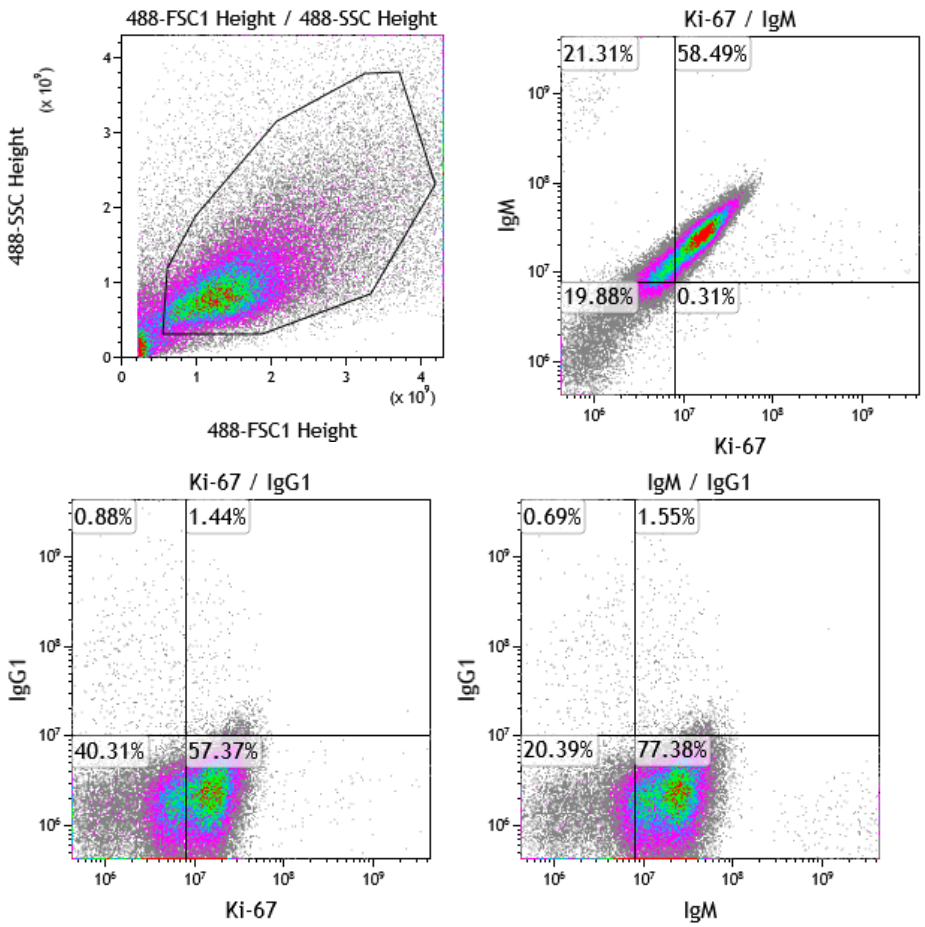


Figure 0.4.E. FACS scatter plots for Ki67, IgM and IgG1 in murine splenic B-cells treated with 100µg/ml 1412EtB. Events were gated for size by forward scatter (FSC) and granularity by side scatter (SSC). Events outside this gate were excluded from further analysis. Quadrant gates are set to the same values as the gates in Figures 5.1 - 5.3. Percentage shown = % positive cells.

50µg/ml 1412EtB

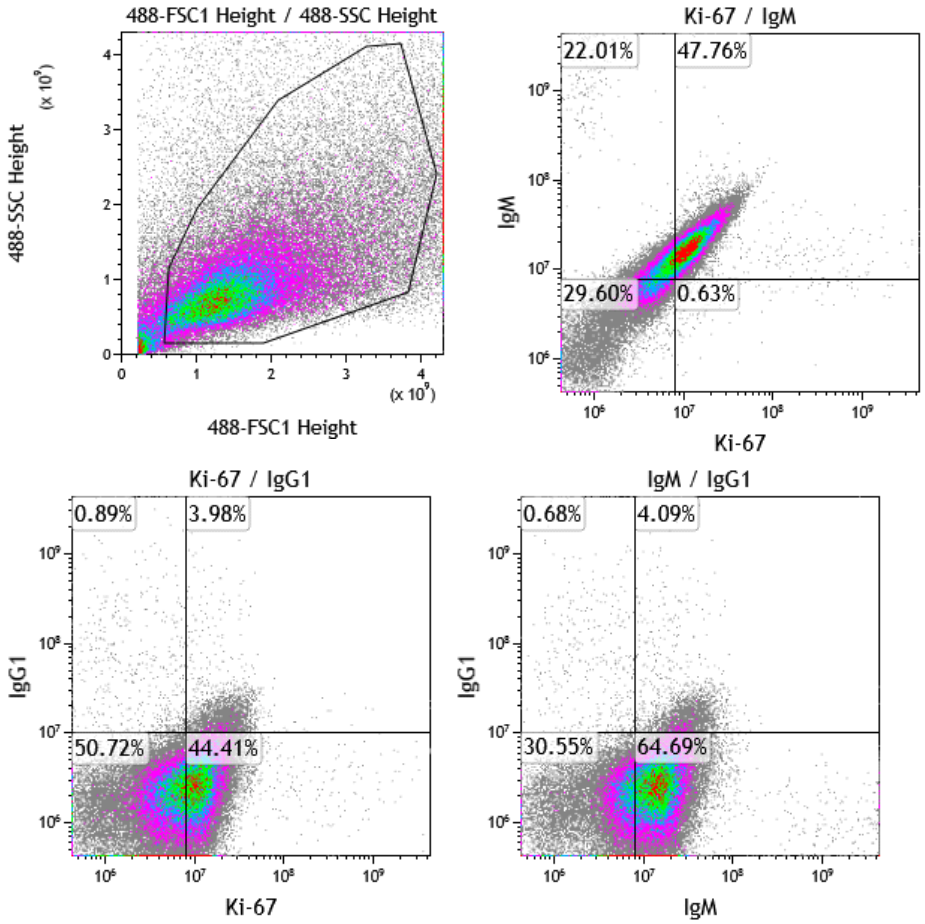


Figure 0.4.F. FACS scatter plots for Ki67, IgM and IgG1 in murine splenic B-cells treated with 50µg/ml 1412EtB. Events were gated for size by forward scatter (FSC) and granularity by side scatter (SSC). Events outside this gate were excluded from further analysis. Quadrant gates are set to the same values as the gates in Figures 5.1 - 5.3. Percentage shown = % positive cells.

1412EtB (acid-treated)

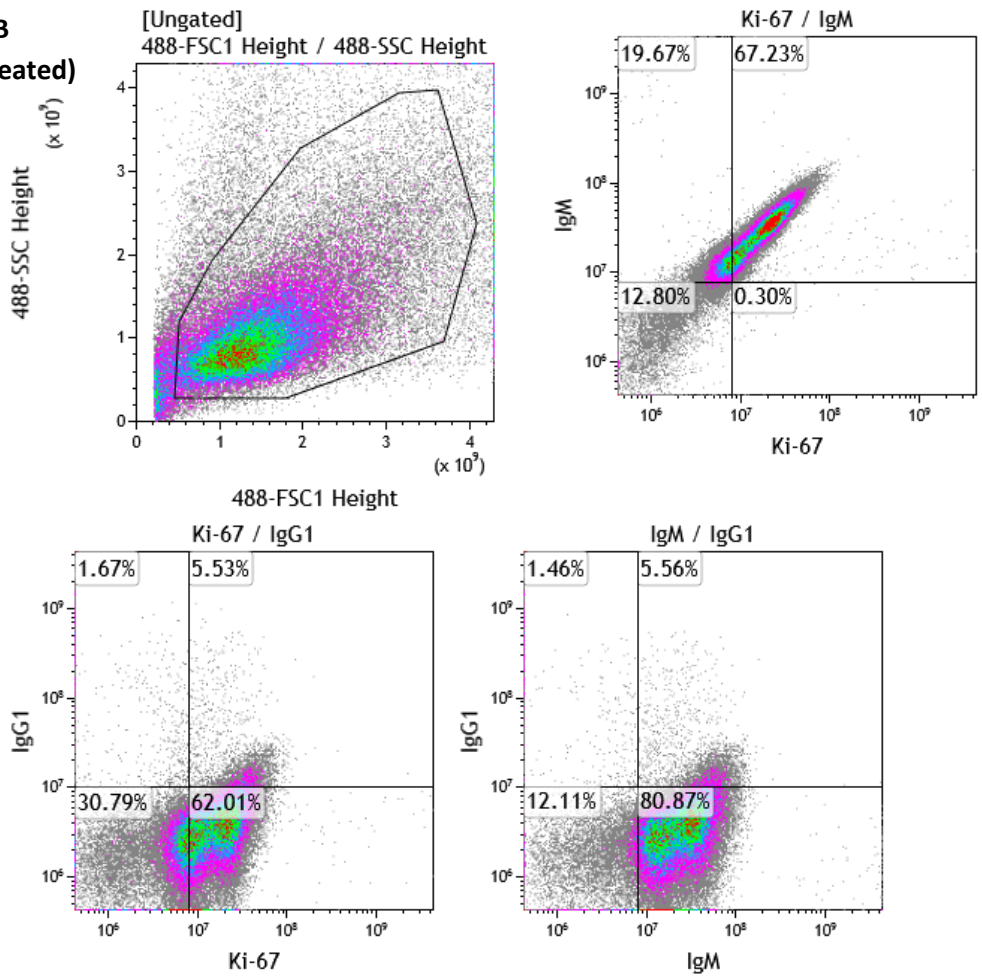


Figure 0.4.G. FACS scatter plots for Ki67, IgM and IgG1 in murine splenic B-cells treated with acid-treated 1412EtB. Events were gated for size by forward scatter (FSC) and granularity by side scatter (SSC). Events outside this gate were excluded from further analysis. Quadrant gates are set to the same values as the gates in Figures 5.1 - 5.3. Percentage shown = % positive cells.

1412EtB (boiled)

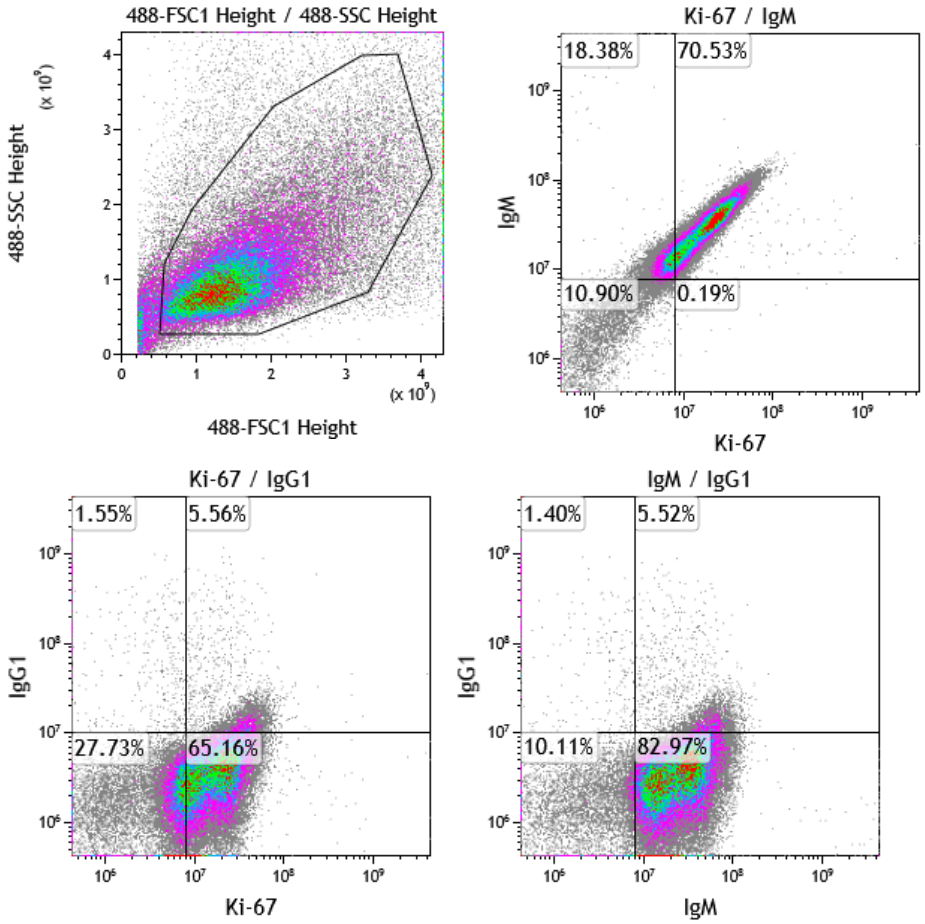


Figure 0.4.H. FACS scatter plots for Ki67, IgM and IgG1 in murine splenic B-cells treated with boiled 1412EtB. Events were gated for size by forward scatter (FSC) and granularity by side scatter (SSC). Events outside this gate were excluded from further analysis. Quadrant gates are set to the same values as the gates in Figures 5.1 - 5.3. Percentage shown = % positive cells.

1412EtB (oxidised)

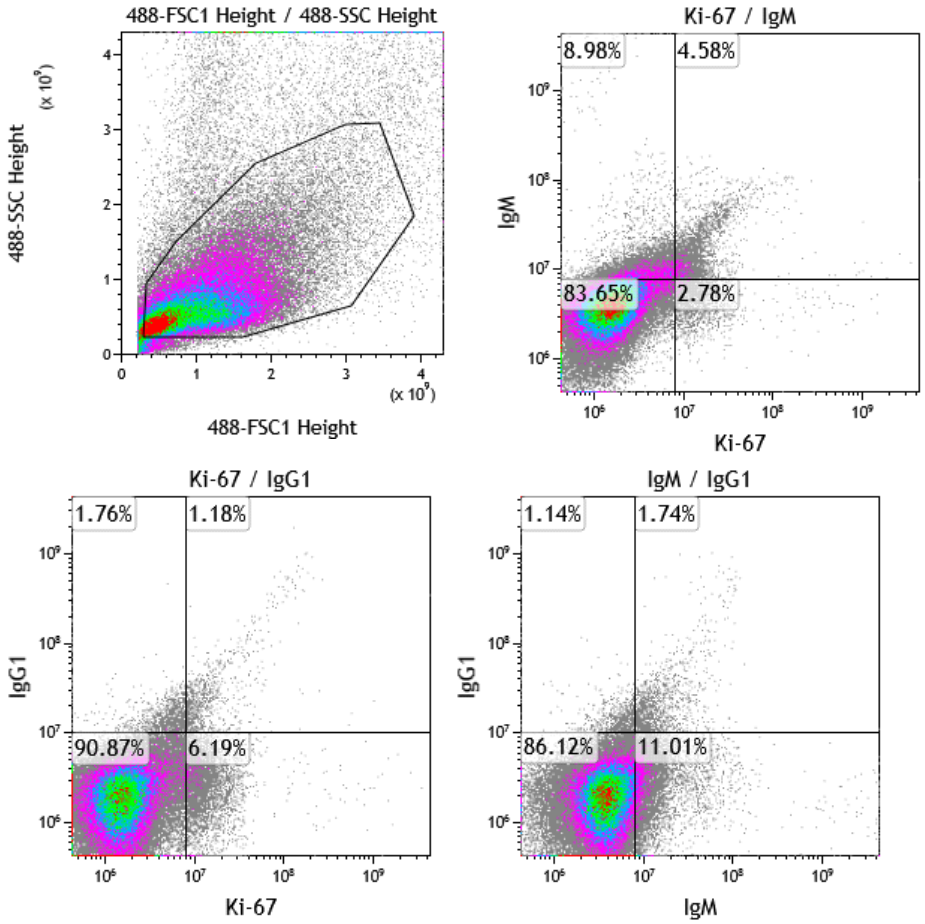


Figure 0.4.I. FACS scatter plots for Ki67, IgM and IgG1 in murine splenic B-cells treated with oxidised 1412EtB. Events were gated for size by forward scatter (FSC) and granularity by side scatter (SSC). Events outside this gate were excluded from further analysis. Quadrant gates are set to the same values as the gates in Figures 5.1 - 5.3. Percentage shown = % positive cells.

100kDa
1412EtB

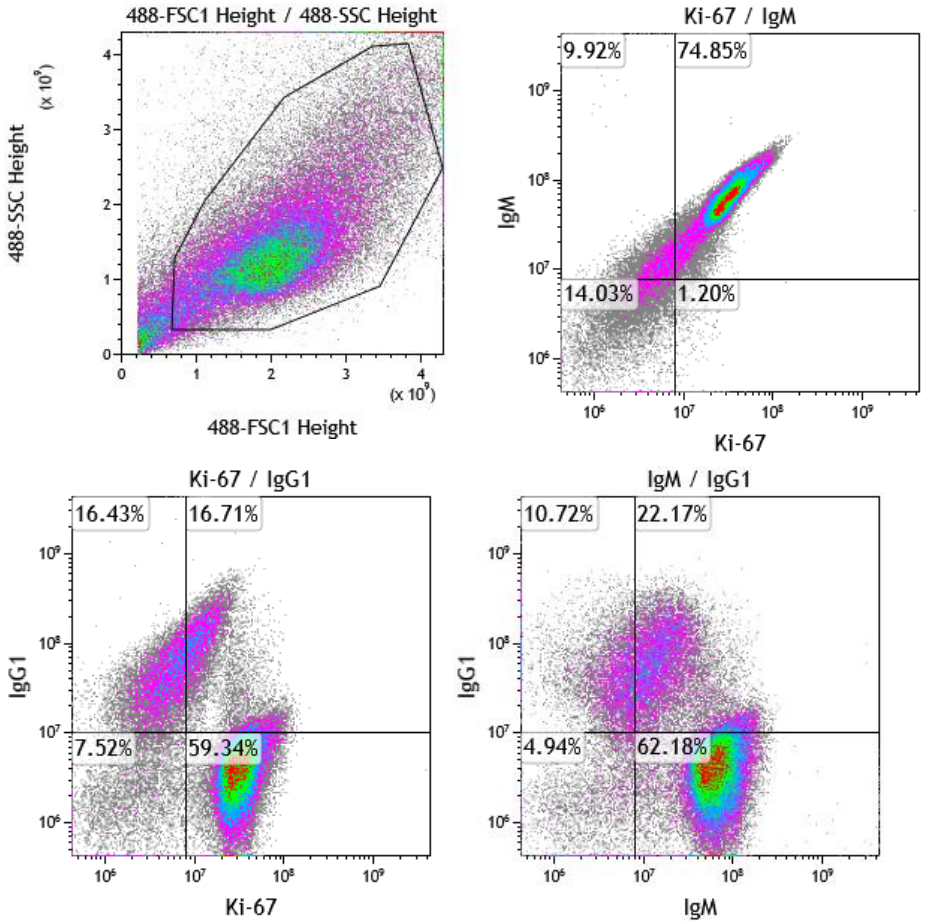


Figure 0.4.J. FACS scatter plots for Ki67, IgM and IgG1 in murine splenic B-cells treated with the >100kDa fraction of 1412EtB. Events were gated for size by forward scatter (FSC) and granularity by side scatter (SSC). Events outside this gate were excluded from further analysis. Quadrant gates are set to the same values as the gates in Figures 5.1 - 5.3. Percentage shown = % positive cells.

Appendix B PIPS Placement with The Naked Scientists

B.1 Note to examiners

This statement is included as an appendix to the thesis in order that the thesis accurately captures the PhD training experienced by the candidate as a BBSRC Doctoral Training Partnership student.

The Professional Internship for PhD Students is a compulsory 3-month placement which must be undertaken by DTP students. It is usually centred on a specific project and must not be related to the PhD project. This reflective statement is designed to capture the skills development which has taken place during the student's placement and the impact on their career plans it has had.

B.2 PIPS report

I undertook my PIPS placement at the office of the award-winning science podcast and BBC radio show The Naked Scientists.

Even before I'd been offered the placement, I could tell that this would be a stimulating place to work. The interview was interesting and made me think, particularly when the interviewer upended a large envelope of seemingly random items onto the table and gave me two minutes to make a science demonstration out of it. I left with a raised pulse but a smile on my face.

On my first day I was immediately made to feel part of the Naked Scientists team and I was thrown straight into the cycle of selecting stories from upcoming press releases, contacting researchers for comment, conducting interviews and editing the raw audio into a four-minute item for the programme. I'd arrived at a particularly busy time because the team was preparing extra shows for the festive break. It was a very exciting start, and even though there was a lot to take in at first I never felt overwhelmed or unsupported. I thrived on the challenge and my first interview was deemed good enough to be part of the main show that week, which is uncommon for interns.

Listening back to that interview now, my ear picks out bad edits, imperfectly-phrased questions and halting delivery, highlighting just how much I learned in a mere three months. I learned how to craft a story, asking the right questions to tell the narrative; I honed my

communication skills in interviews, on the phone, in recorded passages and live on stage. I acquired technical skills that were, for the most part, totally new to me. These included microphone technique, audio editing and the technical aspects of professional podcast production. Through observing the producers and presenters at work on the live broadcasts I also learned a lot about what it takes to put together a live radio show.

I also learned from my mistakes. Picking stories that were unsuitable for communication to a non-scientist audience, or failing to prepare for an interview properly were both causes of aborted efforts. Ultimately, I learned more from some of these stumbles than I did from my successes.

This all culminated in the production of my very own episode of The Naked Scientists. I was given my choice of theme, and there was one firm favourite in my mind: parasites. I've always loved parasites, and I take great pleasure in convincing people of their many endearing features. Fortunately the team agreed and I talked to a whole range of leading parasitologists to construct an interesting, novel and coherent narrative. I finally settled on a lineup that covered the unique benefits and challenges of parasitism, the often-bizarre host-parasite dynamic and the possibility of using some of these interactions in medical research. This included an on-location interview in the insectary at the London School of Hygiene and Tropical Medicine, which was particularly enjoyable.

This internship gave me opportunities and motivation to do things that I wouldn't normally have experienced, like taking part in a live Q&A on BBC Radio Norfolk and entering the FameLab science communication competition. Over the three months many of my pieces went into the Naked Scientists podcast and BBC radio show, ranging from monkey friendship to oceanic plastic. Through local and national radio, as well as the website and podcast, I've reached hundreds of thousands of people, which still amazes me. I also got to meet some absolutely fascinating researchers and communicators along the way, far too many to mention.

Before my placement I was reasonably confident in my abilities as a public speaker, writer and teacher. However, in three short months I sharpened all of these skills almost beyond recognition. In short, this internship has not only given me an insight into a stimulating and exciting field, but also an unforgettable three months working with a wonderful team doing something that I now know I love. I can see science communication either being my career post-PhD, or forming an integral part of it alongside research and/or teaching. I feel very lucky to have had this opportunity, and grateful to the team for making it so.

Appendix C Conferences and meetings attended

- Nottingham BBSRC DTP Spring School 2013
- British Society for Immunology (BSI) Congress, Liverpool, 2013
- Nottingham BBSRC DTP Spring School 2014 **(presentation and poster)**
- Sense About Science "Standing Up for Science" workshop, London, 2014
- Nottingham SVMS Early Career Researcher Presentation Day 2015 **(presentation)**
- Nottingham BBSRC DTP Spring School 2015 **(winner: Best Abstract)**
- Nottingham Immunology Showcase 2016 **(poster)**
- Nottingham BBSRC DTP Spring School 2016